HYPERTROPHIC SCAR THERAPY: PRESSURE-INDUCED REMODELLING AND ITS DETERMINENTS

A Thesis presented for the Degree of Doctor of Philosophy

by

Robert S. Naismith B.Sc.

Bioengineering Unit,
University of Strathclyde,
Glasgow.

June, 1980

ABSTRACT

Hypertrophic scars are cosmetically unattractive products of abnormal wound healing and, if they occur over flexor aspects of joints, considerable functional impairment often results.

Pressure, as a therapy for hypertrophic scarring has considerable attraction since it is effective and non-surgical. Previous reports of this therapy have not quantified magnitudes or durations of pressure required to induce remodelling. Correlation of these parameters is necessary to define guidelines to optimise pressure therapy. Measurement of pressure applied to hypertrophic scars by garments with elastic properties was achieved using a monitoring system based on a thin (0.2mm) flat ($1cm^2$) capacitive transducer. Pressures of 15 - 40mmHg produced, in general, accelerated scar remodelling with superior cosmesis resulting from higher pressures. Clinical studies suggested that 6 - 9 months pressure is sufficient to induce permanent remodelling, although studies of rates of collagen biosynthesis in pressure-treated and untreated scars indicated 9 - 12 months pressure was necessary.

Two types of pressure applying garments, Tubigrip and Lycra, were studied and compared. Tubigrip garments demonstrated superior elastic properties for maintaining pressure with time.

Investigations of two hypotheses for pressure-induced remodelling were performed. A first hypothesis that pressure induces ischaemia in scars, implying remodelling by autolysis, was investigated with vital microscopy using a hamster cheek pouch model. Pressure magnitudes which induced scar remodelling did not disturb the microcirculation sufficiently to cause permanent damage, therefore this hypothesis was thought unlikely to be correct.

A second hypothesis that pressure-induced vascular

changes produce scar resorption via a collagen-based mechanism was investigated using a radioactive isotope assay of the rate of collagen biosynthesis. The time for which the rate of collagen biosynthesis approached normal scar levels was reduced by half in pressure-treated compared to untreated scars.

A two-phase scar remodelling theory was introduced comprising a pressure-magnitude dependent phase followed by a time-dependent phase. The second hypothesis was thought to be partially correct and the complexity of the pressure-induced remodelling mechanism is discussed.

ACKNOWLEDGEMENTS

I welcome this opportunity for formal expression of my thanks to the following for their various contributions to this thesis:-

to my supervisors, Dr. John Evans and Mr. William Reid, consultant Plastic Surgeon, Canniesburn Hospital, Glasgow, my special thanks for guidance over the past three years and for the helpful counsel and suggestions offered regarding my thesis,

to Professors Robert Kenedi and Tom Gibson for introducing me to the problem of hypertrophic scarring and for the facilities provided by the Bioengineering Unit, and Canniesburn Hospital.

to Professor John Paul for his support and encouragement, and for handling the academic and administrative problems that arose from time to time.

to Dr. Anne Simmonds, Department of Biochemistry, Royal Maternity Hospital, Glasgow for patiently educating an engineer ignorant of tissue culture and cell biology, for the provision of laboratory facilities and for her useful comments on tissue preparation procedures described in Chapter 6.

to Mikael Romanus of the Laboratory of Experimental Biology, University of Goteborg, Sweden, for arranging my visit to Sweden, for the provision of laboratory facilities and assistance in performing the experiments contained in Chapter 7, for his critical consideration of Chapter 7, and for the friendship and hospitality bestowed upon me by his family.

to Dr. Martin Ferguson-Pell for his critical consideration of Chapter 4, and for invaluable discussion and shared ideas,

to the medical, nursing and ancillary staff of Canniesburn Hospital and Glasgow Royal Infirmary for their assistance and support. In particular, to Sister Doreen Couper for much help and shared ideas.

to Mr. David Smith for skilled technical assistance on many occasions, and for the preparation of many of the photographs in this thesis,

to Lone Broadhead for her most capable typing, and for her patience, and to her husband for permitting her to work ridiculous hours,

to all the students and staff of the Bioengineering Unit, past and present, who have helped me to the conclusion of this work; in particular to my colleague Anne Tully for close cooperation, useful discussion and shared ideas; also my other colleagues Jack Ferguson, Terry Hanson, Thien How, David Radcliffe, Steve Sherwin, Liz Smith and David Stobbart who assisted the work in many ways,

to Ian Buist whose courage gave me inspiration when it seemed dark,

to the Science Research Council and to the Medical Research Council for providing me with financial support for this study for periods of 1 and 2 years respectively,

to my mother and father for their ever present encouragement and faith in this and all my endeavours,

to my wife Sandra for her patience and most especially for her encouragement of a too-frequently preoccupied and very trying spouse.

CONTENTS

HYPERTROPHIC SCAR THERAPY: PRESSURE INDUCED REMODELLING AND ITS DETERMINENTS

Abstract

Acknowledgement

Contents

List of Figures

1. Introduction

1.1 The Problem of Hypertrophic Scarring 2

1.2 Background of the Investigation 5

1.3 The Scope, Aims and Objectives of the Investigation 6

2. A Comparative Review Between Hypertrophic Scar Tissue and Normal Skin 9

2.1 Introduction 10

2.2 Normal Skin 11

2.2.1 Normal Skin Epidermis 13
2.2.2 Normal Skin Dermis 13

2.2.2.1 The Papillary Layer 14
2.2.2.2 The Reticular Layer 14

2.3 Scar Tissue 15

2.3.1 Scar Epidermis 15
2.3.2 Pre-Elevation Scar Tissue 17
2.3.3 Elevated or Active Hypertrophic Scar Tissue 18
2.3.4 Mature Scar Tissue 20

2.4 Discussion and Conclusions 21

3. The Response of Normal Skin and Hypertrophic Scar Tissue to Mechanical Stimuli 23

3.1 Introduction 24

3.2 The Effect of Mechanical Stimuli on Normal Skin 26

3.2.1 The Response of the Vascular System to Mechanical Stimuli 26
3.2.2 The Response of Normal Skin to Prolonged Pressure 29
3.2.3 The Response of Normal Skin to "Shear" Forces 31

3.2.4 The Reflow Ability of Normal Skin 32
3.3 The Effect of Mechanical Stimuli on Hypertrophic Scar Tissue 33
3.3.1 The Physical Effect 34
3.3.2 The Structural Response of Scar Tissue 35
3.3.3 The Biochemical Response of Scar Tissue 36
3.4 Discussion 36

4. The Development and Construction of an Interface Pressure Measurement System 39

4.1 Introduction 41
4.2 Pressure Transducer Design Criteria 42
4.2.1 Surface Area 42
4.2.2 Transducer Thickness 43
4.2.3 Pressure Range 44
4.2.4 Resolution and Accuracy 44
4.2.5 Response to Physical Variables 45
4.2.5.1 Temperature 45
4.2.5.2 Curvature 45
4.2.5.3 In-Plane or Shear Forces 46
4.2.5.4 Dynamic Response 46
4.2.5.5 Time Dependence 46
4.2.5.6 Hysteresis 47
4.3 Selection of a Pressure Transducer 47
4.3.1 Principles of Operation of the Capacitive Pressure Transducer 48
4.3.1.1 Sensitivity to Pressure 49
4.3.1.2 Temperature Sensitivity 51
4.3.1.3 Sensitivity to Curvature 53
4.3.1.4 Sensitivity to In-Plane or Shear Forces 56
4.3.1.5 Time-Dependent Effects 58
4.3.2 Discussion 59
4.4 Construction of the Capacitive Pressure Transducer 61
4.4.1 Selection of Transducer Construction Method 62
4.4.2 Temperature Conditioning 67
4.5 Evaluation of the Capacitive Pressure Transducer 69
4.5.1 Standing Capacitance 69
4.5.2 Pressure Transducer Calibration 70
4.5.3 The Response to Temperature 72

4.5.4 The Response to Curvature 72
4.5.5 The Response to In-Plane Forces 72
4.5.6 The Response of the Transducer to Constant Load 73
4.5.7 Discussion 74

4.6 Design and Construction of a Signal Processing Circuit 76

4.6.1 Principles of Signal Detection 76

4.6.1.1 Capacitance to Frequency Conversion 76
4.6.1.2 The Capacitance Bridge 77

4.6.2 Design and Construction of Signal Processing Circuitry 79
4.6.3 Comparison between Capacitive Pressure Transducer and Other Interface Pressure Sensors 80

4.7 Summary 82

5. Clinical Investigations of Pressure Applied to Hypertrophic Scars 84

5.1 Introduction 85

5.2 Pressure Applying Materials 85

5.2.1 Lycra Garments 86
5.2.2 Tubigrip Garments 86

5.3 Method Of Measuring Pressure 87

5.3.1 Selection of Measurement Site 87
5.3.2 Calibration of Pressure Transducers 87
5.3.3 Measurement of Pressure 88

5.3.3.1 Pressure Measurements with the Transducer Static 88
5.3.3.2 Pressure Measurements with the Transducer being moved to Different Sites 89

5.4 Experimental Results 89

5.4.1 Case Study No. 6 91

5.4.1.1 Discussion and Conclusions 97

5.4.2 Case Study No. 9 98

5.4.2.1 Discussion and Conclusions 103

5.4.3 Case Study No. 1 104

5.4.3.1 Discussion and Conclusions 106

5.5 Analyses and General Discussion of Results 107

5.6 Summary 113

6. Collagen Biosynthesis Investigations in Pressure Treated and Untreated Hypertrophic Scars 114

6.1 Introduction 115

6.2 Selection of the Method of Determining Collagen Biosynthesis 116

6.2.1 Enzyme-Based Assays of Collagen Synthesis 116

6.2.2 Non-Enzyme Based Assay of Collagen Synthesis 117

6.3 Materials and Methods 118

6.3.1 Tissue Preparation 118

6.3.2 Incubation Conditions 119

6.3.3 Assay of Total Radioactivity and Hydroxyproline Radioactivity 120

6.4 Experimental Design 121

6.4.1 Patient Population 121

6.4.2 Verification of Incubation System 122

6.4.3 Calibration and Verification of the Assay Procedure 122

6.5 Experimental Results 125

6.5.1 Collagen Biosynthesis in Normal Skin and Normal Scar 125

6.5.2 Collagen Biosynthesis in Pressure Treated and Untreated Hypertrophic Scars 127

6.5.3 Discussion and Conclusions 130

6.6 Summary 133

7. An Investigation of the Effect of Constant Pressure and Pressure Gradients on the Microcirculation 135

7.1 Introduction 137

7.2 Microvascular Assessment Techniques: A Review 137

7.2.1 Angiography 137

7.2.2 Radioisotope Clearance Techniques 137

7.2.3 Doppler Ultrasound Blood Flow Monitoring 139

7.2.4 Laser Doppler Anemometry 140

7.2.5 Transcutaneous Optical Blood Content and Oxygenation Assessment Device 141

7.2.6 Development of the Transcutaneous Optical Device 142

7.2.7 Intravital Microscopy 143

7.3 The Effect of Pressure Distributions on The Microcirculation using a Hamster Cheek Pouch Model 144

7.3.1 Materials and Methods 144

7.3.2 Cheek Pouch Preparation 144

7.3.3 Microvascular Response Assessment Criteria 146

7.4 Experimental Design 147

7.4.1 Uniform Pressure Distributions 148
7.4.2 Non-Uniform Pressure Distributions 148

7.5 Experimental Results 149

7.5.1 Microcirculatory Response to "Low" Uniform Pressure Distributions 149

7.5.1.1 40mmHg Applied for 20mins. 149
7.5.1.2 40mmHg Applied for 60mins. 149
7.5.1.3 Discussion 150

7.5.2 Microcirculatory Response to "High" Uniform Pressure Distributions 151

7.5.2.1 400mmHg Applied for 15mins. 152
7.5.2.2 Discussion 154

7.5.3 Microcirculatory Response to Non-Uniform Pressure Distributions 157

7.5.3.1 20mmHg Pressure 157
7.5.3.2 40mmHg Pressure 158
7.5.3.3 Discussion 160

7.6 Summary 164

8. Synopsis 166

Bibliography 169

Appendix A 178

Appendix B 183

Appendix C 240

Appendix D 251

LIST OF FIGURES

2.1 Section of human sole illustrating the layered structure of the epidermis (after Bloom and Fawcett, 1969)

2.2 Section through skin from the shoulder showing the papillae at the epidermis/dermis junction (after Bloom and Fawcett, 1969)

2.3 Distribution and relative size of blood vessels in a vertical section of skin (after Bloom and Fawcett, 1969)

2.4 Light micrograph of a section through an active hypertrophic scar showing the planar papillary layer (PL) at the junction of the epidermis (E) and the dermis (D) (after Tully, 1980)

2.5 Micrographs of collagen filaments (CP) at granulation stage showing apparent loose packing x 10,500 (after Linares et al, 1973)

2.6 Light micrograph of a section through an active hypertrophic scar showing bundles of collagen fibres arranged into whorls (W) separated by septa (S) (after Tully, 1980)

3.1 Diastolic pressure levels in blood vessels of different sizes (after Sewell, 1974)

3.2 Skin blood flow (in ml/min per 100g of tissue) versus applied pressure (after Daly et al, 1976)

3.3 Allowable pressure versus time of application for tissue under bony prominences (after Reswick and Rodgers, 1976)

3.4 Schematic model of small cubical element of flesh with capillary across one diagonal

3.5 Schematic effect of pressure and ischaemia on portions of a rabbit skin flap

3.6 Effect of continuous pressure for 5 months on a skin grafted donor site showing remodelling at pressure treated site (PT) in contrast to the untreated site (UT) which is hypertrophic (after Tolhurst, 1977)

3.7 Photograph of 1½ year old hypertrophic scar which had been pressure treated for one year showing interstitial spaces (IS) between collagen fibres (CF) (after Baur et al, 1976)

4.1 Pressure response of 3-plate capacitive pressure transducer exhibiting output hysteresis between increasing (I) and decreasing (D) pressures

4.2(a) Unloaded triple parallel-plate capacitor

4.2(b) Loaded triple parallel-plate capacitor

4.3 Variation in sensitivity with dielectric thickness (after Ferguson-Pell, 1977)

4.4 Theoretical relationship between error due to temperature sensitivity and dielectric thickness (after Ferguson-Pell, 1977)

4.5 Schematic diagram of section of coaxial cylinders used for calculation of capacitance

4.6 Normal (F_n) and in-plane (F_s) forces acting on skin surface (S) produced by elasticated garment

4.7 Ratio of shear force to normal force acting on a curved surface

4.8 Response of a viscoelastic material to step loading and unloading demonstrating creep behaviour

4.9 Exploded schematic view of a triple parallel-plate capacitive pressure transducer (after Ferguson-Pell, 1977)

4.10 Comparitive size of pressure transducer

4.11 Methods of manufacturing parallel-plate pressure transducers

4.12(a) Response of type I pressure transducers to applied pressure

(b) Response of type II pressure transducers to applied pressure

(c) Response of type III pressure transducers to applied pressure

(d) Response of type IV pressure transducers to applied pressure

4.13 Temperature response of transducer before and temperature conditioning

4.14 Exploded view of calibration chamber with 0.25mm thick latex rubber diaphragm (RD) and latex rubber pad (RP)

4.15 Transducer calibration response with acceptibility limits (AL) and acceptable (A) and unacceptable (UR) responses

4.16 Calibration of sphygmomanometer (S) against mercury column

4.17 Pressure response of loaded transducer to curvature showing true pressure (TP) and pressure modified by curvature (CP)

4.18 Comparison between static transducer outputs (SO) and output when transducer is pulled out of chamber (MO) with 140mmHg applied pneumatic pressure (after Ferguson-Pell, 1977)

4.19 Transducer response to constant applied loads showing creep behaviour

4.20 Capacitance bridge circuit diagram with transducer (T) and variable capacitor (VC) connected in parallel

4.21 Block diagram of capacitive pressure measurement system with buffers (B), differential amplifier (D.A.) and rectifier

4.22 Capacitance bridge pressure monitor

4.23 Complete interface pressure monitoring system

5.1 Lycra pressure garment: short sleeve body vest

5.2 Tubigrip pressure garment: short sleeve body vest

5.3 Transducers (T) attached to skin surface by adhesive tape

5.4 Pressure transducers located beneath elasticated garment to take 'spot' measurements

5.5 Synopsis of pressures measured at selected sites on each patient - Table

5.6 Case study No. 6: Volar surface right arm before pressure applied

5.7 Case study No. 6: Dorsal surface right arm before pressure applied

5.8 Schematic view of pressure measurements pathways and selected measurement sites for case study No. 6

5.9 Pressures measured at interface with new Lycra pressure garment fitted - refer measurement session 29, Appendix B

5.10 Pressures measured at the interface after Lycra garment worn for 6 weeks - refer measurement session 34, Appendix B.

5.11 Temporal variation of pressures measured at the interface at various sites - refer measurement session 29 - 35, Appendix B

5.12 Case study No. 6: Dorsal surface after 8 months pressure therapy

5.13 Case study No. 6: Volar surface after 20 months pressure therapy

5.14 Split photograph showing hypertrophic scar after 10 months pressure of 25mmHg (top) and untreated control scar (bottom)

5.15 Pressure measured at the scar/dressing interface with continuous pressure applied for 6 hours

5.16 Case study No. 9: Right forearm volar surface showing extensive hypertrophic scarring before pressure

5.17 Case study No. 9: Schematic view of pressure measurement pathways and selected measurement sites

5.18 Pressures measured at scar/dressing interface with new Tubigrip garment - refer measurement session 3, Appendix B

5.19 Pressures measured at scar/dressing interface after Tubigrip garment worn for 9 weeks - refer measurement session 7, Appendix B.

5.20 Temporal variation of pressures measured at scar/ Tubigrip interface at various sites - refer measurement sessions 9 - 18, Appendix B

5.21 Case study No. 9: Volar surface after 9 months pressure therapy showing remodelled areas (R) and unremodelled areas (U)

5.22 Pressure profile along path 2 with varying layers of Tubigrip garment

5.23 Case study No. 1: Right hand with hypertrophic scarring before pressure therapy and transducers attached

5.24 Case study No. 1: Schematic diagram of pressure measurement sites - refer table case study no. 1, Appendix B

5.25 Temporal variations of pressures measured at the interface at various sites - refer table case study No. 1, Appendix B

5.26 Both hands after 10 weeks on pressure therapy showing marked cosmetic improvement

5.27 Both hands after 12 months pressure therapy showing 'wrinkled' skin texture

6.1 Time-dependence of the formation of peptide-bound ^{14}C-hydroxyproline by normal human skin in-vitro

6.2 Total protein and hydroxyproline synthesis in normal skin and normal scar - Table

6.3 Collagen biosynthesis in normal skin, normal scar and pressure-treated and untreated hypertrophic scar

6.4 Ratio of collagen biosynthesis to total protein synthesis in normal skin, normal scar, pressure-treated and untreated scars

6.5 Total protein and hydroxyproline synthesis in pressure-treated and untreated hypertrophic scars - Table

6.6 Collagen biosynthesis in pressure-treated scars as a function of scar duration

7.1 A wash-out curve following epicutaneous applications of radioactive tracer (after Kristensen and Wadskove, 1977)

7.2 Pneumatic pressure chamber for investigating blood content and oxygenation.

7.3 Hamster cheek pouch mounted over pressure chamber

7.4 Polaroid photograph of a part of cheek pouch illuminated with U-V light after infusion of FITC Dextran

7.5 Mounting platform for cheek pouch (CP) with pressure chamber (PC),irrigation bath (IB), water column (WC), objective (OB) and condenser (C) (after Romanus, 1977)

7.6 Apparatus for producing pressure gradients by compressing the cheek pouch (CP) against the glass edge by the latex membrane

7.7 Results of microvascular response to uniform pressure distribution of 40mmHg - Table

7.8 Microvascular response to uniform pressure distribution of 40mmHg showing extent of compressed area (CA) and pinched arteriole (A)

7.9 Results of microvascular response to uniform pressure distribution of 400mmHg - Table

7.10 Microvascular response to uniform pressure distribution of 400mmHg showing microthrombi (M) and rouleaux (R)

7.11 Pressure-induced strains in different vessel types - Table

7.12 Average pressure induced strain in different vessel types - Table

7.13 Results of microvascular response to 20mmHg non-uniform pressure distribution - Table

7.14(a) Before the application of pressure showing glass edge (GE) delineating compressed (C) and uncompressed zones

(b) Microvascular response to 20mmHg induced pressure distribution showing the width (W_1) of the occluded area (OA_1) between the compressed (C) and uncompressed areas (NC)

7.15 Results of microvascular response to 40mmHg induced non-uniform pressure distribution - Table

7.16(a) Microvascular response to 40mmHg induced non-uniform pressure distribution showing the width (W_2) between the compressed (C) and uncompressed (UC) areas

(b) Microvascular response following release of 40mmHg pressure showing leakages (L) microthrombi (M), inflammatory response (if), hyperaemia (e), the compressed (C) and uncompressed (NC) areas

CHAPTER 1

INTRODUCTION

1.1. The Problem of Hypertrophic Scarring

1.2. Background to the Investigation

1.3. The Scope, Aims and Objectives of the Investigation

1.1. THE PROBLEM OF HYPERTROPHIC SCARRING

Hypertrophic scars are erythematous, elevated plaques of tissue which are mechanically rigid, inextensible and, which, histologically, consist mainly of collagen bundles fused together and arranged in an amorphous matrix. Their aetiology is presently unknown and their formation is most frequently observed subsequent to the destruction of large areas of skin to the level of the deep reticular dermis such as occurs after burns. In this thesis a hypertrophic scar is defined as an abnormal scar which remains within the original wound boundary after healing. Although similar lesions have been infrequently reported in other animal species, the formation of hypertrophic scars, in their frequency and consistency, is a phenomenon which appears unique to human beings.

Hypertrophic scars are often accompanied by severe cosmetic and functional disablement - contractures occurring over the flexor aspect of joints such as the axillae or the volar neck surface. The socio-economic consequences of hypertrophic scarring can be serious for both the individual and the state; incumbent individuals often undergo intensive rehabilitation therapy, such as surgery and physiotherapy, which is frequently demanding for the community, traumatic for the patient and in the short term has been generally ineffectual; the individuals are often unable to work productively and consequently may be thought of as an added burden to community welfare departments, and the magnitude of the cosmetic and functional debilitation can result in the individual's complete withdrawal from normal society. It has long been recognised that both intrinsic and extrinsic factors are important in producing scar formation, the onset of which is variable depending on the initial wound healing process. Intrinsic factors include age, race, location of lesion and skin tension at the location of the lesion, and extrinsic factors include depth and extent of injury.

The wound contraction process is present in all healing

wounds and normally stops after an unknown predetermined period, however, in wounds which are predisposed to hypertrophy furthercontraction occurs after an indeterminate period resulting in a hypertrophic scar.

The proliferation of hypertrophic scar tissue is rapid and usually begins around the third to fifth week after the initial wound healing process continuing for a period of six to eight weeks thereafter, during which the hypertrophic scar morphology develops and subsequent contraction begins. This process of subsequent contraction can continue for several months. A period of stability of the scar then occurs during which time no further contraction is observed, and later after an indeterminate time, the scar undergoes a natural regression or remodelling process which may be either spontaneous or gradual. The hypertrophic scar is thus transformed into a mature scar during this latter process but the mechanism responsible for initiating and maintaining the remodelling process is unknown. The resulting mature scar has similar mechanical properties and histological features to those of normal scar.

The quality of the mature scar can be improved by treating the active scar to modify the natural remodelling process, and many therapies have been used for this purpose. Such therapies include surgery, irradiation, chemotherapy and external pressure with each type of therapy being reported as providing a better clinical result than that achieved by the natural remodelling process itself. Consequently each therapy has been extensively investigated with a view to producing a universally successful and acceptable routine treatment for hypertrophic scarring.

Surgery was, and still is, a very popular treatment because of expediency. However, recent studies have shown that after a few months lesions treated by surgery alone show a marked tendency to recur. Surgery in combination with other therapies such as irradiation and chemotherapy has been frequently used, but no significant improvement

has been demonstrated over any other individual method.

Irradiation was previously used to treat hypertrophic scars due to the concept that such scars were produced by an abnormal proliferation of fibroblasts, but this type of therapy was not wholly successful; scars frequently did not resolve and atrophy of the treated site and surrounding tissue was common. Consequently, this therapy is no longer used.

Anti-inflammatory agents, such as triamcinolone acetonide have been applied locally to scars, usually by injection, with widely varying results being reported. However, the actual mode of action of the drug remains unknown, since the high internal hydrostatic pressures produced within the scars by the injection may have been responsible for indirectly mediating the scar remodelling process in instances where sucessful results were reported.

Major reasons for the conflicting success reports of the above-mentioned therapies may be the absence or lack of understanding of the aetiology of hypertrophic scarring, and of the natural remodelling process.

Recently, smooth muscle relaxants have been used on fibroblastscultured from hypertrophic scar tissue and have been shown to inhibit contraction within these cells. Hypertrophic scar fibroblasts have also demonstrated contractile properties similar to smooth muscle cells with the presence of actinomyosin groups being identified from biochemical cross-reactions. Hypertrophic scar contraction has been attributed to contractile filaments within the cells,some of which have been termed "myofibroblasts"due to their morphology and biochemical response.

Ultrasound has also recently been used as a treatment for hypertrophic scars, based on the principle that short-wave radiation improves the vascularity of the tissue hence improves the "healing" or remodelling capacity as well as removing pain or pruritis associated with the scar, however, little clinical data has been reported to date.

1.2. BACKGROUND TO THE INVESTIGATION

As a therapy for hypertrophic scarring, the use of pressure is documented in the literature as far back as the early nineteenth century, although its use since then has not been widespread nor the results obtained well documented. The use of pressure as a therapy has more recently been investigated in detail in the U.S.A. where it is now widespread and routinely used for the treatment of hypertrophic scars, particularly at the Shriners Burns Institute, Galveston, Texas. Pressure is applied on the scar surface by elasticated garments. These garments are custom-made for each patient and are worn continuously. The garments have dimensions smaller than the actual anatomical dimensions at the site of the lesion so that the stretching of the garment, when worn, produces elastic forces resisting the stretch which act on the hypertropic scar. The results claimed indicate a superior clinical result over the results obtained by other therapies and additionally, pressure therapy claims the advantages of being non-surgical and non-invasive.

Canniesburn Hospital, Glasgow, is a major centre of Plastic and Reconstructive surgery and has for many years collaborated with the Bioengineering Unit, University of Strathclyde, on a variety of complex clinical problems. This situation is consistent with the Medical Research Council's current policy to encourage and foster multi-disciplinary approaches to skin research (M.R.C.A.R., 1977). Treatment of post-burn hypertrophic scarring is included at the hospital and several scar treatment regimes have been carried out, using surgery and chemotherapy, and more recently, ultrasonics. The results of these previous therapies were variable and generally unsuccessful. Due to a low overall success rate it was therefore realised that a more consistent therapy was required. It was known from research in the U.S.A. that encouraging results in the treatment of hypertrophic scars by pressure were being

obtained. Moreover, on a closer inspection of the results it appeared most of these studies had been incompletely reported,and that further data and information were required before it would be suitable to provide a routine clinical therapy for hypertrophic scarring based on mechanical pressure.

1.3. THE SCOPE, AIMS AND OBJECTIVES OF THE INVESTIGATION

It was apparent that pressure-based treatment offered significant potential as a routine clinical therapy and consequently it was decided to investigate this potential using a multidisciplinary approach according to the following aims and objectives.

(i) To develop and construct an instrumentation system to obtain quantitative values of the magnitude of pressure at the scar/dressing interface.

(ii) To investigate the relationship between pressure magnitude, duration of pressure and the scar remodelling results.

(iii) To investigate the nature of remodelling mechanism induced by the effect of mechanical pressure on scar tissue.

As a preliminary step towards these aims,Chapter 2 compares the structure and function of normal skin and hypertrophic scar. Comparisons are discussed according to anatomical boundaries, and the temporal variation of the hypertrophic scar structure and function is also included. Chapter 3 reviews the effect of mechanical stimuli on normal skin and on scar tissue. Critical threshold parameters for normal skin viability are discussed in relation to pressure-induced scar remodelling. In particular, the absence of quantification in previous

studies of scar remodelling is highlighted and the need for a quantitative approach to the problem is emphasised.

Chapter 4 describes the design and construction of a monitoring system to measure and record pressures present at the scar/dressing interface. In particular, the design criteria for an ideal interface pressure sensor is discussed and the unsuitability of existing devices highlighted. The development of a parallel-plate capacitive pressure transducer is presented with emphasis placed on suitability for use in a clinical environment.

Chapter 5 reports a clinical investigation of pressures developed at the scar/dressing interface carried out on a group of patients with hypertrophic scarring at Canniesburn Hospital, Glasgow. The relationship between pressure magnitude, pressure duration and scar remodelling is discussed, and available pressure applying garments are compared.

Chapter 6 describes an investigation of the mechanism responsible for hypertrophic scar remodelling using a biochemical assay of the rate of collagen synthesis in biopsies taken from pressure-treated and untreated hypertrophic scars.

The effect of constant pressure and pressure gradients on the microcirculation using a Hamster Cheek pouch model is described in Chapter 7. The significance of the results are discussed with regard to the effect of pressures found to induce hypertrophic scar remodelling.

Chapter 8 includes a general discussion of the results of the thesis principally with regard to their clinical significance and application. The conclusions of the investigation are also presented. The requirement for further detailed investigation in certain areas for a better understanding of the remodelling mechanism is emphasised.

This thesis is a part of an integrated study presently being undertaken between the Bioengineering Unit and Canniesburn Hospital into the aetiology and treatment of hypertrophic scarring and includes only the investigation of pressure magnitudes on the remodelling effect of scar

tissue with regard to the changes in collagen biochemistry and vascular behaviour.

For a more complete understanding of the subject the reader is referred to the associated thesis of Tully (1980) which investigates the response of the structure and mechanical properties of hypertrophic scars to applied pressure.

During the latter part of this thesis the author was awarded an M.R.C. Travelling Scholarship to visit the Laboratory of Experimental Biology at Göteborg, Sweden to study the effects of constant pressures and pressure gradients on the vascular system; the results of which are included in Chapter 7 of this thesis.

CHAPTER 2

A COMPARATIVE REVIEW BETWEEN HYPERTROPHIC SCAR TISSUE AND NORMAL SKIN

2.1 Introduction
2.2 Normal Skin
2.2.1 Normal Skin Epidermis
2.2.2 Normal Skin Dermis
2.2.2.1 The Papillary Layer
2.2.2.2 The Reticular Layer
2.3 Scar Tissue
2.3.1 Scar Epidermis
2.3.2 Pre-Elevation Scar Tissue
2.3.3. Elevated or Active Hypertrophic Scar Tissue
2.3.4 Mature Scar Tissue
2.4 Discussion and Conclusions

2.1 INTRODUCTION

In human beings only the epidermis, and to a lesser extent the liver, have the capacity to regenerate tissue which is a duplicate of the uninjured tissue. All other tissues such as nerve, muscle, tendon and dermis must rely on wound healing. Wound healing is an intricate physiological process whereby several different kinds of cells appear at successive intervals in order to absorb foreign matter, destroy bacteria and repair the injury (Peacock and Van Winkle, 1976). The magnitude and nature of the difference between repaired tissue and uninjured tissue is often a function of the initial insult, although the wound healing process per se is generally independent of the form of injury (Ross, 1969).

In the case of skin, the wound repair process produces very acceptable cosmetic and functional results when the area of injury is small, wound contraction closes the wound and granulation tissue forms to provide protection from a hostile environment. However, when damage to the skin involves the destruction of large area of tissue, as often occurs, for example, in burns or avulsion injuries, the wound repair process often becomes abnormal and a post-wound healing phenomenon, characterised by excessive production of collagen and severe contraction, occurs. This phenomenon is clinically described as hypertrophic scarring.

In order to optimise treatment for hypertrophic scarring it is important to investigate and identify differences between the structure and function of hypertrophic scar tissue and normal skin and scar. Such differentiation would assist evaluation of different therapies and, it may also provide a basis for determining the aetiology of hypertrophic scars.

2.2 NORMAL SKIN

The skin forms the outermost surface of the body containing the body's contents under a small internal pressure and is continuous with the mucosal surface of the respiratory, alimentary and urogenital tracts. It forms the interface between the body and the external environment, experiencing large differentials of physical and chemical parameters throughout its thickness.

Skin minimises the potentially injurious effects of mechanical, osmotic, chemical, thermal and other environmental stresses, it provides a barrier against invasion by other micro-organisms and it controls, in part, the exchange of heat by its thermal properties. Additionally, skin is, inter alia; an important sensory surface and sweat, and, it is capable of synthesising metabolic substances such as Vitamin D.

Physically, skin is composed of two essentially adjacent layers, the dermis and the epidermis, the latter being the innermost layer. The epidermis is avascular and consists of six closely packed strata which rely on diffusion for nutrition. The underlying dermis consists of a dense network of fibrous proteins contained in a viscous mucopolysaccharide matrix, often called "ground substance". The adipose layer of tissue beneath the dermis is usually associated in mechanical terms therewith.and it also provides a mobile interface between the skin and the deeper fascia.

Although the most significant differences between skin and scar occur in the dermis, changes have also been observed between the epidermis of normal skin and scar. Characterisation of these epidermal differences may yield information which complements that obtained from the dermis.

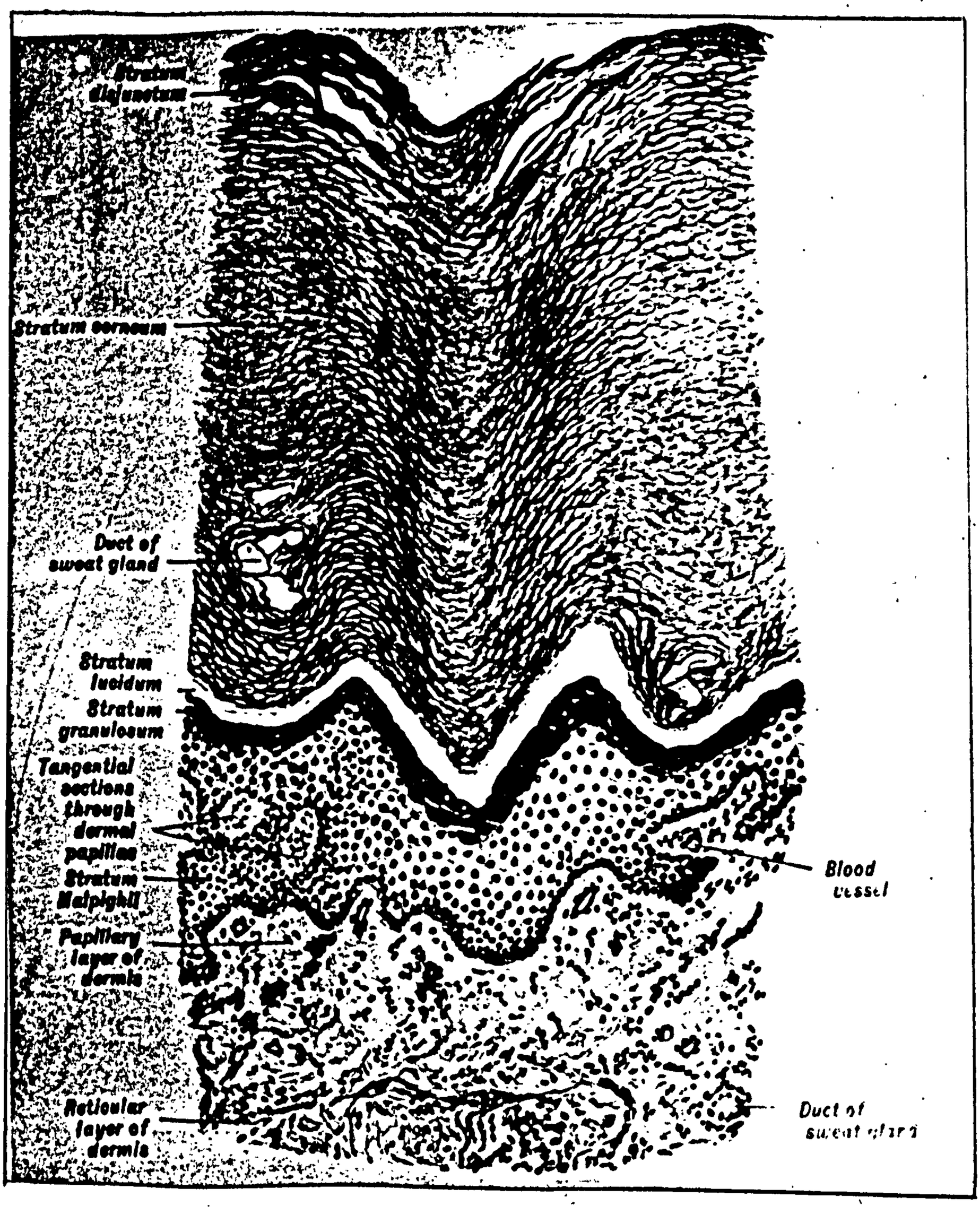

FIGURE 2.1. SECTION OF HUMAN SOLE ILLUSTRATING THE LAYERED STRUCTURE OF THE EPIDERMIS

(After Bloom and Fawcett, 1969)

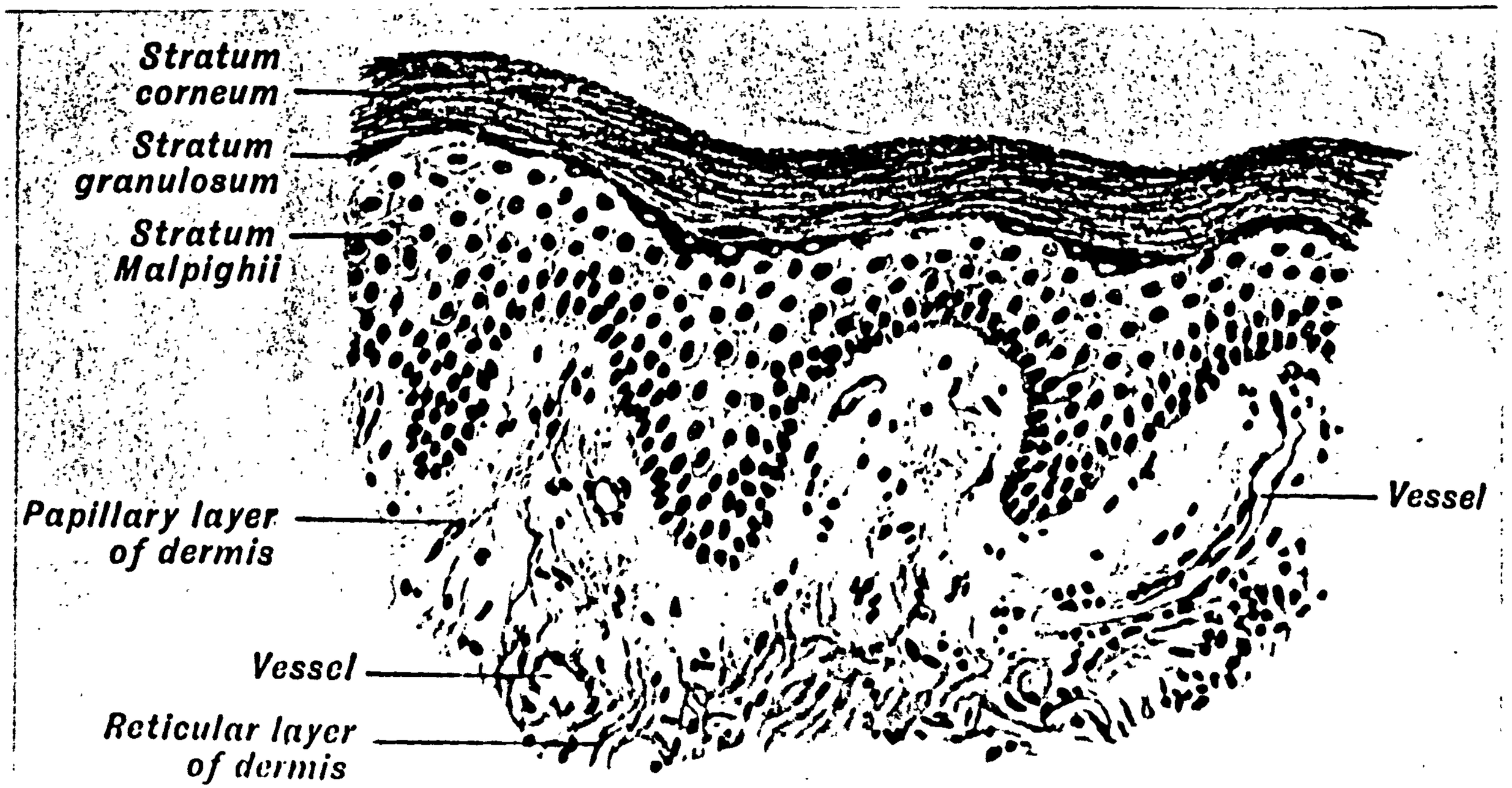

FIGURE 2.2. SECTION THROUGH SKIN FROM THE SHOULDER SHOWING THE PAPILLAE AT THE EPIDERMIS/DERMIS JUNCTION

(After Bloom and Fawcett, 1969)

2.2.1 Normal Skin Epidermis

Normal skin epidermis is avascular and consists of six closely packed strata and, although the thickness of the epidermis varies considerably over the body, the six layer structure is maintained. The structure of the epidermis is flexible, permitting adaptation to differing physiological requirements, notably repeated intermittent loading, in which case hypertrophic epithelium results and the stratum corneum noticeably thickens. The six strata of the epidermis are arranged as illustrated in Figure 2.1 with the stratum basale being the layer of cells immediately above the dermis, followed by: the stratum spinosum, stratum granulosum, stratum lucidum, stratum corneum respectively and, finally, the stratum disjunctum which is the outermost layer.

The cells of the stratum spinosum become elongated and flattened as they approach the stratum granulosum. This flattening process continues in the stratum granulosum and,in the superficial cells,organelles are frequently absent. Desmosomes, intercellular contact media, are commonly observed in the stratum although they appear to lose their structure in the superficial stratum granulosum. Cell nuclei are rarely observed in or about the stratum lucidum.

The junction between epidermis and dermis is characterised by papillae, or rête ridges, which appear as a wavy convoluted pattern in cross-section (Figure 2.2) and which provide a large surface contact area between the epidermis and the dermis. Papillae are most clearly defined at palmar and plantar surfaces where elevated ridges are observed on the surface of the dermis.

2.2.2. Normal Dermis

The dermis adjacent to and beneath the epidermis reflects the major differences between normal skin and scar tissue.

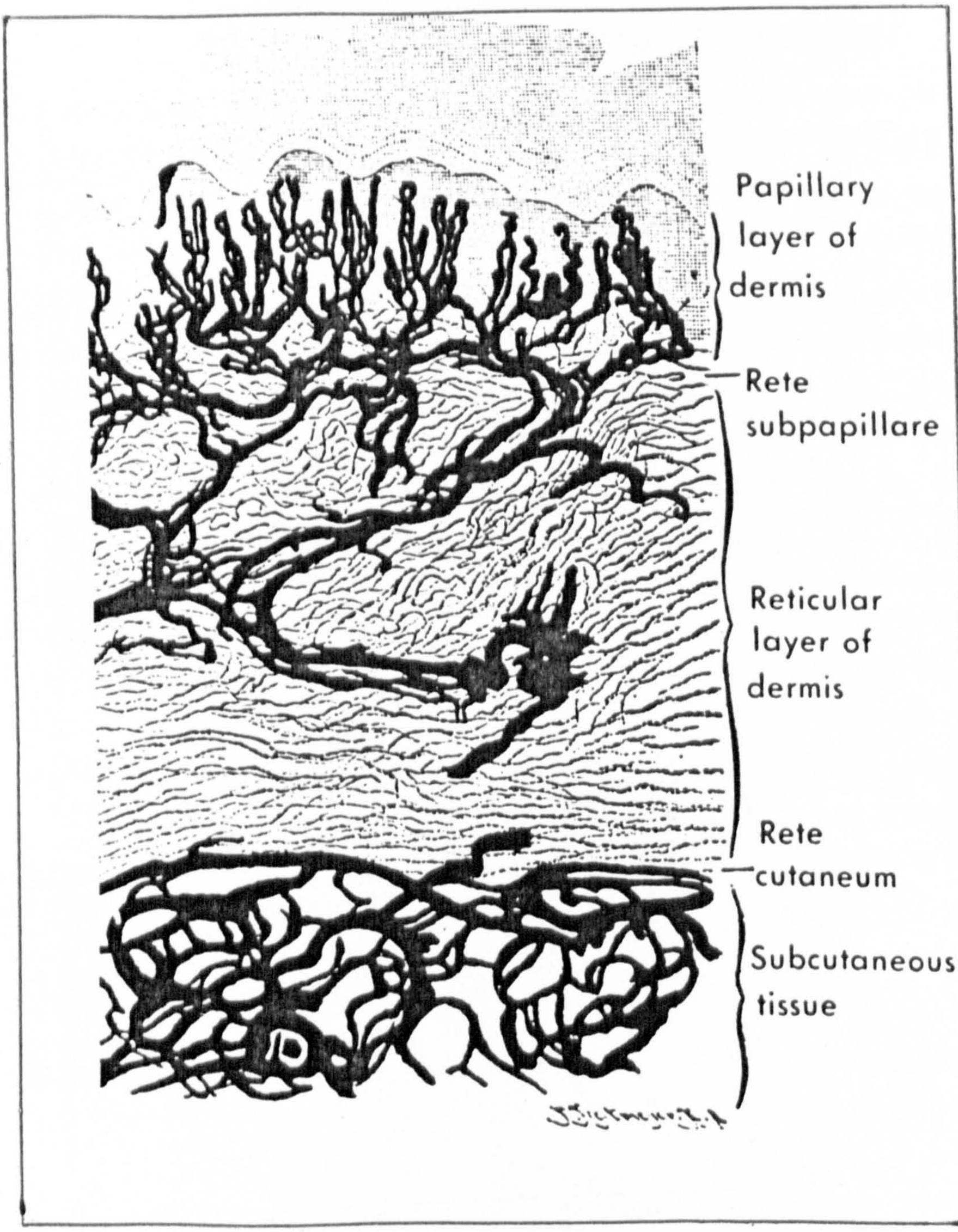

FIGURE 2.3 DISTRIBUTION AND RELATIVE SIZE OF BLOOD VESSELS IN A VERTICAL SECTION OF SKIN.
(After Bloom and Fawcett, 1969)

The dermis is formed from the somatic layer of the mesoderm in the embryo and is highly innervated and vascularised, especially just beneath the papillary layer. The dermis is composed of an irregular network of collagen and elastin fibres contained in a viscuous mucopolysaccharide and glycoprotein matrix, known as "ground substance". It may be structurally divided into two layers, the reticular layer and the papillary layer. The fibroblast, a specific connective tissue cell, is thought to be responsible for the production of most of the extracellular material in the dermis (Ross, 1969, Craig et al, 1973). The fibrous network and viscous matrix are responsible for the tough, resilient charc-teristics of skin. Ground substance is a complex matrix of carbohydrates and glycoproteins synthesised by the fibroblast and the liver respectively, and it has a high water-binding capacity which facilitates the diffusion of metabolites and nutrients. It is also thought to form a mechanical barrier to impede the movement of foreign bodies such as bacteria.

2.2.2.1. <u>The Papillary Layer</u> The papillary layer is adjacent to the stratum basale of the epidermis and consists of loosely arranged non-oriented fibres. It has a rich vascular system, particularly an anastomosing capillary network which is supplied from the reticular dermis by vessels which are quasi-perpendicular to the skin surface (Figure 2.3). The papillary layer also has a large cell population, in particular fibroblasts (Linares et al, 1972). It is continuous with the reticular layer of the dermis and, is structurally differentiated from the reticular layer mainly by the diameter of the collagen fibres although also by differences in vascular patterns.

2.2.2.2. <u>The Reticular Layer</u> The collagen fibres in the reticular layer are wavy in appearance and have an apparent random orientation (Linares et al, 1972, Brown,

1971). The distance between collagen fibrils is considerable and these fibrils are connected at various irregular intervals by collagen filaments, which, unfortunately, have not yet been completely characterised. Linares et al (1972) estimated that collagen fibrils had a diameter between 400Å - 1500Å with a mean value of 1000Å in normal skin. Elastin fibres were frequently observed within the collagenous network, and have been reported as greatly influencing the resilient properties of tissue (Nachemson and Evans 1968, Daly, 1968).

2.3. SCAR TISSUE

In a normal wound repair process, a normal scar results directly from the granulation stage, whereas a hypertrophic scar is essentially an intermediate stage of an abnormal wound repair process. After an indeterminate period which can range from a few months to several years, the hypertrophic scar undergoes a spontaneous natural remodelling process into a "mature scar" which has a similar clinical and histological appearance to normal skin.

The structure and metabolism of scars is therefore a function of scar age and, in the case of hypertrophic scars three main phases are important; the pre-elevation phase, the active or elevated phase and, the mature scar phase. In order to provide a meaningful comparison between the hypertrophic scar and normal skin it is necessary to consider and examine the tissue of each phase in turn.

2.3.1. Scar Epidermis

Scar epidermis, like normal epidermis, is avascular and has the same number and order of cellular layers, however polymorphism has been observed in hypertrophic scar specimens; some specimens exhibited atrophy whereas others showed a normal appearance or varying acanthosis. (Linares et al, 1972). Linares et al, (1973) reported that structures of epidermal origin, such as hair follicles

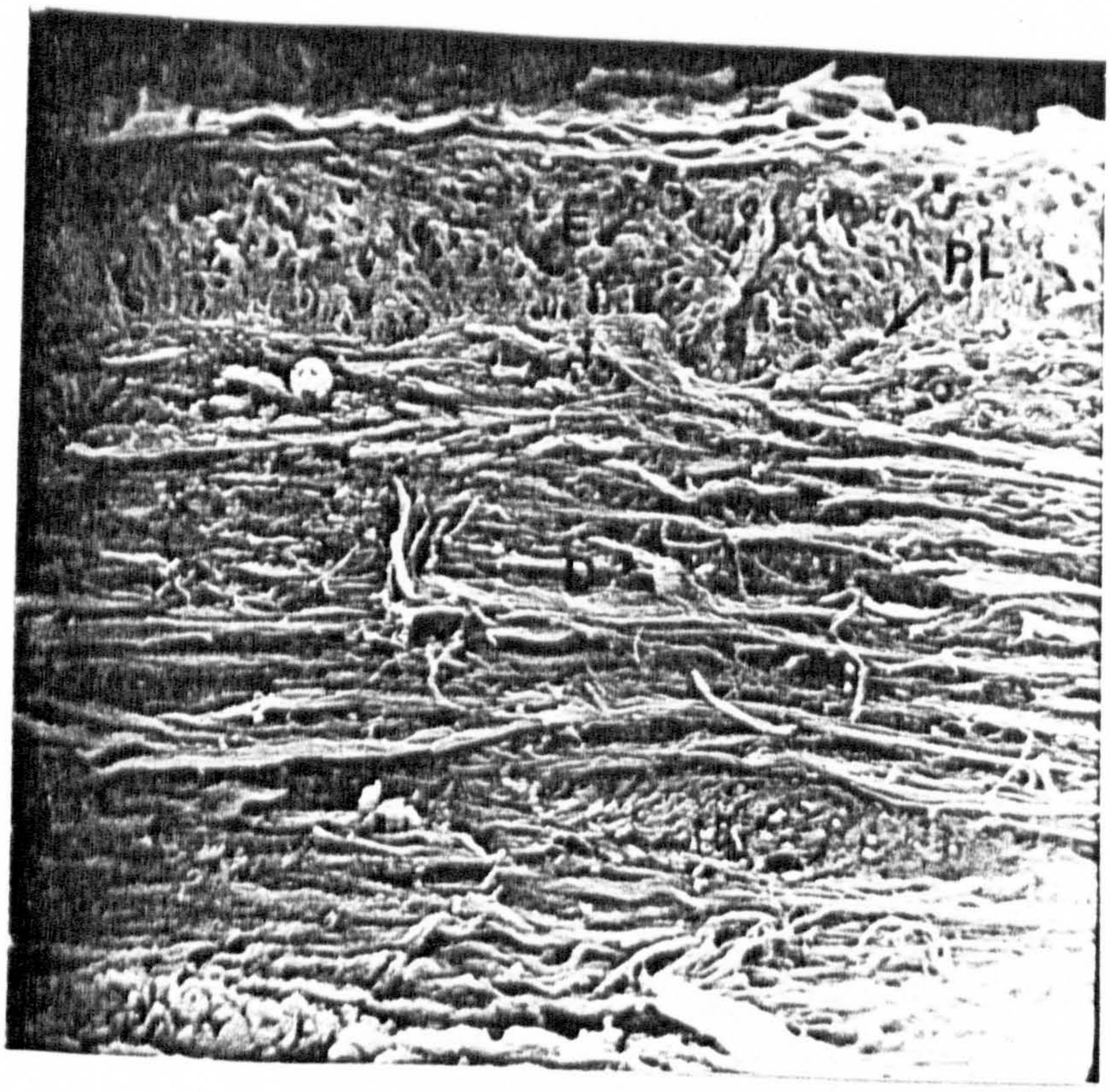

FIGURE 2.4. LIGHT MICROGRAPH OF A SECTION THROUGH AN ACTIVE HYPERTROPHIC SCAR SHOWING THE PLANAR PAPILLARY LAYER (PL) AT THE JUNCTION OF THE EPIDERMIS (E) AND THE DERMIS (D)

(After Tully, 1980)

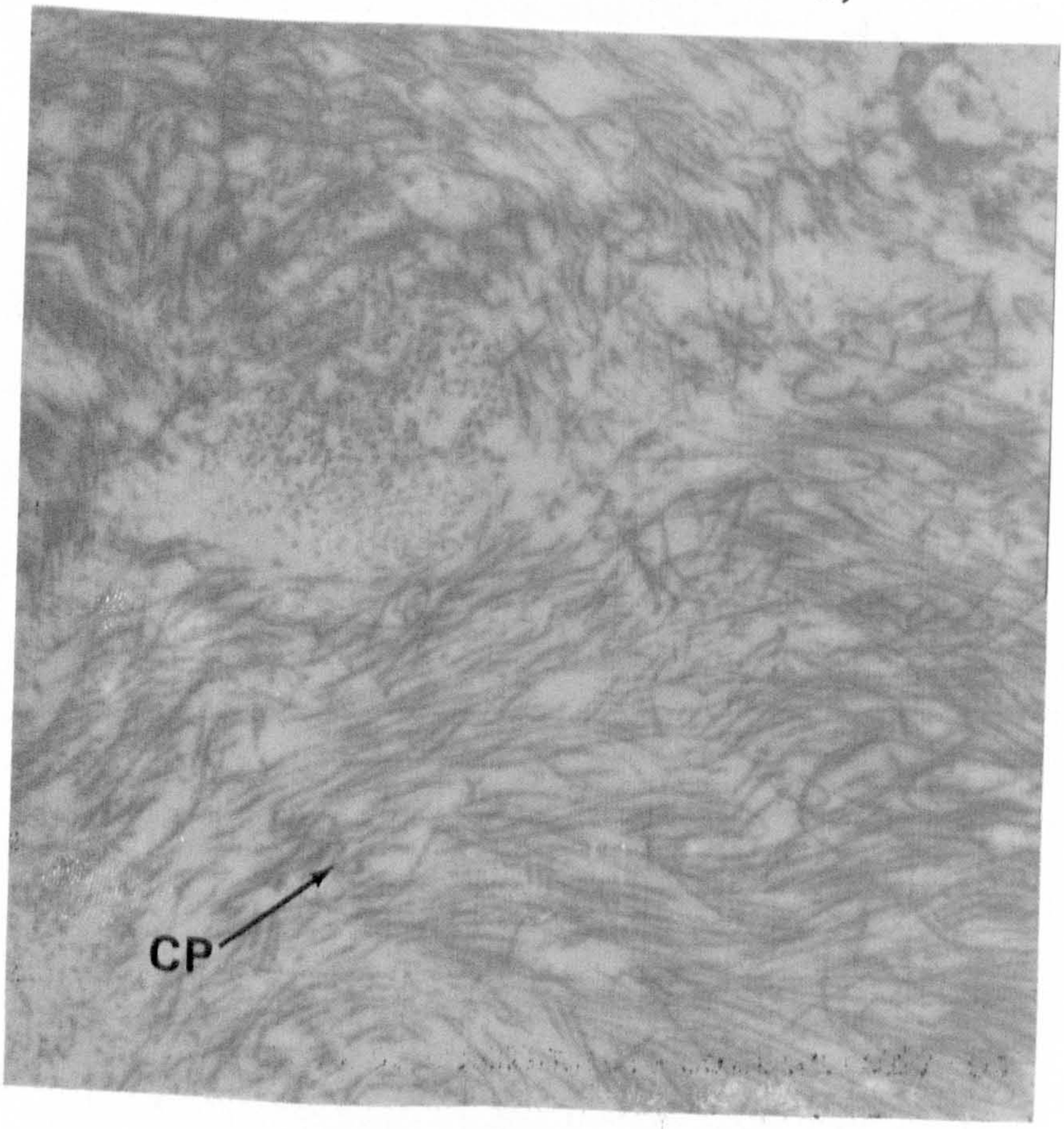

FIGURE 2.5. MICROGRAPHS OF COLLAGEN FILAMENTS (CP) AT GRANULATION STAGE SHOWING APPARENT LOOSE PACKING X 10,500

(After Linares et al, 1973)

and sweat glands, are not consistently observed in hypertrophic scar epidermis. Since deep partial thickness or full thickness injury to the skin destroys most epithelial producing elements, healing is accompanied by epithelial migration from the edges of the wound. Mancini et al (1961) observed that the basal membrane in hypertrophic scar tissue was thin at the initial healing stage, but by the forty-second may of healing its thickness had increased considerably. Tully (1980) has shown that, in active hypertrophic scars the epidermis is considerably thicker than in less active scars, and also reported morphological differences in the appearance of cells in certain layers. In particular, stratum granulosum cells of ovoid shape were observed near to the stratum lucidum which contrasts with observations in normal skin where cells tend to become flatter as they move upwards. As in normal skin desmosomes have been frequently observed at cell to cell junctions in the stratum spinosum (Baur et al, 1975). Brown (1971) found that in skin under tension, the cells of the stratum spinosum were flat. These results may indicate that within the hypertrophic scar skin tension is reduced.

The papillary layer observed between the epidermis and the dermis is usually absent in scar tissue, the boundary being usually planar which is illustrated as linear in cross-section (Figure 2.4). Mancini (1961) noted the absence of papillae and Tully (1980) demonstrated their absence over a wide range of scar specimens.

Tully (1980) found that in preparation of scar tissue specimens, the epithelium was very labile, and sequestration often occurred between the stratum spinosum and the stratum granulosum layers. The observation of both in-vivo and in-vitro lability of scar epidermis may be due, in fact, to the reduced surface contact area at the dermal-epidermal junction, producing inferior epidermal attachment therebetween. Differences in meta-

bolism between the scar and the normal epidermis are also evident, such as the rapid mitosis of cells in the stratum basale of scar.

2.3.2. Pre-Elevation Scar Tissue

Histologically it is difficult to delineate layers in pre-elevation scar tissue phase, the upper scar being very cellular and vascular which accounts for erythema of the scar (Linares et al, 1972). There appears to be no organised pattern to the vascular system as in the papillary layer of normal skin. At the granulation stage, collagen filaments are very loosely arranged and form an irregular pattern in the upper dermis, whereas in the reticular or deeper dermis they appear orientedinto a curvilinear pattern (Figure 2.5). The fibroblast population is more numerous than in normal skin (Baur et al, 1975) and includes a number of fibroblasts containing filaments with supposed contractile properties, termed "myofibroblasts" which have been implicated in the aetiology of hypertrophic scarring (Gabbiani et al, 1971, Majno et al, 1971, Larson et al, 1971, Baur et al, 1975). Perivascular lymphocytes and plasma cells have also been observed, although these are usually only evident in inflammatory reactions.

Few epithelial remnants remain- sweat ducts, sebaceous glands, hair follicles and arrector pilorum muscles are destroyed or displaced by the scar (Linares et al, 1972, Kischer et al, 1975a).

The reticular layer is less cellular and more fibrous with larger fibrils located in the deeper portion near the fat bed. Elastin is rarely observed in the hypertrophic scar at this phase, although it has been implicated in contributing to the inflammatory response (Linares and Larson, 1974).

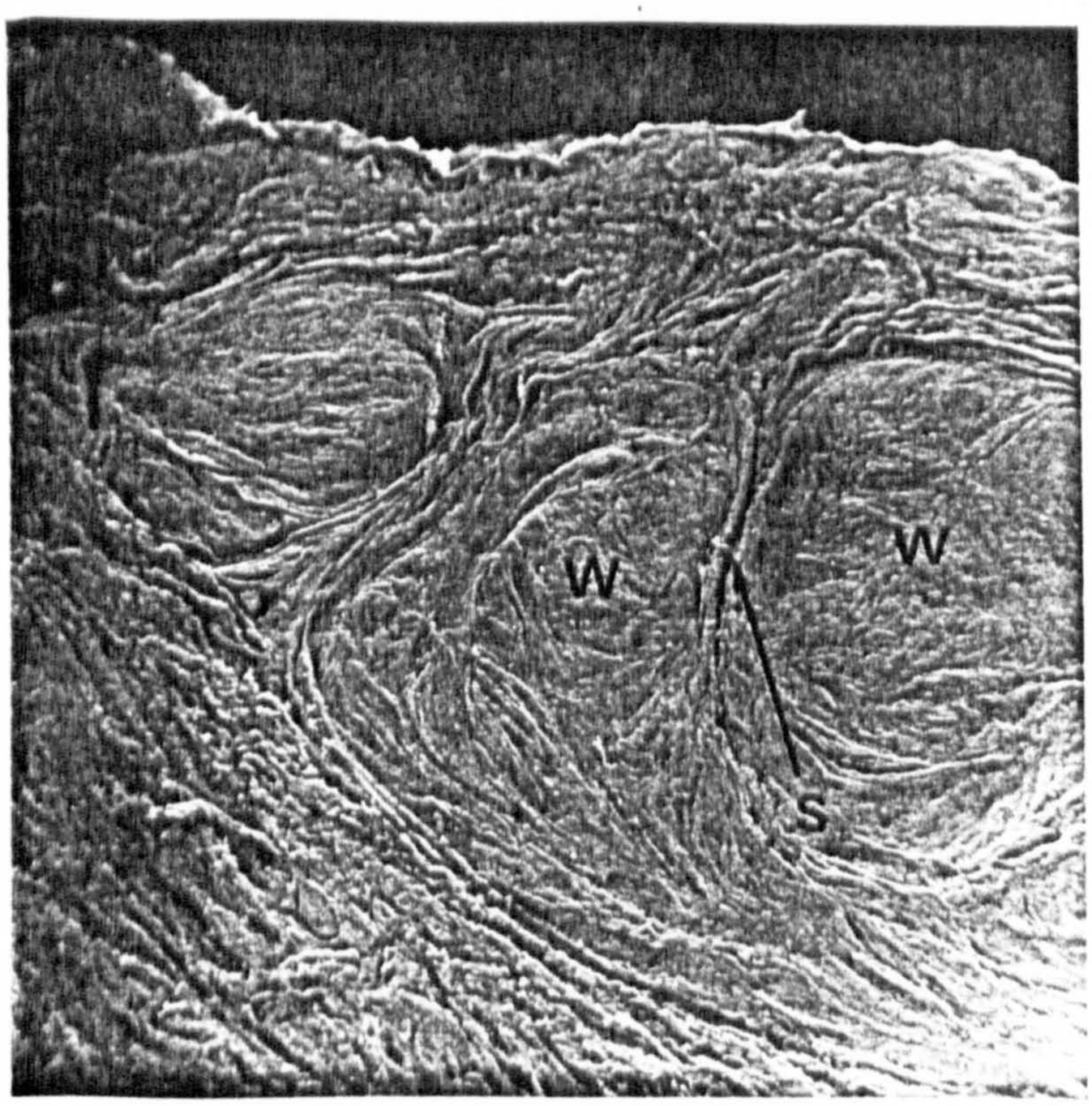

FIGURE 2.6. LIGHT MICROGRAPH OF A SECTION THROUGH AN ACTIVE HYPERTROPHIC SCAR SHOWING BUNDLES OF COLLAGEN FIBRES ARRANGED INTO "WHORLS" (W) SEPARATED BY SEPTA (S)

(After Tully, 1980)

2.3.3. Elevated or Active Hypertrophic Scar Tissue

Classical descriptions of hypertrophic scars almost always enter into this category; in this phase the scar is clinically described as erythemic, elevated, rigid and inextensible (Mowlem, 1951, Larson et al, 1971). The vascular system appears to have no organised pattern and vessels can be seen through the scar surface with the naked eye. Histologically, collagen fibres are densely packed into bundles which then appear to be arranged into "whorls" or "nodules" separated by septa-like structures (Figure 2.6). These nodules have been postulated as originating in granulation tissue prior to hypertrophy (Linares et al, 1973) and are particularly evident in the deep dermis (Larson et al, 1971, Kischer et al, 1975b, Tully et al, 1980). Although it has been suggested that these nodules are spherical and, that, in microscopic cross-sections they are generally observed as ovoid or circular, it has recently been thought that the three-dimensional shape may, in fact, be prismatic (Tully, 1980).

At the periphery of these nodules there appears a rich vascular supply whereas the interior is almost entirely a vascular. From microscopic analysis, it has been reported that many vessels in the hypertrophic scar are partially occluded (Kischer et al, 1975b). Sloan et al (1978) from intradermal measurements of oxygen and carbon dioxide tension, showed that pO_2 in hypertrophic scar tissue was significantly lower than that of normal skin, whereas pCO_2 was relatively unchanged. This result may be due to either high tissue metabolic activity or reduced diffusion of oxygen, however the CO_2 tension is consistent with the former hypothesis whereas the ultrastructure of the scar favours the latter hypothesis. From scanning electron microscopy (S.E.M.) the mean diameter of collagen fibrils has been estimated as 600Å which is significantly smaller than that of normal skin (Linares et al, 1972).

Collagen filaments are more numerous than in normal skin, occupying the interstices in the collagen framework (Kischer et al, 1975a), and are thought to mediate a rigid mechanical bond between collagen fibres. A layer of collagen fibres adjacent the fat layer which is morphologically similar to normal skin has been observed. (Linares et al, 1974, Tully, 1980). This latter observation may indicate that tension across the scar boundaries is very similar to that of normal skin.

Fine elastic fibres have been observed in the papillary layer and in the septa surrounding the nodular areas, however no elastic fibres have been observed within the nodules. (Linares et al, 1973, Tully, 1980).

In contrast to normal skin and pre-elevated scar tissue, mast cells have been frequently observed (Kischer and Bailey, 1972). They also estimated that there is a four-fold increase in the mast cell population in comparison to normal skin, and concluded that this contributes significantly to the persistance of the inflammatory response.

The amount of collagen in active scars has been reported to be increased with respect to other scar types and to normal skin, and it has been demonstrated that the concentration of collagen is also significantly increased (Bazin et al, 1975, Craig et al, 1975b).

Increased collagen biosynthesis in active hypertrophic scars has been widely reported, Cohen et al (1971) and Jeffrey and Eisen (1973) demonstrated a significant increase in collagen biosynthesis in active hypertrophic scars in comparison with that of normal skin, and with that of normal scars, using a prolyl-hydroxylase assay. Craig et al, (1975a) found an increase in collagen biosynthesis using both radiolabelled hydroxyproline and prolyl-hydroxylase assays.

Recently, Weber et al (1978) demonstrated, by electrophoretic distribution patterns of CNBr peptides that type III collagen is dramatically increased in hyper-

trophic scars whereas in normal or mature scars it is only slightly increased above normal skin levels. The distribution pattern for active scar collagen types was found to be very similar to that of fetal dermis, and Linares et al (1972) also reported that collagen in active scars was of the young or immature type.

In addition to the cellular, ultra-structural and vascular differences observed between hypertrophic scars and normal skin and normal and mature scar, there are also differences present between the acid mucopolysaccharide contents. Shetlar et al (1971) showed that acid mucopolysaccharides were increased in hypertrophic scars in comparison to normal scars and normal skin, and Shetlar et al (1972) demonstrated that this mucopolysaccharide increase was due in particular to the increased level of a Chondroitin-Dermatan Sulphate fraction.

Shetlar R. and Shetlar C. (1977) found, by using a histochemical assay followed by electrophoretic studies, that Chondroitin-4-Sulphate was much higher in the scar, and the Dermatan Sulphate (or Chonrdoitin-6-Sulphate) level was much more uniformly distributed through the scar.

2.3.4. Mature Scar Tissue

A mature scar is clinically, histologically and biochemically similar to a normal scar. Clinically the mature scar demonstrates an absence of erythema, however no quantitative or qualitative comparison of blood flow or blood content has yet been published. Sloan et al (1978) found that tissue PO_2 was greater in mature scars than in active scars. However, Sloan also demonstrated that the metabolic activity is lower in mature scars than active scars and concluded that this result was due to less oxygen consumption by the mature scars. Kischer (1975b) observed from scanning electron micrographs that the mean diameter of collagen fibrils were greater than in active scars, although it was still somewhat less than that of normal skin. Individual collagen fibrils were observed and the interfibrillar distance was increased,

but the morphology of normal skin fibrils was not observed. Tully (1980) found that by mechanical analysis on mature scar specimens in comparison with histological observation, that the fibre orientation was in the direction of the lines of maximum skin tension. Collagen synthesis in mature scar tissue was reported as being the same level as in normal scar, but less than in normal skin 2 - 3 years post-wounding (Craig et al, 1975b) although the tissue concentration of collagen had increased relative to normal scars.

Linares et al (1972) found that elastic tissue eventually recurs in mature scar tissue and Bhangoo (1974) found greater amounts of elastin in mature scars than in active scars but still less than in normal skin. Tully (1980) demonstrated by mechanical testing that mature scar tissue has a greater elasticity than that of active scar, and similar to that of normal scar which implies that the pressure induced remodelling process results in a scar being similar to a normal scar.

2.4. DISCUSSION AND CONCLUSIONS

The structural and functional differences between the various phases of hypertrophic scars and normal skin leads to several important aetiological and therapeutic implications. In particular, inspection and examination of these differences provides a picture of a dynamically varying tissue which slowly tends towards a known type of tissue; normal scar.

Studying the scar ultrastructure may also provide explanations for hitherto unexplained clinical phenomena; Hypertrophic scar epidermis is frequently removed by trauma such as abrasions which normal skin would easily tolerate. In scar tissue there are various observations which may account for this effect, for example, there is an absence of rête ridges, or dermal papillae, at the epidermal/dermal junction in hypertrophic scar tissue which means that for a given surface area there is a

reduced contact area at the junction which could result in inferior attachment and consequently susceptibility to small loads and strains. Tully (1980) noted the presence of ovoid cells in the upper stratum granulosum of scar in contrast to flat cells found in normal skin, and found that during preparation of scar tissue samples epidermal sequestration frequently occurred just superficial to this layer. Simple geometry implies that the contact area between ovoid cells is due to point contact and is much less than the contact area for an equivalent number of planar cells, and as such may augment the susceptibility of the scar epidermis to minimal trauma. A further observation is that the rête ridges in normal skin are extensible, and as such can deform to take up applied loads whereas scar tissue has a much lower "load take-up strain' consequently is more affected by small trauma.

The major differences between hypertrophic scar and normal skin occur in the dermis where the scar tissue is composed of bundles of fused collagen fibres frequently arranged into nodules. This collagen structure is responsible for most of the mechanical characteristics of the scar. The natural remodelling process results in a 'mature' scar which is almost indentical structurally and physiologically to a 'normal' scar.

Thus, although scar tissue exhibits a wide variety of structural and physiological changes from normal skin in almost every aspect, it would appear that for practical purposes a more sensible comparison should be made between hypertrophic scar and normal scar. Thus certain parameters common to both hypertrophic and normal scars could be selected and compared to those of the hypertrophic scar observed during the natural remodelling process. This would support objective evaluation and comparison of the efficiency of hypertrophic scar therapies, in contrast to the present subjective evaluations which may be responsible for much of the conflict and uncertainty which presently surrounds attempts to understand the remodelling process.

CHAPTER 3

THE RESPONSE OF NORMAL SKIN AND HYPERTROPHIC SCAR TISSUE TO MECHANICAL STIMULI

3.1. Introduction

3.2. The Effect of Mechanical Stimuli on Normal Skin

- 3.2.1. The Response of the Vascular System to Mechanical Stimuli
- 3.2.2. The Response of Normal Skin to Prolonged Pressure
- 3.2.3. The Response of Normal Skin to "Shear" Forces
- 3.2.4. The Reflow Ability of Normal Skin

3.3. The Effect of Mechanical Stimuli on Hypertrophic Scar Tissue

- 3.3.1. The Physical Effect
- 3.3.2. The Structural Response of Scar Tissue
- 3.3.3. The Biochemical Response of Scar Tissue

3.4. Discussion

3.1. INTRODUCTION

The interaction of mechanical stimuli and the body via the medium of skin is of such important clinical significance that numerous investigations have been performed in attempting to qualify and quantify the response phenomema. A succinct treatise on the "state of the art" has been published (B.S.B., Ed. Kenedi, 1976) and many reviews on the subject exist, of which Ferguson-Pell's (1977) is perhaps the most thorough. When considering the effects of mechanical stimuli on tissue, it is important to specify the nature of the stimuli as the tolerance and the response of the tissue can vary considerably. In the case of skin, stimuli such as loads, strains, forces inter alia can be classified into hydrostatic and non-hydrostatic components.

There are two generally accepted main forms of such stimuli; transient mechanical insults and prolonged mechanical insults, although the author considers only the latter to be within the scope of this thesis and, therefore, relevant.

In considering prolonged mechanical insults, two important limitations are evident which adversely affect the accuracy of experimental results:

Firstly, measurements of mechanical insults are usually made at the surface of the skin, which is the interface between the internal and the external environments. However, most stimuli induced phenomena occur <u>within</u> the skin and prediction of the stimuli parameters thereat are exceedingly difficult. Therefore, correlations between applied mechanical stimuli and most response phenomena and <u>approximate</u>;

Secondly, skin is a biological organ and as such, is continually adaptive maintaining a tissue homeostasis despite neurological, hormonal and metabolic changes which may occur in addition to those induced by mechanical stimuli.

The tolerance of skin is known to be very high to hydrostatic loading with a figure of ¼ million p.s.i. (1688 MPa) being required to disrupt the normal function of a cell as the pressure difference across the cell remains relatively unchanged. The tolerance to non-hydrostatic loading is decidedly lower, non-hydrostatic components, such as uniaxial and biaxial stresses and strains produce distention of the skin which results in an interruption of blood flow.

This effect is critical in determining the tolerance threshold and the response of the skin; since many important physiological processes cease when the circulation is arrested; thermoregulation ceases, innervation is lost and epithelial components such as sebum and sweat glands are disrupted. Mass transfer functions necessary for cellular activity are disrupted due to the arrest of blood flow.

In normal skin, three major aspects characterise the nature of the response; the tolerance of the vascular system to mechanical insults, the response of the constituents of skin to prolonged ischaemia and the ability of the tissue to support reflow consequent to prolonged ischaemia.

In the case of hypertrophic scar, it has been known for some years that the application of mechanical stimuli to the scar will result in a remodelling process, the result of which is fortuitously therapeutic. The use of mechanical stimuli to remodel hypertrophic scar tissue on a widespread scale is recent (Fujimori et al, 1968, Larson et al, 1971, Tolhurst, 1977), the applied mechanical stimuli used being pressure.

Changes between "before" and "after" the application of pressure have been reported for a variety of skin parameters such as clinical appearance (Larson et al, 1971) histological (Shetlar et al, 1972, 1977) and skin gas tensions (Sloan et al, 1978), inter alia.

The results of such studies were construed to provide hypotheses for a mechanism responsible for the remodelling process. However, a close inspection of the results leads back to a requirement for a clear and a more fuller understanding of the structure and physiology of the hypertrophic scar tissue. It is important to determine the effect of varying parameters such as the magnitude, duration and nature of the stimuli on the remodelling process and on the final clinical result.

Although such data are lacking in the case of hypertrophic scar tissue, normal skin has been investigated and much documentation exists in the aspects concerned. Extrapolation of normal skin results to scar tissue is disputable, and indeed wrong, for many parameters. However parameters such as pressure magnitude threshold tolerances and the duration of pressure are relevant and should, at least, be considered when investigating the response of scar tissue to mechanical stimuli. As for normal skin, there are three major factors to consider when assessing the effect of mechanical stimuli on hypertrophic scar tissue; the threshold magnitude required to initiate and maintain the remodelling process; the duration over which the threshold pressure is maintained; the response of the constituents of scar tissue to the stimuli and their effect on mediating the remodelling process.

3.2. THE EFFECT OF MECHANICAL STIMULI ON NORMAL SKIN

The response of each of the three major aspects which characterise in normal skin is examined under the following sub-sections.

3.2.1. The Response of the Vascular System to Mechanical Stimuli

In order for mechanical stimuli to occlude the flow of blood in a particular vessel, mechanical stimuli in the form of "normal" pressure, applied to the skin

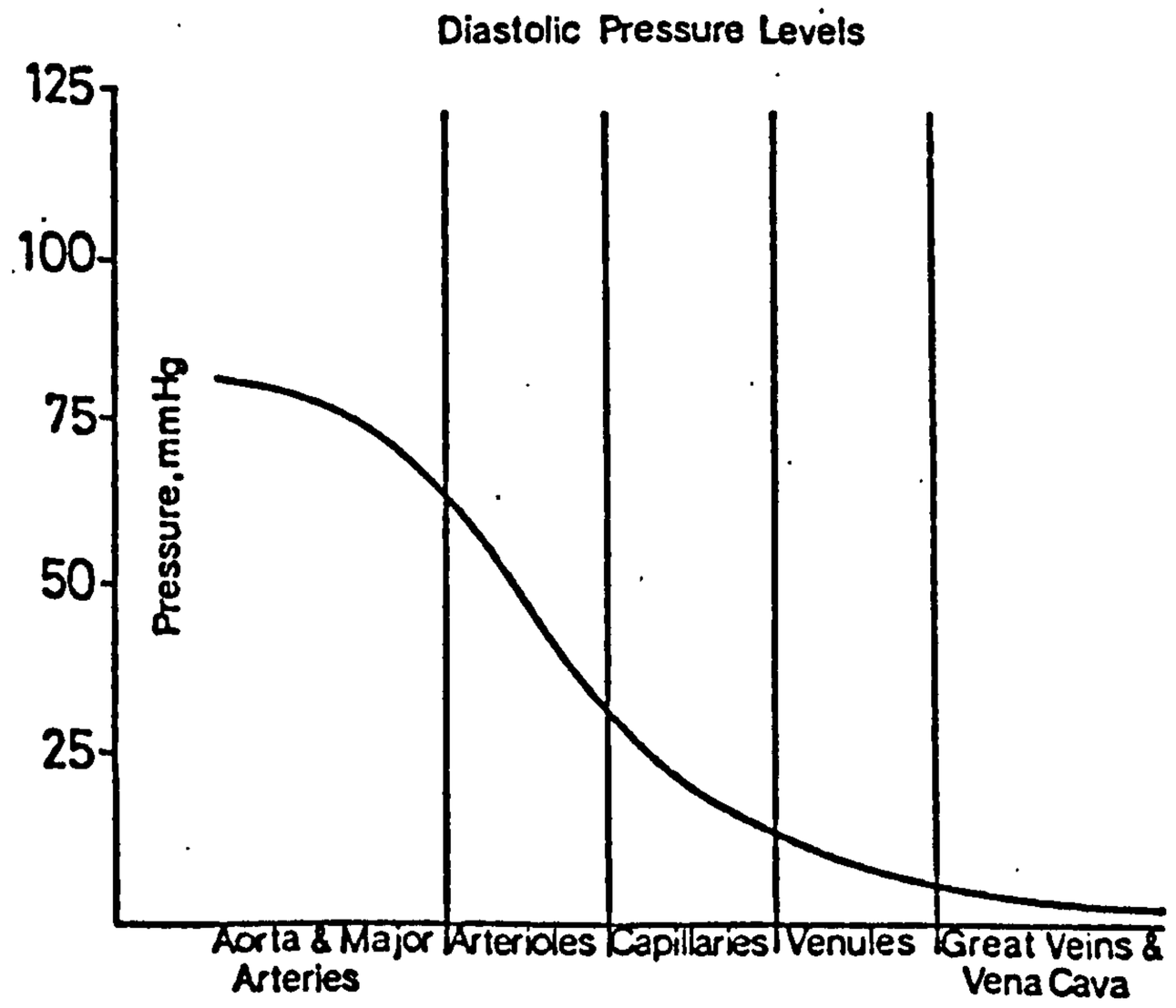

FIGURE 3.1. DIASTOLIC PRESSURE LEVELS IN BLOOD VESSELS OF DIFFERENT SIZES

(After Sewell, 1974)

must be equal to or greater than, the hydrostatic pressure within the vessel plus the pressure drop across the skin.

Venous occlusion plethysmography and occlusive cannulation are the two main techniques used to determine intravascular hydrostatic pressure. The latter technique involves the use of small bore pipettes attached to manometers and is particularly well suited for use in small vessels such as capillaries and venules (Krogh et al, 1929). Landis (1930) using the cannulation technique, demonstrated that the average pressure in a capillary loop was about 32mmHg, varying from about 48mmHg at the proximal end to about 12mmHg at the venule end. It was also reported that the average capillary pressure could be altered by various stimuli, such as temperature, injury and histamine, and related compounds by as much as 100% in some cases.

Many studies have verified the results of Landis and a presently accepted normal range for mean capillary pressure (m.c.p.) is 22 - 35mmHg. It seems unlikely therefore that pressures within this range, when applied to skin, will significantly affect capillary flow, however, they may well impair the flow in venules which have a much lower Hydrostatic pressure than that of capillaries (Figure 3.1).

Few investigations of the effect of external forces, pressure, etc. on skin blood flow have been documented. However, pressures lower than the mean capillary pressure have been reported as affecting tissue viability in supine subjects (Campion et al, 1968). Sabri (1971) investigated the effect of inflating a plastic splint to pressures between 5 - 150mmHg on the legs of patients undergoing surgery for varicose veins and found that a pressure of 15mmHg applied below the knee significantly decreased the blood flow in the femoral vein ofpatients by about 15%, and increased the peripheral resistance.

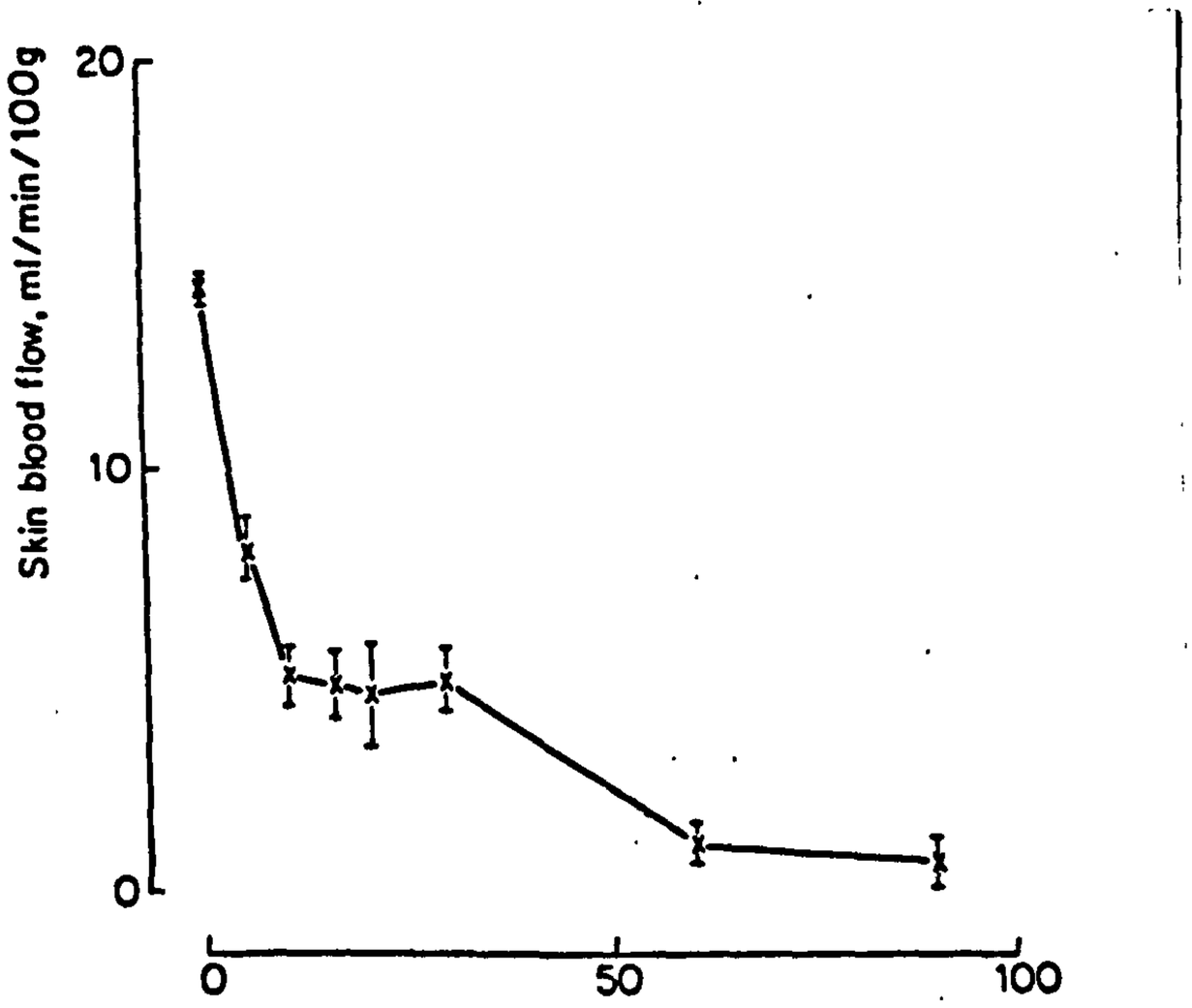

FIGURE 3.2. SKIN BLOOD FLOW (IN ml/MIN PER 100g. OF TISSUE) VERSUS APPLIED PRESSURE

In contrast, Sigel (1975), on a study of the effect of elastic compression stockings on lower limb blood flow found that if an external pressure gradient of 18 to 8mmHg was applied distally to proximally on the limb, an increase in the femoral vein blood flow velocity of 138% was increased. Pressures between 20 - 30mmHg were found to reduce the blood flow slightly and above 30mmHg a significant reduction in blood flow was reported. However, Gardner (1966), using an inflatible "G-splint" to compress tissue with angiography to measure the vascular response, reported that, compression of a traumatised limb between 20 - 30mmHg does not significantly reduce blood flow in the limb. Unfortunately, these results represent the blood flow in subcutaneous tissue and skin and it is virtually impossible to decouple only the response of skin therefrom.

Hickman et al, (1965) used a radiosodium (Na^{24}) tracer technique to investigate skin blood flow and found that the application of 25mmHg by a pneumatic piston reduced the normal skin blood flow in the human forearm by only 10%.

Daly et al, (1976) investigated the effect of pressure on skin blood flow using a radioactive tracer technique with Xenon (Xe^{133}). The rate of clearance of the Xe^{133}, in response to pressure applied to a small area of skin by a metal ring, was estimated using on-line computer analysis which provided highly accurate results. The results are shown in Figure 3.2. There is a considerable reduction in blood flow (about 50%) for a small increase in pressure, up to about 15mmHg. A quasi-steady state exists thereafter up to about 30mmHg. Increasing pressure produces a further decrease until at between 60 - 90mmHg the flow rate is around 10% of the original value. The quasi-steady state phase is thought to be due to the action of an autoregulatory mechanism, probably neurologically mediated,which provides a minimum blood flow rate in order

to maintain the basic metabolic requirements of skin.

3.2.2. The Response of Normal Skin to Prolonged Pressure

The application of prolonged pressure of a magnitude sufficient to overcome the hydrostatic pressure and the intrinsic compensatory mechanism of the vessels in the skin will ultimately induce cell death and necrosis (Kosiak, 1959, Landau, 1961, Fernie, 1973, Ferguson-Pell, 1977).

During ischaemia, the skin metabolism becomes anaerobic as oxygen is consumed. This process can be monitored biochemically by pH and tissue lactate measurements, (Karpf et al, 1974). Once the cells change to anaerobic metabolism the cell membrane disintegrates and lysosomal enzymes are released which autolyse the skin causing necrosis.

The aforedescribed process has been defined as pressure induced ischaemia in which ischaemia is taken to mean complete circulatory arrest, (Romanus, 1977).

Between the initiation of ischaemia and necrosis, the temporal response of skin is complex and is responsible for a variety of clinical phenomena such as oedema. Fibroblast activity is also reported as being receptive to mechanical stimuli mediating the response of the skin to ischaemia (Guttman, 1976).

Ethical considerations have restricted destructive investigations of pressure induced ischaemia to animals. Results of animal investigations are difficult to extrapolate to humans due to differences between the structure and composition of the tissues, however, some studies have also been performed on human volunteers (Brånemark, 1971). Husain (1953) on a series of experiments in which rat legs were occluded for varying times at similar pressures concluded from the results that once

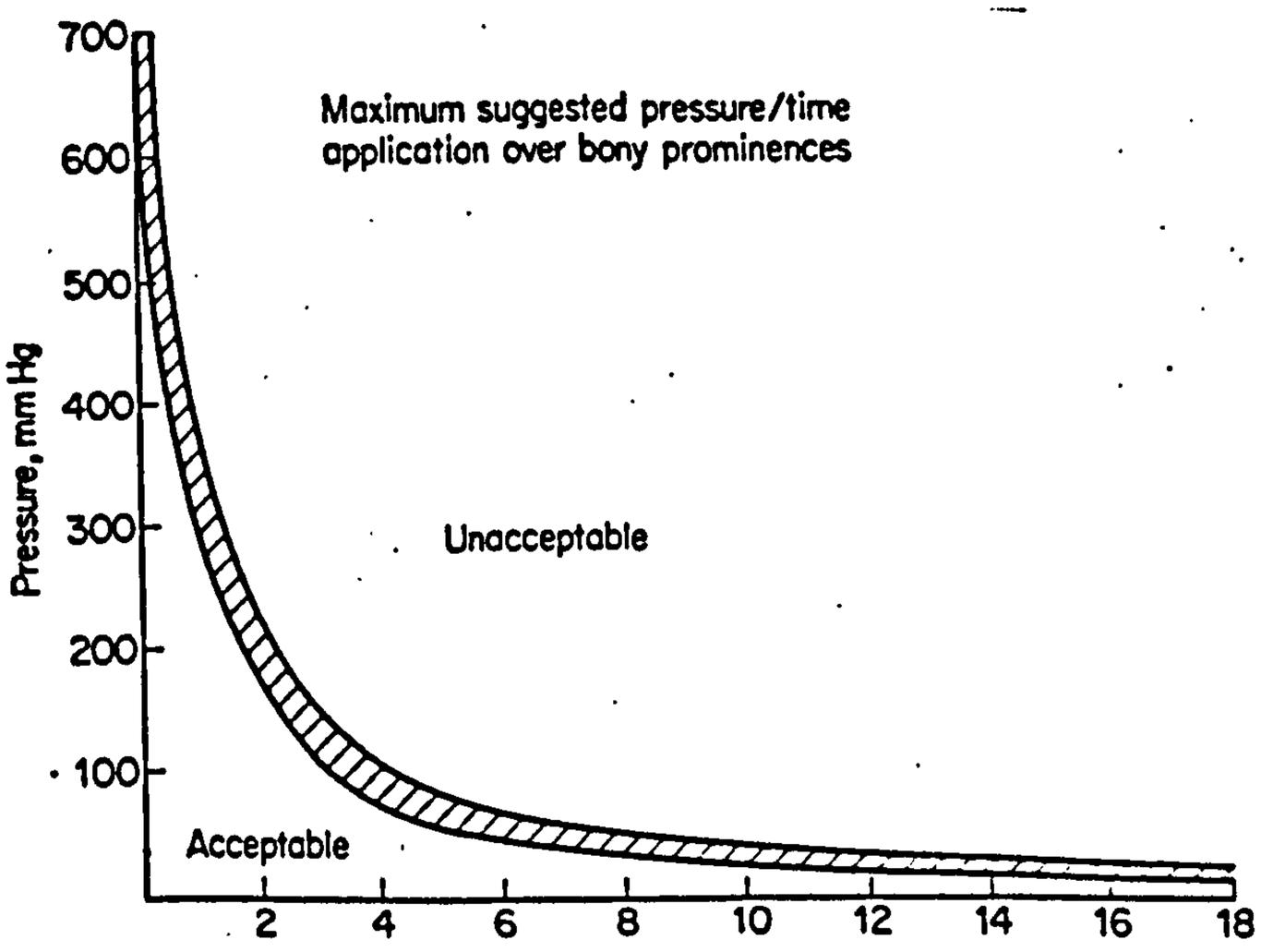

FIGURE 3.3. ALLOWABLE PRESSURE VERSUS TIME OF APPLICATION FOR TISSUE UNDER BONY PROMINENCES.

(After Reswick and Rodgers, 1976)

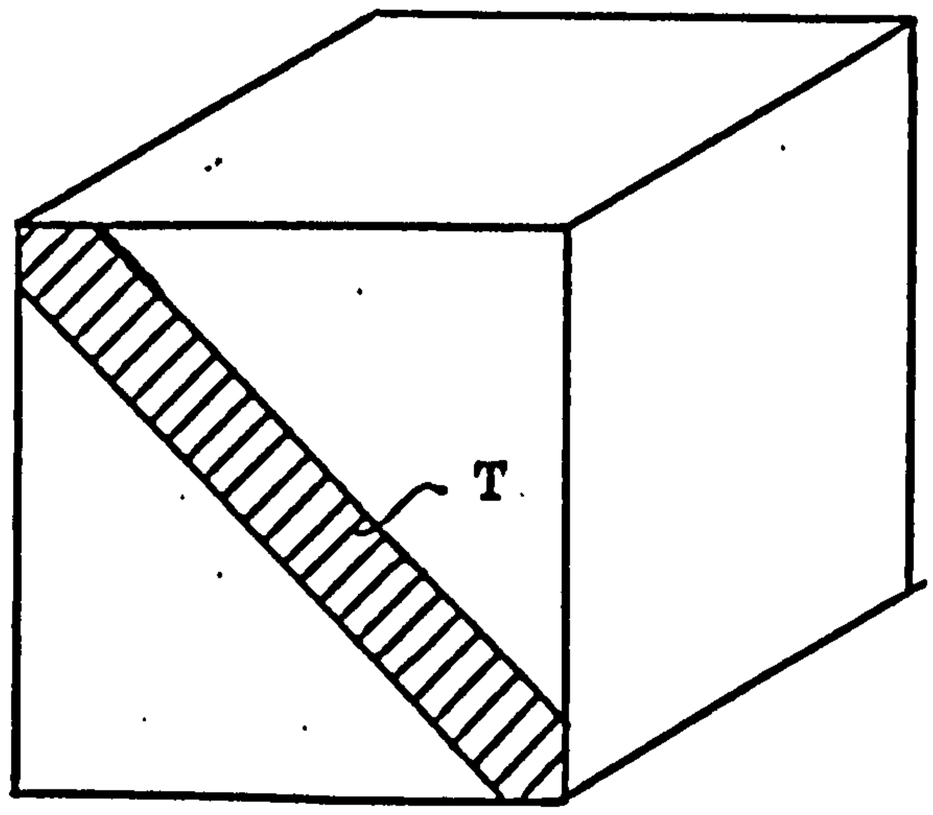

a) Unloaded: No Distortion

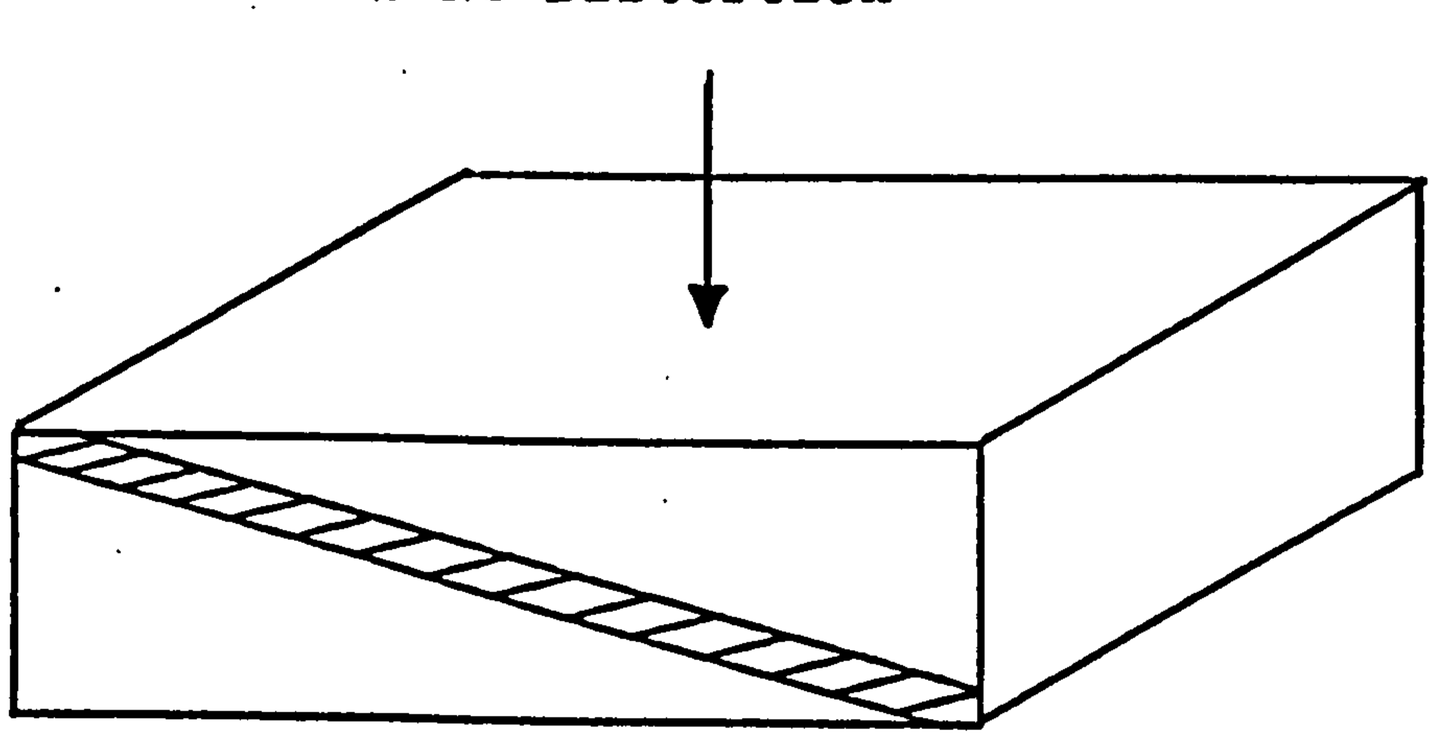

b) Loaded in Uniaxial Compression: Distortion

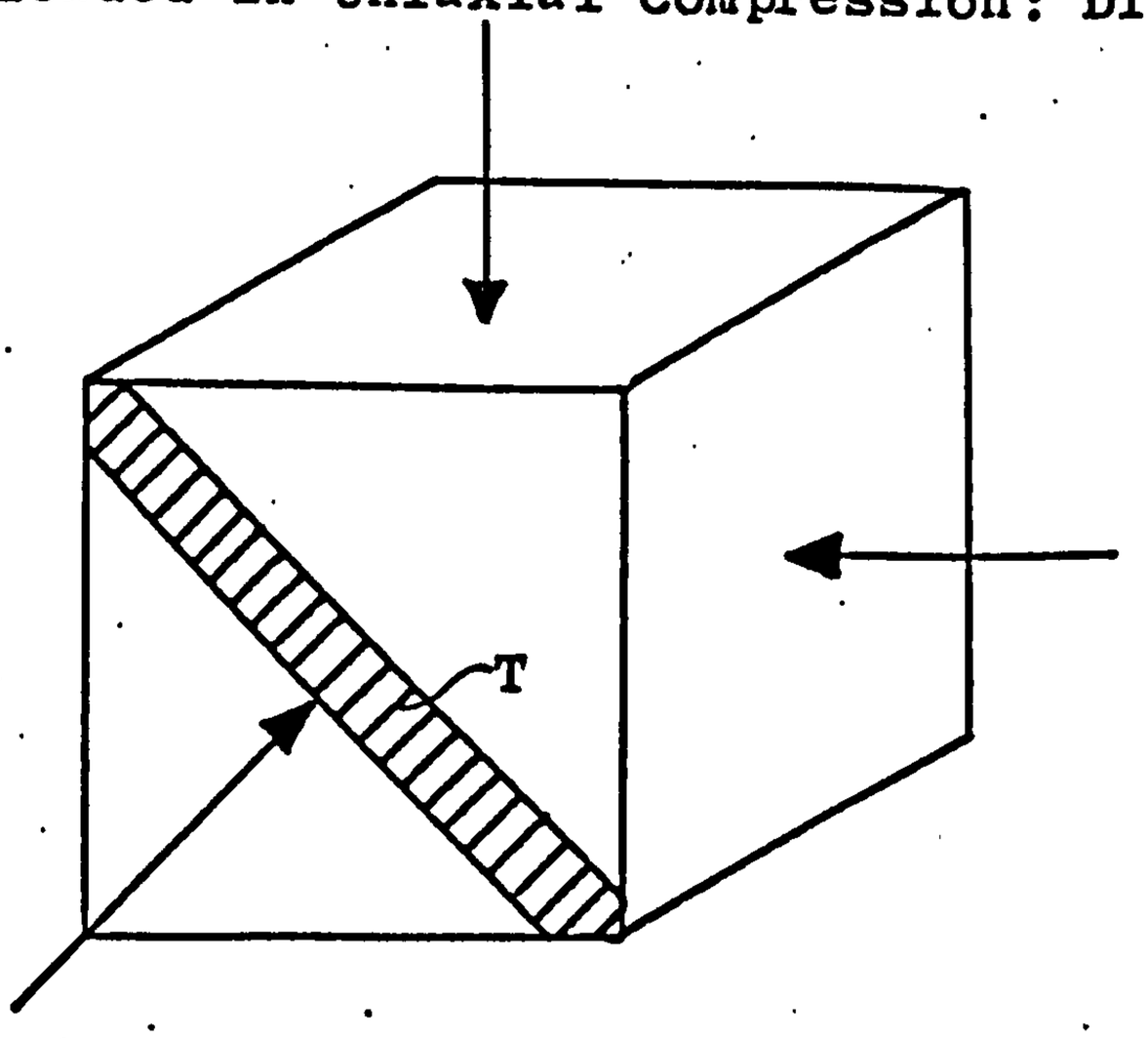

c) Loaded in Hydrostatic Compression: No Distortion.

FIGURE 3.4. SCHEMATIC MODEL OF SMALL CUBICAL ELEMENT OF FLESH WITH CAPILLARY ACROSS ONE DIAGONAL. TRANSVERSE LINES (T) ACROSS CAPILLARY INDICATE NO DISTORTION WHEN UNLOADED OR WHEN LOADED HYDROSTATICALLY (a and c). DISTORTION IS SHOWN WHEN LOADED UNIAXIALLY (b)

a threshold pressure was applied time was the major factor determining tissue viability. Kosiak (1959) demonstrated a clear inverse relationship between pressure magnitude and the duration of ischaemia required to induce breakdown from a series of experiments in which varying pressures were applied to the trochanteric region of dogs. This relationship was confirmed with humans by Reswick and Rodgers (1976) on a study of recumbent patients (Figure 3.3). Sachs (1976) stated that a minimum continuous pressure of 70 - 80mmHg is required to induce tissue breakdown. However this minimum level may be optimistically high, since recent experimental clinical evidence shows that the maximum value of continuously tolerable pressure may, in fact be as low as 50mmHg (Barbenel, 1978).

The aforedescribed skin responses to prolonged pressure are generally understood to be a consequence of "normal pressure" in which the pressure is applied approximately perpendicular to the skin surface, although other stimuli have also been reported as greatly influencing the skin response, in particular, shear forces.

3.2.3. The Response of Normal Skin to "Shear" Forces

It has been reported that "shear" forces, stresses, strains, etc., produce significantly more skin damage than equivalent magnitudes of normal pressures, acting mainly via vascular occlusion (Reichel, 1958). Dinsdale (1974) reported increased tissue susceptibility to frictional stresses during repeated pressure applications of 45mmHg in paraplegic swine. Chow et al (1976) stated that distortions of capillaries in skin are produced in response to shear strains (Figure 3.4), which can reduce, and even prevent, blood flow in the capillaries. Rydevik and Lundborg (1977) found that when a section of rabbit tibial nerve was compressed at 400mmHg for 4 hours, damage was most severe at the boundaries of the pressure area where the pressure gradient and shear forces were highest.

Quantitative investigations of response of skin to shear forces are lacking since at present there is no satisfactory physiological shear force transducer.

available. Lewis and Nourse (1978) produced a shear transducer which operated on a pneumatic principle, however no clinical data has been reported hitherto. It has been thought that the value of shear-related stimuli required to induce skin damage may be as much as an order of magnitude less than the equivalent critical normal pressure values.

At the cellular level, two immediate consequences of ischaemia are oedema and endothelial damage. Diana and Laughlin (1974) showed oedema to be a function of pressure duration. The cellular porosity was increased dramatically from 34Å to 54Å when the ischaemic period was extended from 1 to 3 hours. Oedema of the perivascular cells lining the capillary wall has been shown to increase the vascular resistance and completely occlude vessels (Strock & Majno, 1969, Leaf, 1973). The diffusion distance for oxygen, nutrients and metabolites is increased by oedema and may therefore contribute to the susceptibility of skin to pressure.

3.2.4. The Reflow Ability of Normal Skin

The duration of pressure induced ischaemia required to produce irreversible tissue damage is short. Brånemark, (1971) using intravital microscopy on a human pedicle flap raised on the volar arm surface which could be occluded by pneumatically controlled cuffs, demonstrated that irreversible changes in the microvascular system occurred after 7 hours' ischaemia. Romanus (1977) found that 60mmHg applied to a hamster cheek pouch for 4 hours produced changes which were not reversible within 120mins. post-pressure. However Larsson (1977) showed that metabolic alterations after 1 - 3 hours' ischaemia were normalised within 30 - 40mins. reflow. Pressure and ischaemia have been reported as producing more damage than either pressure or ischaemia per se, (Lauritzen, Personal Communication, 1978). Sufficient pressure was applied to compress the medial portion of a rabbit skin flap to produce ischaemia in the

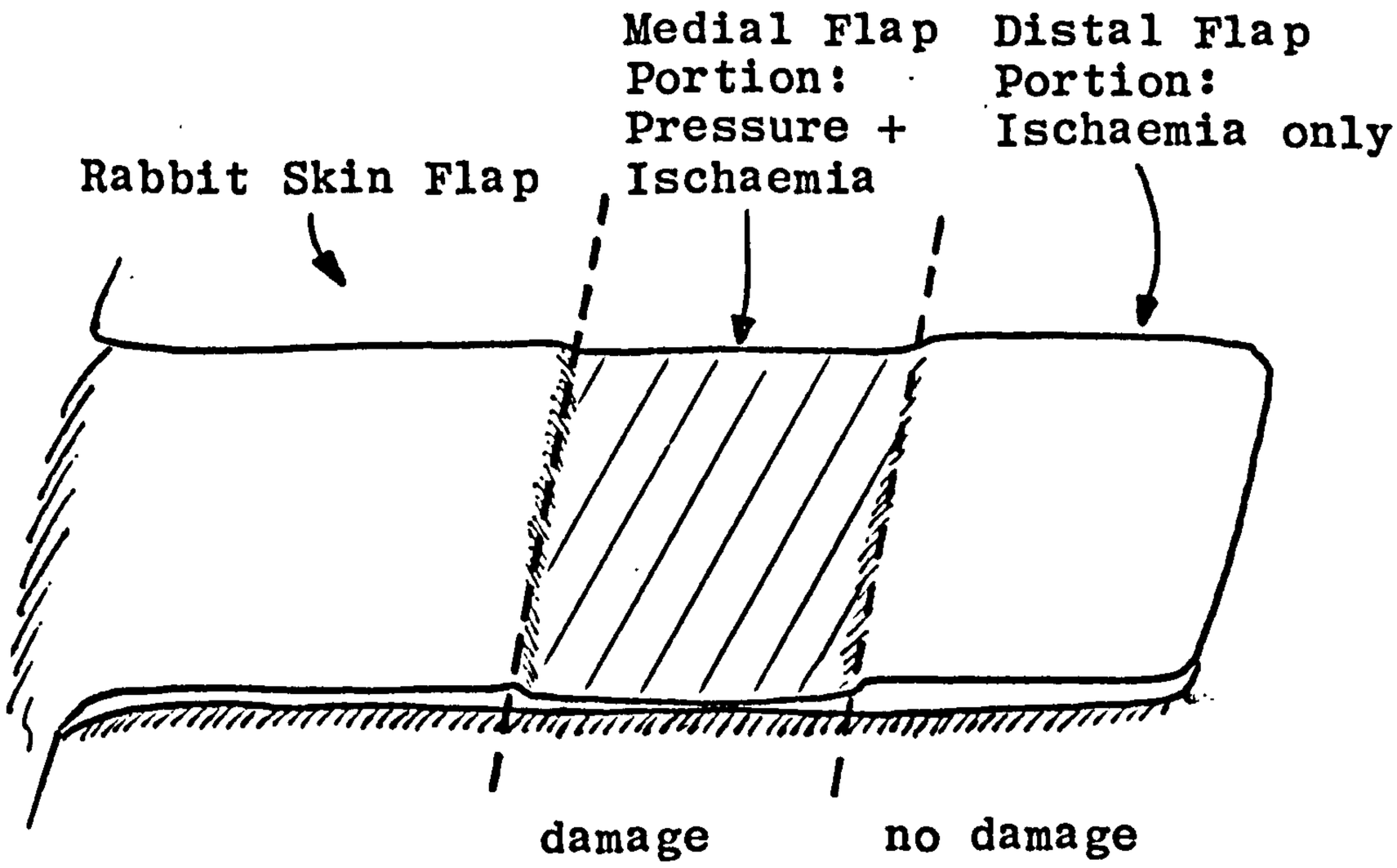

FIGURE 3.5. SCHEMATIC EFFECT OF PRESSURE AND ISCHAEMIA ON PORTIONS OF A RABBIT SKIN FLAP.

distal portion which was not compressed (Figure 3.5.). For equivalent pressures and durations of ischaemia, greatest permanent pressure induced change was always observed in the compressed and ischaemic region.

Factors other than mechanical stimuli have been reported as influencing skin breakdown, Husain, (1953) suggested that vitamin C deficiency reduces the skin tolerance to prolonged ischaemia, and it is commonly known that vitamin C deficiency is associated with scurvy, a disease which is characterised by an abnormality in collagen cross-linking (Peacock and Van Winkle, 1971). Protein deficiency has been reported as reducing the skin tolerance to ischaemia (Rudd, 1962) and endocrine substances injected systemically (Selye 1967) implied a reduced incidence of irreversible tissue damage for severely stressed cases. Innervation is considered an important factor in determining the response of skin to prolonged pressure and although the healing rates of normal and denervated skin in rabbits are similar (Muren and Zederfeldt, 1966, Guttman, 1976) it has been shown that, in a study of healing spinal laminectomies, the rate and the quality of healing is a function of innervation (Whimster,1976).

There appears to be no specific value of either pressure magnitude or duration associated with the response of normal skin since most experiments have beem performed over widely varying environmental conditions which greatly vary both the local and systemic vascular systems. However, critical pressures of 60 - 70mmHg and durations of 6 - 8 hours are generally recognised as being limitations beyond which there is a high probability of tissue breakdown. Once a critical threshold has been overcome, time appears to be the crucial factor.

3.3. THE EFFECT OF MECHANICAL STIMULI ON HYPERTROPHIC SCAR TISSUE

The response of hypertrophic scar tissue to externally applied mechanical stimuli may be considered under the following sub-sections.

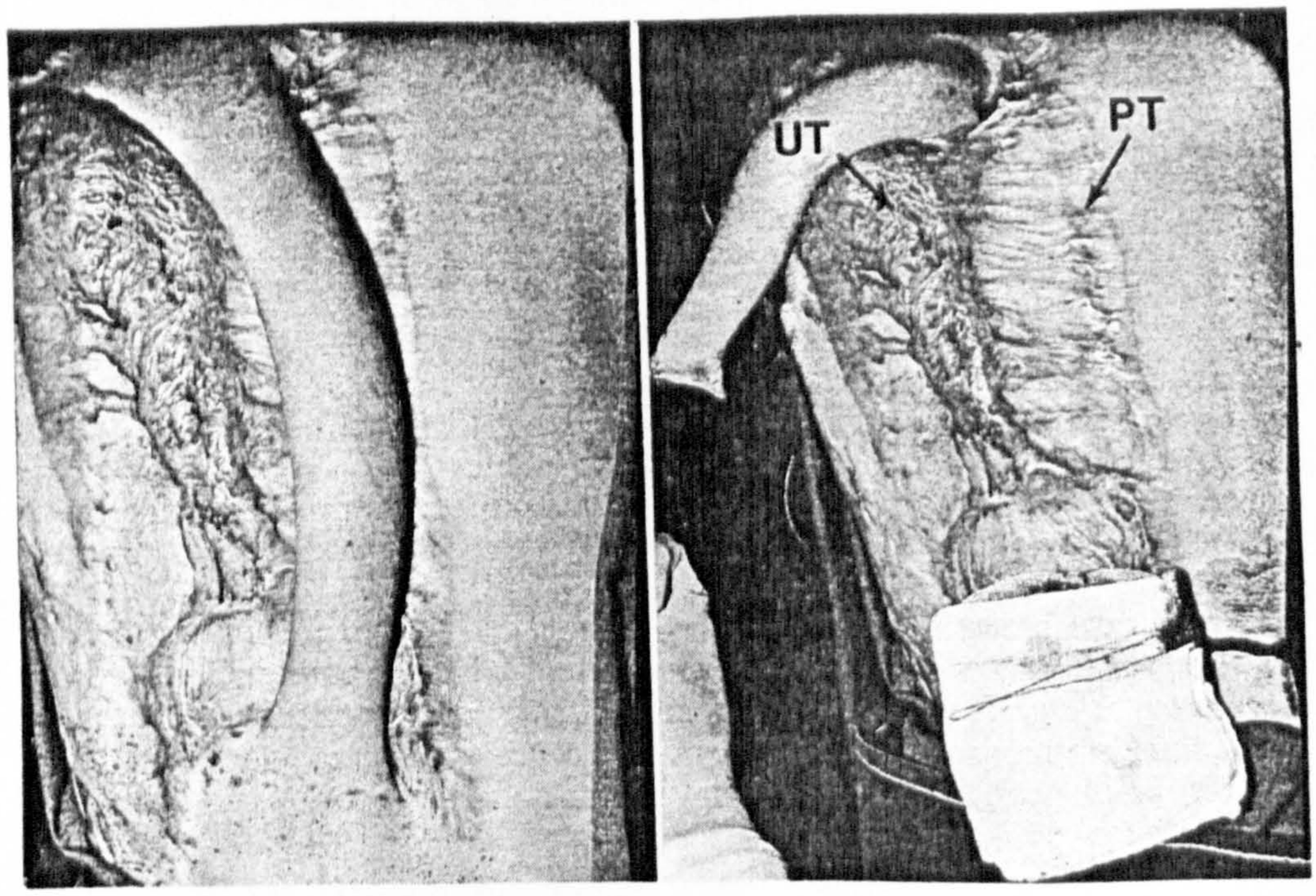

FIGURE 3.6 EFFECT OF CONTINUOUS PRESSURE FOR 5 MONTHS ON A SKIN GRAFTED DONOR SITE SHOWING REMODELLING AT PRESSURE TREATED SITE(PT) IN CONTRAST TO THE UNTREATED SITE (UT) WHICH IS HYPERTROPHIC.
(After Tolhurst, 1977)

3.3.1. The Physical Effect

It has been known for many years that hypertrophic scar tissue can be remodelled by the application of mechanical stimuli commonly applied in the form of pressure. Fujimori et al (1968) found that the application of pressure to hypertrophic scar tissue by a sponge fixation method resulted in considerable cosmetic and functional improvement; no values of pressure were given but the pressure was maintained until the scar appeared less erythemic. Larson et al, (1971), found that traction induced strain applied to joint contractures by isoprene splints halted and reversed the contraction process. Larson also found that hypertrophic scar areas which had been pressured by these splints were remodelled i.e.,flat and pale in contrast to adjacent unpressured areas which remained hypertrophic. A minimum period of six months continuous pressure was then thought necessary to produce permanent remodelling of the scar. Larson et al (1974) stated that the period of constant pressure should be at least 9 months. A clear demonstration of the efficiency of continuous pressure was reported by Tolhurst (1977). A tube pedicle donor site had one half subjected to continuous pressure for 5 months by a combination of mesh, immobilised pedicle flap and a elasticated vest, whereas the other half of the donor site was relatively uncompressed. After transfer of thepedicle the pressurised area was effectively remodelled in contrast to the untreated area which exhibited gross hypertrophy (Figure 3.6). Five months after removal of pressure this compressed area remained remodelled.

In clinical terms,mechanical stimuli in the form of pressure, when applied to active hypertrophic scar tissue induces a remodelling process which produces an end result similar to that which occurs as a consequence of the natural remodelling process, although greatly accelerated. Pressure applied to injured sites predisposed to hypertrophy

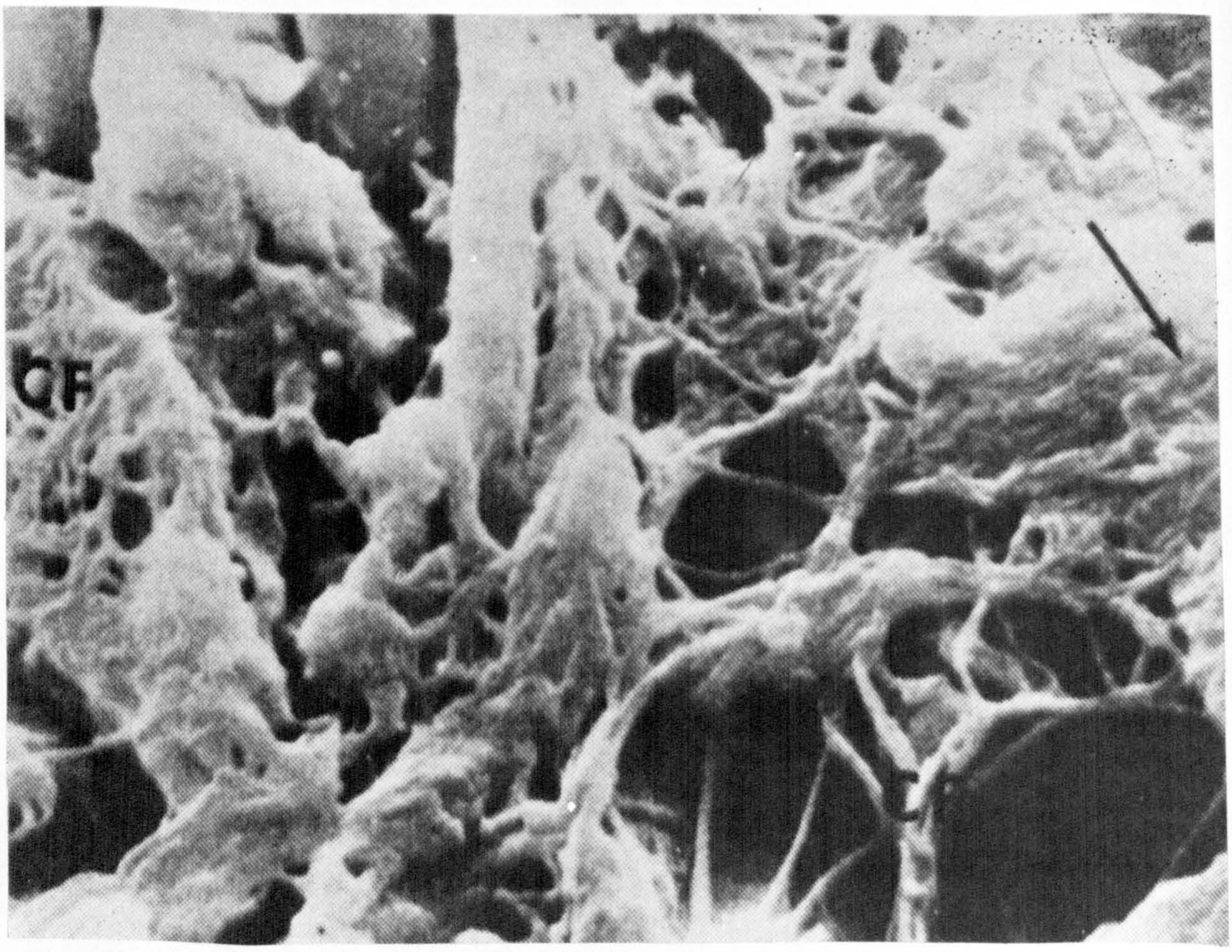

FIGURE 3.7 PHOTOGRAPH OF $1\frac{1}{2}$ YEAR OLD HYPERTROPHIC SCAR WHICH HAD BEEN PRESSURE-TREATED FOR 1 YEAR SHOWING INTERSTITITAL SPACED (IS) BETWEEN COLLAGEN FIBRES (CF)

(After Baur et al, 1976)

and to grafted donor sites, has also been reported as preventing the formation of hypertrophic scars in contrast to uncompressed sites (Cronin, 1961, Larson et al, 1971).

Structural, physiological and biochemical changes also occur in response to mechanical stimuli and characterisation of these changes may not only aid the understanding of the remodelling process but also identify and provide optimum remodelling results.

3.3.2. The Structural Response of Scar Tissue

Although the clinical effect of pressure induced remodelling has been known for some time only recently have comparisons between pressure treated and untreated hypertrophic scars been initiated (Larson et al, 1971). Larson found that pressure treated scar tissue demonstrated a clear absence of nodules in contrast to untreated scar tissue, which exhibited typical nodular formation.

In untreated hypertrophic scars, large nodules are frequently observed in sections of scar tissue, particularly in the deeper dermis and, in several cases they are large enough to be seen with the naked eye. Several distinct morphological differences between pressure-treated and untreated scars have been reported (Kischer et al, 1975b, Baur et al, 1976). The morphology of the fibres in scars which had been pressure treated continuously for one year resembled the morphology of fibres in naturally remodelled scar tissue (Baur et al, 1976). Nodules were not observed in the pressure treated scars. Large interstitial spaces between the fibres were observed (Figure 3.7) which are thought to be due to the loss of mucopolysaccharide ground substances (Kischer et al, 1975b, Baur et al, 1976).

The type and population of cells present in active hypertrophic scars were also reported as being affected by continuous pressure. A slight reduction in fibroblasts, mast cells and plasma cells were observed in SEM's and cellular components, such as endoplastic reticulum, golgi

bodies and mitochondria, exhibited similar temporal changes.

3.3.3. The Biochemical Response of Scar Tissue

As a corollary to structural investigations, assays of certain biochemical constituents in scars have been performed; Kischer et al (1975b) found that scars treated with continuous pressure had much lower levels of Chondroitin-4-Sulphate than untreated scars, which were similar to mature scar and normal scar levels; pressure increased the level of hyaluronic acid whereas the level of dermatan sulphate (Chondroitin Sulphate B or Chondroitin-6-Sulphate) remained substantially unchanged from the levels reported for normal skin and mature scar (Shetlar et al, 1972).

In pressure treated scars an absence of granulating mast cells have been reported, which have been thought to be indirectly responsible for stimulating collagen production (Kischer et al, 1972).

Such studies performed to date have been qualitative only and further investigations of the relationship between for example, the level of Chondroitin-4-Sulphate and the magnitude and duration of applied pressures appear necessary if critical values of pressure parameters are to be obtained, and used clinically.

3.4. DISCUSSION

Although the nature of mechanical stimuli applied to skin requires clarification with regard to the terminology used, results from numerous investigations imply that there appears to be no specific value either of pressure magnitude or duration associated with the response of normal skin since most experiments have been performed over widely varying experimental conditions which affect both the local and systemic vascular response.

However, critical normal pressures of 60-70mmHg for a

duration of at least 6 - 8 hours are generally accepted as being limitations beyond which there is a high probability of producing a tissue breakdown response.

In contrast, characterisation of the hypertrophic scar remodelling process by physical parameters is based on much less experimental evidence; a minimum duration of 9 - 12 months continuous pressure of a magnitude greater than mean capillary pressure i.e. 22mmHg - 30mmHg is proposed (Larson et al, 1974), based almost entirely on clinical evidence.

Kischer et al, (1975b) suggested that a value of 22mmHg pressure increases the already present tissue hypoxia to a level at which a percentage of the fibroblast population undergoes anaerobic metabolism and states that this favours collagen degradation and scar remodelling. Ultra-structural analysis of pressure treated scars have, however, produced no results or observations, such as cellular remnants, to substantiate this theory, although substantial reductions in the population of cells were reported after a period of at least six months (Baur et al, 1976, Kischer et al, 1975b).

Pressure induced scar remodelling has also been thought to be due to a mechanism controlled by changes in the collagen biochemistry. Ritzmann et al (1973) found that serum proteins, in particular the α-globulins, were elevated above normal levels in burn patients up to 8 weeks after injury. This coincides with the period in which hypertrophic scar formation has been reported as first occurring (vide 1.1). Serum α-globulins have been found to suppress collagenase in-vivo (Eisen et al, 1971). Thus high serum α-globulins present in the tissue during the wound healing process may inhibit collagen degradation leading to a net increase in the amount of collagen synthesised, which may be in part responsible for the formation of hypertrophic scar tissue.

Conversely, it has been suggested that if pressure

reduces the blood flow, and hence serum proteins, to scars then the collagenase may not be inhibited and will then initiate or accelerate the natural remodelling process (Baur et al, 1976).

In addition, if collagenase levels are increased it is likely that collagen biosynthesis levels are reduced or collagen degradation increased during accelerated remodelling. Craig et al (1975b) found that collagen biosynthesis in hypertrophic scars decreases with time, and it has also been found that collagenase levels in normal skin and hypertrophic scar were not significantly different (Milsom and Craig, 1973) therefore it is also possible that pressure reduces collagen biosynthesis in-vivo. Sloan et al, (1978) found that pO_2 levels in hypertrophic scars were low, and pCO_2 levels high, which indicates increased metabolic activity in the scar rather than hypoxia. Therefore it is also possible that pressure reduces the pO_2 levels such that the collagen synthesis-degradation balance is biased towards of the latter favouring resorption of the hypertrophic scar tissue.

The clinical or experimental evidence available to support any of the abovementioned hypotheses of the pressure included scar remodelling process is generally incomplete, although the principal tissue parameters requiring investigation appear to be scar blood flow, blood content and oxygenation, and collagen biosynthesis.

In investigating the response of hypertrophic scar tissue to pressure produced by elasticated garments, it is desirable to obtain a quantitative description of the pressures developed at the scar/dressing interface. The relationship between pressure duration, pressure magnitude and the remodelling of the scar tissue may establish basic thresholds of pressure and time required to induce scar remodelling. Such fundamental data could be used to provide a baseline from which to quantitatively investigate the nature of the mechanism responsible for scar remodelling and resorption.

CHAPTER 4

THE DEVELOPMENT AND CONSTRUCTION OF AN INTERFACE PRESSURE MEASUREMENT SYSTEM

4.1. Introduction

4.2. Pressure Transducer Design Criteria

- 4.2.1. Surface Area
- 4.2.2. Transducer Thickness
- 4.2.3. Pressure Range
- 4.2.4. Resolution and Accuracy
- 4.2.5. Response to Physical Variables
  - 4.2.5.1. Temperature
  - 4.2.5.2. Curvature
  - 4.2.5.3. In-Plane or shear Forces
  - 4.2.5.4. Dynamic Response
  - 4.2.5.5. Time Dependence
  - 4.2.5.6. Hysteresis

4.3. Selection of a Pressure Transducer

- 4.3.1. Principles of Operation of the Capacitive Pressure Transducer
  - 4.3.1.1. Sensitivity to Pressure
  - 4.3.1.2. Temperature Sensitivity
  - 4.3.1.3. Sensitivity to Curvature
  - 4.3.1.4. Sensitivity to In-Plane or Shear Forces
  - 4.3.1.5. Time-Dependent Effects
- 4.3.2. Discussion

4.4. Construction of the Capacitive Pressure Transducer

- 4.4.1. Selection of Transducer Construction Method
- 4.4.2. Temperature Conditioning

4.5. Evaluation of the Capacitive Pressure Transducer

- 4.5.1. Standing Capacitance
- 4.5.2. Pressure Transducer Calibration
- 4.5.3. The Response to Temperature
- 4.5.4. The Response to Curvature
- 4.5.5. The Response to In-Plane Forces

4.5.6. The Response of the Transducer to Constant Load

4.5.7. Discussion

4.6. Design and Construction of a Signal Processing Circuit

4.6.1. Principles of Signal Detection

4.6.1.1. Capacitance to Frequency Conversion

4.6.1.2. The Capacitance Bridge

4.6.2. Design and Construction of Signal Processing Circuitry

4.6.3. Comparison between Capacitive Pressure Transducer and Other Interface Pressure Sensors

4.7. Summary

4.1. INTRODUCTION

In order to identify a relationship between applied pressure and the hypertrophic scar remodelling process it is necessary to quantify the magnitudes of the applied pressure. Quantification of pressure should, in this physical system, assist critical evaluation of different regimes of pressure therapy, and of the materials used to apply pressure.

Most pressure measurement studies concerned with evaluating interface pressures between the body surface and the external environment have been performed on support systems for paraplegics, geriatrics, (Kósiak, 1959, Sachs, 1974, Ferguson-Pell, 1977), and also on rehabilitation engineering devices such as prosthesis and orthosis.

The results of many of these studies indicate that the normal component of external force applied to the skin surface is readily measurable. Consequently, most available pressure transducers operate on the principle of integrating the average normal component of force over a given sensing area to provide a measurement of pressure. Although "shear" or in-plane forces have been demonstrated as having a significantly adverse affect on tissue viability (vide 3.2.3.) no clinically acceptable transducer for measuring this parameter has yet been reported to the author's knowledge. In addition to the effects produced by "normal" and "shear" forces, other physical factors exist which influence the viability of the tissue to an appreciable degree; a very high pressure gradient has been shown to produce tissue damage, (Rydevik and Lundborg, 1977), (vide 7.4.).

In hypertrophic scar literature, "pressure" resulting from elasticated dressings, although not further specified

is assumed to act normal to the skin surface (Larson et al, 1971, Baur et al, 1976) and, as the most readily measurable component of pressure is normal to the scar surface, a pressure transducer should ideally be designed to be responsive to only this component so that the accuracy of the pressure measured is optimised.

4.2. PRESSURE TRANSDUCER DESIGN CRITERIA

Ideal characteristics for a pressure transducer are relatively easy to identify (NASWPFM, 1968), but are difficult to quantify. The major ideal characteristics required for a pressure transducer for the present application are discussed in the following sub-sections. In the present study the range of pressures normally encountered at the skin surface/dressing interface requires to be determined in order to facilitate quantification of the transducer characteristics, and also the transducer dimensions which affect the value and accuracy of the pressures measured at the interface require to be specified. In addition to morphological and technical design criteria, clinical and safety criteria are also introduced in which the latter cannot sensibly be compromised at any stage.

A further design constraint is introduced in that the electrical safety of transducers and associated equipment should comply with B.S.I. 76/30975 DC* which advises and directs the use of electrical equipment in medical practice.

4.2.1. Surface Area

Ideally, the surface area of a pressure transducer should be as small as possible in order to resolve sharp pressure gradients which could occur at scar/normal tissue boundaries. This criterion is also consistent with a transducer having a high spatial resolution. The shape of the pressure transducer should be conveniently circular to facilitate manufacture and comparison between like devices since the area of the transducer is a constant ratio to the diameter.

---

* Equivalent to Hospital Technical Memorandum No. 8 (H.T.M.8)

Ferguson-Pell (1977) calculated that the maximum diameter for producing results, within a certain accuracy, was given by the equation

$$r < \frac{EP_o}{200k} \qquad 4.1$$

where E is the % accuracy of measurement,
P_o is the local peak pressure, and
k is the pressure gradient

Therefore, from an inspection of equation 4.1 , if the radius is increased the error in the accuracy of the measurement also increases. In order to maintain the accuracy within certain limits for circular transducers the diameter or radius must be controlled. However, if the value of E chosen is very low, i.e. of the order of 1% - 2½% then very difficult manufacturing conditions are imposed by virtue of the small transducer diameter required. A compromise between the accuracy of measurement and the transducer diameter must therefore be selected; a diameter of 10mm with a peak pressure of 60 - 70mmHg and a pressure gradient of 0.5mmHg/mm is capable, theoretically, of resolving pressures measured to within ± 7% of the local peak pressure which the author deems to be very acceptable for use in biological investigations.

4.2.2. Transducer Thickness

It has long since been demonstrated that measurement of a variable in any physical system produces changes in the value of the variable measured, i.e. the measurand. This principle is analogous to Heisenberg's Uncertainty principle. Therefore, to maximise the accuracy of measurement, the measurement process *per se* should produce minimal changes in the measurand.

When a transducer is placed on the surface of the skin and the skin is compressed via the transducer, the

transducer is thus said to be at an interface. However its presence thereat modifies the mechanical properties of the skin and also affects the accuracy of the pressure measured.

The effect of thickness-induced perturbation by various transducers placed on skin has been reviewed by Ferguson-Pell (1977). The critical factor in producing minimal perturbation appears to be the ratio of transducer radius to thickness, the "aspect ratio". The higher the aspect ratio the less perturbation due to the transducer.

4.2.3. Pressure Range

Reports, in the literature, of pressure applied by elasticated garments state that the value of pressure required to induce and maintain scar remodelling should be greater than mean capillary pressure value which is usually taken as 25 - 30mmHg (vide 3.3.1). Furthermore if a pressure magnitude exceeds 70 - 80mmHg continuously for several hours there is a real risk of irreversible tissue damage (vide 3.2.1). Therefore a transducer should be capable of measuring up to values of at least 100mmHg. In addition, as high overload transients frequently occur during loading and unloading of the transducer by the elasticated garment, a reasonable safety margin of 100% of the maximum calculated pressure value should be provided. This means that a pressure transducer should have an operational range of at least 200mmHg.

4.2.4. Resolution and Accuracy

From inspection of preliminary studies with elasticated garments it appears that a wide range of interface pressures may be encountered depending on parameters such as garment tension, anatomical location and the mechanical properties of the tissue thereat. Consequently, in order to provide accurate measurements of peak pressures less than 15 - 20mmHg, it is essential that the transducer and instrumentation system should have a resolution of at least 1mmHg and preferably $\simeq$ 0.5mmHg. With a resolution of 0.5mmHg then even at

10mmHg peak pressure the accuracy would be within ± 5% of the true pressure value.

4.2.5. Response to Physical Variables

Although an ideal transducer has same characteristics as defined in 4.2.1 to 4.2.4. real transducers invariably respond to physical variables, and the ideal response to variables considered relevant in the present study are described under the following headings.

4.2.5.1. Temperature The variation in surface temperature of scar and of normal skin may be as much as 3°C from one anatomical site to another (Naismith and Evans, 1977, unpublished data) and may also vary considerably on the same site over short intervals of time (Fernie, 1973). Most materials used in the construction of transducers demonstrate significant temperature sensitivities over the normal scar and skin temperature range which results in inaccurate pressure readings being produced if variations in temperature occur during measurement. The ideal transducer should be sensibly independent of temperature over the range of normal body surface temperature.

4.2.5.2. Curvature The surface of the body is highly contoured, many locations having curvatures which frequently change radius during body movements, such as sites over joints and muscle. It is a prerequisite that the transducer must not distort the surface at the curved interface, and to achieve this, the transducer itself must be flexible, adapting its shape to that of the anatomical site opposite. However, if the transducer is insufficiently flexible and the interface is forced to comply with the shape of the transducer, pressures are not measured normal to the interface but normal to the transducer. Furthermore, inflexible transducers may produce inaccurate results whereby changes in output are produced due to the production of stresses within the transducer itself.

The ideal transducer should be essentially independent of the range of radii of curvature normally encountered on the body.

4.2.5.3. In-Plane or Shear Forces The errors introduced to pressure measurements by transducers which respond to in-plane forces are difficult to assess when the magnitude of in-plane forces at the garment-scar surface interface is unknown. Fernie (1973) suggested that it may be possible to decouple certain types of transducers mechanically to prevent generating in-plane forces in the transducer although in practical terms this is extremely difficult. Until in-plane force measurements are practical it would seem reasonable to assume that in-plane stresses,of the same magnitudes normal stresses, may be present. A reasonable and generally accepted design value for artefacts of the transducer due to in-plane stresses is less than 10% of the pressure measured.

4.2.5.4. Dynamic Response The dynamic response of transducers proposed for use at the scar/pressure garment interface is a particularly demanding constraint. Significant body movements do not appear to occur with a periodicity of less than a few seconds in sedentary subjects and therefore a similar time constant for a pressure transducer is anticipated. The time rate of loading may substantially alter the sensitivity of transducers to pressure if their response is mainly due to materials which are predominantly time-dependent in nature. Furthermore, for scar/pressure garment interface evaluation, the rate of loading may vary considerably. Therefore, ideally, transducers should have a repeatable response over a large range of loading rates.

4.2.5.5. Time-Dependence Transducers which are expected to be located under elastic garments continuously or for long periods should exhibit acceptable long term stability of calibration and output under constant load applications. Changes in output leading to significant errors may occur due to the creep compliance of components in the materials used in the construction of the transducer. This characteristic of many transducers reported in the literature is rarely evaluated. Transducers used to evaluate the

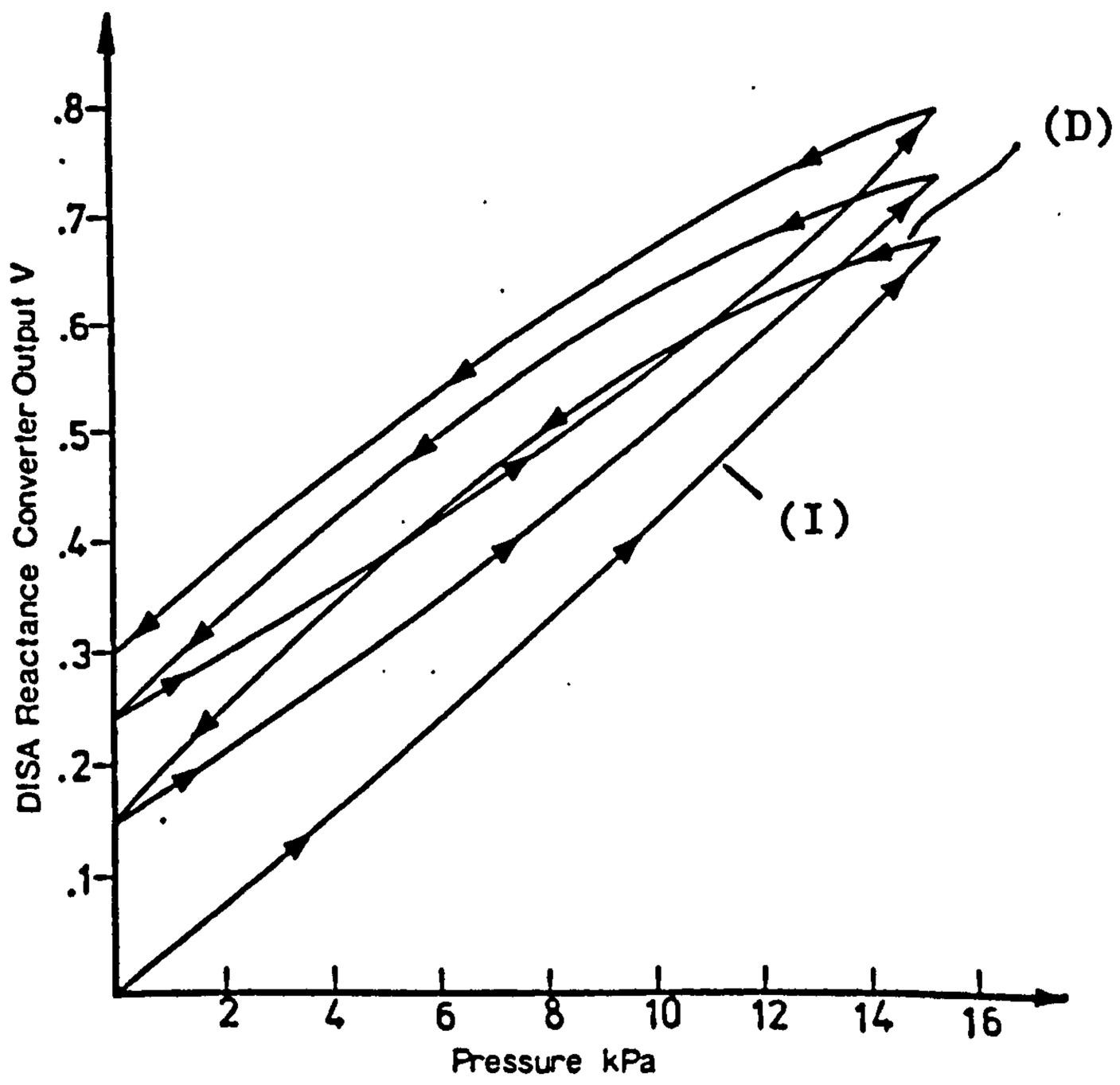

DIELECTRIC = 3M'S TYPE 451 DOUBLE-SIDED ADHESIVE TAPE

FIGURE 4.1 PRESSURE RESPONSE OF 3-PLATE CAPACITIVE PRESSURE TRANSDUCER EXHIBITING OUTPUT HYSTERESIS BETWEEN INCREASING (I) AND DECREASING (D) PRESSURES

interface pressure-time characteristics due to elasticated pressure garments require to have a long term stability so that the value measured by the transducer is ideally independent of the duration of pressure application.

4.2.5.6. Hysteresis Many transducers, especially those employing "elastic" materials for detection, exhibit severe hysteresis; the relationship between output and pressure during the loading sequence being different from that during the unloading sequence. In some cases transducer outputs do not return precisely to zero when the transducer is completely unloaded indicating a long term deformation. Repeated loading frequently results in a series of ascending hysteresis curves giving substantial uncertainty of the pressure value for a given output signal and can therefore result in extremely inaccurate results. An example of hysteresis behaviour is shown in Figure 4.1. where double-sided adhesive tape was used as a compliant dielectric in a parallel-plate capacitive pressure transducer (Ferguson-Pell, 1977). Reports of many of the transducers evaluated in the literature do not quote the errors likely to occur due to hysteresis, although in fact they may be extremely high. Accordingly, the ideal transducers designed and used should have negligible hysteresis particularly if they are to be used over a long period of time as described in 4.2.3.5.

4.3. SELECTION OF A PRESSURE TRANSDUCER

Ferguson-Pell (1977) thoroughly reviewed the two types of available pressure transducers; those which make single pressure readings (snap-shot transducers), and those which continuously record interface pressure measurements (dynamic transducers) for suitably of measuring body/support interfaces pressure with paraplegic and geriatric subjects. The objective of his study was to provide temporally related interface pressure information and it was concluded that dynamic pressure transducers showed greatest

UNLOADED

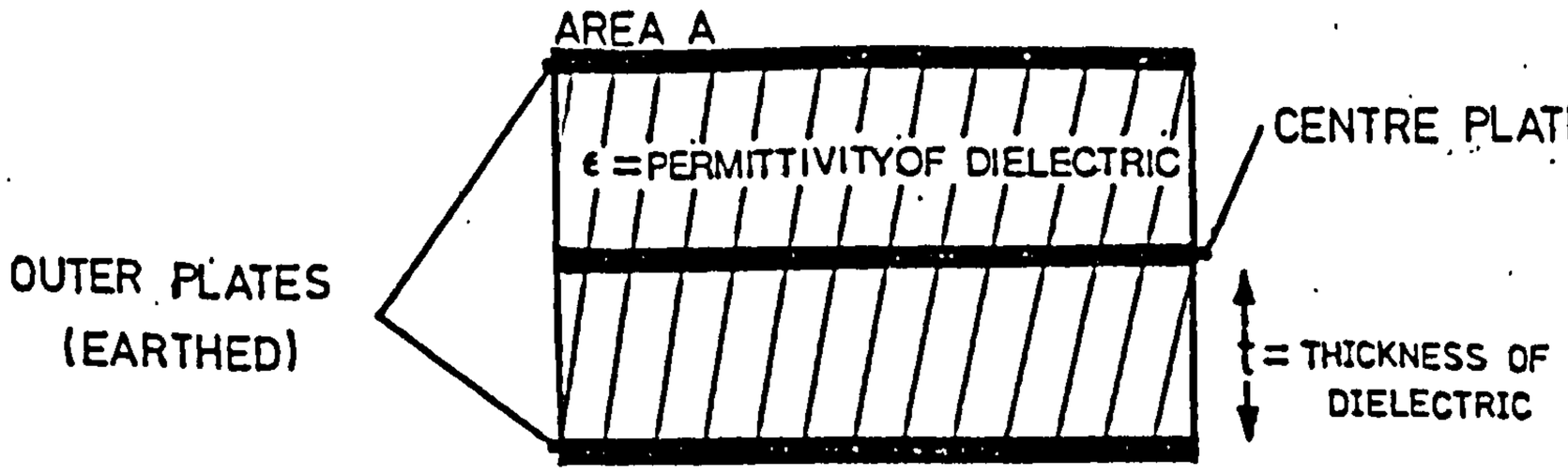

$$\text{CAPACITANCE } C = \frac{2A\epsilon}{t}$$

FIGURE 4.2a UNLOADED TRIPLE PARALLEL-PLATE CAPACITOR

LOADED

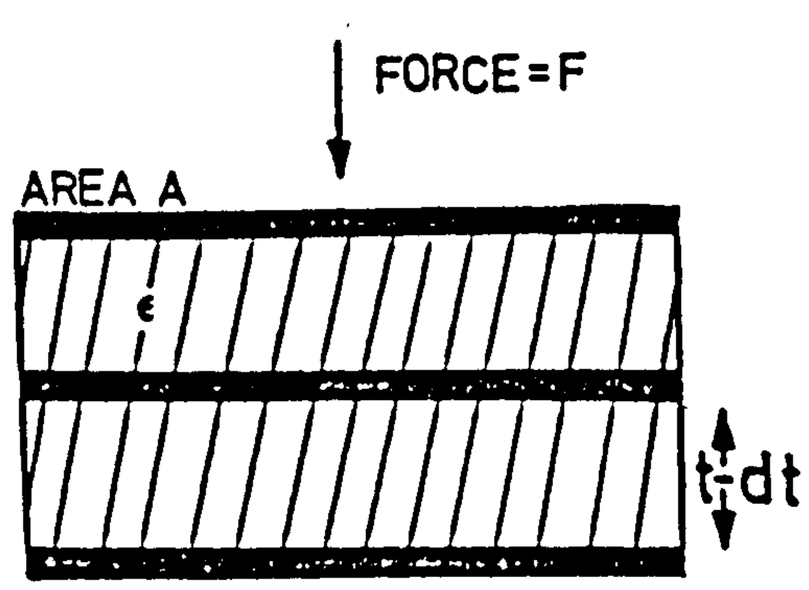

$$\text{CAPACITANCE } C + dC = \frac{2A\epsilon}{t - dt}$$

FIGURE 4.2b LOADED TRIPLE PARALLEL-PLATE CAPACITOR

potential in fulfilling this requirement.

With hypertrophic scars, it is also essential that a temporal recording of pressure distribution be obtained, since it may be possible to relate the temporal interface pressure profiles with remodelling of the scar morphology, and with other parameters such as blood flow rate or blood content. Therefore a continuously recording or dynamic transducer is desirable to obtain fundamental clinical data.

Within the range of dynamic pressure transducers there are many different types available such as those operating on inductive, resistive and capacitive principles; strain-gauged beam transducers; pressure sensitive semi-conductor transducers; and diaphragm transducers. From a detailed study and analysis of each of these afore-mentioned dynamic transducers Ferguson-Pell (1977) concluded that the capacitive pressure transducer was the most suitable for measuring interface pressures.

The author, after extensively reviewing and considering the comparitive study of Ferguson-Pell decided that the capacitive pressure transducer offered superior potential for use as an interface pressure measurement sensor.

4.3.1. Principles of Operation of the Capacitive Pressure Transducer

If two conducting surfaces carrying equal charges, +Q and -Q respectively, are separated by a dielectric material of thickness t and relative electrical permittivity ϵ_r the ratio of the charge on the surface of one conductor to the potential difference (V) between conductors is defined as capacitance (C) between the conductors. The capacitance of any physical arrangement of conductors is a function of the geometry of the conductors.

A schematic diagram of 3 parallel conducting plates is shown in Figure 4.2a. If the lateral dimensions of the plates are large in comparison to their separation, then it can sensibly be assumed, from basic theoretical

considerations, that the electrical field between the plates is uniform and normal to the plates. If the outer two plates of area A are grounded and are separated from the centre plate by a dielectric of a thickness t then the capacitance of the transducer is a function of the area of the conducting plates and the thickness of the dielectric

$$C = f(A,t)$$

$$\text{in fact} \qquad C = \frac{2A\epsilon}{t} \qquad 4.2.$$

where $\epsilon = \epsilon_r \epsilon_o$

ϵ_o = permittivity of free space (vacuo)

ϵ_r = 1 for air

The capacitance shown in equation 4.2 is present when the transducer is unloaded and will be hereinafter referred to as the static or "standing" capacitance.

4.3.1.1. Sensitivity to Pressure If the plates of the 3 parallel-plate capacitor are separated by a compliant dielectric then loads or forces applied normal to the plane of the plates compress the dielectric resulting in a reduction in the thickness of the transducer (Figure 4.2b). From equation 4.2 it can be seen that a reduction in dielectric thickness increases the overall standing capacitance of the transducer.

In order to accurately analyse the response of the transducer to normal loads an assumption is made that the electric field edge effects are small at the periphery of the transducer, and when the compliant dielectic is free to expand radially when loaded by a force F acting normal to the plates then

$$E_c = \frac{-dF}{dt} \cdot \frac{t}{A} \quad \text{in compression} \qquad 4.3$$

where E_c is the compressive stiffness of a linear dielectric material

if $dP = \frac{dF}{A}$ is defined as the change in pressure acting normal to the plates then 4.3 becomes

$$E_c = \frac{-dP \cdot t}{dt} \qquad 4.4$$

and differentiating equation 4.2 with respect to t gives

$$\frac{dc}{dt} = -\frac{2A\epsilon}{t^2} \qquad 4.5$$

and combining equations 4.4 and 4.5 gives an expression of the sensitivity of the transducer to pressure

$$\frac{dc}{dP} = \frac{2A\epsilon}{tE_c} \qquad 4.6$$

by inspection of equation 4.6 the change in capacitance due to normal pressure is directly proportional to the area of the transducer and inversally proportional to the thickness and compressive stiffness of the dielectric material. Thus, superficially, it appears that the sensitivity of the transducer to applied pressure can be predetermined by purely geometrical considerations and selection of a suitable dielectric, and the thinner the transducer the greater its sensitivity to pressure. Many dielectrics have, however, a high bulk compressibility which means that changes in thickness have to be maintained by changes in shape to maintain the volume of material constant. This change in shape occurs by bulging at the sides of the dielectric creating a mechanical edge effect which effectively increases the stiffness of the material, E_c, under compression which in turn reduces the sensitivity of the transducer to pressure.

One method of increasing the sensitivity to pressure is to reduce the friction between the conducting plates

FIGURE 4.3. VARIATION IN SENSITIVITY WITH DIELECTRIC THICKNESS (After Ferguson-Pell, 1977)

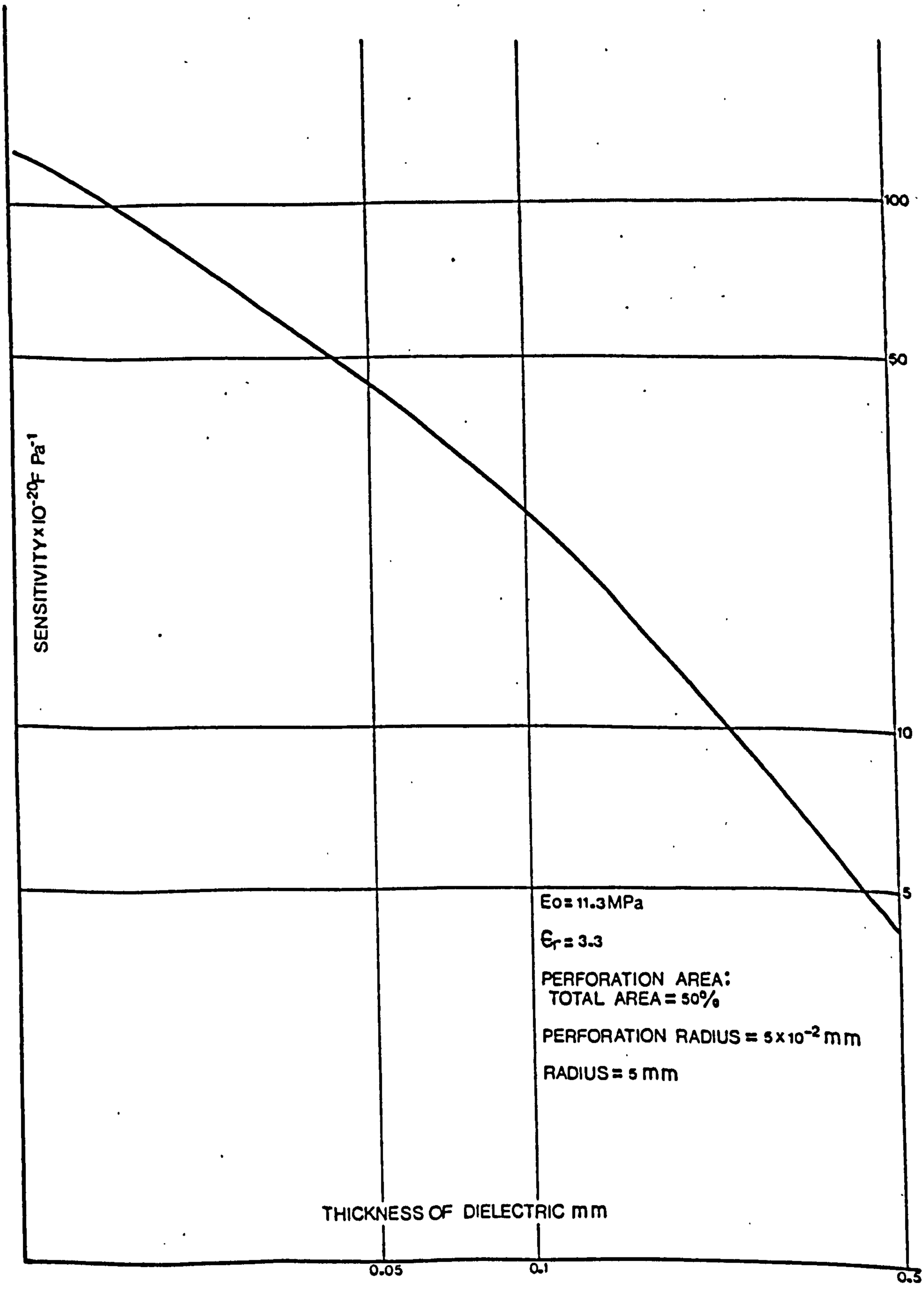

and the dielectric, however, this necessitates lubrication or sophisticated construction, requirements which conflict with a low cost, practical and easy to use concept of a transducer.

An alternative method would be to use extensible conducting plates for the capacitor, or to modify the geometry of the dielectric, however experiments performed using this latter method reported only indeterminate results (Frank and Gibson, 1954). High permittivity materials have been used in an attempt to practically increase the sensitivity, however the usefulness of many such materials e.g carbon-filled rubber, is limited by excessive hysteresis. Ferguson-Pell, (1977) found that, by using compliant conducting plates made of aluminium with a conductive elastomeric adhesive as a dielectric the criteria of mechanically bonding the transducer to the dielectric was satisfied. Ferguson-Pell (1977) also showed, from a theoretical model, that the sensitivity of the dielectric could be improved by increasing the dielectric load free area to 50% of the total dielectric area, and that the sensitivity was increased with decreasing thickness for a given dielectric area and a perforation load free area. (Figure 4.3).

4.3.1.2. Temperature Sensitivity The model below used to predict the behaviour of the parallel-plate capacitor in response to thermal variations is considerably simplified; all thermal effects in an air perforated dielectric being assumed to be due solely to the thermal properties of the dielectric; and the dielectric constant is independent of temperature over the useful range, which is taken from room temperature ($18^{o}C$) to body temperature ($33-35^{o}C$).

The thermal coefficient of expansion, β, of the dielectric is defined as

$$\beta = \frac{1}{V_o}\frac{\partial V}{\partial \theta} \qquad 4.7$$

where V_o = the initial volume of the material

θ = temperature

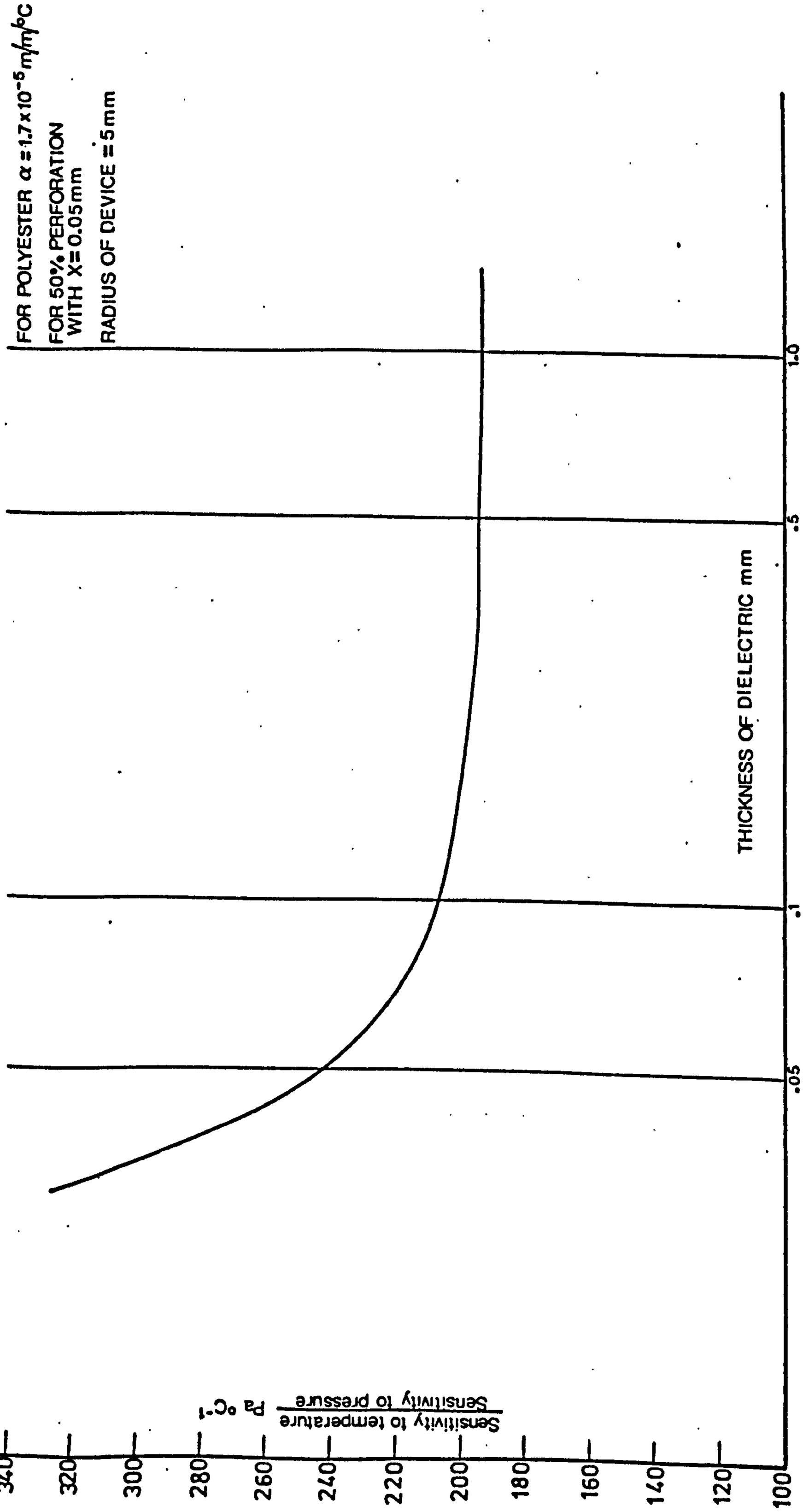

4.4. THEORETICAL RELATIONSHIP BETWEEN ERROR DUE TO TEMPERATURE SENSITIVITY AND DIELECTRIC THICKNESS (After Ferguson-Pell, 1977)

FIGURE 4

It is also assumed that the conducting plates are independent of thermal effects and permit no expansion of the dielectric perpendicular to the plane of the plates.

The dielectric linear thermal coefficient of expansion, α , is defined as

$$\alpha = \frac{1}{t \quad \frac{\partial t}{\partial \theta}} \qquad 4.8$$

where t = initial thickness of the material

Since the standing capacitance of a parallel capacitor for a thickness t is defined in equation 4.1 as $C = \frac{2A\epsilon}{t}$ then

$$\frac{\partial C}{\partial t} = \frac{2A\epsilon}{t^2} \text{ and } \frac{\partial t}{\partial \theta} = \alpha t \qquad 4.9$$

$$\text{therefore} \quad \frac{\partial C}{\partial \theta} = \frac{-2A\alpha\epsilon}{t} \qquad 4.10$$

which is the sensitivity of the device to thermal changes

and using equation 4.6 then

$$\frac{\text{sensitivity to temperature}}{\text{sensitivity to pressure}} = \frac{\frac{\partial C}{\partial \theta}}{\frac{\partial C}{\partial p}} = \frac{-\frac{2A\alpha\epsilon}{t}}{\frac{2A\epsilon}{E_c t}} = -\alpha E_c \qquad 4.11$$

Ferguson-Pell (1977) found that applying equation 4.11 to a perforated theoretical dielectric model gave a relationship between dielectric thickness and relative temperature response as shown in Figure 4.4. For a dielectric thickness less than 0.1mm, the thermal sensitivity increases rapidly obviating any high sensitivity obtained by having a thin dielectric less than 0.08mm. Little advantage is apparent if transducers are made

having a thin dielectric less than 0.08mm. The same situation is apparent if dielectrics are made thicker than 0.2mm. From this evidence the dielectrics of transducers should be made between 0.1mm and 0.2mm thick.

The above theory also predicts that if a dielectric with a positive linear temperature coefficient of expansion is used, for example 10^{-4} m/m /^{o}C, then raising the temperature reduces the value of the standing capacitance of the transducer.

The difference between normal room-temperature (20^{o}C) and scar or skin surface temperature (34^{o}C) is 14^{o}C and this change causes the dielectric to expand thus increasing the thickness of the transducer and reducing the capactiance. This is manifested as a negative pressure change equivalent to 20mmHg. This means that with certain polyester dielectrics, if the transducer is calibrated at room temperature and then placed on a subject at the scar/dressing interface the value of pressure measured will be 20mmHg less than the true value once the temperature of the transducer equilibrates with the surface temperature. Errors of this magnitude are clearly unacceptable and some means of temperature compensation must be provided.

4.3.1.3. Sensitivity to Curvature It has been stated that, for an ideal transducer, the change in output due to curvature per se of the body surface should be negligible (vide 4.2.4.3) however in the case of the parallel plate transducer using a compliant elastomer as a dielectric, bending the transducer from an initially planar surface over a curved surface will produce stresses within the transducer leading to distortion of the transducer geometry and consequently the output signal.

In addition to internally produced stresses a change in capacitance will occur if the transducer is flexed over a cylindrical or spherical surface. This change is due to the geometrical nature of capacitance.

$$C_c = \frac{2\Pi\epsilon\phi\ell}{\ln_e (r_2/r_1)}$$

FIGURE 4.5 SCHEMATIC DIAGRAM OF SECTION OF COAXIAL CYLINDERS USED FOR THE CALCULATION OF CAPACITANCE

Consider the situation for a cylindrical capacitor comprising two coaxial cylindrical conductive surfaces of radius r_1 and r_2 separated by a dielectric with permittivity ϵ. The capacitance per unit length is defined by

$$C_c = \frac{2\Pi\epsilon}{\ln_e(r_2/r_1)} \qquad 4.12$$

C_c = capacitance per unit length between coaxial cylindrical surfaces

Consider a section of the cylinder as shown in Figure 4.5 which subtends an angle Ø at the centre and has a curved surface area equivalent to that of a square of side length ℓ. The capacitance of the coaxial cylindrical sector (angle Ø) length is given by

$$C_C = \frac{2\Pi\epsilon\,\phi\,\ell}{\ln_e(r_2/r_1)\cdot\ 2\Pi} \qquad 4.13$$

where r_1 = radius of outer shell
r_2 = radius of inner shell

A planar surface can be assumed to be an extension of part of a spherical or cylindrical surface with an infinite radius of curvature. Therefore for a parallel plate capacitor with an infinite radius of curvature.

$$r_1 \gg r_1 - r_2$$

In the case of spherical surfaces if a two plate capacitor is represented by unit area on two concentric surfaces, the area is given by $\Phi r_1^2 = 1$

where Φ is the solid angle subtended by the unit area.

The proportion of the total capacitance, C_p, of the section of spheres is

$$C_s = \frac{4\Pi\epsilon\, r_1 r_2}{r_1 - r_2} \cdot \frac{\Phi}{4\Pi} \qquad 4.14$$

$r_1 - r_2 = t$, the dielectric thickness and $\Phi = \frac{1}{r_1^2}$ 4.15

thus $$C_s = \frac{\epsilon(r_1 - t)}{t\, r_1} \qquad 4.16$$

In the planar case $r_1 - t \rightarrow r_1$ therefore

$$C_s \rightarrow C = \frac{\epsilon}{t} \quad \text{(unit area)} \qquad 4.17$$

$$\text{thus } C_s - C = \Delta C_1 = \frac{\epsilon(r_1 - t)}{t\, r_1} - \frac{\epsilon}{t} = -\frac{\epsilon}{r_1} \qquad 4.18$$

where ΔC_1 = change in capacitance due to pressure and for area A and three plates

$$\Delta C_2 = \frac{-2A\epsilon}{r_1} \qquad 4.19$$

which is independent of the transducer thickness. For a transducer with a radius of 5mm and an elastomeric polyester dielectric 0.1mm thick perforated with 5×10^{-2}mm holes over 50% of its area, a change in capacitance of 4.6×10^{-2}pF would occur if it were made to conform to a speherical surface of radius 100mm (a common anatomical radius of curvature). This is equivalent to a pressure reading of 100mmHg and would be the error caused by conforming the transducer shape to that of the spherical surface.

The errors introduced by altering the geometry of the transducer at curved surfaces are clearly large, and it is not suitable to prevent these errors by making the transducer inflexible as perturbation of the surface may introduce inaccuracies of a similar magnitude. It is unfortunate that this sensitivity to curvature is an intrinsic geometrical property of transducers operating on capacitive principles and it may only be negligible in its effect if the transducers are as sensitive to pressure changes as possible. In addition to geometrically produced changes in capacitance during flexion, the presence of internal stresses within the dielectric may lead to significant artefacts which are difficult to predict

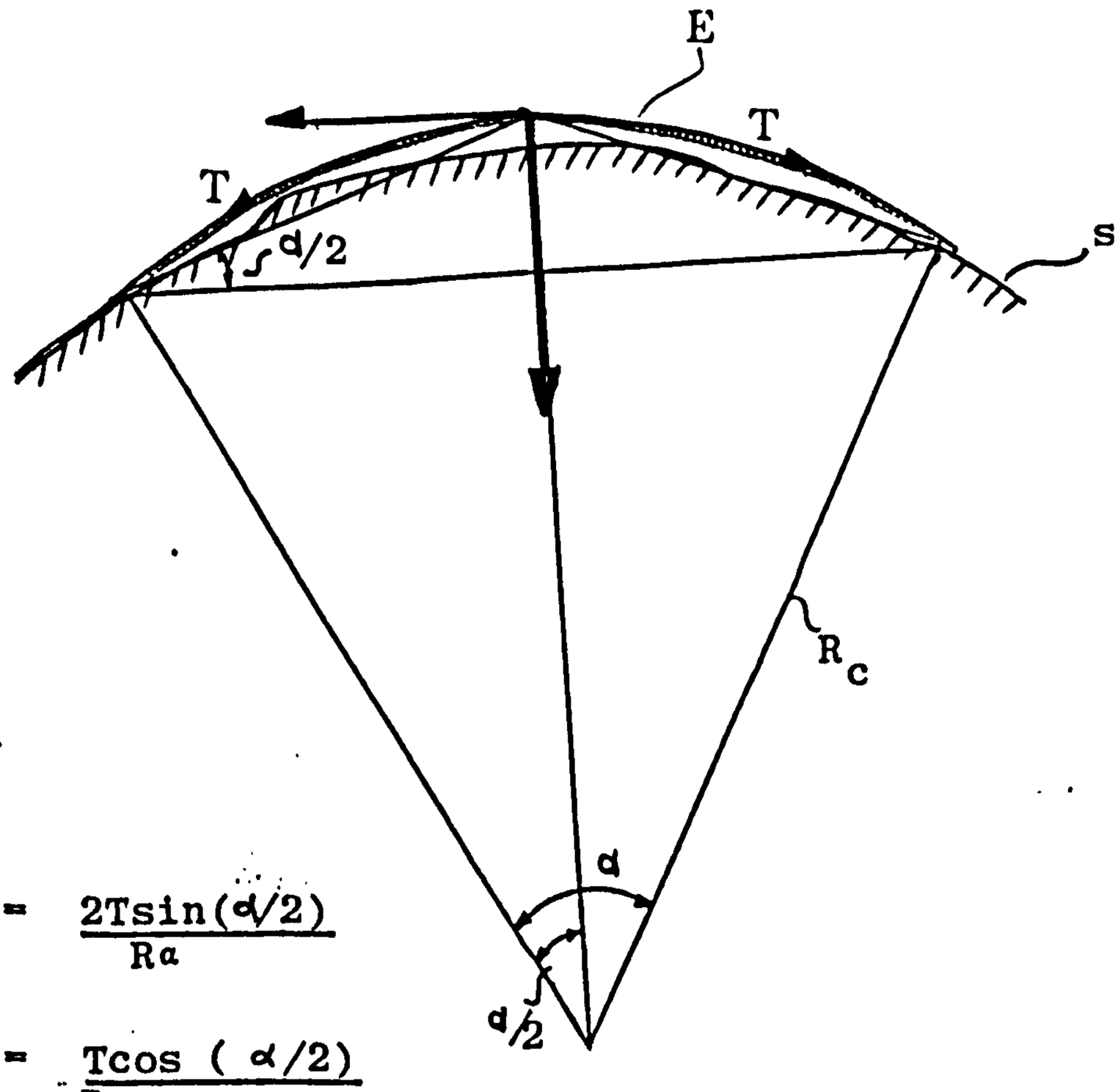

$$F_n = \frac{2T\sin(\alpha/2)}{R\alpha}$$

$$F_s = \frac{T\cos(\alpha/2)}{R\alpha}$$

FIGURE 4.6 NORMAL (F_n) AND IN-PLANE (F_s) FORCES ACTING ON SKIN SURFACE (s) PRODUCED BY ELASTICATED GARMENT (E)

theoretically.

4.3.1.4. Sensitivity to Shear or In-Plane Forces When the transducer is located at the interface between tissue and the elasticated garment it may be assumed that the forces acting on the transducer are produced only by elastic forces within the garment and that no frictional forces are present. The actions of these forces are shown in Figure 4.6 which is a simple schematic diagram of the elastic forces as seen by the transducer at the interface.

The force due to the component of elastic tension, acting normal to the skin, F_n, is given by

$$F_n = \frac{2T \sin \alpha/2}{R\alpha} \qquad 4.20$$

where T = circumferential elastic tension in the garment
R = radius of curvature of the location of the transducer
α = angle subtending a unit area of the surface on which the transducer is located

and the in-plane or shear force, F_s, due to the component of elastic tension acting in the plane of the transducer is given by

$$F_s = \frac{T \cos \alpha/2}{R\alpha} \qquad 4.21$$

and the ratio of in-plane force, in one direction, to normal force is therefore

$$\frac{F_s}{F_n} = \frac{1}{2\tan(\alpha/2)} \qquad 4.22$$

The ratio of F_s/F_n is plotted against α and shown graphically in Figure 4.7. From the graph it is seen that in order that the magnitude of shear force or in-plane force component is less than 10% of the normal component as is required by 4.2.5.3, it is necessary to select an angle of between $\simeq 150^o$ and 210^o which maximises the contribution due to the normal component of force. Theoretically this means that, once the transducer is placed on a flat surface or a surface having a very high radius of

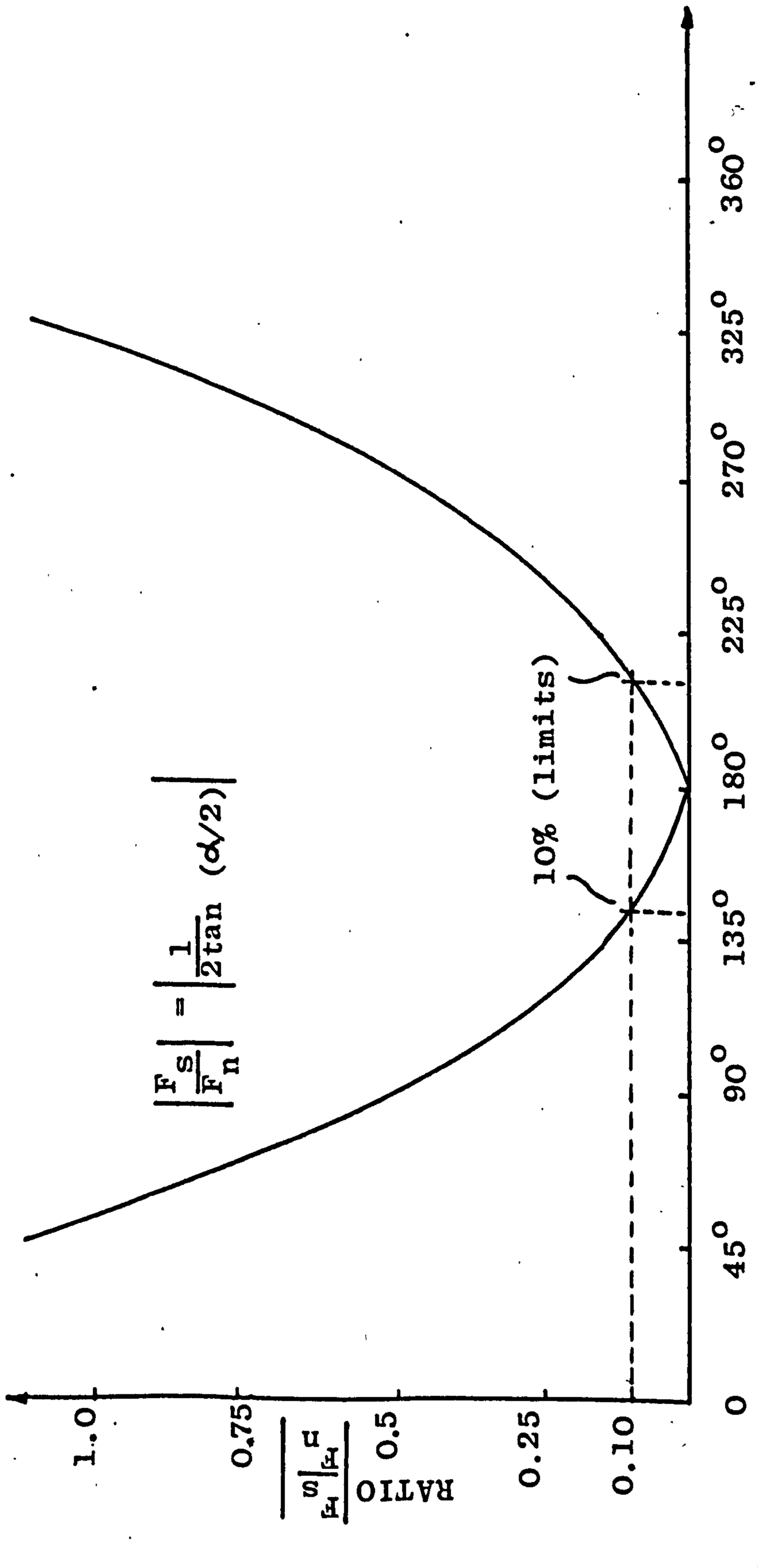

FIGURE 4.7 RATIO OF SHEAR FORCE TO NORMAL FORCE ACTING ON A CURVED SURFACE

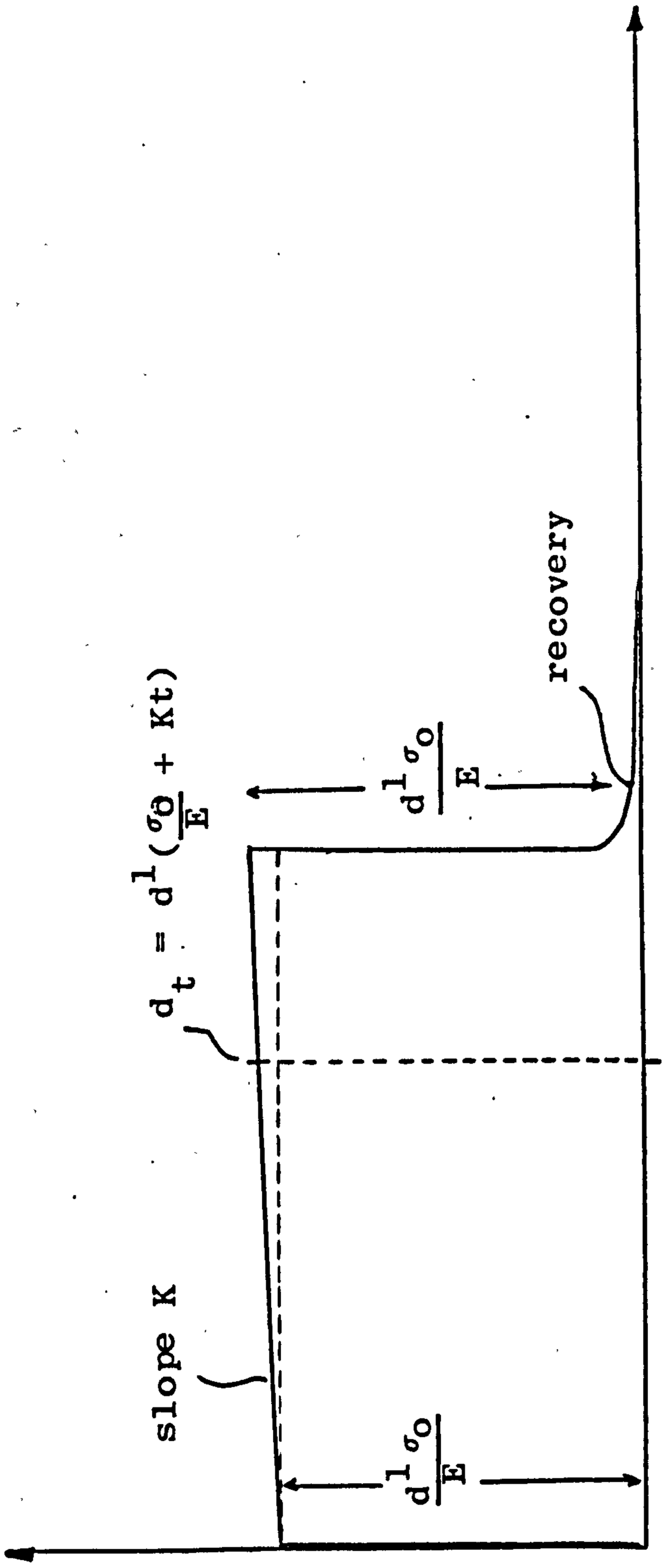

FIGURE 4.8 RESPONSE OF A VISCOELASTIC MATERIAL TO STEP LOADING AND UNLOADING DEMONSTRATING CREEP BEHAVIOUR

curvature.beneath an elasticated garment in tension, any output measured is almost entirely due to in-plane forces. However if there is likely to be a reasonable curvature at the interface, such as on an extremity, then the transducer output is minimally influenced by in-plane or shear forces, being of the order of 10% or less.

Therefore, when interface pressure measurements are recorded it is important that the anatomy at the site being measured is described.

4.3.1.5. Time-Dependent Effects When a dielectric material of thickness d_o is loaded by a compressive force F_o there is provided a stress σ_o which acts on the area of the dielectric and which will produce an immediate initial deformation d^1 in the dielectric. The stress σ_o can be related to the original thickness d_o by a strain ϵ_o. If we assume that the mechanical properties of the compliant dielectric are representative of the whole transducer and that the dielectric has a linear viscoelastic fluidic response, then the behaviour subsequent to the initial deformation is shown in Figure 4.8 and may be described by

$$d_t = d^1 (\sigma_o/E + Kt) \qquad 4.23$$

where d_t = is the deformation after time t
E = elastic modulus of the material
K = material constant

and on release of the applied force, F_o, the residual deformation is given by

$$d_R = d^1 Kt \qquad 4.24$$

consequently the thickness of the dielectric is

$$d_o - d^1 Kt \qquad 4.25$$

Thus the standing capacitance and sensitivity to pressure will be altered accordingly, However, what this means in practical terms is that, if the transducer

dielectric behaves as a linear viscoelastic material, then when the transducer is located at the scar/elastic dressing interface the constant pressure will result in a change in transducer output with time i.e. a time-dependent effect; creep. Thus the transducer output will display a greater value of pressure then is actually present, the error being dependent on the magnitude of applied pressure and the mechanical properties of the dielectric. It is rather difficult to predict the magnitude of errors due to creep as the mechanical properties of many of the elastomeric polyester materials are unknown, however limiting values for the creep response can be roughly specified.

If we assume that 60mins. is an upper time limit for a transducer being located at an interface and limit the maximum acceptable error over this period to 5% of the maximum measured pressure then for a true measured maximum pressure of 40mmHg, 2mmHg creep per hour or 0.033mmHg/min are acceptable values for creep errors (5%).

As creep errors are directly proportional to the duration of the transducer's presence at the interface, some control of the measurement procedure is clearly required.

4.3.2. Discussion

The simple theory used to predict the response of the parallel-plate capacitive pressure transducer having a compliant dielectric to variations in certain physical parameters provides objective criteria for the selection of materials used in the construction of the transducer. In particular, soft rubber-based materials which exhibit undue hysteresis, temperature sensitivity and time-dependent effects such as creep are excluded by the theory.

The pressure sensitivity of the transducer, once a suitable dielectric is selected, is dependent on the geometry of the transducer and, for practical purposes

only the thickness thereof; the pressure sensitivity increasing with decreasing transducer thickness. The transducer thickness is limited by increasing temperature sensitivity which offsets any increase in pressure sensitivity. Theoretically, the sensitivity to decreasing dielectric thickness also increased by introducing perforations into the dielectric to modify its shape. Inspection of this model shows that the introduction of perforations into the dielectric is consistent with minimising the response due to thermal changes. The response of the transducer to curvature is unfortunately an intrinsic geometrical property of capacitance-based transducers and can only be relatively minimised by ensuring that the transducer is as sensitive as possible to pressure.

The predicted influence of shear forces may be thought to be negligible unless the transducer is located at an interface over a large radius of curvature where in-plane forces generated by the garment may be of the same order as the normal force components. However this is inconsistent with the response of the transducer to curvature.

Time-dependent effects could result in large measurement errors being produced which are difficult to predict as the mechanical properties of many of the viscoelastic dielectrics are unknown. This means that the duration of measurement must be carefully examined with regard to such errors.

The predicted response or behaviour of the transducer according to simple theoretical models is based on assumptions which may be frequently invalid. In addition, measurement errors due to temperature changes, curved interfaces and shear forces and time-dependence are likely to be substantial. Nevertheless the models provide a description of the transducer behaviour to separate variables and therefore facilitate analyses of experimental results where the transducer response may be a result of an unclear combination of variables. In addition the models also provide means by which improvements and developments of the transducer can be quantified and compared.

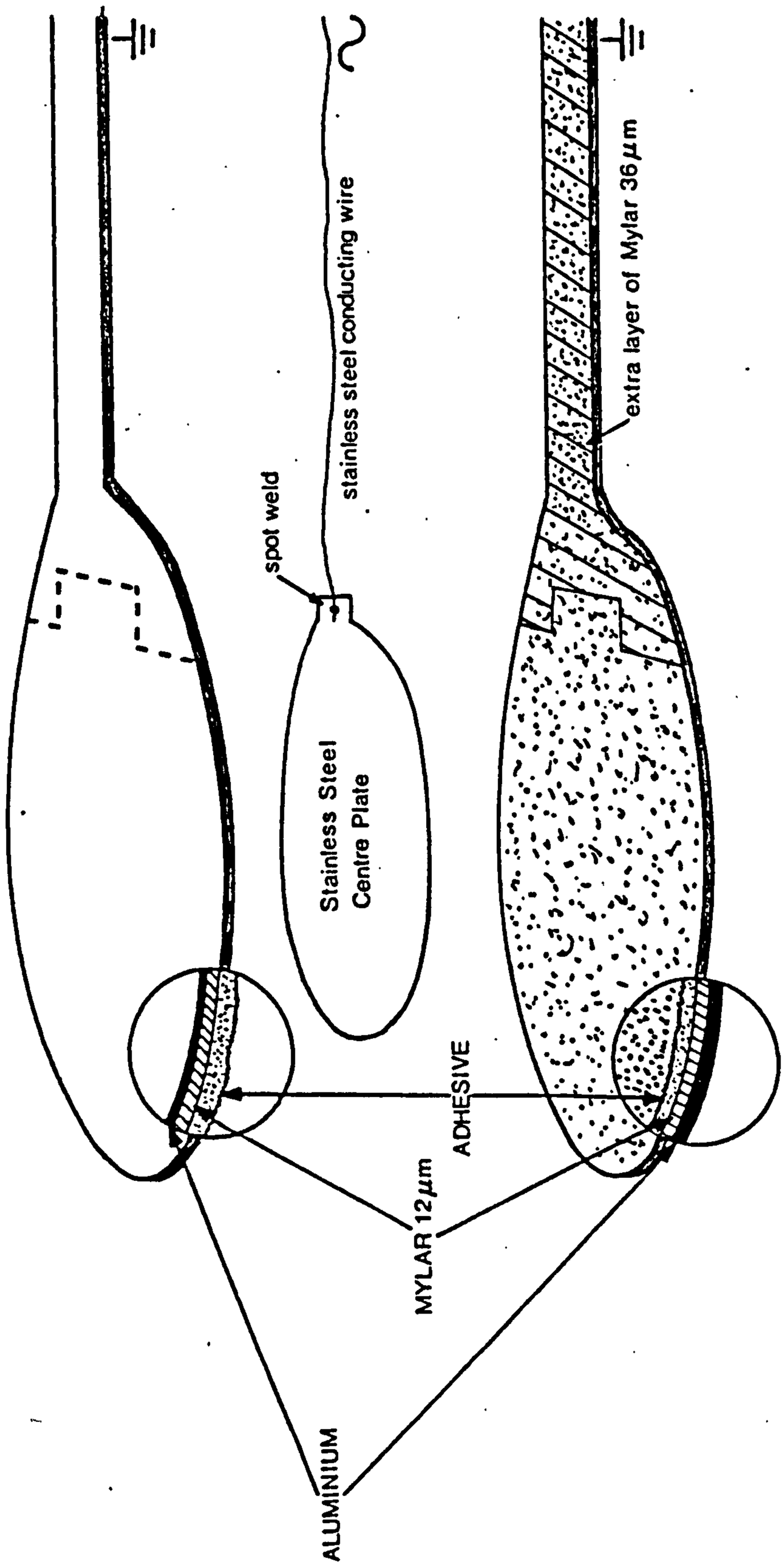

FIGURE 4.9 EXPLODED SCHEMATIC VIEW OF A TRIPLE PARALLEL PLATE CAPACITIVE PRESSURE TRANSDUCER (After Ferguson-Pell, 1977)

4.4. CONSTRUCTION OF THE CAPACITIVE PRESSURE TRANSDUCER

The construction of the parallel plate pressure transducer having a compliant dielectric has been described in great detail and the reader is referred to Ferguson-Pell (1977) for a full treatise on this matter. A synopis of the construction is provided below.

An exploded schematic view of a transducer is shown in Figure 4.9. The transducer is a triple plate capacitor with a compliant dielectic positioned between the two outer conducting plates and a conducting centre plate. The outer plates are a laminate of Aluminium Foil 9μm thick and a Mylar* (polyethylene terapthalate) insulating film 12μm thick (Metal Box Ltd., U.K.). The centre plate is punched out of 12μm thick EN58E 18/8 stainless steel (i.e. 18% chromium, 8% Nickel), (Goodfellow Metals, Cambridge, U.K.). Aluminium and 18/8 stainless steel are practically non-magnetic and were selected to minimize inductive effects from external electromagnetic fields. The central plate is connectable to electronic processing means by a 50μm diameter 18/8 stainless steel wire which is spot welded to a tag on the centre plate.

The compliant dielectric is formed from a 17% solution of a polyester adhesive (No. 49002-solid, No. 4671-solution, Du Pont de Nemons, U.K.), in a solvent (methylene chloride) and is thinly and evenly spread on the Mylar* side of the aluminium/mylar laminate and left to dry until tacky. When tacky the stainless steel centre plate is placed on one tacky adhesive surface and the other tacky surface is placed on top of the centre plate and the plates are pressed together forming a sandwich construction. Ferguson-Pell found it necessary to place a strip of Mylar 36μm thick between the tag portion of the stainless steel centre plate and the laminate as the spot weld frequently penetrated the thin 12μm Mylar film and short circuited the signal carried on the central conductor to the outer

---

* Mylar is a registered Trade Mark for polyester film Du Pont (U.K.) Ltd.

FIGURE 4.10. COMPARATIVE SIZE OF PRESSURE TRANSDUCER

TRANSDUCER TYPE	ADHESIVE SURFACE	STAINLESS STEEL CENTRE PLATE
I	SMOOTH	EMBOSSED
II	SMOOTH	SMOOTH
III	TEXTURED	SMOOTH
IV	TEXTURED	EMBOSSED

FIGURE 4.11. METHODS OF MANUFACTURING PARALLEL PLATE CAPACITIVE PRESSURE TRANSDUCERS

aluminium plates, which are grounded.

The diameter of the stainless steel centre plate used was 10mm and is taken as the active sensing area of the transducer. The overall diameter of the transducer head used by Ferguson-Pell is about 12mm and the "in-use" thickness about 200 - 300 μm. The size of the transducer is comparatively displayed in Figure 4.10.

Four different combinations of centre plate and dielectric were employed by the author in the manufacture of the capacitive pressure transducer designed, principally, to vary the shape factor of the compliant dielectric (Figure 4.11). The stainless steel centre plate was pressed onto a surface of a "bastard" file by a rubber pad to produce a uniform pattern embossed thereon and a "stipled" or textured surface of the dielectric was produced by brushing the adhesive in orthoganal directions when tacky.

4.4.1. Selection of Transducer Construction Method

In order to identify the most suitable type of transducer construction to be used, batches of ten transducers of the four different types of transducer used (I - IV) were constructed by the author. Each transducer was connected to signal processing apparatus (4.6.2) and was then placed in the pneumatic diagraghm calibration chamber and the response of each transducer to incremental and decremental changes of pressure was recorded. The results are displayed graphically in Figures 4.12 a,b,c and d.

From preliminary inspection of the graphical results, the response of transducers type IV, constructed with the emhossed centre plate and textured adhesive, displayed reasonably consistant outputs with less variation between transducers than in the other types, and also there was less hysteresis in each transducer output. Therefore it appeared that, initially, the transducer constructed with the embossed centre plate and textured dielectric, type IV, was most suitable with regard to the requirements of section 4.3.

FIGURE 4.12a RESPONSE OF TYPE I PRESSURE TRANSDUCERS TO APPLIED PRESSURE

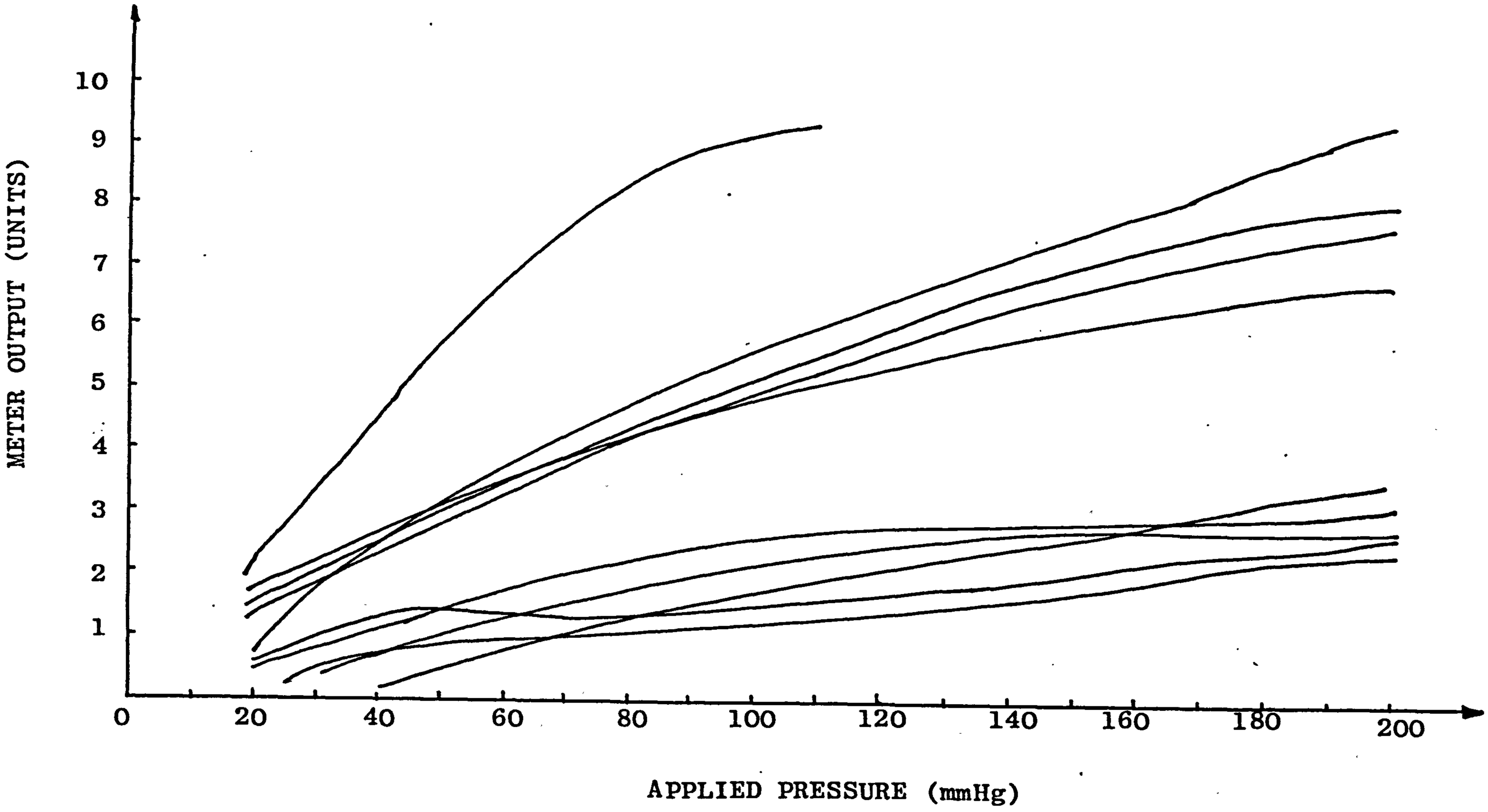

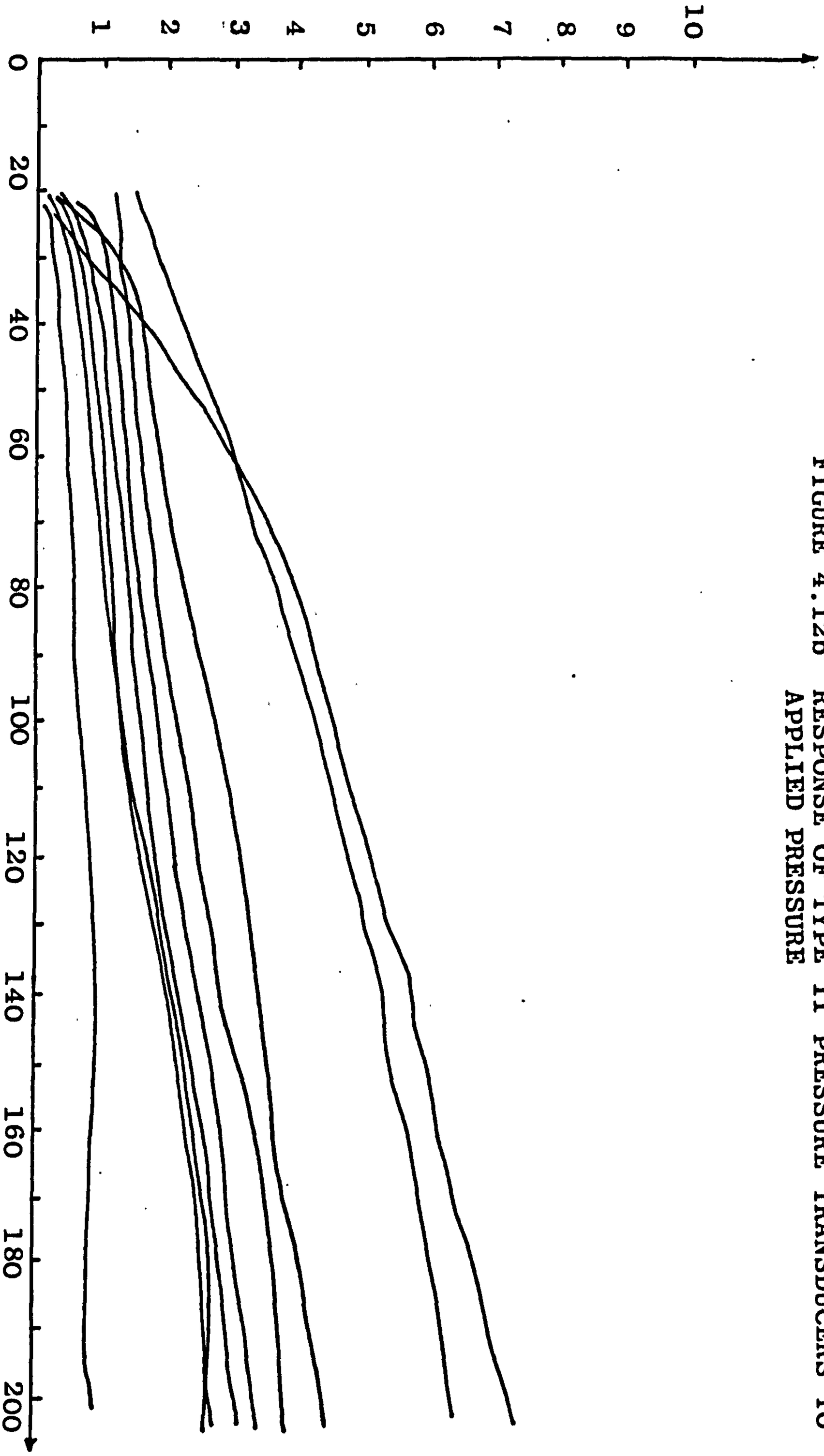

FIGURE 4.12b RESPONSE OF TYPE II PRESSURE TRANSDUCERS TO APPLIED PRESSURE

FIGURE 4.12c RESPONSE OF TYPE III PRESSURE TRANSDUCERS TO APPLIED PRESSURE

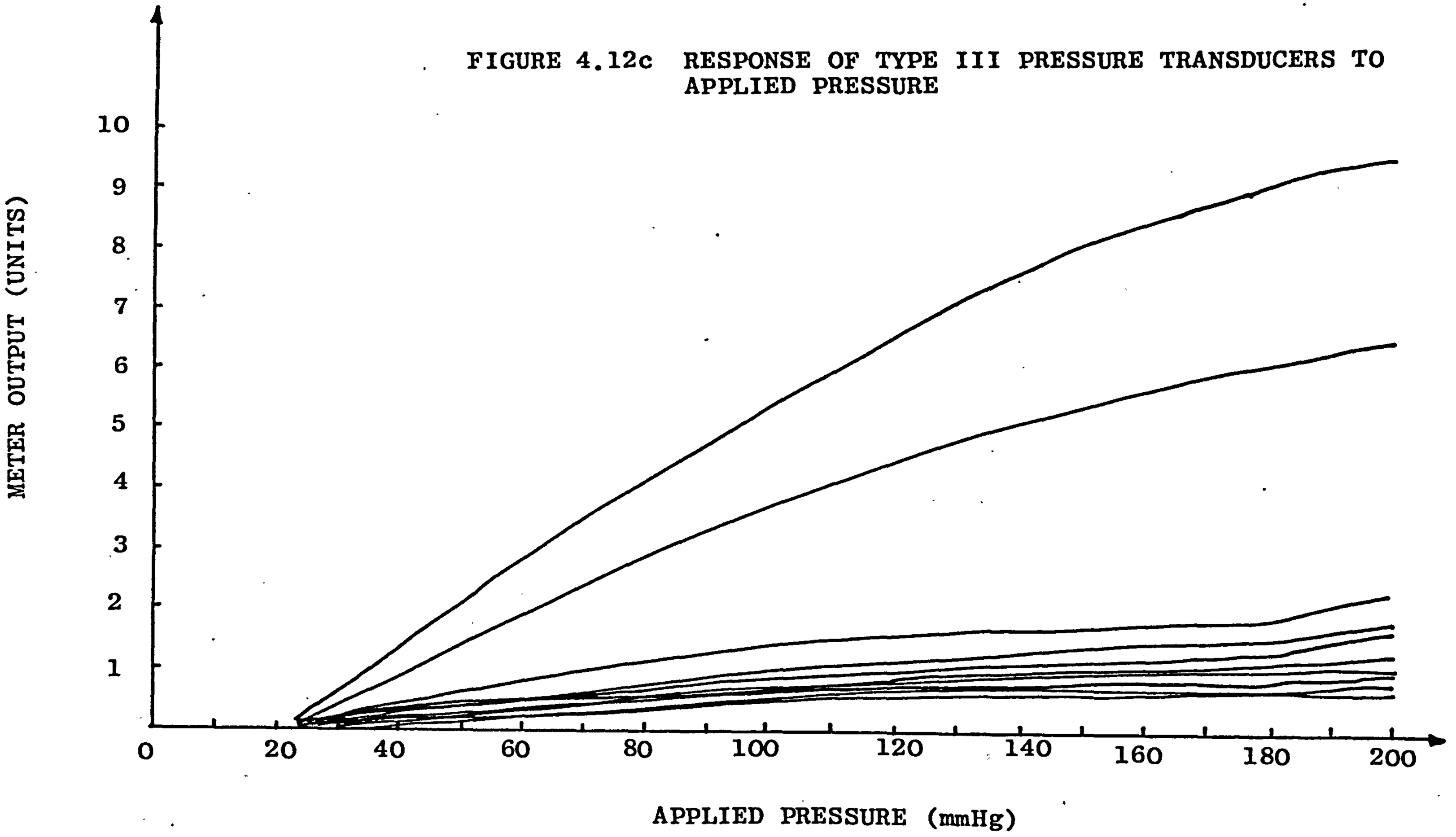

FIGURE 4.12d RESPONSE OF TYPE IV PRESSURE TRANSDUCERS TO APPLIED PRESSURE

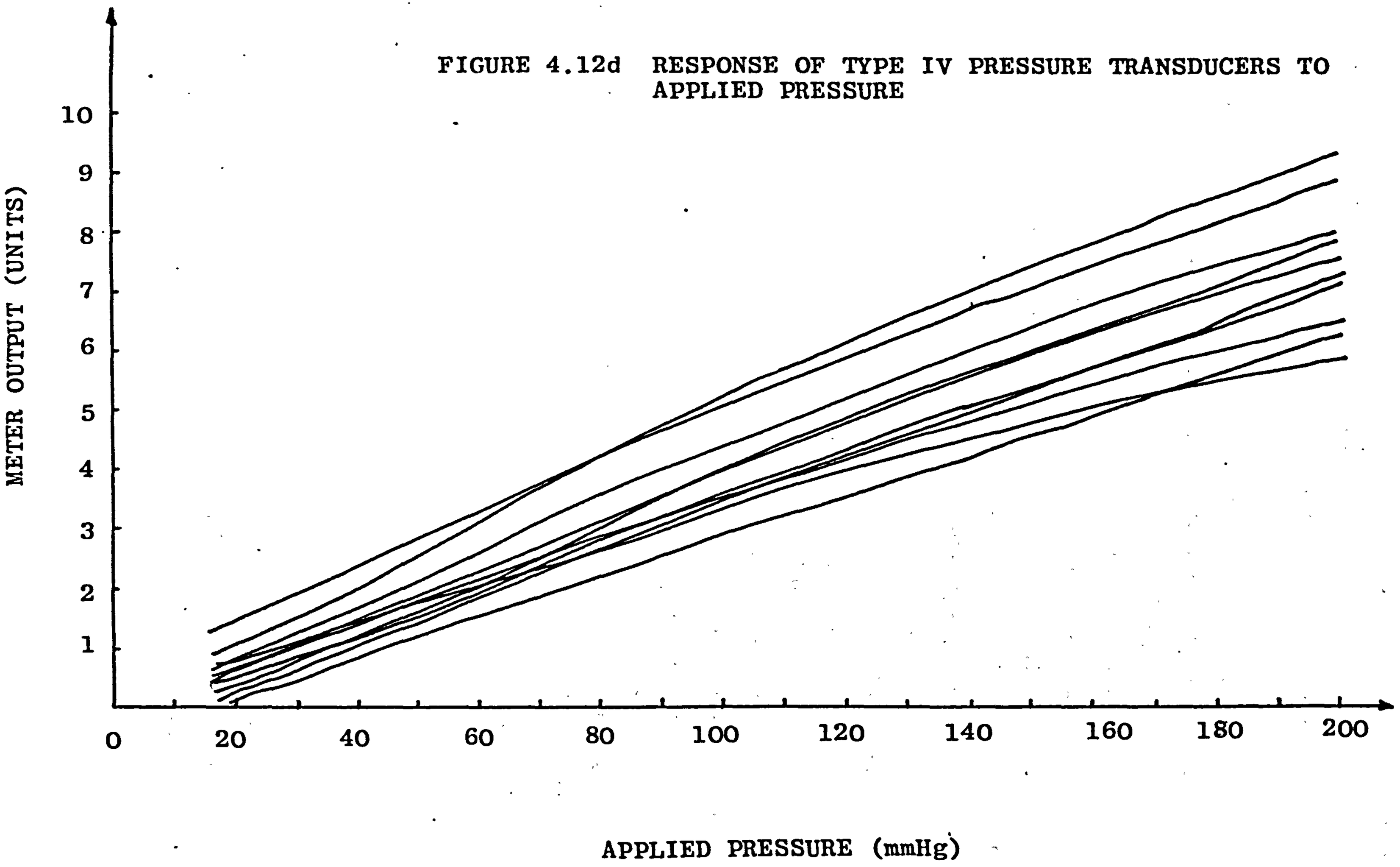

4.4.2. Temperature Conditioning

The transducers used by Ferguson-Pell were particularly susceptable to variations in temperature which as discussed (vide 4.3.1.2) can result in significant measurement artefacts. Reasons for this variation were thought to be due to incomplete drying of solvent in the dielectric and also perhaps to poor adhesion between the transducer plates resulting in the presence of air gaps contributing excessively to the temperature response.

The temperature response of each transducer was obtained by placing it in a variable temperature oven, accurate to $\pm .1^{o}C$ of the true thermostatic value, then the temperature of the oven was then raised slowly from room temperature ($18^{o}C$) to $40^{o}C$. The temperature in the oven was recorded continually by a thermistor placed in proximity with the active sensing area of the transducer at regular intervals, using a Mycalex Series 5 data logger system (Ferguson-Pell, 1977). The output from each transducer was continually recorded simultaneously to facilitate correlation between the temperature and the transducer output.

The temperature response of a typical transducer before temperature conditioning is shown in Figure 4.13 . The average temperature sensitivity of each transducer was calculated and construed as equivalent to a pressure change in $mmHg/^{o}C$. The average temperature sensitivity of the temperature preconditioned transducers was $-2.5mmHg/^{o}C$ which exceeds the value predicted theoretically in 4.3.1.2 by a factor of $\simeq 2$.

Each transducer was then temperature conditioned by placing it in an oven for at least 6 hours at a temperature of $100^{o}C$. Temperatures higher than $120^{o}C$ were found to adversely affect the mechanical properties of the polyester dielectric. After temperature conditioning each transducer was also calibrated by the pneumatic diaphragm calibration chamber to determine the pressure response, and was then placed within the variable temperature oven to determine

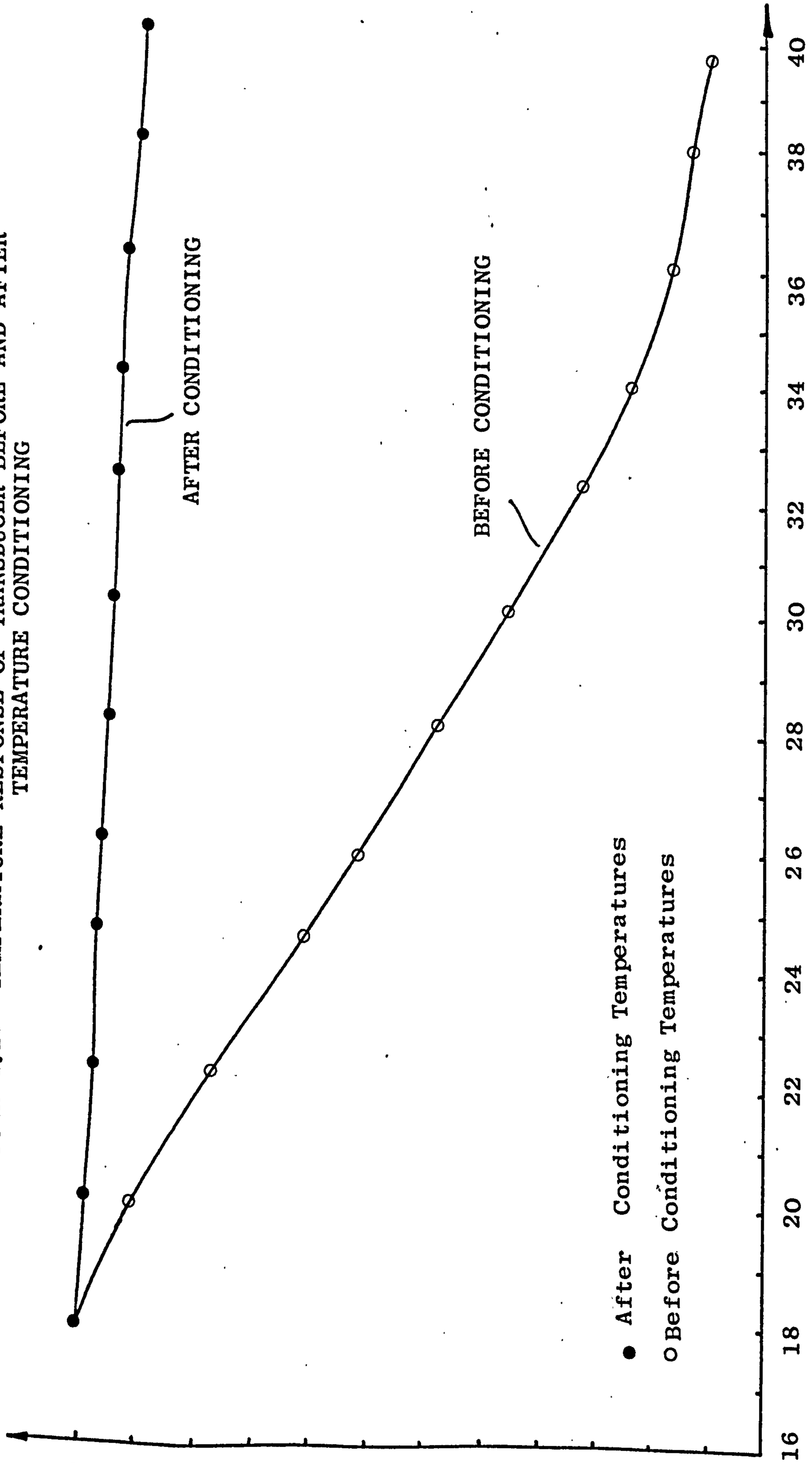

FIGURE 4.13 TEMPERATURE RESPONSE OF TRANSDUCER BEFORE AND AFTER TEMPERATURE CONDITIONING

the temperature response in a manner identical to that before the temperature conditioning. The average equivalent pressure change after conditioning was estimated to be 0.22 mmHg/^{o}C which is a reduction in temperature sensitivity by about one order of magnitude (Figure 4.13).

In addition, the average pressure response was found to be slightly linearised.

If the temperature difference between the calibration temperature and the interface temperature is assumed to be a maximum of 20^{o}C, and with the equivalent pressure change across this temperature difference limited to 1% of the calibration pressure range which is 100mmHg (vide 4.6.1.), i.e. 1mmHg, then the maximum equivalent pressure change over 20^{o}C is 0.15mmHg/^{o}C. Therefore if the scar surface temperature varies by 2 or 3 degrees celsius, the maximum error produced would be $\pm$ (0.1 - 0.15) mmHg/^{o}C which, in the case of a true pressure reading of 10mmHg, is about 1% - 1.5% of the true value.

Using the above criteria the results of the pressure and temperature responses were analysed: it was clearly confirmed by inspection that the temperature conditioned transducers had a much reduced average temperature sensitivity of 0.22mmHg/^{o}C which is much closer to the desired value of $\pm$ (0.1 - 0.15)mmHg/^{o}C.

Statistical validation of these results is, in view of the differences, unnecessary and would not contribute to the selection criteria due to the clearly superior pressure and temperature response of the temperature conditioned type IV transducer. These relatively simple tests carried out on varying transducer constructions clearly demonstrate the superiority and suitability of capacitive transducers constructed with an embossed centre plate and textured dielectric, in terms of pressure and temperature response.

Consequently, transducers of this type were selected to provide the basis for transducers which would be used clinically to measure pressures developed at the interface between hypertrophic scars

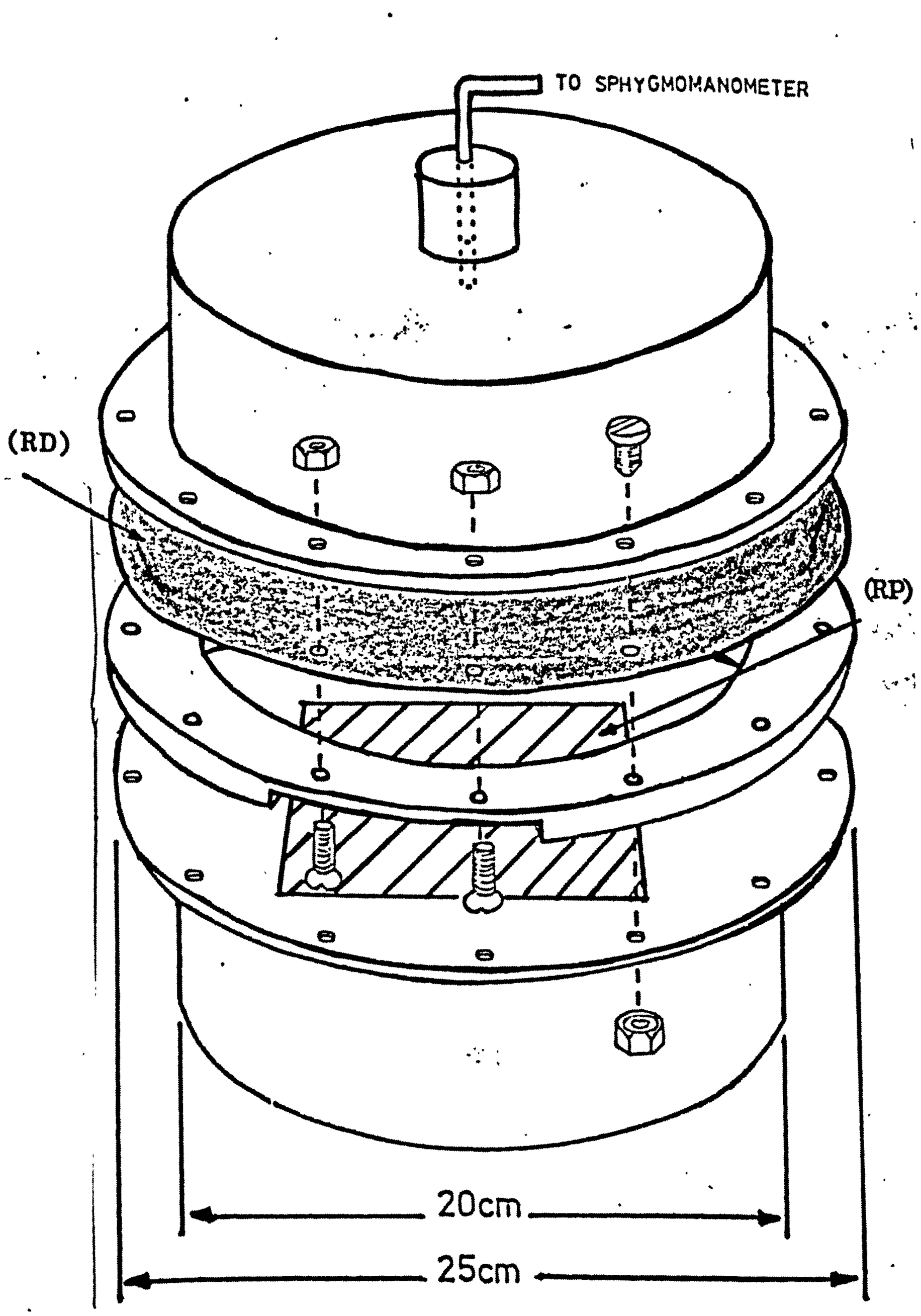

FIGURE 4.14 EXPLODED VIEW OF CALIBRATION CHAMBER WITH 0.25mm THICK LATEX RUBBER DIAPHRAGM (RD) AND LATEX RUBBER PAD (RP)

and elasticated garments. The transducer, however, requires yet further evaluation of its performance with regard to the theoretical limits imposed on the parameters specified in 4.3.

4.5. EVALUATION OF THE CAPACITIVE PRESSURE TRANSDUCER

Interfacing the transducer to suitable instrumentation which accurately reproduces the response of the transducer to pressure is essential before any practical investigation is performed. Ferguson-Pell (1977) initially used a Wayne Kerr Universal Bridge, B221A, with an autobalance adaptor AA221 operating at 1592KHz to perform laboratory evaluation of the transducer but later developed and used; a portable single channel capacitance monitoring device; and a 32-channel multiplexer capable of handling transducer arrays simultaneously for clinical work. Both the monitor and the multiplexer operation were based on capacitance bridges relying on pressure induced modulation of a 1KHz oscillator frequency, to provide a change in the bridge output.

The author further developed the single channel monitor of Ferguson-Pell (1977) inter alia ,to include five independent measurement channels, which could be selected by the operator (vide 4.6.2), and which was used to process signals detected by the capacitive pressure transducer.

Each pressure transducer was evaluated using the multiple-channel pressure monitor in accordance with a flow system specifically designed to evaluate the response of the transducer to the variables likely to be encountered in-situ (Vide 4.2.4.). A brief description of each of the important evaluation stages of the transducers are described below:

4.5.1. Standing Capacitance

The standing capacitance, C_o, was measured immediately after the completion of manufacture using a small capacitance meter. The size of the capacitors used in the capacitance

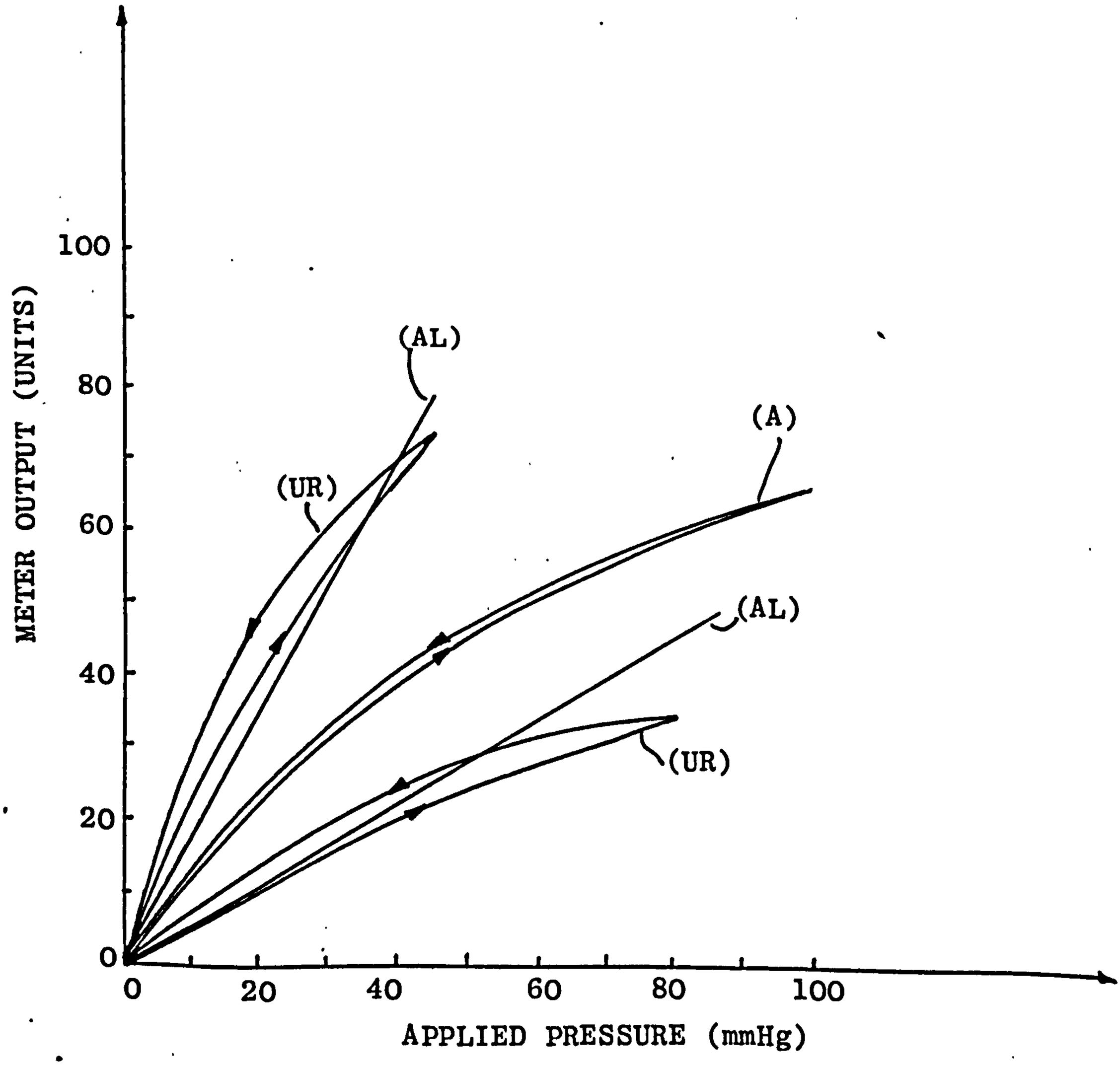

FIGURE 4.15 TRANSDUCER CALIBRATION RESPONSE WITH ACCEPTABILITY LIMITS (AL) AND ACCEPTABLE (A) AND UNACCEPTABLE (UR) RESPONSES

bridge dictated that standing capacitance values of the transducer should be within the range of 60 - 100pF if satisfactory operation of the monitoring system was to be achieved. Those transducers which lay within 60 - 100pF were then temperature conditioned for at least 6 hours at 100^{o}C and then the standing capacitance was remeasured using the same criteria; transducers outside the specified limits were rejected.

4.5.2. Transducer Calibration

Proper calibration of any measuring device is probably the most important procedure in the measurement of a parameter and may be a major item affecting accuracy of the measurand. The transducer was calibrated using both a primary and a secondary calibration procedure. The secondary calibration procedure consisted of placing a transducer between a latex rubber diaphragm connected to a pneumatically pressurisable chamber and a flat perspex plate, the perspex plate being secured to the pressurisable chamber by removable bolts as shown in Figure 4.14. The pneumatic chamber was pressurisable by a sphygmomanometer hand-pump which had an analogue scale display in mmHg.

Calibration was performed by inflating the membrane against a latex rubber mat located on the perspex plate and recording the transducer output for both increasing and decreasing changes of pressure in mmHg. Measurements were taken at a number of locations on the latex rubber mat and the variation between measured pressures, during the application of constant pressure, was negligible. A calibration curve, considered as acceptable, is shown in Figure 4.15. From inspection it is seen that the transducer response to increasing pressure is different from the response to decreasing pressure: a apparently greater output resulting in the decreasing pressure response for the same value of applied pressure. This is hysteresis (vide 4.2.4.6).

From studying a large range of pressure transducer calibration responses (>100), it was possible to specify criteria for which each transducer had to meet to prove

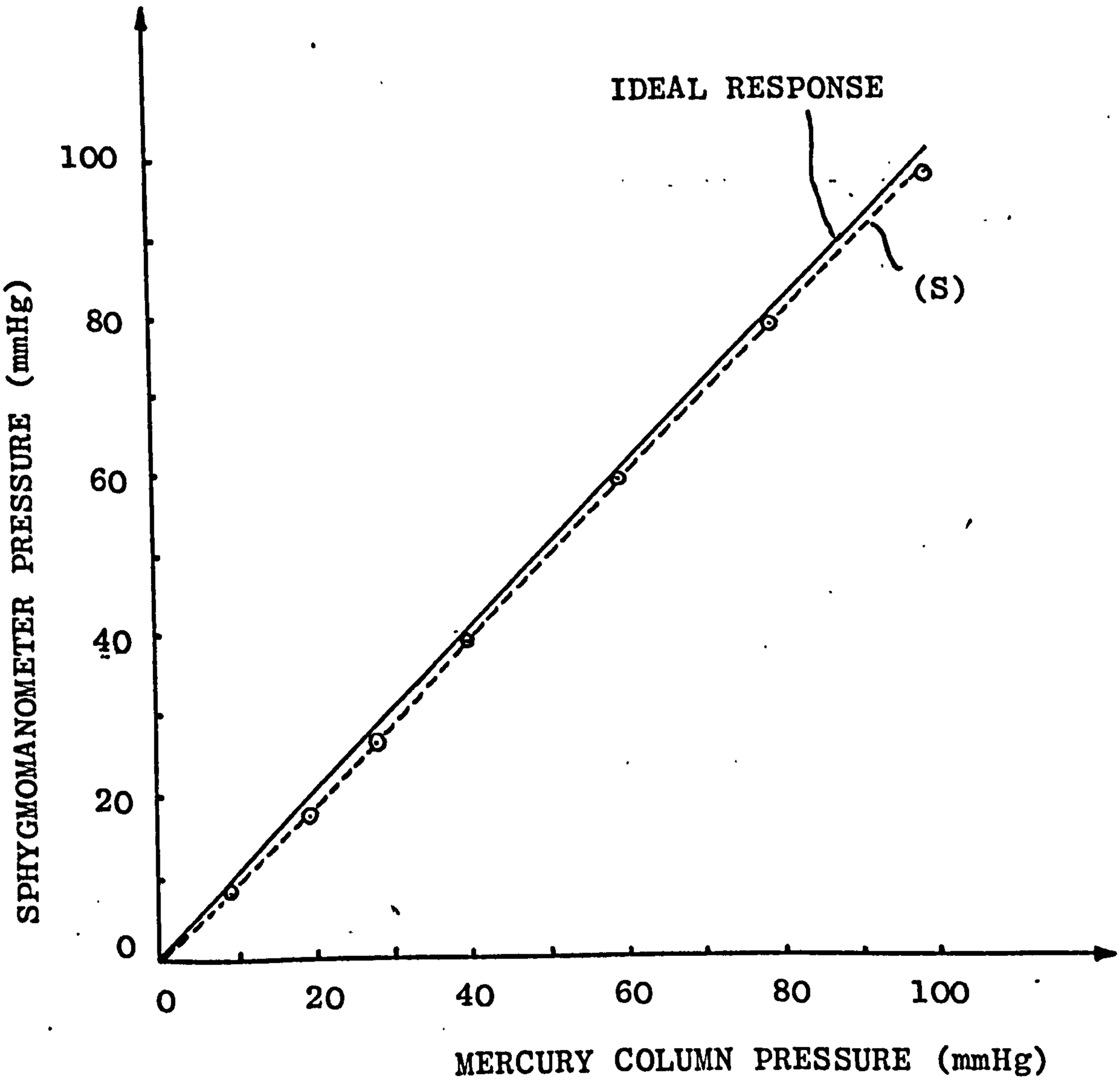

FIGURE 4.16 CALIBRATION OF SPHYGMOMANOMETER (S) AGAINST MERCURY COLUMN

suitable; very low sensitivity and also very high sensitivity transducers produced the largest hysteresis errors. The limits for evaluating the suitability of calibration response is shown in Figure 4.15, with unacceptable calibration responses also shown. Although not an absolute test for determining suitability of the transducer response to pressure these criteria were later justified by consistent in-situ transducer responses (Chapter 5).

Another important factor was the magnitude of the residual transducer output on removal of pressure after calibration. High residual outputs are obviously unacceptable since they can represent large equivalent pressures. From studying the same group of transducer calibration responses as above 2 - 3mmHg as an upper "zero" limit was deemed to be acceptable by the author.

The transducer responses arising from secondary calibration procedure were reanalysed by the primary calibration procedure in which the pneumatic sphygmomanometer hand-pump was calibrated against a mercury column so that the output of each transducer could be directly and accurately expressed in mmHg. The primary calibration of the hand-pump is shown in Figure 4.16 and it is evident that the transducer outputs have to be modified considerably especially at low pressures (< 30mmHg), to provide accurate results.

The author examined in great detail the possibility of presenting the transducer output directly in units of pressure, particularly mmHg, however the technical problems which were not inconsiderable were greatly overshadowed by the variation between transducer pressure calibration responses which made modelling by present electrical technology virtually impossible.

Thus, each transducer was calibrated in mmHg using the primary and secondary calibration procedures. Transducers failing to satisfy the criteria hereinbefore described were rejected.

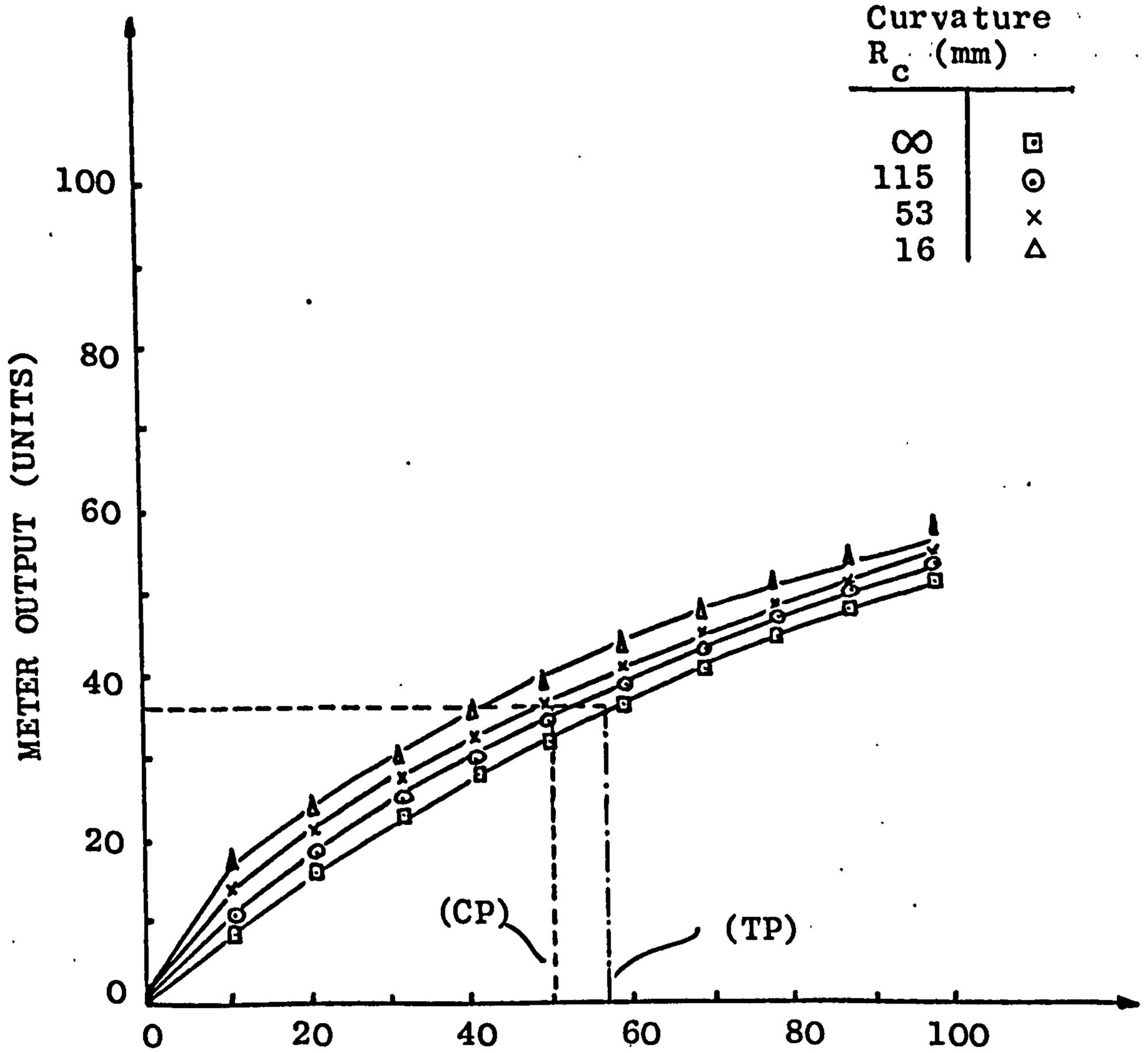

FIGURE 4.17 PRESSURE RESPONSE OF LOADED TRANSDUCER TO CURVATURE SHOWING TRUE PRESSURE (TP) AND PRESSURE MODIFIED BY CURVATURE (CP)

4.5.3. The Response to Temperature

Each transducer was tested for temperature sensitivity as specified in 4.4.2. and those which did not meet the specification described therein were rejected. It should be noted that, after temperature conditioning, the response of the transducer to temperature was similar to that predicted by the theory (vide 4.3.1.2).

4.5.4. The Response to Curvature

A transducer was secured to curved surfaces of plaster-cast objects by adhesive tape, so that the transducer head was conformed to the curvature of the shape thereunder. The transducer was then located in the calibration chamber (4.5.2) and the response of the transducer to varying radii of curvature was recorded in mmHg as shown in Figure 4.17. It is immediately apparent that there is a considerable increase in the error produced by decreasing radii of curvature.

In particular, if the transducer is conformed over a surface with a radius of curvature of 53mm, the output from the graph is equivalent to 100mmHg whereas the true equivalent pressure for infinite radius of curvature is 116 mmHg i.e. there is an error of 16mmHg or ≏14% of the true value. In addition, as the pressure measured is due to a combination of both curvature and normal and in-plane membrane forces it is difficult to quantify the error due to curvature alone, other than by simple subtraction. This method of evaluating the transducer response to curvature is however fairly representative of the clinical measurement situation in which the transducer is loaded when deformed although there is scope for further characterisation of the behaviour of the transducer under load when deformed by curvature, without membrane effects being present.

4.5.5. The Response to In-Plane Forces

The design of an experiment in which known shear forces are applied and to which the output of a transducer is compared is extremely difficult to implement from both

FIGURE 4.18 COMPARISON BETWEEN STATIC TRANSDUCER OUTPUTS (SO) AND OUTPUT WHEN TRANSDUCER IS PULLED OUT OF CHAMBER (MO) WITH 140mmHg APPLIED PNEUMATIC PRESSURE
(After Ferguson-Pell, 1977)

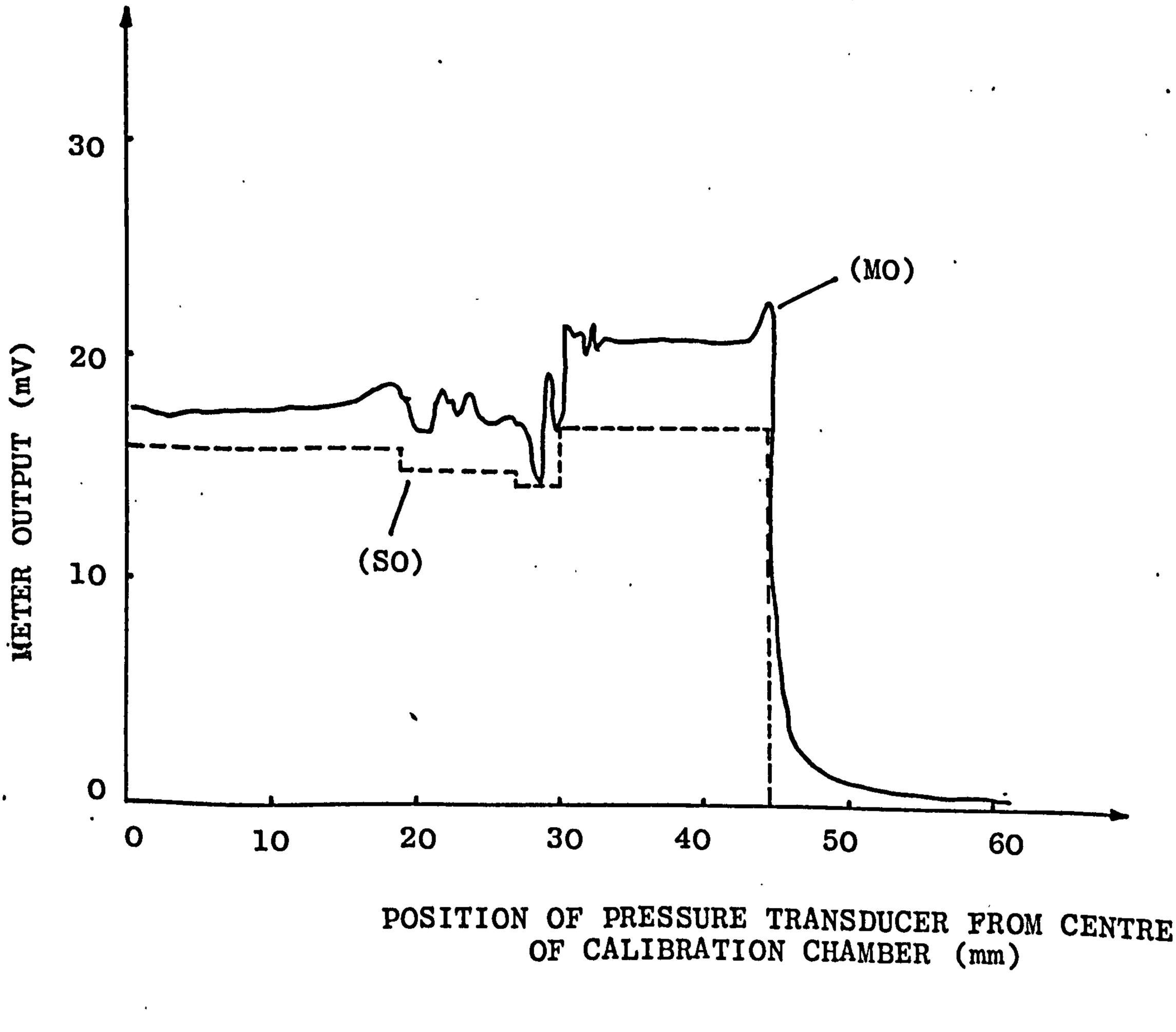

theoretical and practical viewpoints. A conventional method of applying shear force consists of fixing the plates in the measurement direction followed by applying a deformation in an orthogonal direction thereto; this method, however,is not possible with the present pressure transducer since the transducer dimensions, and mechanical properties of the construction materials, are fundamentally incompatible with such a method.

Ferguson-Pell (1977) developed a method of assessing the sensitivity of a transducer to in-plane forces when the transducer was under a normal load. The transducer was placed in the calibration chamber and the pneumatic chamber pressurised to 140mmHg, the transducer being compressed between the diaphragm and the perspex plate. The transducer was then pulled slowly from the chamber, the output of the transducer being recorded during this procedure.

Static pressures were also recorded at distances from the centre of the diaphragm after removal of the transducer. The difference between the transducer output when the transducer is static and when "in-plane" forces are applied is shown in Figure 4.18. Although superficially it appears that the "in-plane" forces are a significant proportion of the static pressure it must be understood that the "in-plane" forces were <u>not</u> static and they may be artificially high due to motion-induced transient pressures hence the true contribution of in-plane forces could in fact be considerably smaller. The author believes that a deeper examination of the influence of in-plane forces would significantly contribute to the development of the capacitive pressure transducer.

4.5.6. <u>The Response of the Transducer to Constant Load</u>

Each transducer was located on a flat surface and was loaded with 1, 5 and 30Kg weights respectively all the weight being assumed to act through the active sensing area of the transducer. Thus on the $1cm^2$ active area respective pressures of 750mmHg, 3750mmHg and

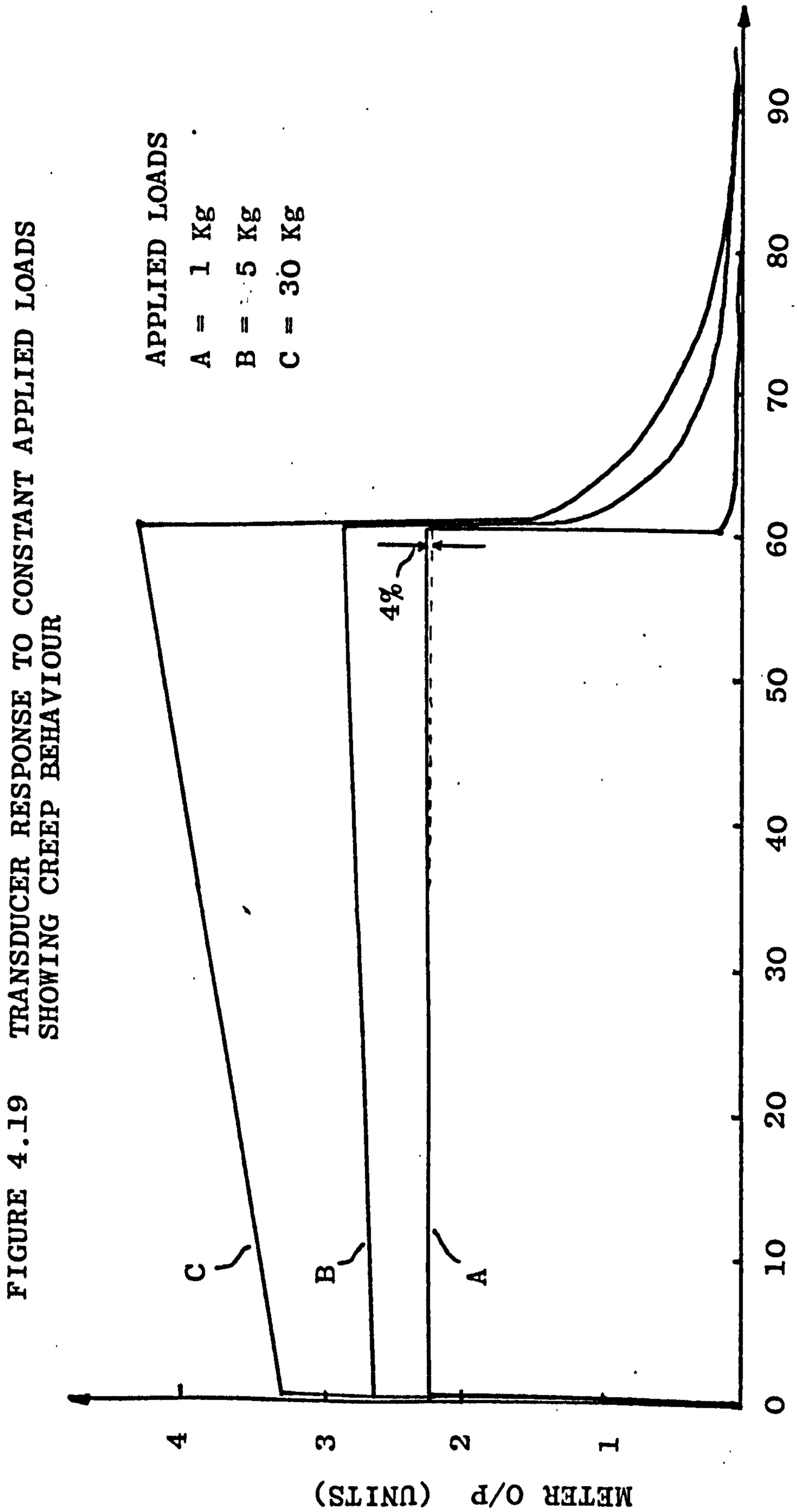

FIGURE 4.19 TRANSDUCER RESPONSE TO CONSTANT APPLIED LOADS
SHOWING CREEP BEHAVIOUR

2.25×10^4mmHg were applied. Each weight was maintained on the transducer for a period of 60mins. which was thought to be an acceptable duration for evaluating the response of the transducer (Figure 4.19). Under constant load the transducer response, which is assumed to be wholly due to the mechanical properties of the dielectric (vide 4.3.1.1.), exhibited behaviour similar to that of a linear visco-elastic material (vide 4.3.1.5.).

The maximum change in output due to 750mmHg occured after 60mins. and was less than 4% of the applied pressure value. The maximum output change is within the limiting value (5%) specified in 4.3.1.5. Consequently, as the designed range of pressure is 0 - 200mmHg, and with measured values of pressure at the scar dressing interface expected to be somewhat less than 100mmHg, it is reasonable to assume that the error due to creep of the transducer dielectric would, in normal clinical use, be negligible.

4.5.7. Discussion

One major problem with the pressure transducer construction technique developed by Ferguson-Pell (1977) was that four different methods of manufacturing the transducer were employed. Consequently no one type of transducer was made continuously, and this may have been responsible for the inconsistent transducer responses reported. The restriction of transducer manufacture to a single technique, in theory, should improve the consistency of transducer response . The four sets of different transducer types constructed by the author demonstrated widely varying group responses to pressure. By inspection the transducer type having an embossed centre plate and smooth dielectric showed the most consistent pressure response and also the least hysteresis error. Improvement of the transducer response requires optimisation of the manufacturing technique; basic and thorough investigation is required to identify the effect of each stage of manufacture on the integrity of the pressure transducer.

The improvement in the temperature response of the transducer following temperature conditioning is dramatic however the means by which the improvement is effected remains unclear; removing the solvent from the adhesive; removing air bubbles trapped in the adhesive; and modification of the structure of the dielectric are possible explanations which require further investigation. The reduction in temperature sensitivity by an order of magnitude following temperature conditioning is a significant improvement, and means that pressures measured clinically should have a maximum error, due to temperature changes, of about $\pm$ 0.5mmHg.

Experiments to determine the response of the transducer to physical variables do not entirely comply with the theory due to practical and technical considerations. Therefore, in comparing predicted and measured responses the results of the experiments should be tentatively construed. The most significant error is due to curvature. It is possible to minimise the curvature error by constructing a set of calibration curves with the transducer loaded over various known radii of curvature, measuring the radius of curvature of the site being measured and then selecting an appropriate calibration curve from which to find the pressure in mmHg. This method requires that each transducer has a set of calibration curves produced before each measurement session for various radii of curvature, and is both time-consuming and labourious.

An alternative method of minimising the curvature error is to position the transducer on a curved surface and adjust the monitor output until the display reads zero. After the garment is fitted, the output recorded is converted to pressure from a typical calibration curve. Experiments indicated that this method is satisfactory for radii of curvature from ∞ to 40mm, however the errorrapidly increases with decreasing radius of curvature below 40mm.

Although the error due to curvature appears to be less than that predicted by the theory it is still likely to be the most significant artefact in the pressure value.

4.6. DESIGN AND CONSTRUCTION OF A SIGNAL PROCESSING CIRCUIT

There are several methods by which capacitive changes in the parallel-plate capacitive pressure transducer may be detected and measured. The principle of detection uses the change in the standing capacitance of the transducer which occurs when the transducer is loaded. The sensitivity to change is defined as the ratio

$$\frac{\text{change in capacitance}}{\text{standing capacitance}} = \frac{\Delta C}{C}$$

In order to facilitate detection, the ratio $\frac{\Delta C}{C}$ should be as large as possible. In practice, the effective standing capacitance is greatly increased over the actual pressure transducer standing capacitance due to capacitive coupling of connecting leads, switches, plugs etc. between the transducer and the detecting circuit as "seen" therefrom. Thus the ratio $\Delta C/C$ is reduced, in turn reducing the sensitivity of the detecting circuit.

4.6.1. Principles of Signal Detection

Two principal methods for detecting capacitive changes are conversion of the capacitance change to frequency and measurement of the capacitance change by a capacitance bridge.

4.6.1.1. Capacitance to Frequency Conversion The principle of this method involves connecting the transducer, as a passive component, to a tuned oscillator circuit the natural frequency of which is determined by the reactance of each of the passive components. When the transducer is loaded the capacitance and hence the reactance vary thereby modulating the oscillator frequency.

The Gouriet-Clapp oscillator utilises this principle and the change in frequency of the oscillator may be related to the change of capacitance by

$$V = \frac{V_o \Delta C}{4C}$$

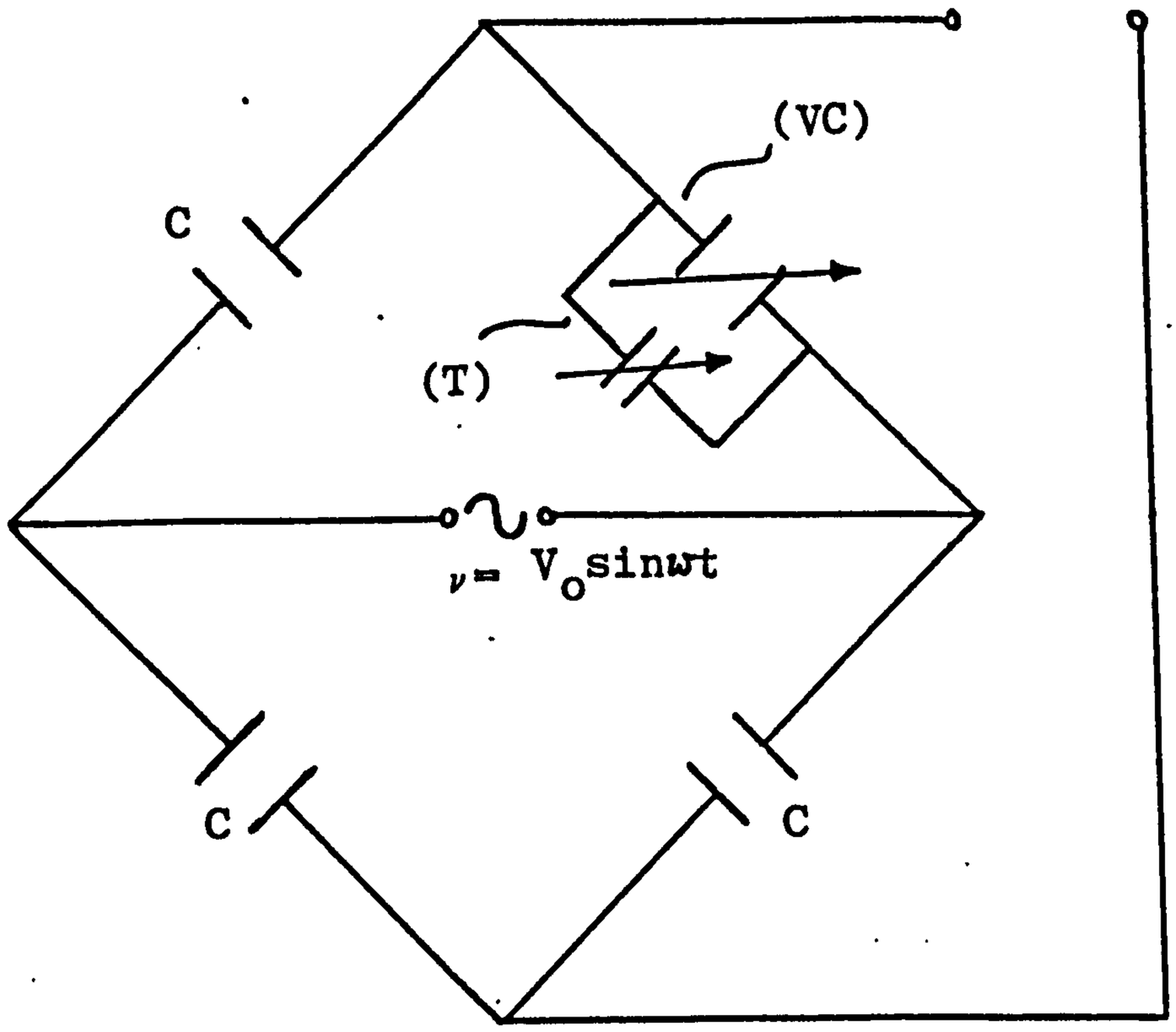

FIGURE 4.20. CAPACITANCE BRIDGE CIRCUIT DIAGRAM WITH TRANSDUCER (T) AND VARIABLE CAPACITOR (VC) CONNECTED IN PARALLEL

$$\Delta f = \frac{-\Delta C}{4\Pi^2 f_o L C^2} \qquad 4.25$$

Inspection of equation 4.25 shows that the change in frequency, Δf, is inversally proportional to the square of the standing capacitance of the transducer, which implies a low sensitivity to capacitance changes. Indeed, the Gouriet-Clapp oscillator is designed to avoid frequency instability due to component manufacturing tolerances, temperature sensitivities and stray capacitance. Thus the principle of operation of the oscillator conflicts with the concept of the capacitive pressure transducer which requires that a small change in capacitance should produce a large change in oscillator frequency. The oscillator frequency should also be independent of the standing capacitance of the oscillator.

4.6.1.2. The Capacitance Bridge The capacitance bridge is similar in construction and operation to a full a.c. energised Wheatstone bridge except that the arms of the bridge include capacitors instead of resistors. Three of the bridge arms have known values of capacitors, two being fixed and one being variable. An unknown capacitance, in this case the transducer, forms the fourth arm of the bridge as shown in Figure 4.20. An important advantage is using a capacitance bridge is that the phase difference between the bridge input and output signals is independent of capacitance change i.e. only the amplitude of the bridge output signal in dependent on the magnitude of the capacitance change.

The relationship between the bridge output signal and the change in capacitance of the bridge is given in Appendix A , and states that for a bridge having identical values of capacitors, and for a change in capacitance of the transducer less than 10% of the standing or unloaded value, the sensitivity of the bridge is defined as

$$\frac{\Delta V}{\Delta C} = \frac{V_o \Delta C}{4C} \qquad 4.26$$

V = the amplitude of the bridge a.c. excitation voltage.

Over the range of the anticipated capacitance change, the sensitivity of the bridge ($\Delta V / \Delta C$) is independent of phase. Section 4.5.1. stated that the standing capacitance should be between 60pF and 100pF. When the transducer is connected to the capacitance bridge the effective capacitive "seen" by the bridge is the transducer standing capacitance plus the capacitance of the coaxial cable used (Filotex 50 VMTx, Waycom Ltd., Bracknell, U.K.). The nominal cable capacitance is 85pF/m and the average length of cable used to connect the transducers to the pressure monitor was about 1.5m. The effective standing capacitance of the transducer "seen" from the bridge was between 200pF - 250pF.

The average maximum capacitive change recorded from the transducers tested was about 4pF over the range 0 - 200mmHg and the relationship between capacitance change and bridge output voltage was approximately linear. This gives a maximum sensitivity to capacitance to change of about 2% which is able to be processed with fairly basic electronic circuitry.

The energisation frequency of the capacitance bridge is freely selectable however a 2V peak to peak 1 kilohertz (1 KHz) frequency supplied from a Wein oscillator was found to be very stable and easy to preset in the oscillator. The standing capacitance of the pressure transducer is variable using a 180pF capacitor (Jackson (London) Ltd., U.K.) connected in parallel with the transducer. This enables the bridge to be balanced to give a minimum, or zero, output for zero pressure input for any transducer. Additionally, the a.c. energising frequency was adjusted to oscillate about earth potential so that the a.c. time average voltage was zero. This provided an earth screen to prevent capacitive coupling of the transducer.

The capacitance bridge satisfied the technical

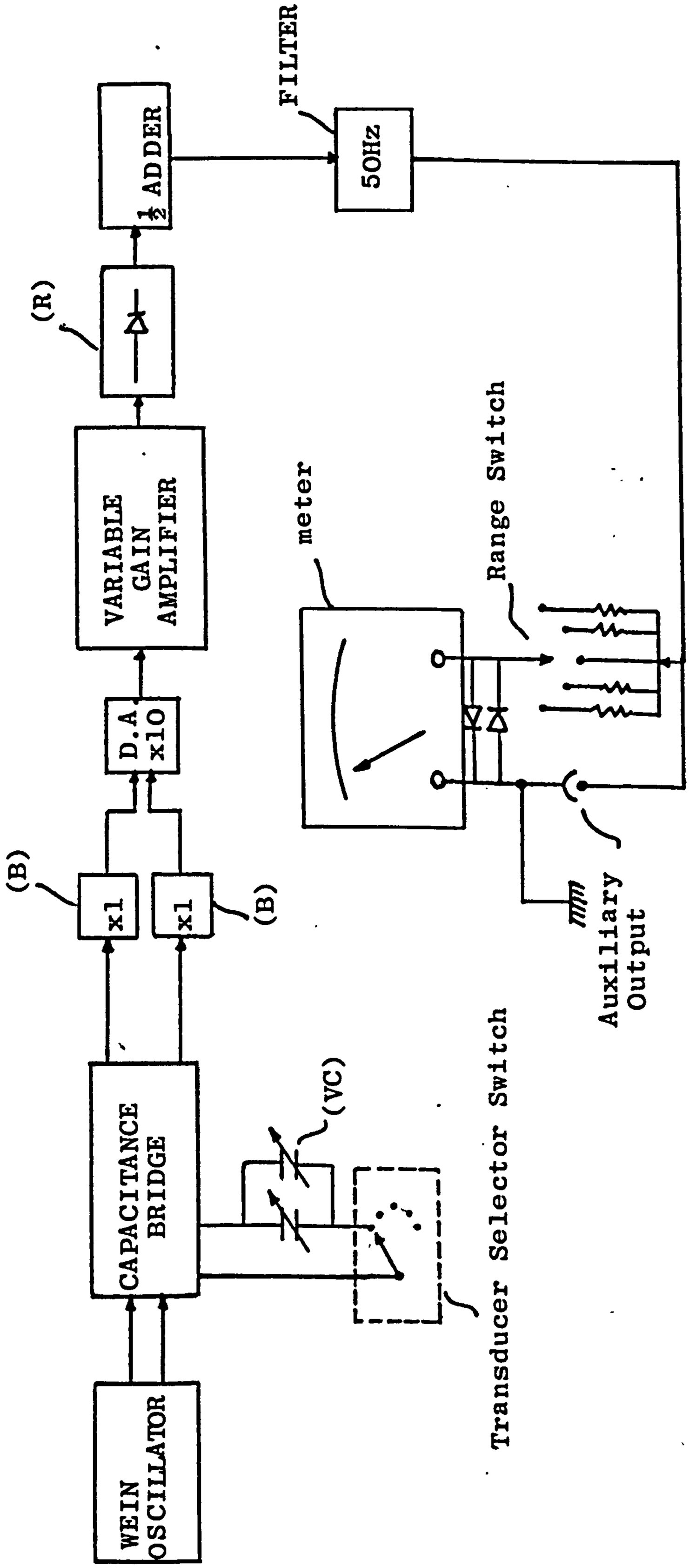

FIGURE 4.21 BLOCK DIAGRAM OF CAPACITIVE PRESSURE MEASUREMENT SYSTEM WITH BUFFERS (B), DIFFERENTIAL AMPLIFIER (D.A.) AND RECTIFIER (R)

requirements of producing a readily measurable output signal for small capacitance changes, an approximately linear relationship between change in capacitance for change in output voltage and the usability with any capacitive pressure transducer by virtue of the standing capacitance compensation facility.

4.6.2. Design and Construction of Signal Processing Circuitry

An amplitude modulation circuit was designed to process the bridge output signal so that the monitor output signal would be clearly related to the applied pressure.

Frequency stability of the Wein oscillator signal, although satisfactory, was not critical. Fluctuations in the amplitude of the oscillator signal were prevented by using back-to-back diodes in the oscillator feedback loop. Figure 4.21 is a block diagram of the signal processing circuit and a detailed circuit diagram of the same is given in Appendix A .

The output signal taken across the bridge was fed through two unity gain bootstrapping amplifiers arranged in parallel each of which perform two major functions; the unity gain prevents spurious or transient bridge signals from being efficiently processed; and the "bootstrapping" is a technique which prevents distortion of signals due to the occurance of small capacitance changes in the cables carrying the signals. The outputs of the unity gain amplifiers were fed to a differential amplifier having a gain of 10 which amplifies the small signal appearing across the bridge output to a level which can be processed easily without undue distortion or noise artefacts being produced. The output of the differential amplifier was connected to a non-inverting amplifier with a variable gain which could be switched by the operator to give amplifications of 100, 200, 500 and 1000. The output frequency of the non-inverting amplifier was 1 KHz and was converted to d.c. by a full-wave rectifier. "Rippling" on the d.c. rectified signal was removed by a low-pass filter.

FIGURE 4.22. CAPACITANCE BRIDGE PRESSURE MONITOR

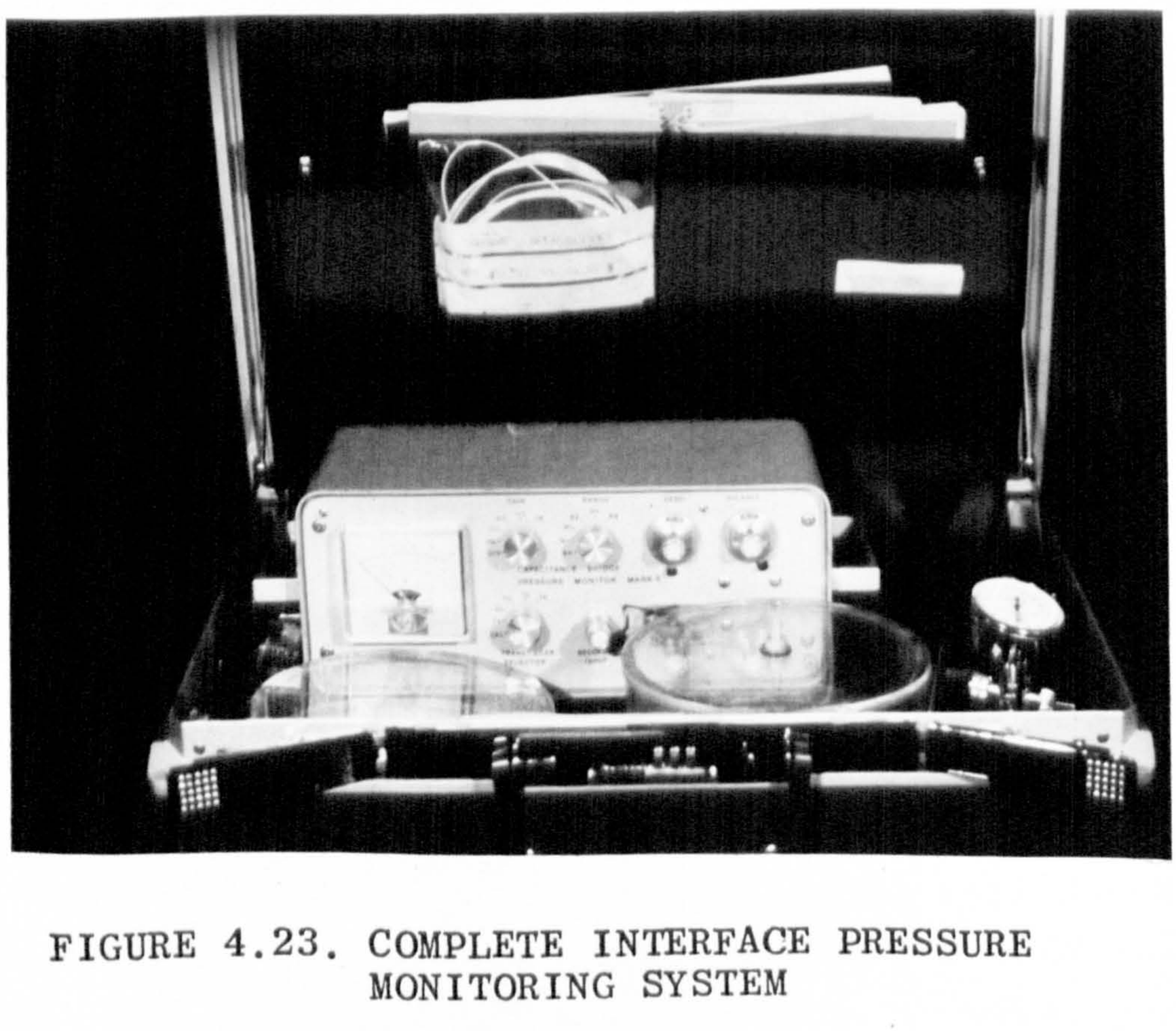

FIGURE 4.23. COMPLETE INTERFACE PRESSURE MONITORING SYSTEM

A visual output of the transducer response was displayed on a moving coil meter (Radio Spares Ltd., U.K.) by connecting the filter output signal thereto. The output from the filter was also connected to a BNC socket to provide an auxiliary output and permit a permanent recording of the monitor output signal, if required, onto a chart recorder. The resolution of the pressure monitoring system was 1mmHg but the accuracy was determined by the moving coil meter which was 2.5% of the full scale deflection (FSD). Therefore if the meter FSD was set to display a pressure range of 100mmHg the accuracy of the system is $\pm$ 2.5mmHg.

The circuit was powered by two 9volt carbon/zinc cells, and was housed in a portable casing. (Figure 4.22). The pressure monitor was, before full laboratory evaluation or clinical use, tested for electrical safety in accordance with the Bioengineering Unit Safety Regulations and H.T.M.8 and was found to satisfy the specified safety criteria.

The complete interface pressure monitoring system consisting of the transducers, pressure monitor and calibration chamber was completely portable and easily carried in a conventional attatche case (Figure 4.23).

The pressure monitoring system was evaluated and gave a stable output signal. The output sensitivity of the capacitance monitor was found to have ample flexibility, accommodating a wide range of transducer sensitivities to pressure. The range of the back-off facility was found to be adequate and is easily controlled. A complete description of the setting up, calibration and usage procedure of the interface pressure monitoring system is presented in Chapter 5.

4.6.3. Comparison between Capacitive Pressure Transducer and Other Interface Pressure Transducers

Although the capacitive pressure transducer was selected as the most suitable transducer with which to measure interface pressures (vide 4.3.), its success is also dependent on other factors such as cost effectiveness, and ease of use for the technically untrained person

(nurse , physiotherapist) who is likely to operate the pressure monitoring system. Of the other interface pressure transducers available two types predominate as likely competitors; a strain-gauges diaphragm transducer (Gaeltec Ltd., Skye, U.K.) and a pneumatic pressure transducer (Talley Scimedics Ltd., U.K.).

A technical comparison between the capacitance pressure transducer and the Gaeltec transducer was performed by Ferguson-Pell (1977) who showed that, despite the superior claimed accuracy of the Gaeltec transducer, the low aspect ratio and high sensitivity to in-plane forces obviated its use as a suitable interface pressure transducer. An additional disadvantage of the Gaeltec is that, as <u>each</u> transducer costs in the region of £250 and the signal processing circuit about £750, the capital equipment cost is very much greater than the capacitive system.

The pneumatic pressure transducer comprises a mitred inflatable plastic sac about 25mm in diameter and about 1 - 2mm thick with an electrical contact or electrode secured to each inner opposite face of the bag so that when the bag is inflated the contacts separate and when the bag is uninflated the contacts close. The pneumatic transducer is attached to a hand control which includes a gauged sphygmomanometer and a light which illuminates when the contacts are closed. When in use, the bag is placed at an interface and loaded. The bag is then inflated so that the contacts just separate; when this happens the light goes out and the pressure on the gauge is taken as a measure of pressure at the interface.

The aspect ratio of the pneumatic transducer is less than the capacitive transducer by a factor of 3 which indicates that its perturbation effect is greater. The pneumatic transducer also has a lesser spatial resolution than that of the capacitive transducer.

In terms of cost effectiveness, the cost of a single capacitive pressure transducer <u>per se</u>, estimated to be about £10 - 11, is comparable with the cost of a pneumatic

system is, at present, about £50 - 60 whereas the prototype pressure monitor cost about £100 to construct. Therefore although the capital cost of equipment is greater for the capacitance device, the cost/transducer is comparable and if the manufacture of the transducers and the monitor was put into production, the total unit cost could be significantly reduced.

Thus, for the purpose of the present investigation, the technical performance of the capacitance transducer is superior to that of comparable devices. In addition, the capacitance pressure monitoring system compares favourably, on a cost effective basis, with the pneumatic system which is probably the cheapest commercially available system.

4.7. SUMMARY

The geometrical requirements of an interface pressure transducer are defined. In particular, the amount of interface perturbation produced by the transducer is related to the surface area of the transducer and the thickness thereof. The ideal response of the transducer to physical variables other than pressure is discussed. A parallel-plate capacitive pressure transducer was selected to measure interface pressures in the present investigation. Theoretical models of the transducers response to physical variables other than pressure during measurement demonstrated that the physical variables are responsible for the occurance of significant errors in the pressure measured. Limitations of the transducer's response appears to be principally concerned with the choice of dielectric material and the intrinsic dependence of the capacitive transducer on geometrical changes.

Of four methods used to construct the capacitive pressure transducer the method using an embossed centre plate and a textured dielectric resulted in pressure transducers with a more consistent and less hysteretic response to applied pressure. The overall dimensions of the capacitive

pressure transducer were highly satisfactory with regard to the ideal design criteria; 12mm in diameter and about 0.2 - 0.3mm thick.

Temperature sensitivity of the dielectric was almost entirely obviated by temperature conditioning the transducer for at least 6 hours at 100^{o}C; the temperature sensitivity being reduced by about an order of magnitude.

A transducer evaluation program was developed to improve and eventually optimise transducer manufacture although more basic information is required to control the variables present during manufacture. The transducer was quickly and accurately calibrated using a pneumatic secondary and a mercury column primary calibration system.

The experimental response of the transducer to physical variables is similar to the response predicted by the theoretical models, except in the case of curvature, which was much less than predicted.

An a.c. capacitance bridge detection circuit was found to be a suitable circuit for measuring capacitance changes occuring when the transducer is loaded. The capacitance bridge circuit was interfaced to a signal processing circuit which amplitude modulated and processed the bridge output signal to a d.c. signal. The displayed d.c. output signal is calibratable in mmHg. The entire interface pressure monitoring system had a resolution of 1mmHg and an accuracy of $\pm$ 2.5% of the meter full scale deflection.

The performance of the capacitive pressure transducer is shown to be technically superior to the pneumatic pressure sensor and to the strain-gauged diaphragm transducer.

In cost effective terms the monitoring system compares favourably with commercially available devices.

The capacitive parallel-plate pressure monitoring system although not ideal is believed to constitute a satisfactory system with which to measure pressure developed at the hypertrophic scar surface/elasticated dressing interface.

CHAPTER 5

CLINICAL INVESTIGATIONS OF PRESSURE APPLIED TO HYPERTROPHIC SCARS

5.1. Introduction

5.2. Pressure Applying Materials

- 5.2.1. Lycra Garments
- 5.2.2. Tubigrip Garments

5.3. Method of Measuring Pressure

- 5.3.1. Selection of Measurement Site
- 5.3.2. Calibration of Pressure Transducers
- 5.3.3. Measurement of Pressure
  - 5.3.3.1. Pressure Measurements with the Transducer Static
  - 5.3.3.2. Pressure Measurements with the Transducer being moved to Different Sites

5.4. Experimental Results

- 5.4.1. Case Study No. 6
  - 5.4.1.1. Discussion and Conclusions
- 5.4.2. Case Study No. 9
  - 5.4.2.1. Discussion and Conclusions
- 5.4.3. Case Study No. 1
  - 5.4.3.1. Discussion and Conclusions

5.5. Analyses and General Discussion of Results

5.6. Summary

CHAPTER 5

5.1. INTRODUCTION

The pressure monitoring system described in Chapter 4 was shown, from the laboratory tests conducted, to be satisfactory for measuring pressures developed at the scar/dressing interface. There are, in the literature, no reports of the values of pressures measured beneath pressure garments however, from a personal communication with D.L. Larson (1978) the author discovered that a biophysicist had been involved in measuring pressures beneath Jobst Lycra* garments. Again, no values of pressure were provided although it was stated that pressure should be constant and above the mean capillary pressure; 25mmHg. No mention of the technique employed to measure pressure was given.

The population used in this study was drawn entirely from patients who had post-burn hypertrophic scarring. In the Glasgow area, most of these patients had attended the Glasgow Royal Infirmary during the healing phase of the burn wound. Follow-up of these patients was carried out at the Plastic and Reconstructive Surgery Unit at Canniesburn Hospital, Bearsden, Glasgow. There was no discrimination of patients on an age or a sex basis. Patients were selected for the study entirely on the initial clinical judgement of the scar type (i.e. whether hypertrophic or not) by the same clinician using the criterion of section 1.1. Complete data was obtained for 16 patients from a total of 22 patients who were examined over periods varying from 4 to 22 months; the average length of the period of examination being about 12 months.

5.2. PRESSURE APPLYING MATERIALS

There have been many different materials (such as foam sponge, leather and plastics) and combinations of materials

---

* Lycra is a registered Trade Mark, Du Pont Co. (U.K.) Ltd.

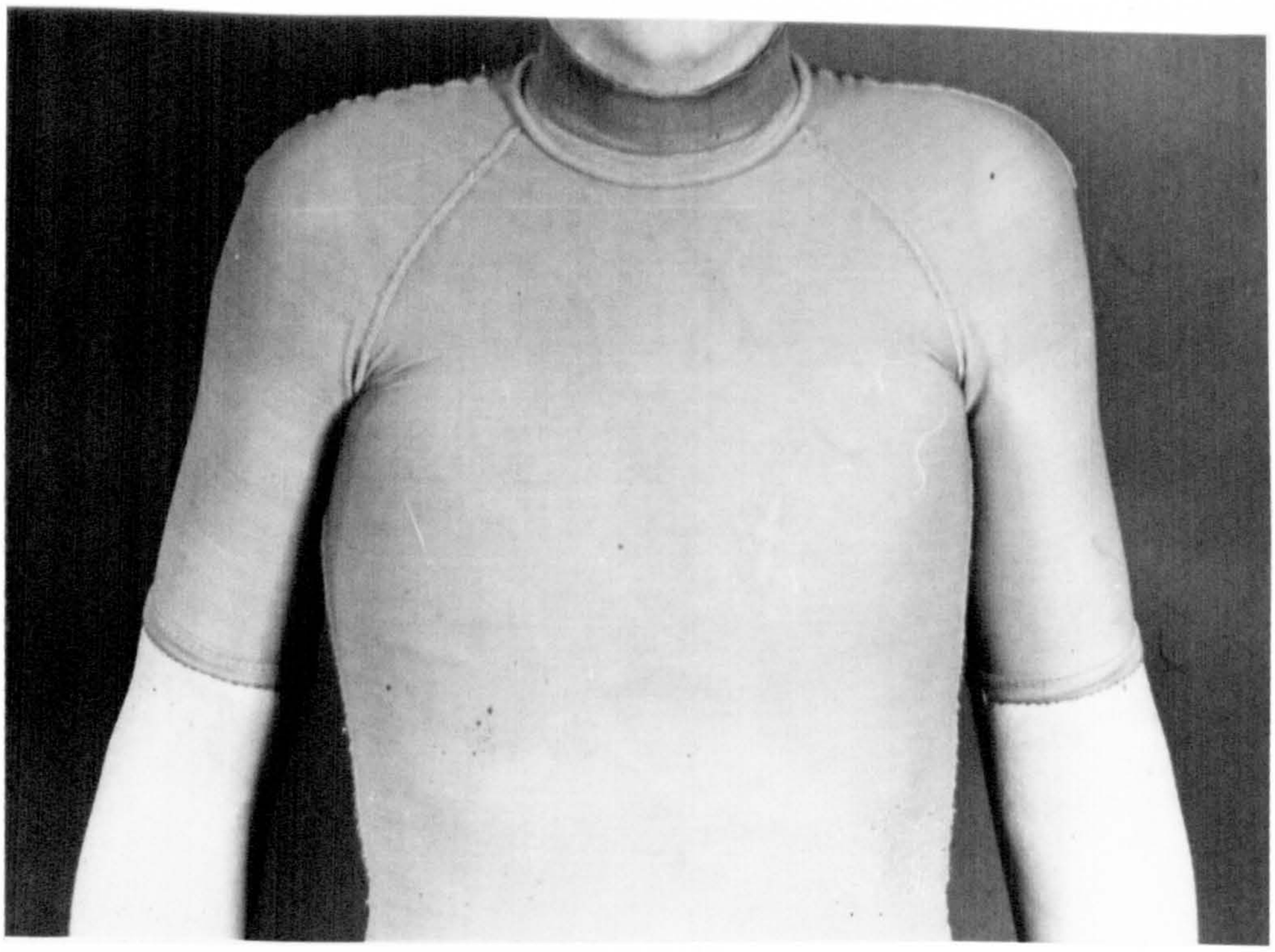

FIGURE 5.1. LYCRA PRESSURE GARMENT:
SHORT SLEEVE BODY VEST.

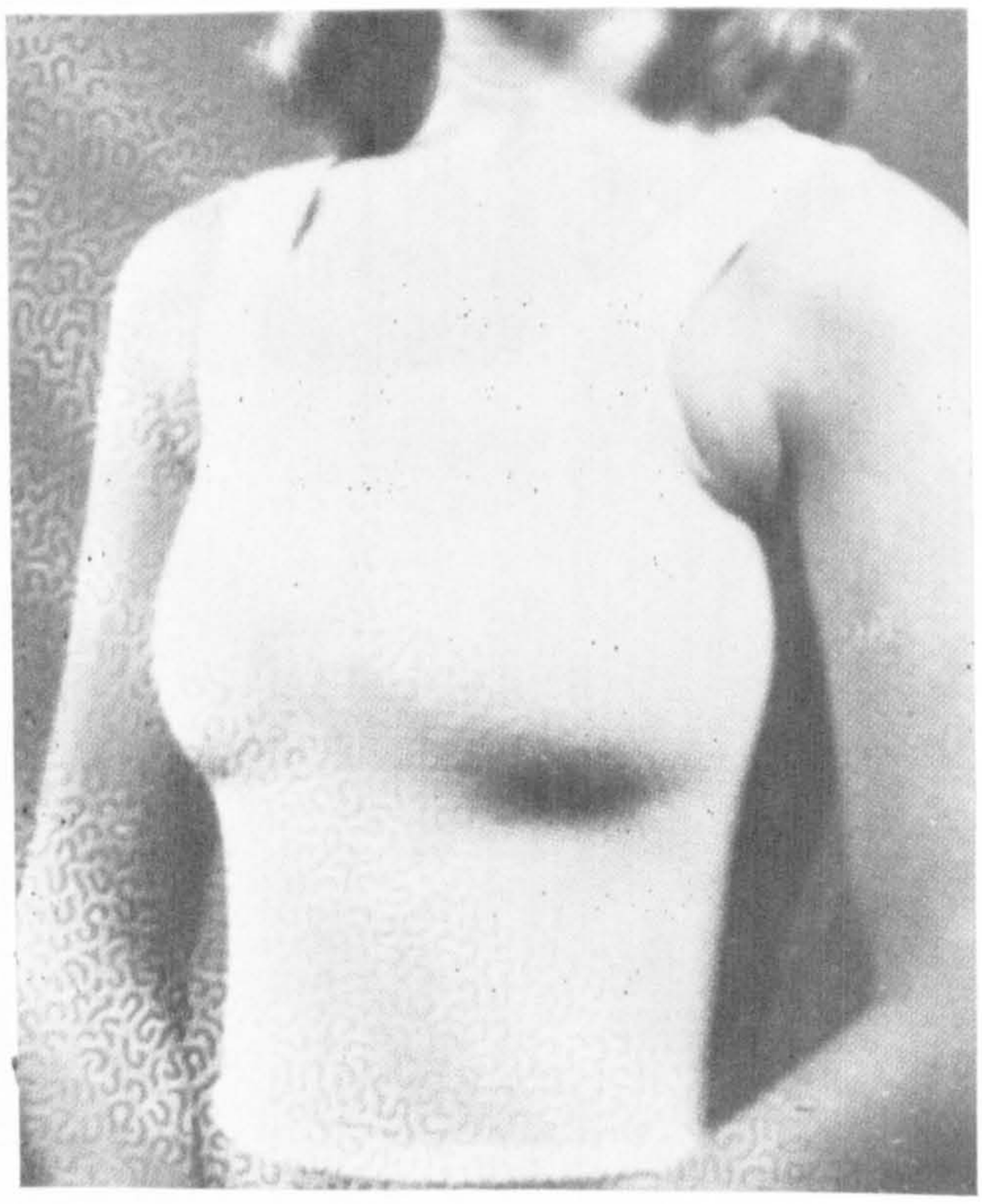

FIGURE 5.2. TUBIGRIP PRESSURE GARMENT:
SHORT SLEEVE BODY VEST

used to apply mechanical pressure to hypertrophic scar tissue (Blair V.P., 1924, Fujimori et al, 1968, Larson et al, 1971, Tolhurst, 1977), the most promising of which appear to be garments with elastic properties. These garments are worn in the stretched condition resulting in elastic forces which act on the scar surface (vide 4.3.1.4). These garments are, in theory, easily removable, enabling the patient and the garment to be washed separately; they are light, and permit ventilation of the skin surface; and they do not restrict movement. The elasticity of the garment also distributes force over the scar surface. Two materials, representative of the types of elasticated garments available which are suitable for applying pressure to hypertrophic scar are Lycra (Figure 5.1) and Tubigrip[+] (Figure 5.2.).

5.2.1. Lycra Garments

Pressure garments made from Lycra are manufactured and distributed by the Jobst Institute, Inc., Toledo, Ohio, U.S.A. Lycra is a spandex fibre material which comprises 80 - 85% polyurethane. In pressure garments the fibre is woven into a two-dimensional fabric which has anisotropic mechanical properties, having different stiffness in two principal directions (Appendix B). The pressure garment consists of a woven monolayer of Lycra except at seams and edges where it is stiffened by additional material and stitching.

5.2.2. Tubigrip Garments

Tubigrip garments are manufactured by Seton (U.K.) and consists of a rib-weave stockinette and a covered latex rubber, neither of which contain optical bleach. The rubber yarn is specially covered to reduce the risk of allergic reactions and is introduced into the stockinette as a continuous length in a spiral fashion, so that the yarn appears to be circumferentially extending and uniformly dispersed along the length of the stockinette. Tubigrip

---

[+] Tubigrip is a Trade Mark of Seton Products (U.K.)

material has marked anisotropic mechanical properties, being elastic only in the radial or circumferential direction of the Stockinette (Appendix B). Tubigrip stockinettes are manufactured in a range of different diameters and body garments can be made from different tubes sizes joined together. They can either be supplied ready to wear, or, since the completion of this investigation, ready made.

It was not known which of these materials was better in terms of providing clinical remodelling of scars. In addition, in any comparison, other factors such as cost, patient acceptability and garment life are required to be taken into consideration. It was decided initially to use both types of garments in order both to provide a comparison and to investigate the effect of pressure therapy in general.

5.3. METHOD OF MEASURING PRESSURE

Prior to clinical proper investigations, a technique for measuring the pressure beneath pressure garments was developed and tested during preliminary trial runs. The following protocol was adopted in each measurement session.

5.3.1. Selection of Measurement Site

Several sites were selected beneath the pressure garment on each patient used in the study; these sites included normal skin as well as hypertrophic scar. In addition, sites on hypertrophic scar tissue were also selected according to anatomical position thus defining the mechanical properties of the underlying tissue and the radius of curvature. Furthermore, where appropriate, an untreated area on a pressure treated scar was used as a control for the pressure therapy. Alternatively, an untreated scar was used as a control, on an adjacent site to the pressure treated scar.

5.3.2. Calibration of Pressure Transducers

Each pressure transducer was calibrated as described in section 4.5.2. and a calibration curve of pressure

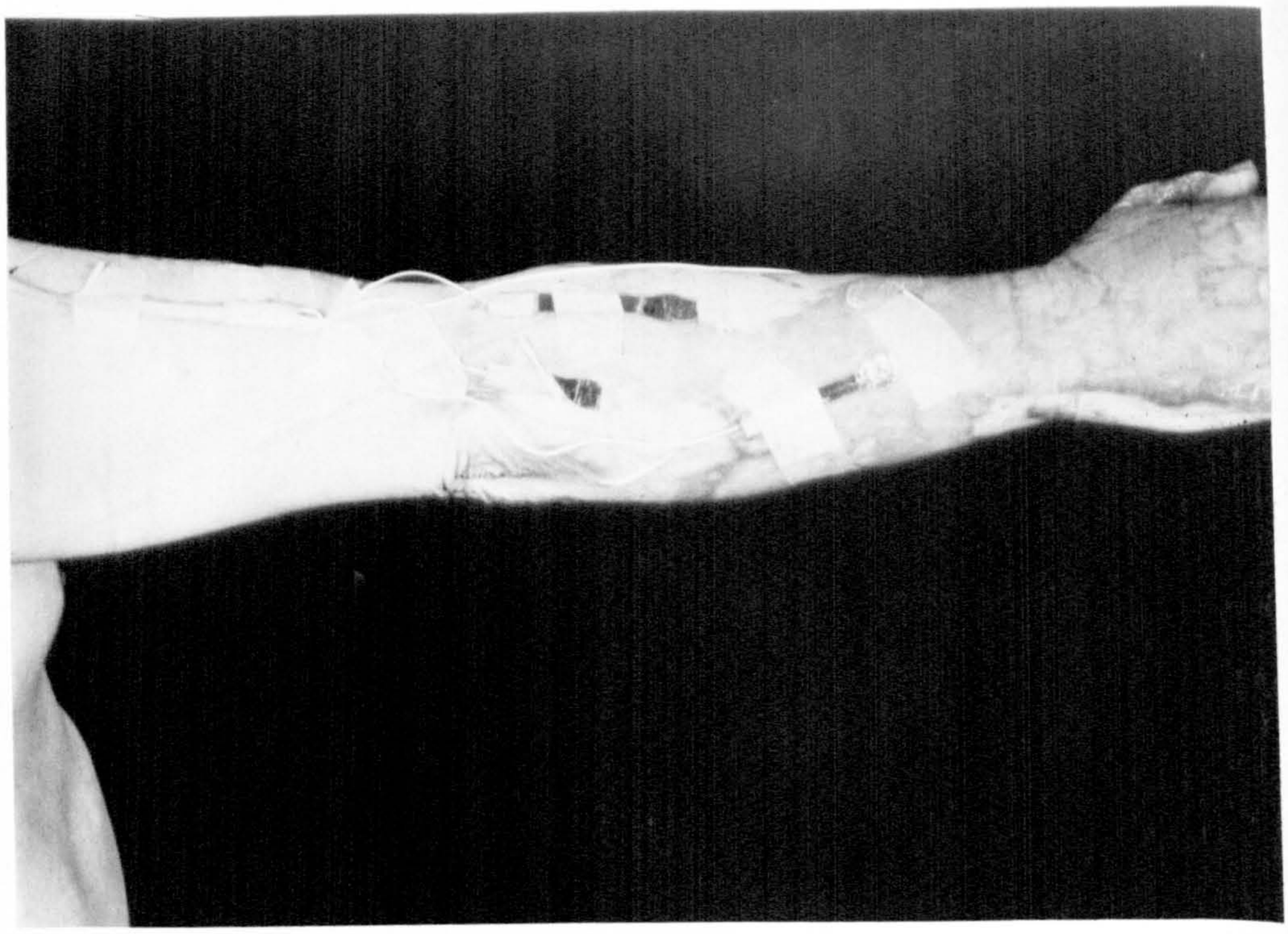

FIGURE 5.3. TRANSDUCERS (T) ATTACHED TO SKIN SURFACE BY ADHESIVE TAPE

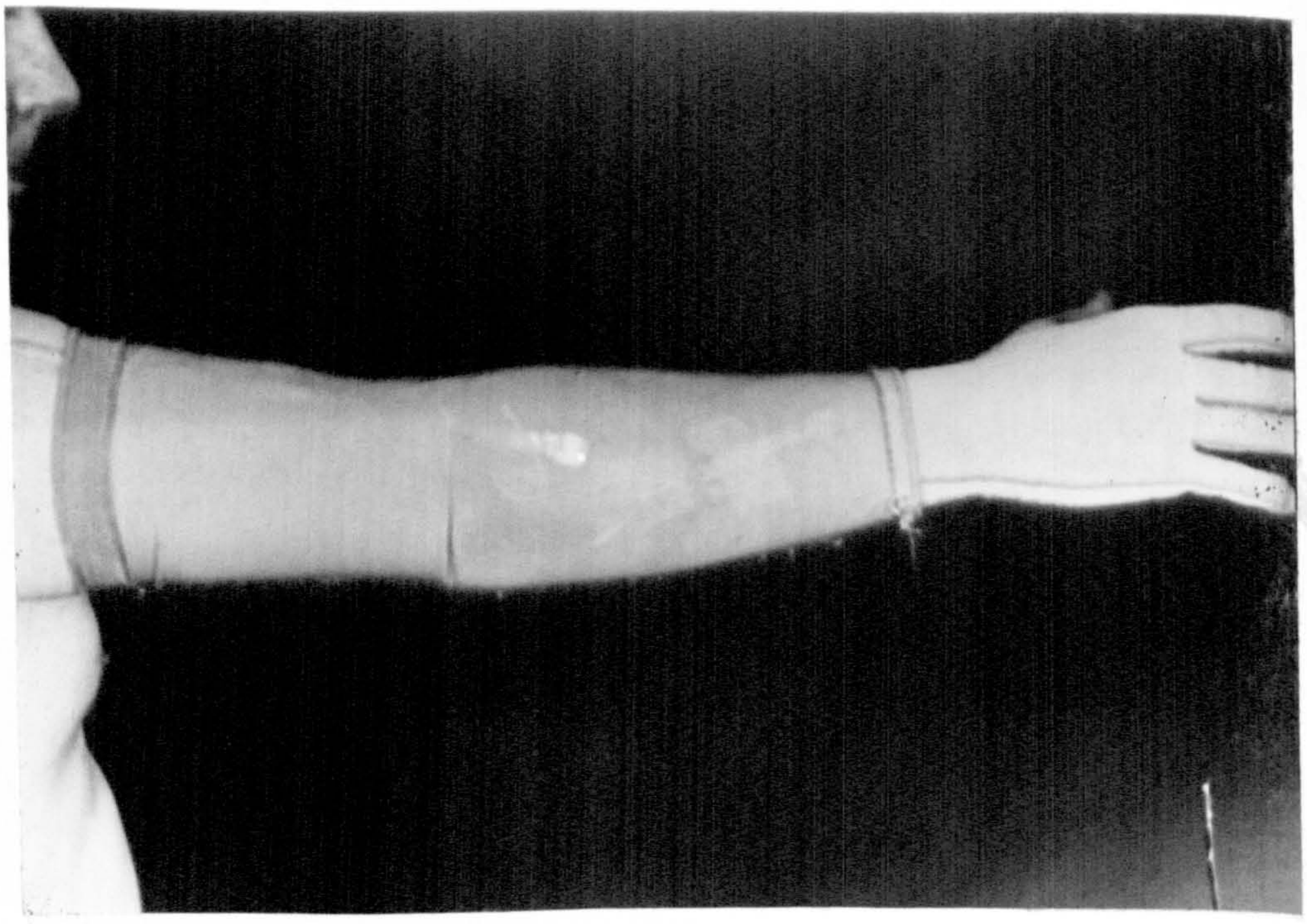

FIGURE 5.4. PRESSURE TRANSDUCERS LOCATED BENEATH ELASTICATED GARMENT TO TAKE "SPOT" MEASUREMENTS

meter output against the pneumatic sphygmomanometer pressure was drawn using the standard data sheet produced (Appendix B). Any unusual developments were noted and that particular transducer was not used.

5.3.3. Measurement of Pressure

There were two ways in which pressure was measured; by taking 'spot' measurements at one location with the transducer static, and the other by using the transducer to obtain an indication of pressure along the length or breath of an area by moving it beneath the garment to different sites.

5.3.3.1. Pressure Measurements with the Transducer Static

Each transducer was positioned at various sites on normal skin and on hypertrophic scar, the same sites being used for repeated tests on one patient. The transducer was then attached by its edge to the skin surface with Blenderm tape (3M Company, U.K.) which was both easy to use and also acceptable to the patients (Figure 5.3). Care was taken to ensure that the transducer was located adjacent to the tissue surface. Once the transducers were in position the elasticated garment was replaced, carefully, and left to 'settle' for a few minutes to avoid any transient or artificially high pressure being recorded, which could be due to the garment being 'caught' on the transducer (Figure 5.4.). The pressure beneath the garment was then read-off from the meter and was then converted to mmHg from the appropriate calibration curve. Conversion to absolute mmHg was later performed using the mercury column calibration curve (vide 4.5.2.). After pressure had been measured, the garment was removed and the transducers were then recalibrated and the pre-measurement and the post-measurement calibration curves were compared to establish if drift or creep had occurred during measurement outwith the limits established in Chapter 4. If any such situation occurred the results were disregarded and pressure from the site in question was remeasured with a reliable transducer.

FIGURE 5.5 SYNOPSIS OF PRESSURES MEASURED AT SELECTED SITES ON EACH PATIENT

Case No	Duration of Pressure (months)	Age (yrs)	Sex	Average Pressures at Sites (mmHg)				
				Site 1	Site 2	Site 3	Site 4	Site 5
1	13	36	M	15(R)	20(B)	28(B)	27(B)	25(B)
2	22	43	F	16(R)	18(B)	15(R)	-	-
3	10	3	F	28(B)	26(B)	34(B)	31(B)	35(B)
4	8	6	M	10	16	28	20	11
5	7	15	M	34	32	35	38	-
6	22	45	M	28(B)	23(B)	15(R)	14(R)	10
7	15	49	M	36(B)	27(B)	31(B)	-	-
8	14	12	M	24	28	26	26	-
9	16	36	M	10	21(B)	15 (B)	-	-
10	12	65	M	13	14	12	-	-
11	16	15	M	14	17(R)	15	13	19(B)
12	16	28	M	24	28	22	-	-
13	6	9	F	26	29	32	34	-
14	4	11	M	18	16	14	17	-
15	5	8	F	39(B)	42(B)	47(B)	-	-
16	10	10	M	16	10	10	11	-

M - Male
F - Female

(B) Denotes sites at which a better cosmetic result was achieved

(R) Denotes Remodelling

5.3.3.2. Pressure Measurements with the Transducer being Moved to Different Sites The elasticated garment was removed and the transducer was placed at the selected position and lightly held at one edge by a piece of Blenderm tape. The garment was replaced and the transducer was then gently 'pulled' to free it from the tape. The transducer was then drawn beneath the garment over a preselected anatomical line covering scar, and or normal skin in most cases, and pressures were recorded at specific distances from the datum point. Pressures were never measured when the transducer was moving, but were measured with the transducer stationary at each appropriate distance to avoid in-plane artefacts being produced. In this way, a spatial pressure profile could be quickly recorded over the entire surface of a scar.

After measurement the transducers were recalibrated and rechecked as described in the previous section. In general, the transducer was used 'dynamically' to obtain the greatest amount of fundamental clinical data.

5.4. EXPERIMENTAL RESULTS

A synopsis of the experimental results obtained from each patient are shown in tabulated form (Figure 5.5.). The pressures indicated under each site and the average pressures calculated at that site over the durations for which pressures were measured. Each average pressure was calculated from the total number of pressures measured.

From inspection of the results it is evident that pressures vary from site to site on the same patient and from patient to patient. Comments on the remodelling achieved at each site are also shown in Figure 5.5. in brackets at the pressures. In general, remodelling was achieved at each site with a pressure greater than 14 - 15mmHg however the quality of remodelling in terms of cosmesis appeared to vary with the magnitude of pressure. In general, the higher the average pressure measured, the better the cosmetic result. It is difficult to express this in words although those sites which displayed a 'better cosmetic result' are indicated by B. There are several patients (case studies 4,5,8,12,13)

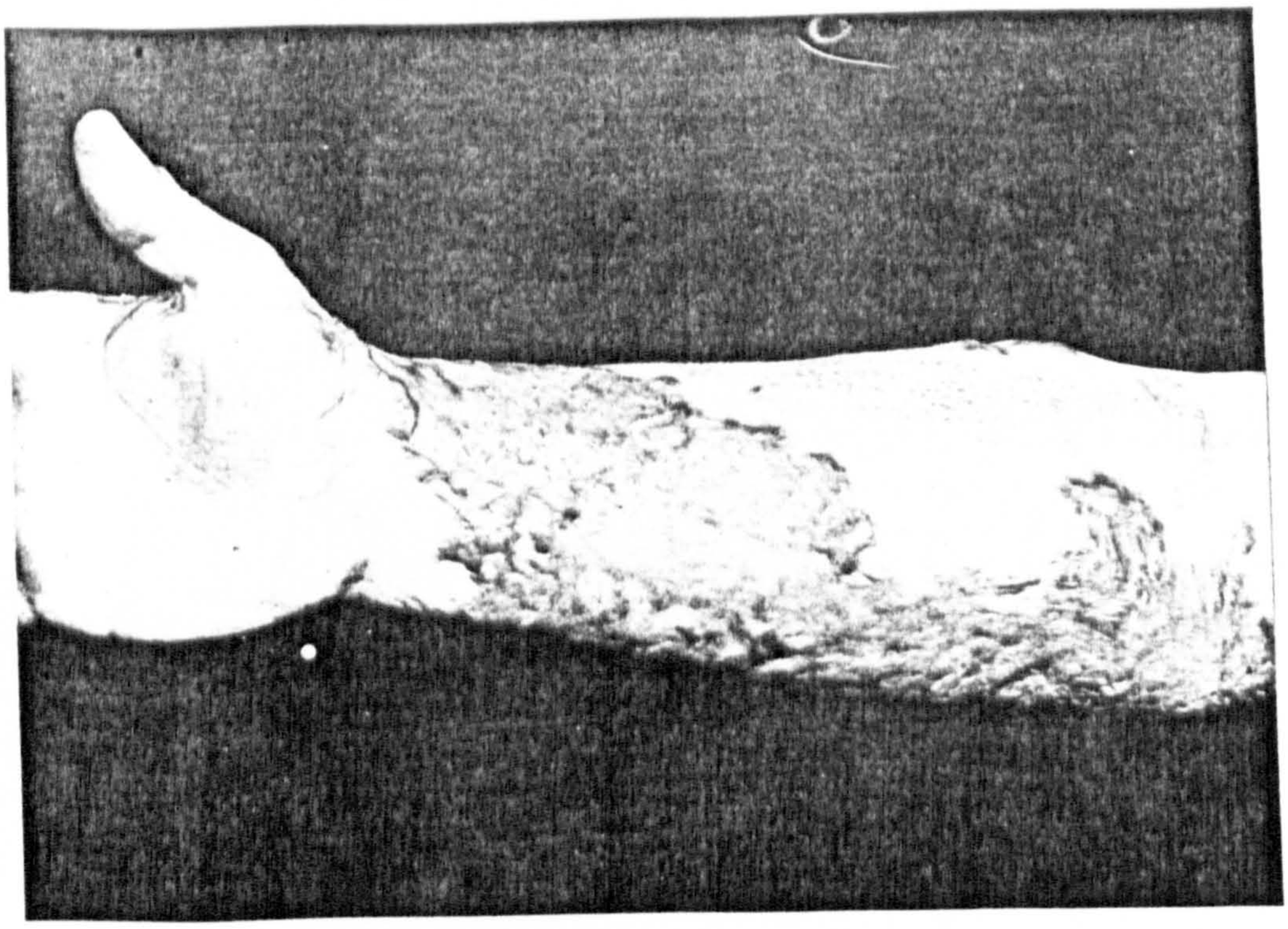

FIGURE 5.6. CASE STUDY NO. 6: VOLAR SURFACE RIGHT ARM BEFORE PRESSURE APPLIED

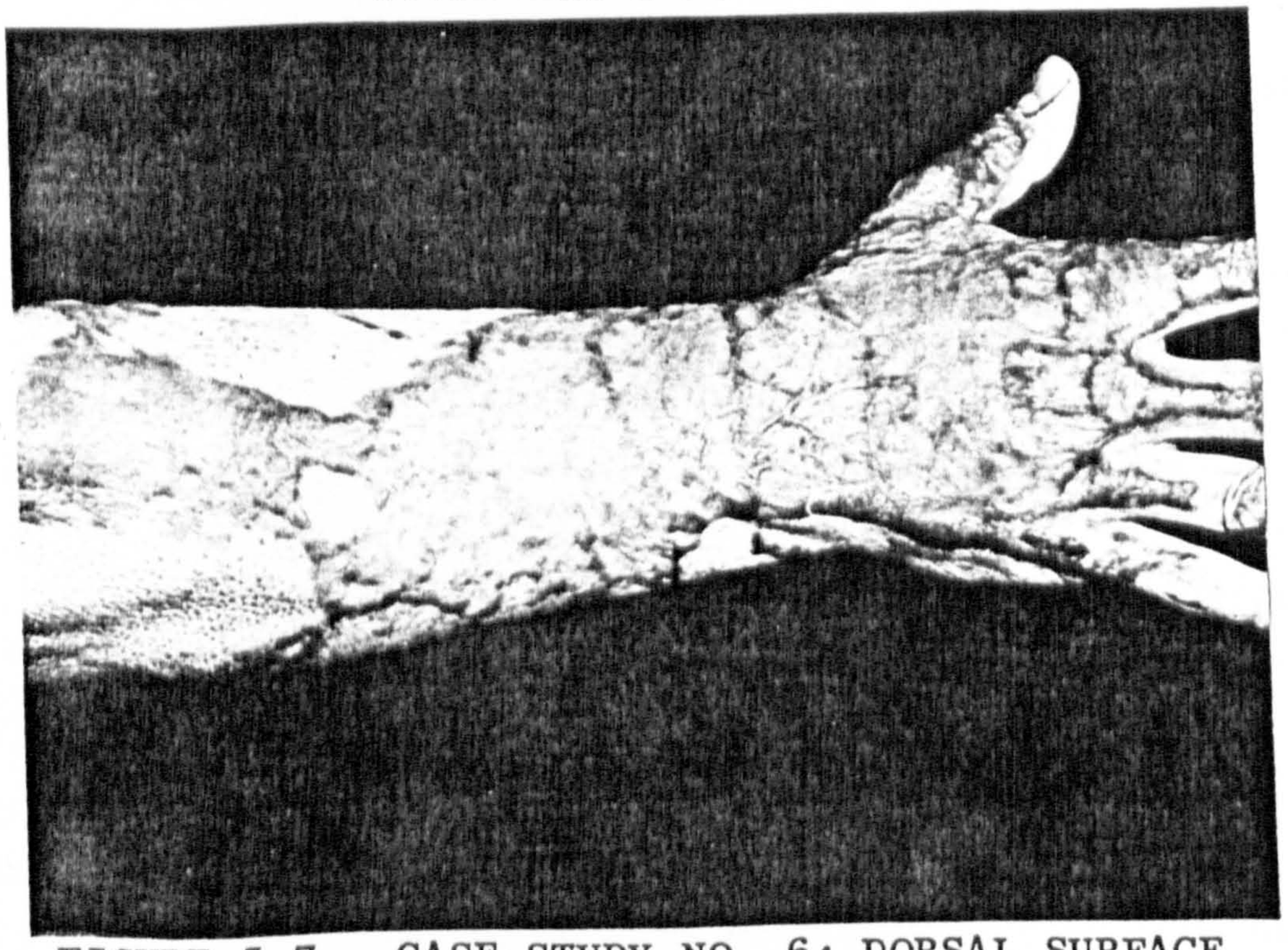

FIGURE 5.7. CASE STUDY NO. 6: DORSAL SURFACE RIGHT ARM BEFORE PRESSURE APPLIED

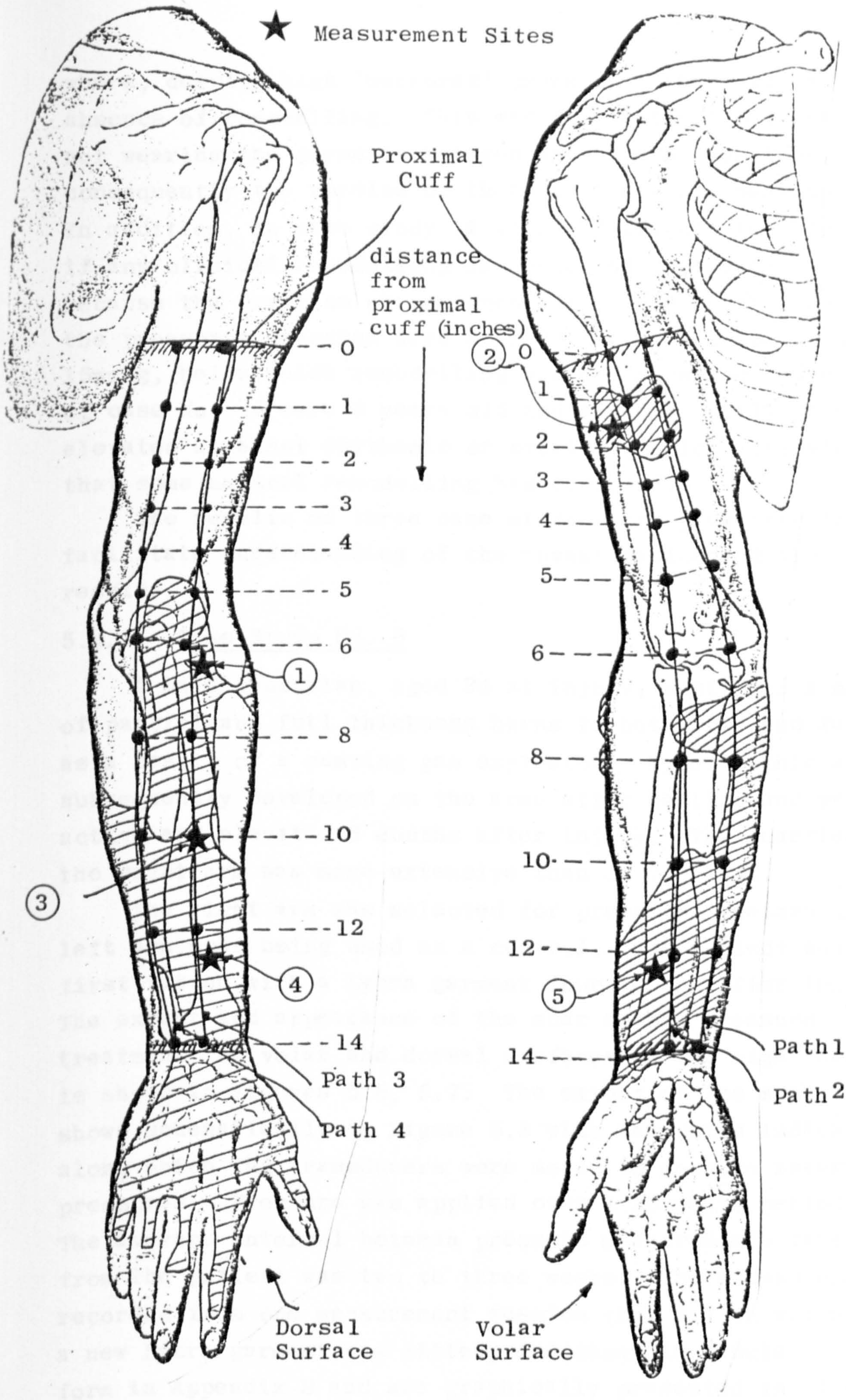

FIGURE 5.8 SCHEMATIC VIEW OF PRESSURE MEASUREMENT PATHWAYS AND SELECTED MEASUREMENT SITES FOR CASE STUDY NO. 6

where, despite high 'measured' pressures, there was an absence of remodelling. This was due to these patients not wearing the garments between measurement sessions, consequently the results of these patients are meaningless. In addition, in case study 14 it was difficult to judge if any clinical remodelling had occurred presumably because the duration of pressure was only 4 months and the pressures measured were near to the value, about 14 - 15mmHg, below which remodelling was not observed. The scars of case No. 16 were 3 years old and although still slightly elevated were not erythemic or pruritic, which indicated that some natural remodelling had occurred.

The results of three case studies are presented to facilitate understanding of the investigation and the results.

5.4.1. Case Study No. 6

A male caucasian, aged 34 at injury, sustained a mixture of partial and full thickness burns to both arms and face as a result of a camping gas explosion. Hypertrophic scars subsequently developed on the arms after healing and were active and elevated 3 months after injury. The scarring on the right arm was more extensive than on the left.

The right arm was selected for pressure treatment, the left arm scar being used as a control. The patient was first fitted with a Lycra garment four months after injury. The extent and appearance of the scar before pressure treatment, on volar and dorsal surfaces of the right arm is shown in Figures 5.6, 5.7. The extent of the scar is shown schematically in Figure 5.8 with the paths indicated along which the transducers were moved to measure interface pressures. Pressure was applied over a 22 month period. The average interval between pressure measurements taken from the patient was two to three weeks. The pressures recorded from one measurement session (No. 29) in which a new Lycra garment was fitted, are shown in tabulated form in Appendix B and are graphically presented in Figure 5.9.

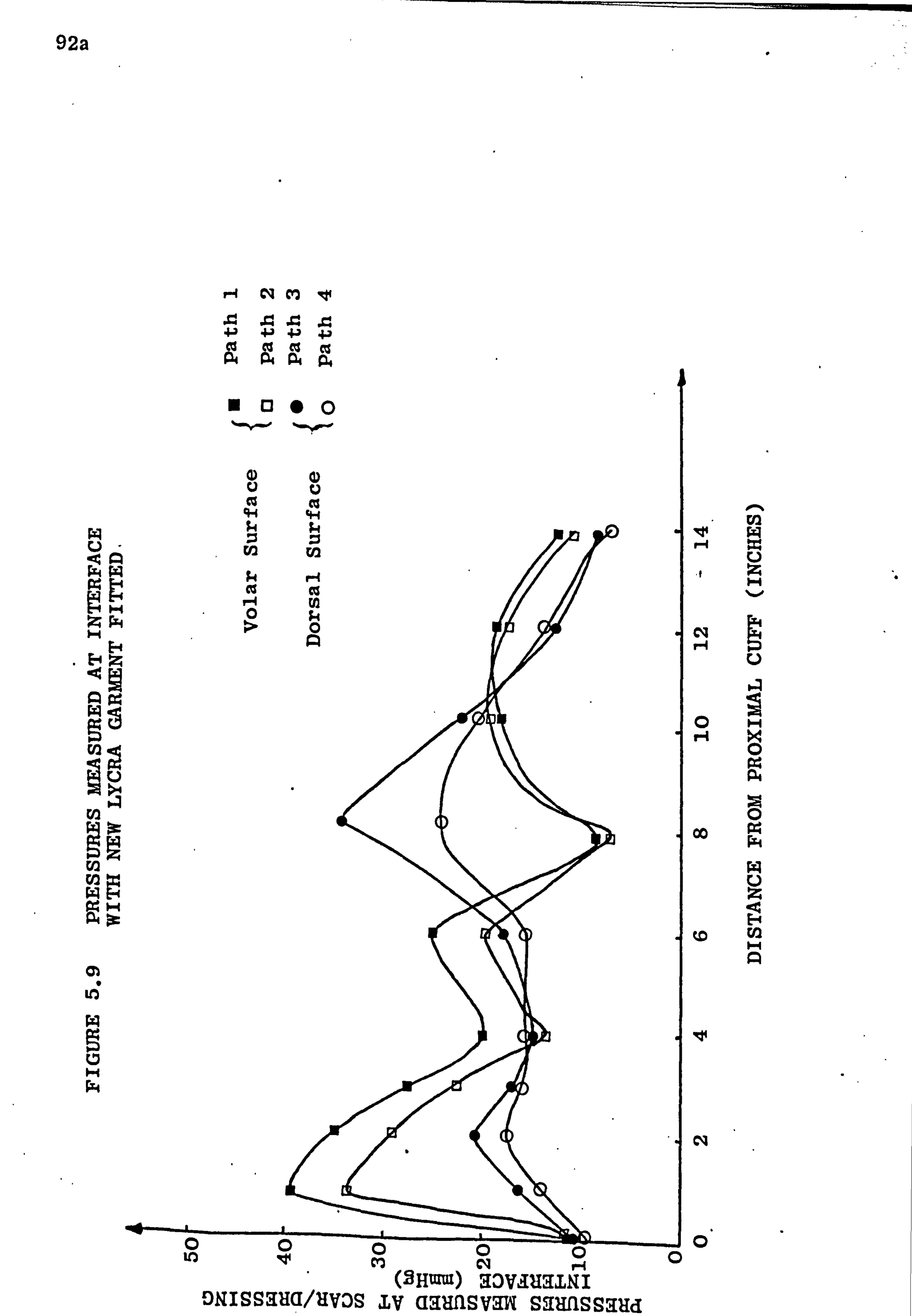

FIGURE 5.9 PRESSURES MEASURED AT SCAR/DRESSING INTERFACE WITH NEW LYCRA GARMENT FITTED.

FIGURE 5.10 PRESSURE MEASURED AT THE INTERFACE AFTER LYCRA GARMENT WORN FOR 6 WEEKS

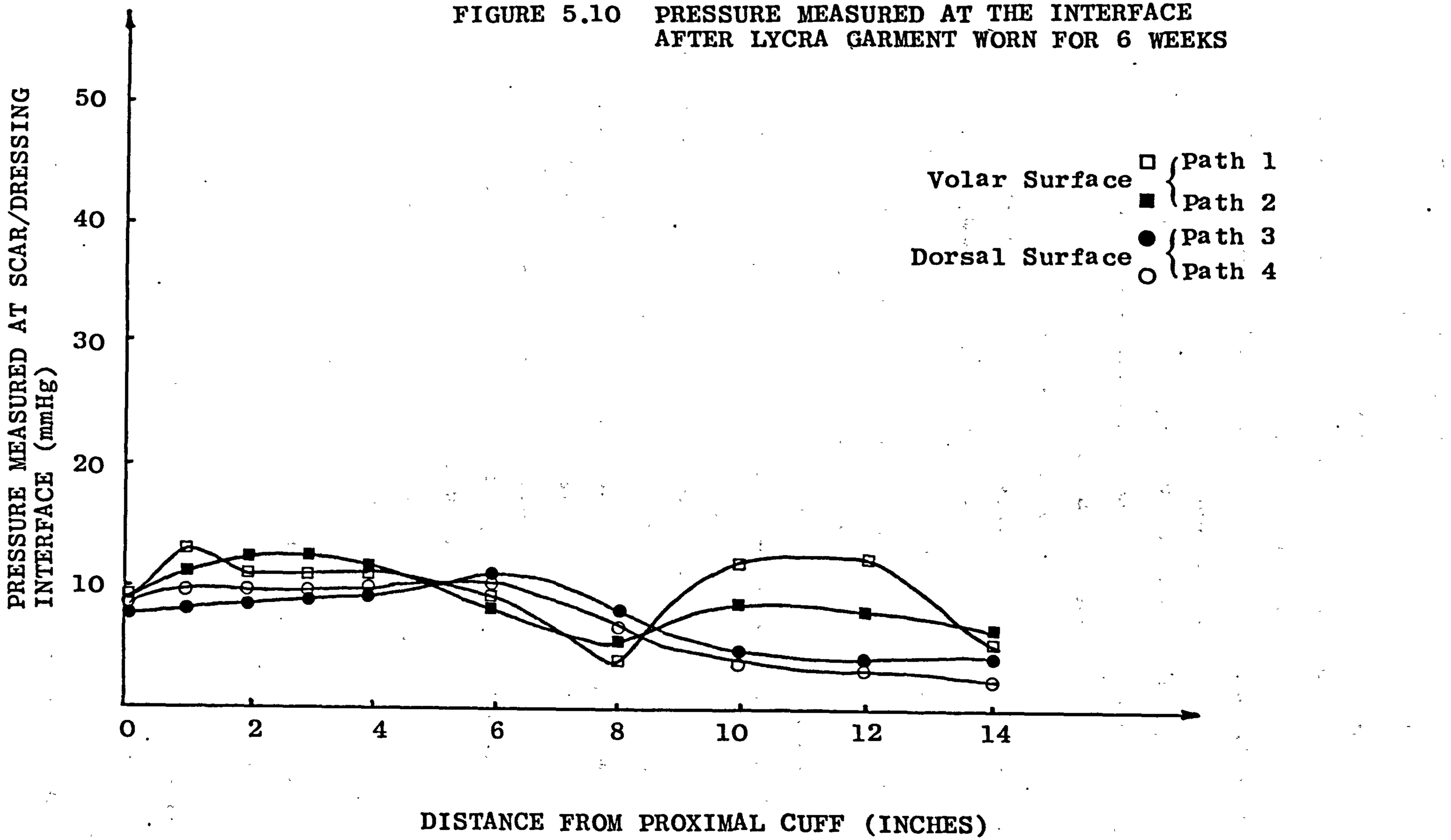

From Figure 5.9 it is evident that pressures vary in both the proximal - distal direction and in the lateral direction. In general, the pressures on the volar surface increase rapidly to about 35 - 40mmHg then fall to a minimum value of about 8 - 9mmHg eight inches from the proximal cuff. The pressures then rise to a value of about 20mmHg over the main plaque of scar tissue and then gradually fall off as the distal cuff is approached. In contrast, the pressures on the dorsal surface rise gradually from about 10mmHg at the proximal cuff to about 18 - 22mmHg just proximal to the elbow joint; the pressures then increase rapidly over the bony tissue reaching 36mmHg about 8 inches from the cuff (Path 3) just superficial to the ulna. The pressure then rapidly falls to around 8 - 10mmHg at 11 inches from the proximal cuff and stays approximately constant thereafter until the distal cuff is reached.

From preliminary inspection of the pressures obtained it is evident that the plaque of scar tissue on the volar surface 1 - 2 inches from the proximal curve has between 30 and 40mmHg pressure applied, whereas the pressure applied to the lower scar surface is about 20 - 22mmHg maximum. On the dorsal surface the plaque of scar tissue extending from the elbow to the cuff has pressure between 35 and 10mmHg applied thereto; pressures greater than 15mmHg being applied to the major portion of the scar tissue.

Pressures were again measured as before when the same garment had been worn for 6 weeks (Measurement Session No. 34, Appendix B); the results are graphically displayed in Figure 5.10. From an inspection of the graph it is evident that the pressures are considerably lower along each measurement pathway, than for the new garment, all pressures measured being less than 15mmHg. The greatest reduction in pressure was measured where the highest pressures had been recorded previously; at proximal cuff and at the distal plaque of scar tissue on the volar arm surface and at the scar tissue distal to the elbow joint on the dorsal arm surface. The Lycra garment, upon inspection, did not

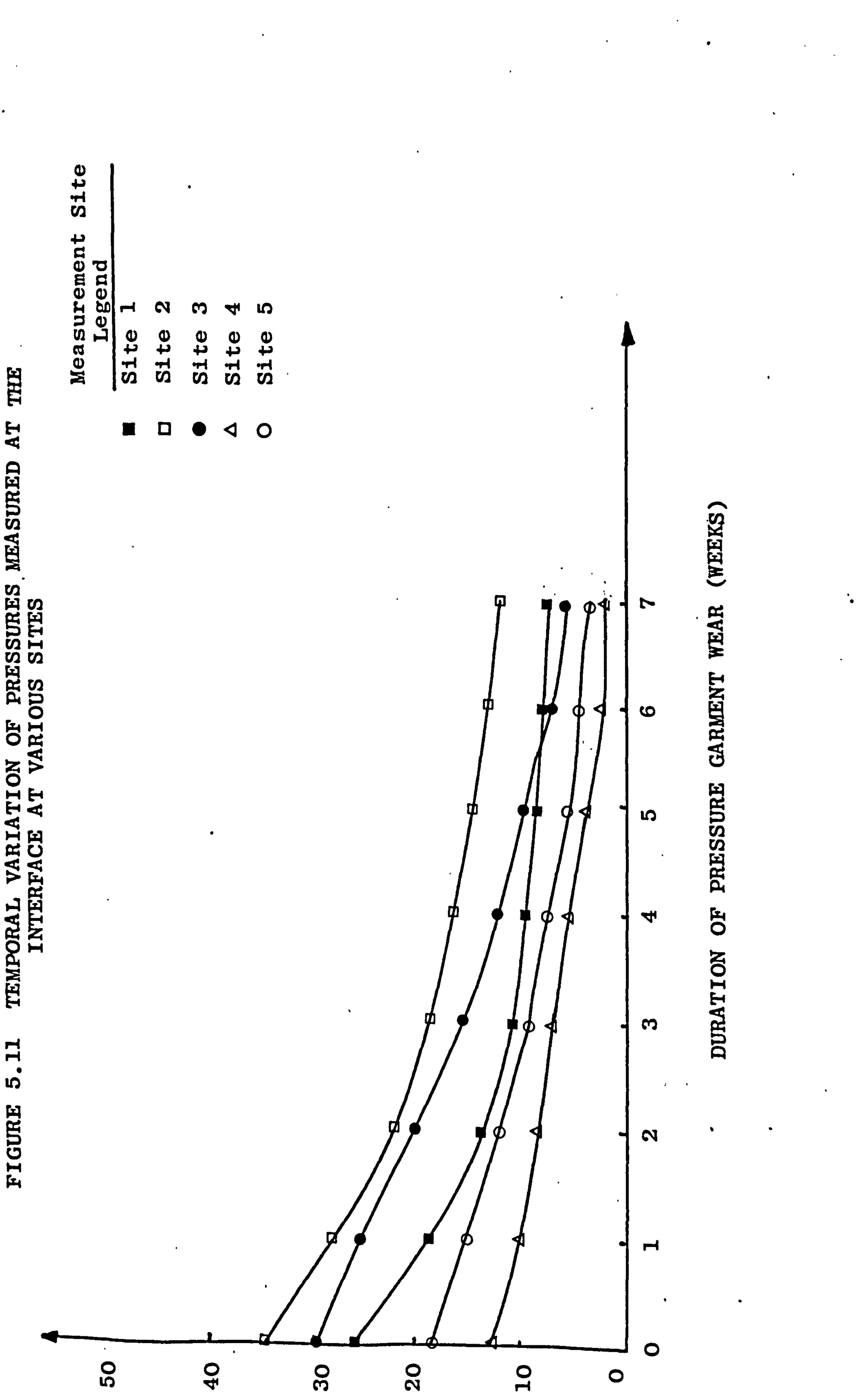

FIGURE 5.11 TEMPORAL VARIATION OF PRESSURES MEASURED AT THE SCAR/DRESSING INTERFACE AT VARIOUS SITES

appear slack however the pressures recorded indicated that some loss of elasticity may have had occurred.

The temporal variation of pressure at selected sites at the scar/dressing interface is shown in Figure 5.11. Pressures were measured at the scar/dressing interface when the dressing was first fitted (Measurement Session No. 29). and thereafter at the time intervals indicated in Figure 5.11 until the garment was replaced. The measurement sites were selected principally because of the different mechanical properties of the tissue underlying each site. The location of each site is shown in Figure 5.6.

Site 1 was on the scar/normal tissue boundary superficial to the lateral edge of the radius. The radius of curvature at this site was large and the underlying tissue was rigid in response to compression.

Site 2 was located on the plaque of scar tissue superficial to the edge of the humerus and to the biceps. The radius of curvature was large, and the underlying tissue was rigid in response to compression.

Site 3 was located on the scar tissue on the dorsal surface of the right forearm superficial to the ulna and radius bones, and the tissue was quite compliant in response to compression.

Site 4 was located distal to site 3, and was also superficial to the radius. The radius of curvature was very large, the tissue being almost flat. The underlying tissue was quite rigid in response to compression.

Site 5 was located on the volar forearm surface superficial to the edge of the radius, however the underlying tissue was soft and the radius of curvature was large.

From Figure 5.11 it is clear that at the sites with the highest initial pressures,sites 1, 2, 4 the pressure falls most rapidly, in general falling to less than 15mmHg (Sites 1, 4) within 4 weeks of the garment being fitted. The pressure measured on site 1 was always greater than 15mmHg, which is somewhat surprising since the pressure on an adjacent site in path 2 had fallen to 10mmHg after 6 weeks

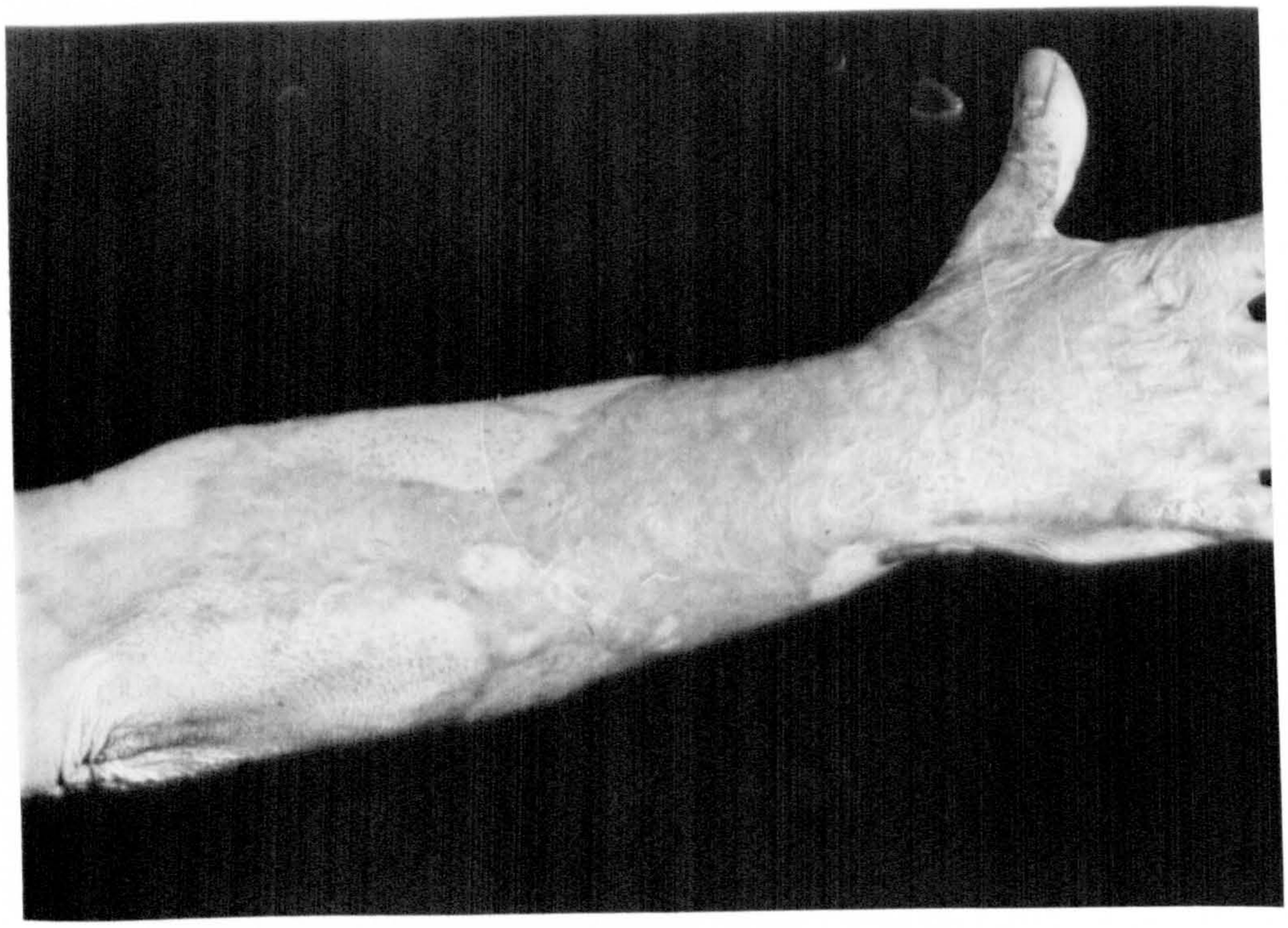

FIGURE 5.12 CASE STUDY NO. 6: DORSAL SURFACE AFTER 8 MONTHS PRESSURE THERAPY

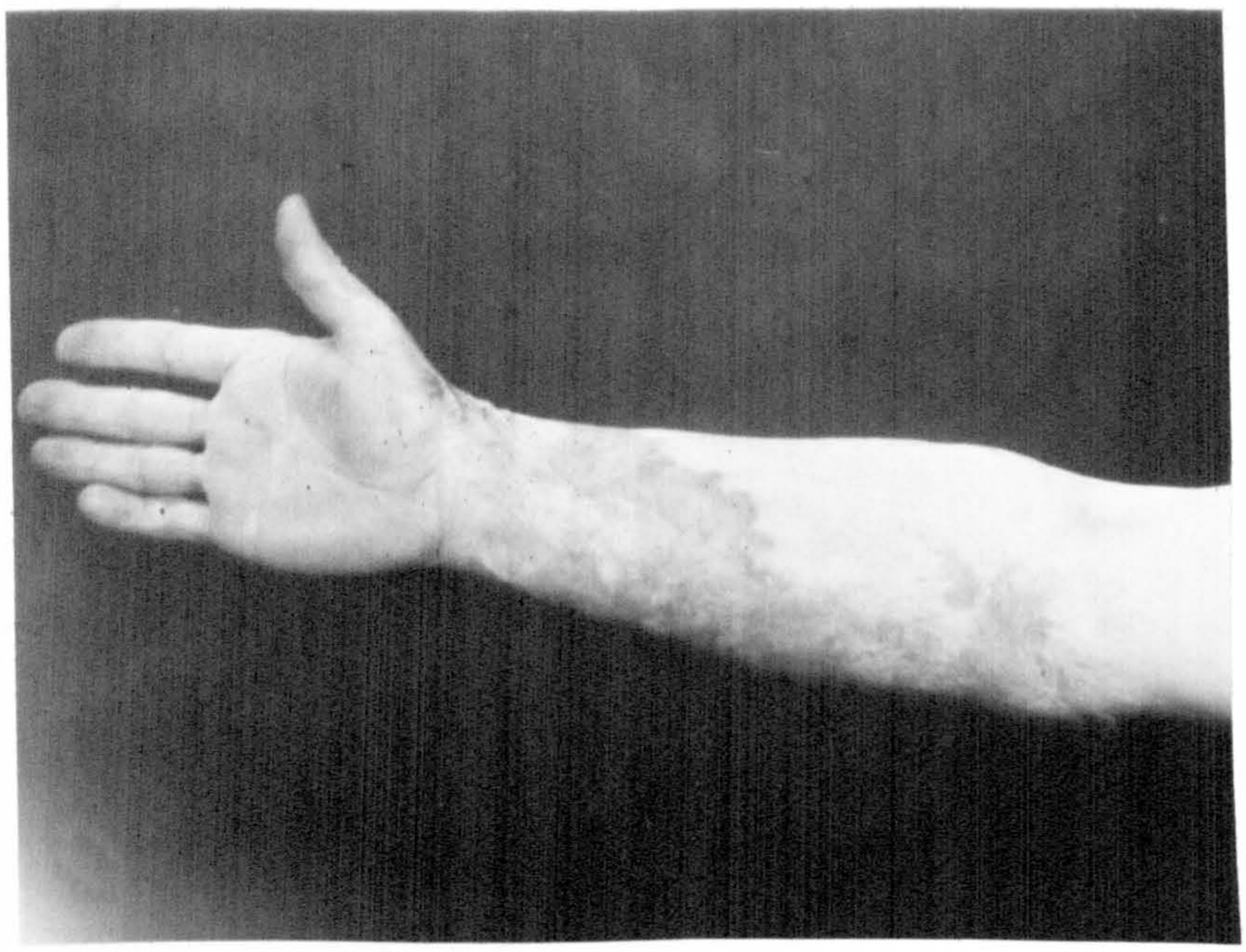

FIGURE 5.13. CASE STUDY NO. 6: VOLAR SURFACE AFTER 20 MONTHS PRESSURE THERAPY

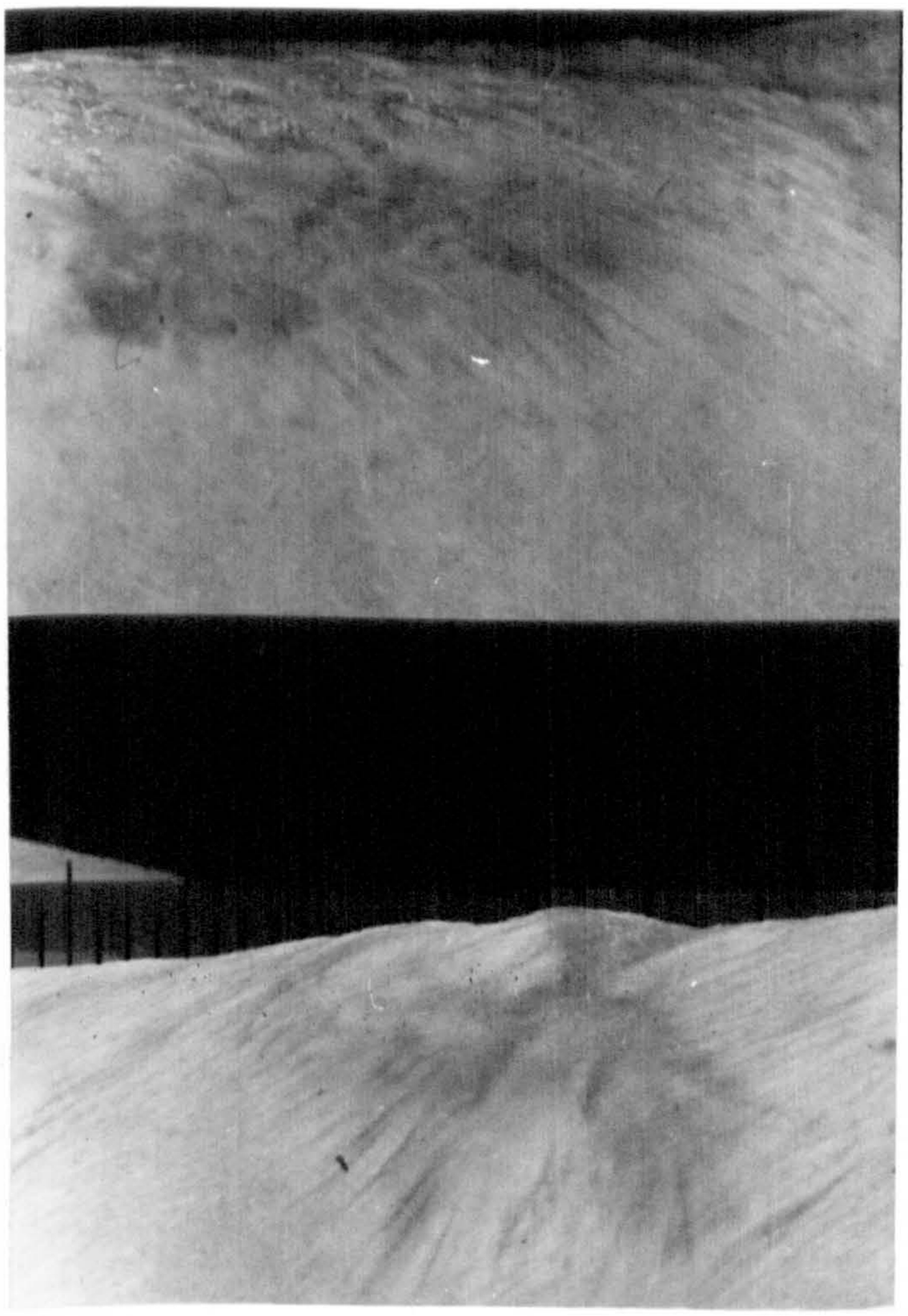

FIGURE 5.14. SPLIT PHOTOGRAPH SHOWING HYPERTROPHIC SCAR AFTER 10 MONTHS PRESSURE OF 25mmHg (top) AND UNTREATED CONTROL SCAR (bottom)

which was considered, generally, too low and the garment was replaced thereafter, on average, every 6 - 7 weeks.

Clinical remodelling of the scars after 8 months pressure on the dorsal surface and after 20 months pressure on the volar surface are shown in Figures 5.12 and 5.13 respectively. There is, at eight months, a considerable reduction in erythema surface roughness and scar elevation and at 20 months a further reduction in erythema and surface roughness although scar elevation at this time was more difficult to assess. The average pressures at sites 1 - 5 are, to be the nearest mmHg, 25mmHg, 20mmHg, 15mmHg and 19mmHg respectively. The degree of scar remodelling achieved at each of sites 1 - 4 was good, even after 8 months duration of pressure; site 5 with an average pressure of 9mmHg, did not show satisfactory remodelling and remained slightly elevated and erythemic.

The application of average pressures greater than 14mmHg resulted in remodelling over most of the hypertrophic scar although the cosmetic result achieved was generally thought to be superior at sites where average pressures were highest i.e. at sites 1 and 2.

Biopsies for investigation of collagen biosynthesis were taken from near site 2 on the right arm and from a symmetrical untreated scar on the left arm, which acted as a control. The pressure treated and control sites are shown in Figure 5.14, an average pressure of 25mmHg having been applied at site 2 for 10 months when these photographs were taken. The photographs show a clear difference between the clinical appearance of the pressure treated scar, which is flat and smooth compared to the untreated scar which is rough textured and elevated.

This patient was also the subject of an experiment to investigate the 'long' term effects of continuous pressure; pressure transducers were calibrated and positioned on the arm as for static measurements at the sites 1 - 5 shown in Figure 5.6. The temperature of the environment was maintained constant throughout the experiment. The garment had been worn for two weeks from fitting. Pressures were continuously recorded via the pressure monitor output onto a chart recorder (Bryan's,U.K.).

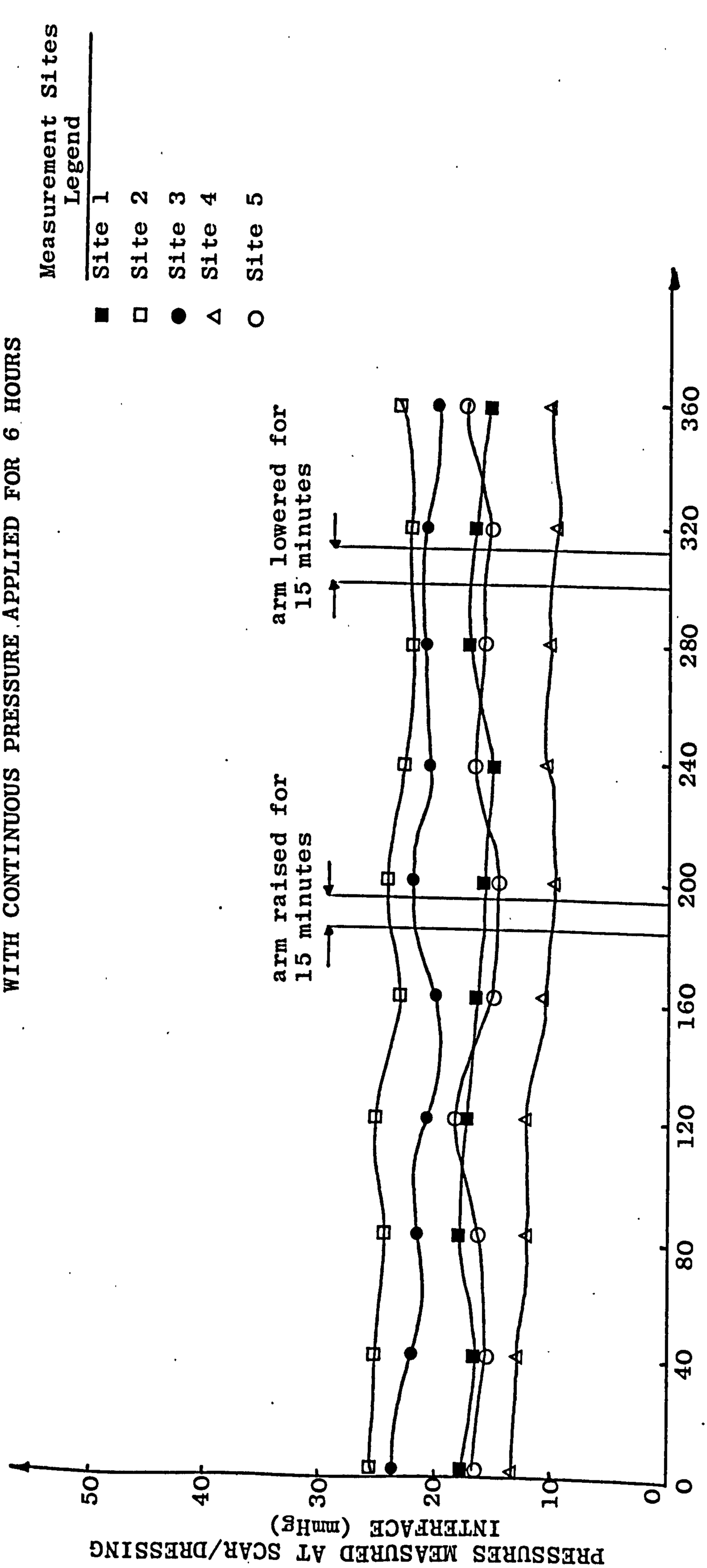

FIGURE 5.15 PRESSURES MEASURED AT THE SCAR/DRESSING INTERFACE WITH CONTINUOUS PRESSURE APPLIED FOR 6 HOURS

The variation in pressure with time for each recorded transducer output is shown in Figure 5.15, which is a graph of pressure magnitude against duration of pressure. From the graph it is evident that there is no constant pressure at any of the sites; pressures varying by about 4 - 5mmHg, on average, over the entire 6 hour experiment. The values of pressure were roughly consistent with pressure values shown in Figure 5.10 for a garment with two weeks wear. The patient was in the supine position throughout the experiment however at the times indicated, the arm with the pressure garment was raised and lowered for periods of 15 minutes respectively to see what effect that this would have on the pressures developed at the interface. The only change noted was a slight increase in the pressure measured at site 2 on raising the arm which, however, was not reversed when the arm was again lowered. In general, the effect of raising and lowering the arm was not reflected by changes in pressure at the scar/dressing interface.

5.4.1.1. Discussion and Conclusions The interface pressures measured were found to vary from site to site being principally influenced by the radius of curvature at each site, the mechanical properties of the underlying tissue and the elasticity of the garment. Pressures were greatest at sites where the underlying tissue was rigid and the radius of curvature was small (i.e. about 100 mm).

Average pressures of 13 - 15mmHg were found to result in scar remodelling. This is in conflict with existing reports (Larson et al, 1971) which requires pressure greater than mean capillary pressure (25mmHg) to be produced at the scar/dressing interface in order to effect remodelling. In general, superior cosmetic results were produced at those sites at which higher pressures were measured, indicating that some sites are more susceptible to pressure induced remodelling than others, for example site 2 where an average pressure of 25mmHg over 10 months resulted in a flat, smooth scar in contrast to the untreated control site scar.

In addition, the Lycra garment lost much of its tension quickly as a result of changing material properties which

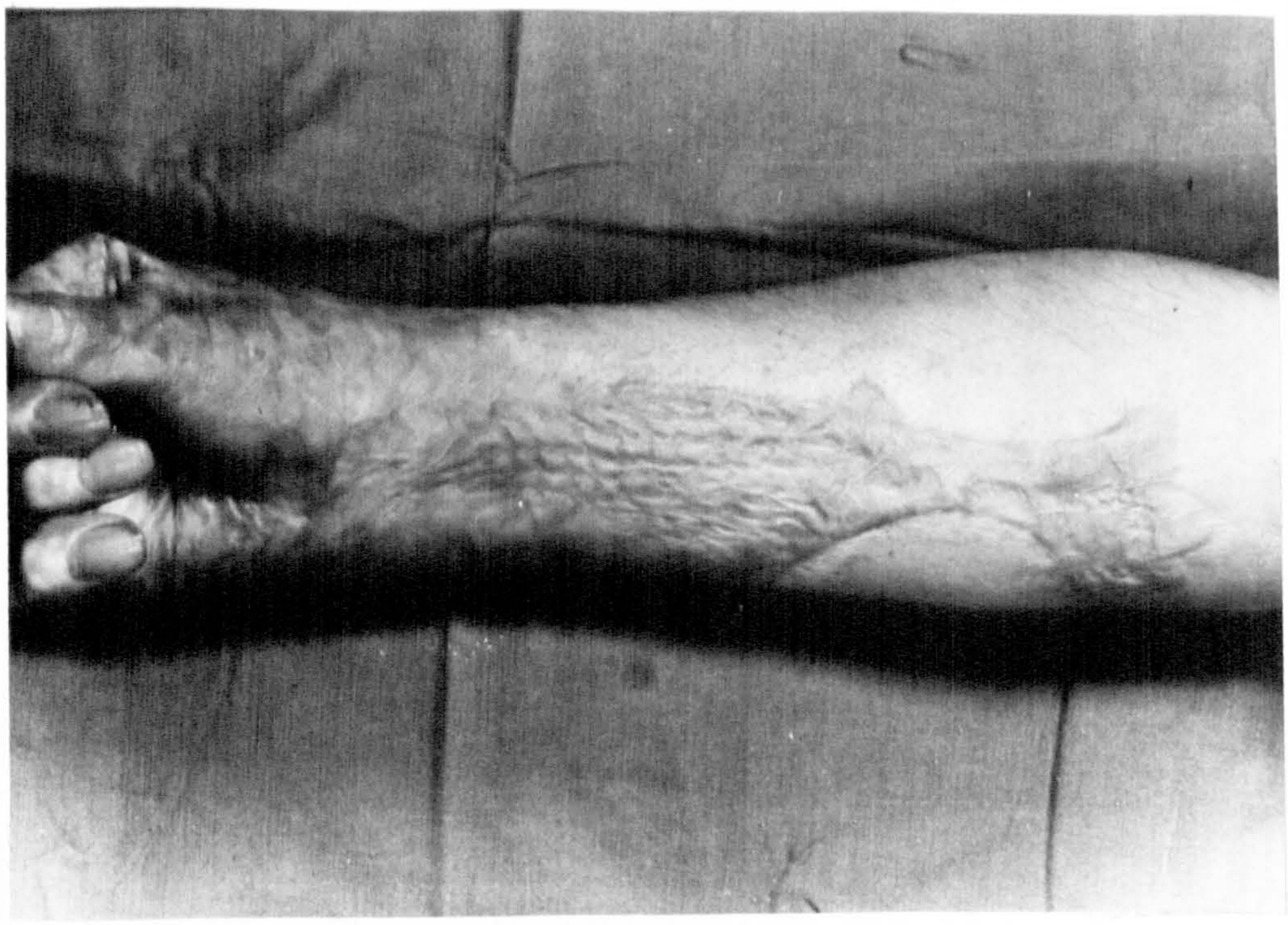

FIGURE 5.16 CASE STUDY NO. 9: RIGHT FOREARM VOLAR SURFACE SHOWING EXTENSIVE HYPERTROPHIC SCARRING BEFORE PRESSURE

FIGURE 5.17 SCHEMATIC VIEW OF PRESSURE MEASUREMENT PATHWAYS AND SELECTED MEASUREMENT SITES: CASE STUDY NO. 9

was accompanied by a reduction in the pressure measured at the scar dressing interface. Pressures were reduced by about 50% of their original values 3 to 4 weeks after fitting and to levels less than 12mmHg, in general, after 5 weeks. Pressures less than 12mmHg did not, in this case, produce satisfactory scar remodelling.

The investigation of pressure over the 6 hour period demonstrated that there are temporal interface pressure variations as well as spatial variations to consider. The temporal variations shown in Figure 5.15 are more difficult to explain however it seems unlikely that changes in the elastic properties of the garment per se are responsible.

It has been found that the volume of a limb is not constant with time, but fluctuates slightly (B.R.A.D.U. Internal Report, 1977). This is probably due to a homeostatic control mechanism acting in response to both extrinsic environmental changes and intrinsic physiological changes. Variation in limb volume may have resulted in the garment tension being altered, which in turn would result in variations in the pressures applied to the scar or skin surface. It was thought that these pressure changes, which appeared to vary about a mean value by a few mmHg were not critical to the remodelling process.

5.4.2. Case Study No. 9

A male caucasian, aged 34 at the time of injury, suffered a mixture of partial and full thickness burns on the right forearm following an accident when a petrol tank ignited. Hypertrophic scars and contractures of the scar tissue developed within 4 months of the injury, the scarring on the volar surface of the right forearm was elevated and erythemic (Figure 5.16). Contractures of the fingers of the right hand were present which prevented pressure treatment with a Lycra glove, therefore a Lycra sleeve, with a glove portion for retaining the sleeve, was fitted to the forearm only. The extent of the scarring is also shown schematically in Figure 5.17 with the paths

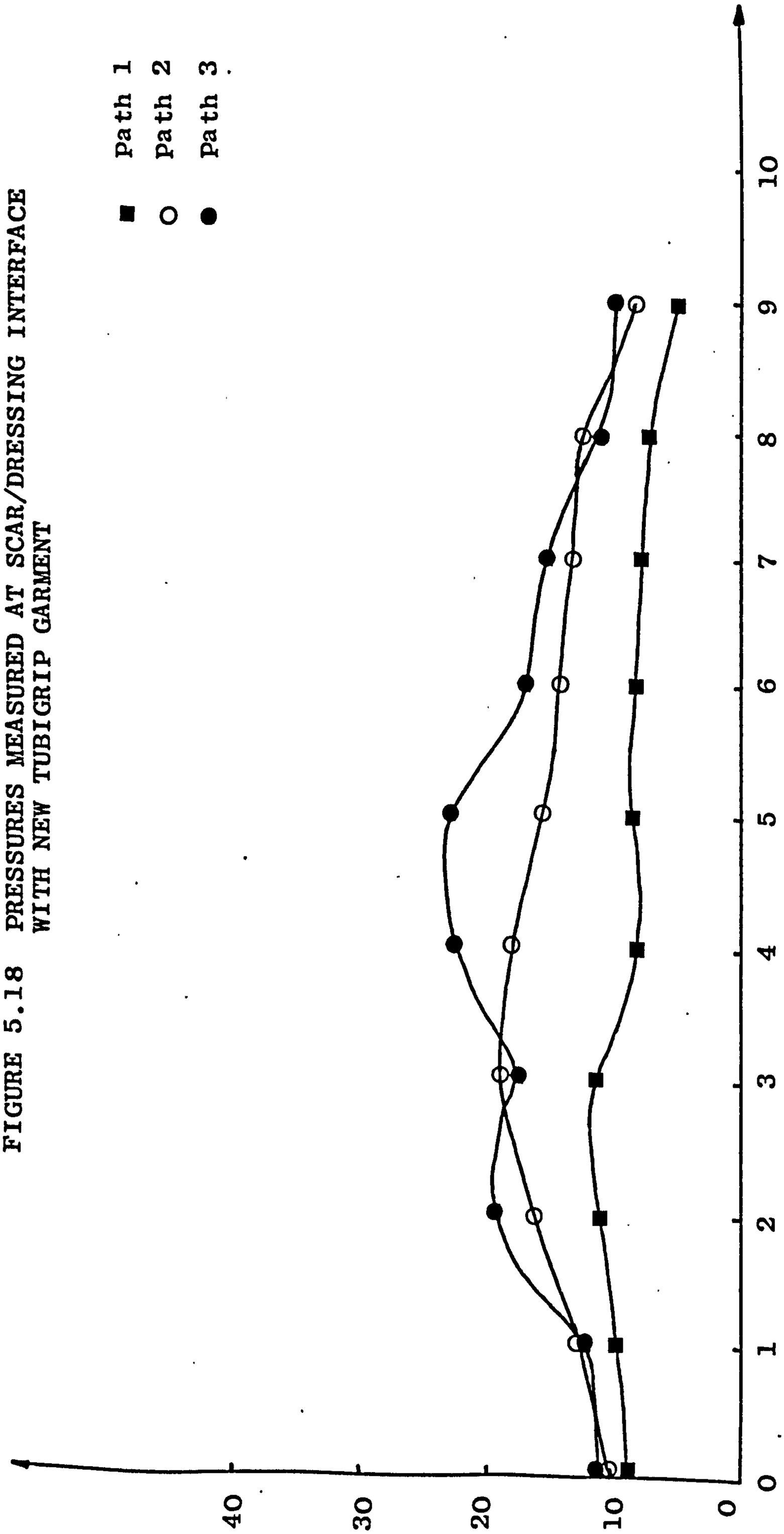

FIGURE 5.18 PRESSURES MEASURED AT SCAR/DRESSING INTERFACE WITH NEW TUBIGRIP GARMENT

FIGURE 5.19 PRESSURES MEASURED AT SCAR/DRESSING INTERFACE AFTER TUBIGRIP GARMENT WORN FOR 9 WEEKS

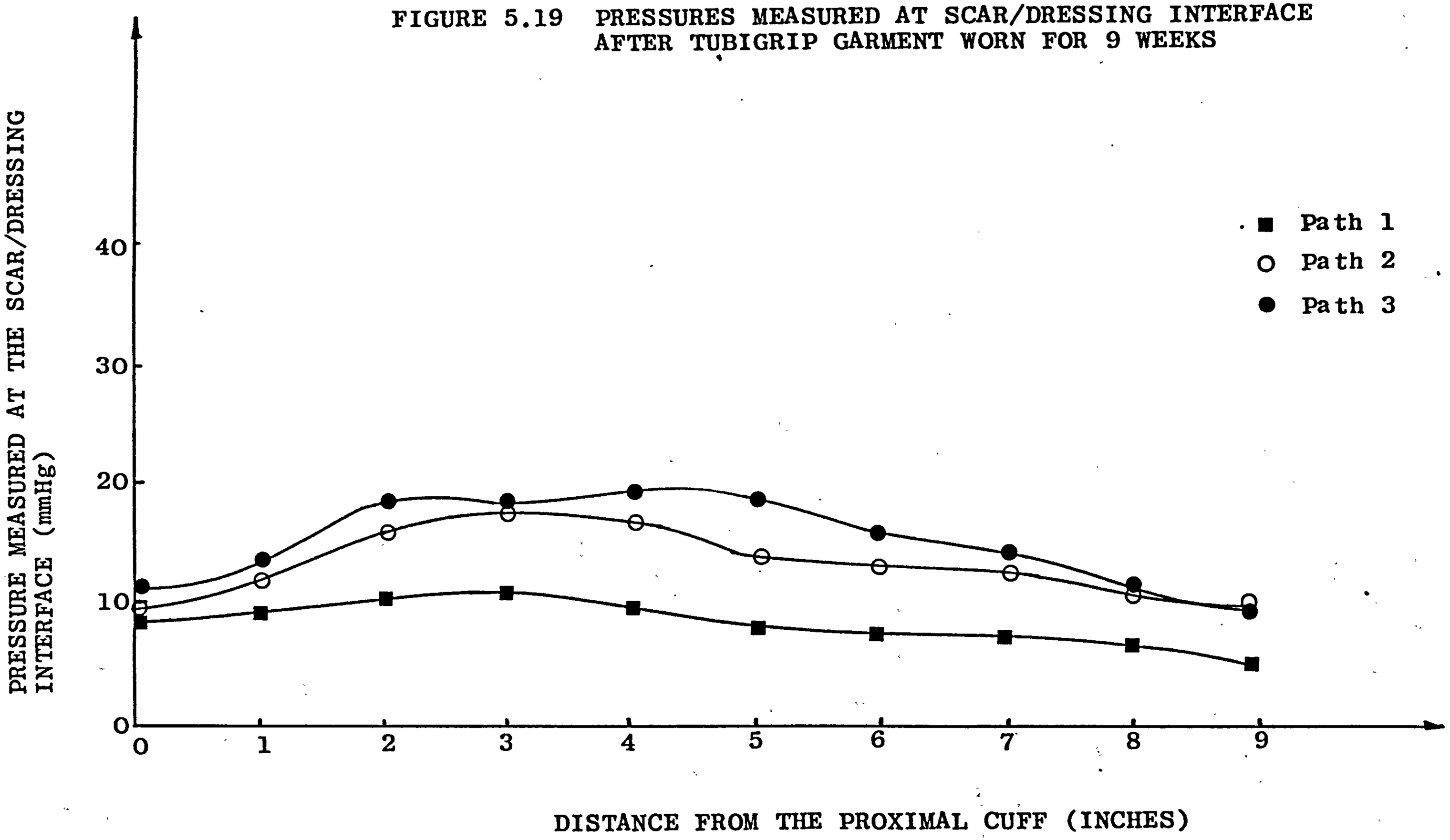

indicated along which transducers were moved to record pressures. Initially pressure was applied with a Lycra garment however after only two weeks the tension of the garment had been reduced so much that negligible pressures were present. Thereafter, a Tubigrip sleeve was provided on top of the Lycra garment which was now slack. The average interval between pressure measurements was two weeks and the pressures recorded from each measurement session are tabulated in Appendix B. Figure 5.18 is a graph of the results of one measurement session (No. 3) with an unworn Tubigrip sleeve fitted; pressures in mmHg were measured along the selected pathways (Figure 5.17), at the distances indicated, from the proximal cuff of the sleeve. The results indicate that pressures vary over the length of each path and also laterally. In the case of path 1 the pressure does not rise much above 10mmHg at any point and, on average it is less than 10mmHg. In contrast, pressures measured on paths 2 and 3 increase from the proximal cuff to about 18 - 20mmHg at the beginning of the plaque of scar tissue and remain at least around this level until about 1 or 2 inches from the distal cuff when they gradually decrease to about 10mmHg. From these results it is seen that the 'average' pressure applied over the scar surface is about 15 - 20mmHg except at the boundary of scar tissue and normal tissue near path 1, where pressures are lower.

The pressures were again measured as above after the Tubigrip garment had been worn for 9 weeks (Measurement Session No. 7, Appendix B), and the results are displayed in Figure 5.19 which is a graph similar to Figure 5.18. Comparing the graphs initially shows little difference between the two sets of data; the pressures measured along each of the pathways after 9 weeks wear being only slightly reduced from their original values. In particular the average pressure developed by the garment along paths 2 and 3 was about 3 - 4mmHg lower over the plaque of scar

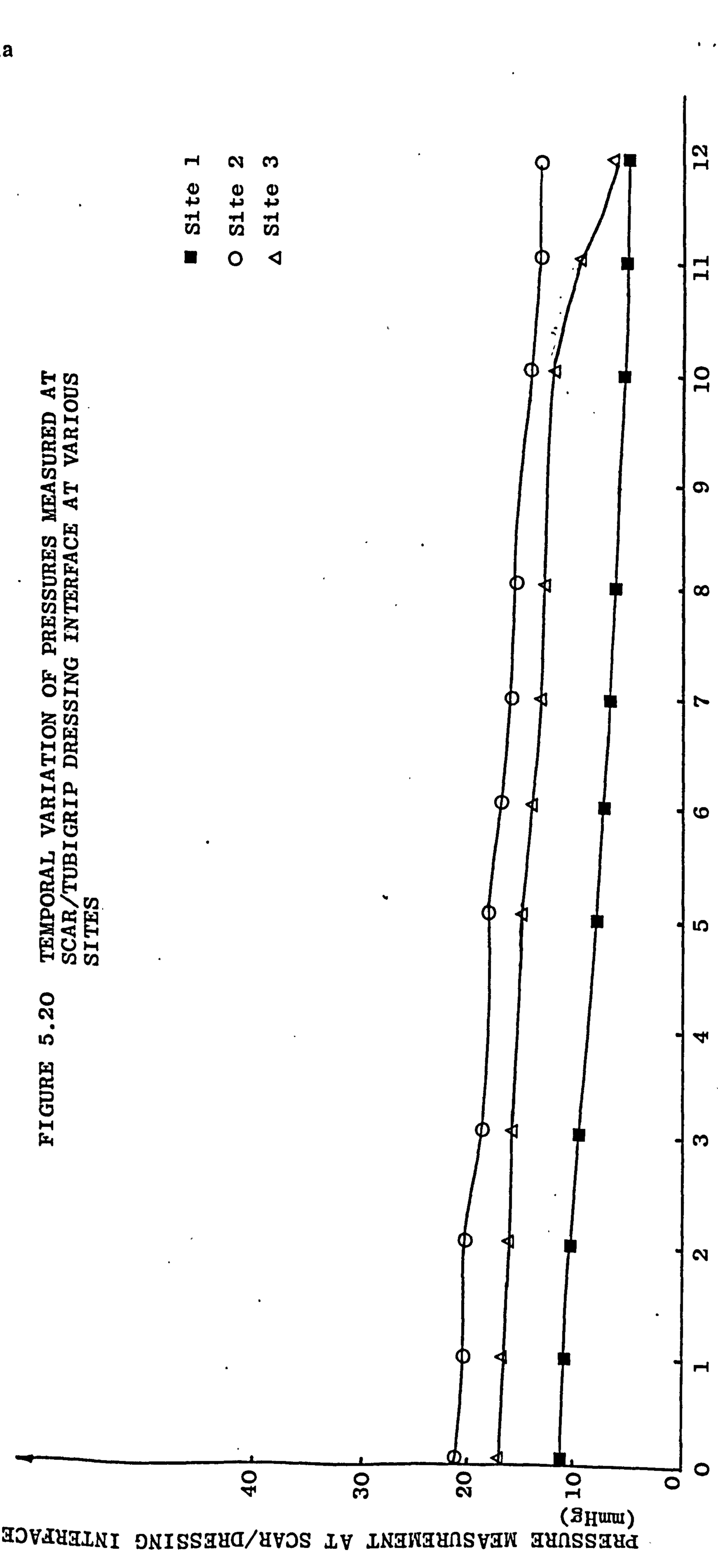

FIGURE 5.20 TEMPORAL VARIATION OF PRESSURES MEASURED AT SCAR/TUBIGRIP DRESSING INTERFACE AT VARIOUS SITES

tissue. The Tubigrip garment did not appear stretched although it was soiled and had begun to fray at both cuffs. It was decided to replace the garment, for cosmetic and hygienic reasons rather than loss of elastic properties which only occurred at the cuffs. In practice, 8 weeks was found to be an appropriate period after which to replace garments.

The temporal variation of pressures at specific sites developed by a Tubigrip garment was investigated over a period of 12 weeks at the time intervals indicated, in the case of one garment. The results are tabulated in measurement sessions 9 - 18 (Appendix B). Three sites were selected, one located on each measurement path; each site was selected principally because of the mechanical properties of the underlying tissue in response to compressive forces (Figure 5.17).

Site 1 was located on the lateral aspect of the scar on path 1 superficial to the radius bone. The surface of the tissue was flat and the radius of curvature was large. The underlying tissues were quite compliant in response to compressive forces.

Site 2 was located on the scar/normal skin boundary. The surface of the scar tissue was not flat and the underlying tissue felt rigid when compressed. It was thought that high pressures could be developed at this site.

Site 3 was located on the scar proximal to the distal cuff edge of the sleeve and superficial to the ulna. The radius of curvature was large and the underlying tissues were rigid when compressed or indented.

The results of the temporal variation in pressure are illustrated in Figure 5.20 and it is evident upon initial inspection that the pressures at each of the sites remain sensibly constant during most of the period in which the garment was worn. However there is a gradual loss of pressure over the 12 week period at sites 1 and 2 and a gradual loss over 10 weeks at site 3 followed by a large loss in weeks 10 - 12. This was accompanied by

FIGURE 5.21. CASE STUDY NO. 9: VOLAR SURFACE AFTER 9 MONTHS PRESSURE THERAPY SHOWS REMODELLED AREAS (R) AND UNREMODELLED AREAS (U)

significant fraying at the distal cuff of the tubigrip sleeve which was thought to be responsible for the reduction in pressure measured. The pressure at site 1 was less than 10mmHg overalmost the entire duration of wear. The pressures at site 2 was reduced from 20mmHg to about 18mmHg after 12 weeks wear and the pressure at site 3 was reduced from 18mmHg to 14mmHg after 10 weeks wear. These results are, surprisingly perhaps,in close agreement with the manufacturers claims (Seton Ltd. U.K.) that the garments should be replaced every three to four months. As a consequence of these results it was decided to leave the same Tubigrip garments in the scar for as long as possible. However this period was principally dictated by wear and the appearance of the garment.

Pressure was applied using Tubigrip garments for 16 months; the clinical appearance of the scar on the volar surface forearm after 9 months pressure is shown in Figure 5.21. Although the photographic reproduction is poor it still shows that the elevation of the scar and erythema are reduced on the medial side (at path 1) the scar was still elevated and active looking in parts indicating little effective scar remodelling had occurred.

The average pressures at sites 1, 2 and 3 after 9 months were 9, 19 and 16mmHg respectively, and after 16 months were 10, 21 and 15mmHg respectively. At site 1 there was no evident remodelling whereas at sites 2 and 3 considerable remodelling had occurred (Figure 5.21); i.e. 15mmHg average pressure resulting in scar remodelling whereas 10mmHg did not produce remodelling. Scar tissue with at least 15mmHg pressure applied exhibited some degree of remodelling and where pressure was highest, e.g. site 2, the remodelling was usually cosmetically superior and quicker.

In an additional experiment, pressures were measured beneath an unworn Tubigrip sleeve which was double,and/or triple, layered by folding. A pressure profile of the scar/ dressing interface was recorded along path 2 only; the results are displayed in Figure 5.22. With 2 layers of

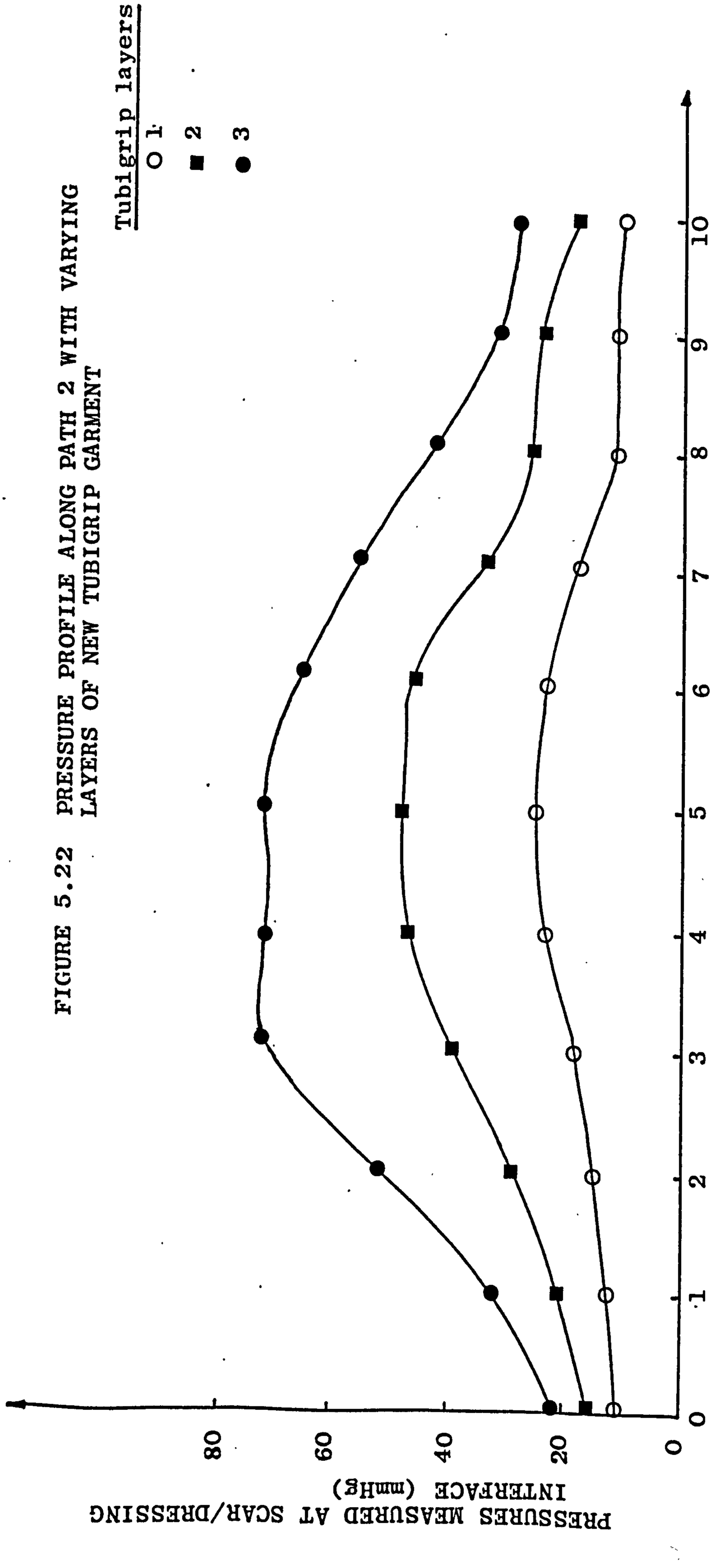

FIGURE 5.22 PRESSURE PROFILE ALONG PATH 2 WITH VARYING LAYERS OF NEW TUBIGRIP GARMENT

Tubigrip pressures were about doubled between 2 and 9 inches from the proximal cuff to 40 to 50mmHg. At all other points the pressure was increased above those produced by the single layer although the effective change at the cuffs was small. In the case of three layers, pressures were increased to 60 - 75mmHg between 2 and 7 inches from the proximal cuff. Initially this was thought to be advantageous, however the subject complained of paresthesia, within 5 - 10 minutes of wearing the triple layered Tubigrip and within 40 - 50 minutes of wearing the double-layered garment. In view of these effects only one layer of Tubigrip was used when fitting garments.

5.4.2.1. Discussion and Conclusions The pressures measured were found to vary from site to site at any one time. Of the three sites investigated pressure was found to be highest where the underlying tissue was most rigid; at site 2 where the average pressure over 16 months was 21mmHg. Significant remodelling occurred at 9 months at site 3 where the average pressure was 15mmHg. Remodelling by the pressures reported was accompanied by a significant improvement in function with the patient being able to extend the wrist through an angle of 30^{o} more after 9 months pressure. No significant remodelling was observed at site 1, at 9 or 16 months, where the average pressure was 9 and 10mmHg respectively. The small reduction in pressure, 20% on average over 6 weeks, indicates that the Tubigrip garment did not lose much of its elastic properties when worn. Therefore garment replacement due to stretching was not a problem. However, the Tubigrip garment was replaced at 6 - 8 weeks for reasons of hygiene and expediency. Multiple layers of Tubigrip, whilst producing much higher interface pressures were not used since parethesia was induced in the patients fingers shortly after fitting. Satisfactory hypertrophic scar remodelling was achieved in this case by pressure of 15mmHg over 9 months.

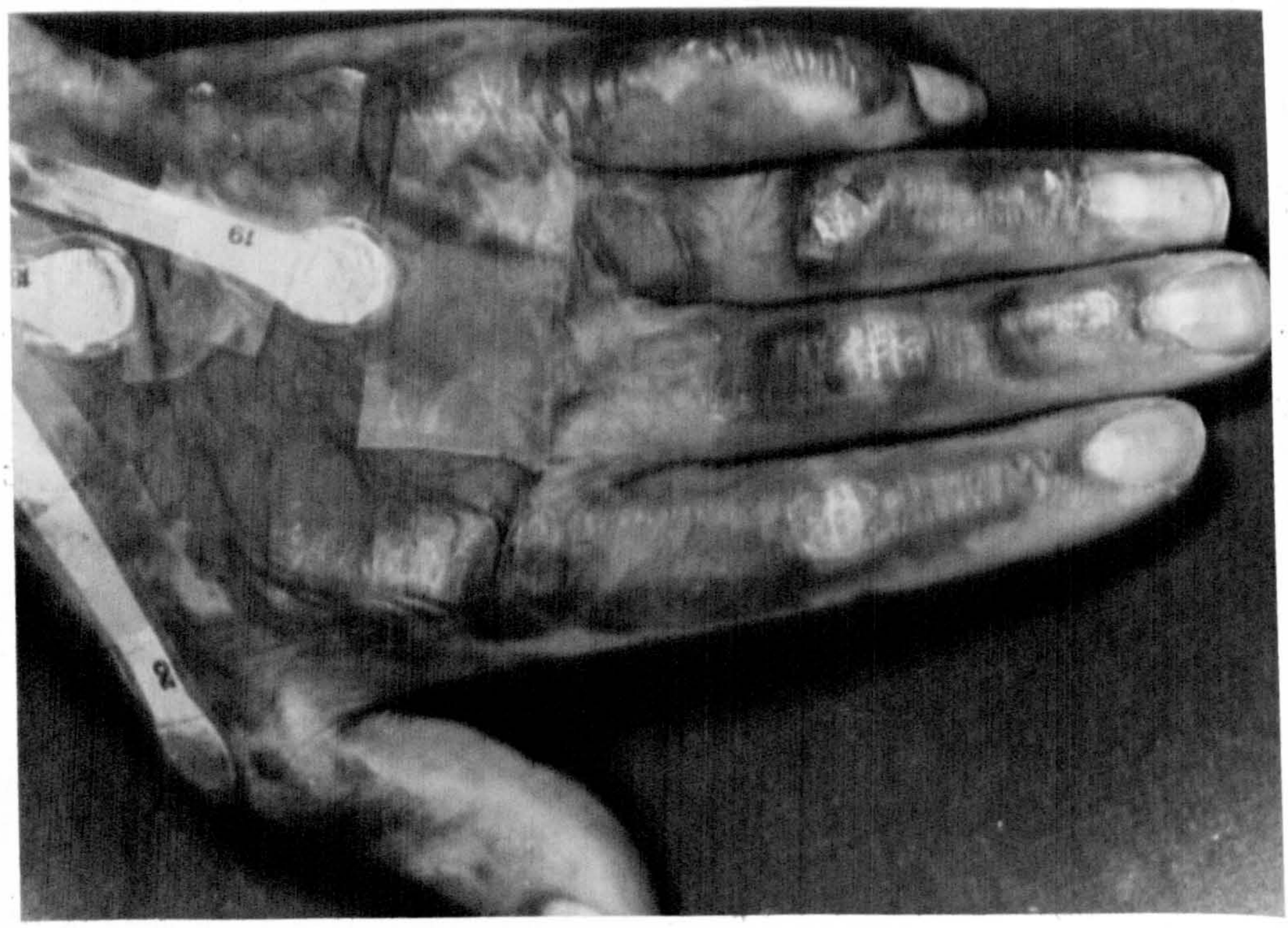

FIGURE 5.23. CASE STUDY NO.1: RIGHT HAND WITH HYPERTROPHIC SCARRING BEFORE PRESSURE THERAPY AND TRANSDUCERS ATTACHED

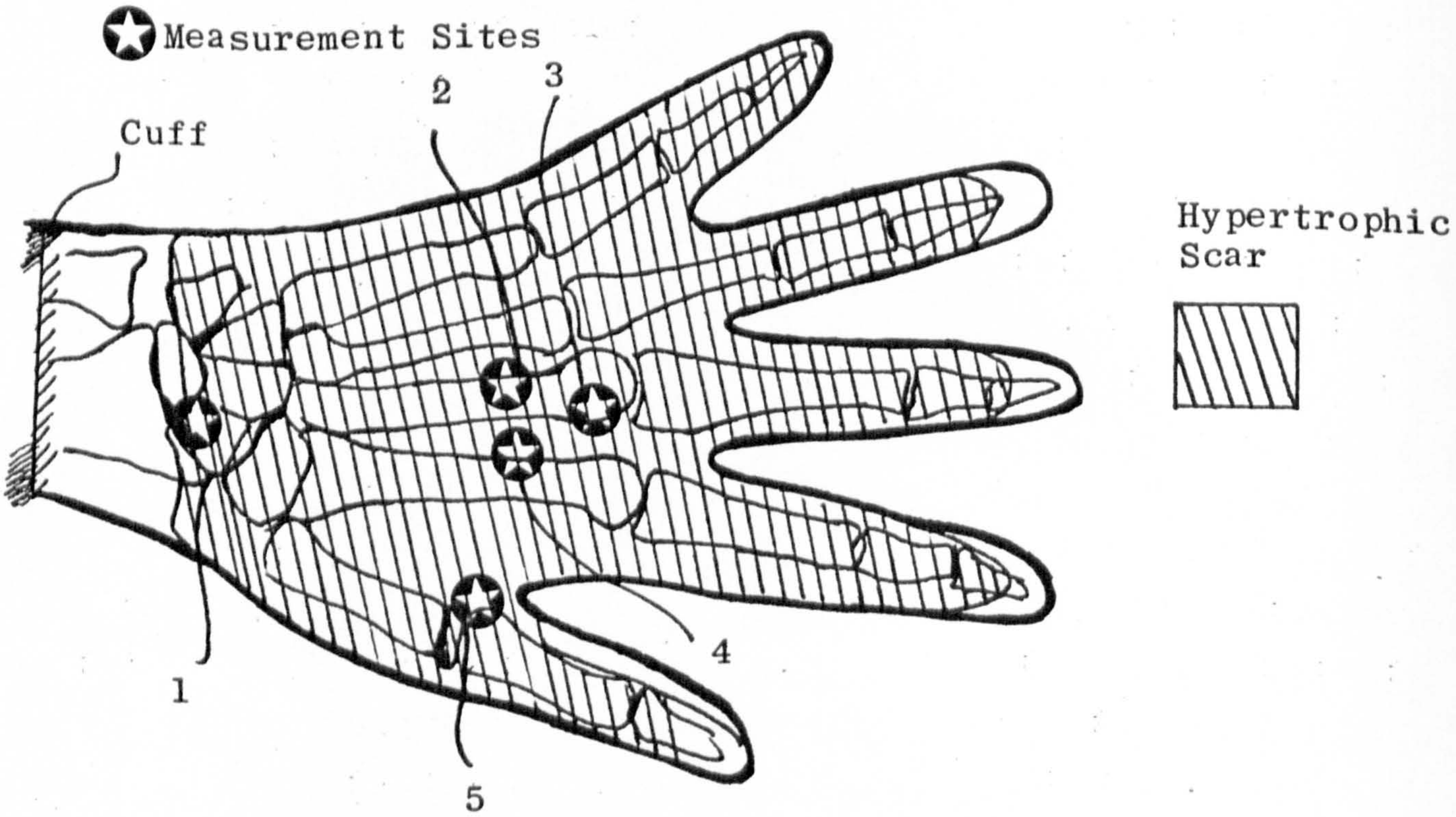

FIGURE 5.24 CASE STUDY NO. 1: SCHEMATIC DIAGRAM OF PRESSURE MEASUREMENT SITES

5.4.3. Case Study No. 1

A male caucasian, aged 33 at the time of injury, sustained burns to both hands in a chemical explosion. Hypertrophic scarring developed subsequent to wound healing and 4 months after injury elevated erythemic scars were present on the dorsal surface of both hands. Figure 5.23 shows the scarring on the right hand only. Lycra gloves were first fitted to the patient two months after the scars developed. The extent of the scarring is shown diagrammatically in Figure 5.24 and the sites at which the transducers are located, on the left hand only, are also shown.

Site 1 was located on scar tissue distal to the scar/normal skin boundary. The underlying tissue was rigid in response to compression.

Sites 2, 3 and 4 were located on the dorsal surface of the hand as shown. The underlying tissues were rigid in response to compressive forces.

Site 5 was located on the thumb or first digit superficial to the metacarpal bone, the underlying tissue was fairly compliant.

The transducer located at site 5 was expected to record any changes in pressure with movement of the metacarpal phalangeal (mp) joint.

Pressures were recorded every 2 and 3 weeks. The pressures recorded at each site during each measurement session are tabulated in Appendix B.

At any given measurement session the pressures recorded vary from site to site; pressures being highest on sites 3, 4 and 5 followed by site 2 and site 1 respectively. Where a Lycra garment was initially fitted the pressures measured at each site was above mean capillary pressure (m.c.p.) (25mmHg). The pressures measured at each site during the life of any one Lycra glove descreased with time, falling to less than m.c.p. after 7 to 8 weeks continuous wear. Consequently, the gloves were replaced at about this frequency

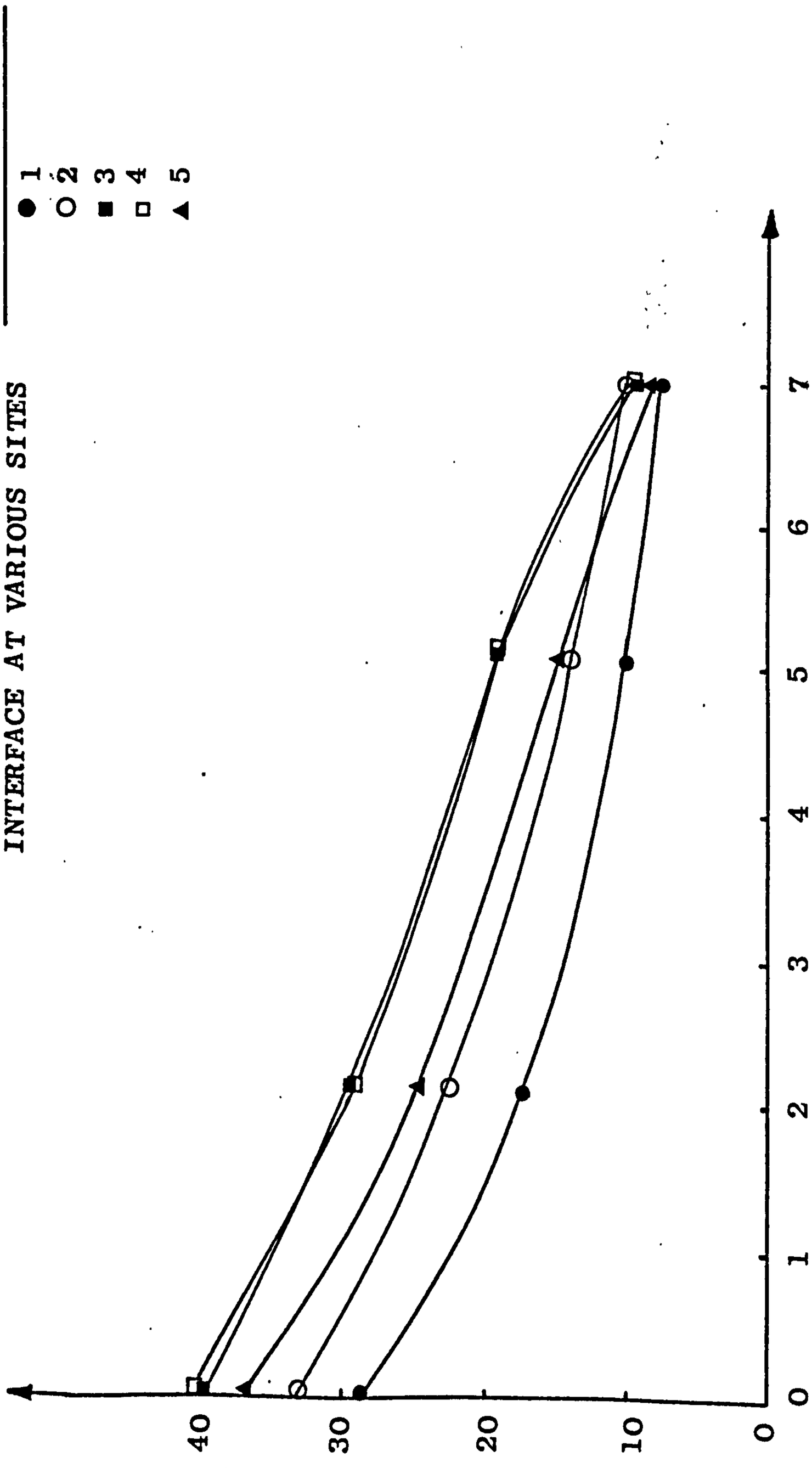

FIGURE 5.25 TEMPORAL VARIATIONS OF PRESSURES MEASURED AT THE INTERFACE AT VARIOUS SITES

Pressure developed by the Lycra glove at the scar/dressing interface (Measurement Session 13 - 16, Appendix B) are displayed graphically in Figure 5.25 from which it is seen that the pressures were reduced by half of their original value within 5 weeks of the glove being fitted. However, even after 7 weeks wear, pressure was considerably reduced below 15mmHg only at site 1. The average pressures developed at each of sites 1, 2, 3, 4 and 5 were calculated to be nearest mmHg, 18, 24, 33, 31, 29mmHg respectively after 10 weeks pressure. Figure 5.26 shows the clinical appearance of the dorsal surface of both hands after 10 weeks of pressure therapy. At each site at which pressure was measured remodelling of the scar tissue had taken place; in particular the remodelling achieved at site 1, due to 18mmHg average pressure, was good. In general the average pressure over the scar surface appeared to be between 18 and 28mmHg; the scar appeared much flatter and paler than before treatment and the scar tissue pliability and extensibility was increased. Both hands showed the same appearance after 10 weeks pressure (Figure 5.26). After 50 weeks of pressure, the average pressure at sites 1, 2, 3, 4 and 5 being 15.5, 20.2, 28.4, 26.6 and 25 which are very similar to the average pressures after 9 months treatment, the clinical appearance of the scar was further improved; erythema was reduced further and the 'normal' pigmentation appeared to have returned to the scar tissue/normal skin boundary was not distinguishable by differences in elevation (Figure 5.27) . Prurities was also reduced.

In addition, the skin showed a more normal 'wrinkled' texture and the extensibility of the skin was further improved. At site 1, an average pressure of 15mmHg over about 12 months induced scar remodelling, however, those sites having higher average pressures applied did not appear cosmetically superior.

Pressures were also measured at each site when the patient made 'fists' with both hands; the pressures at sites

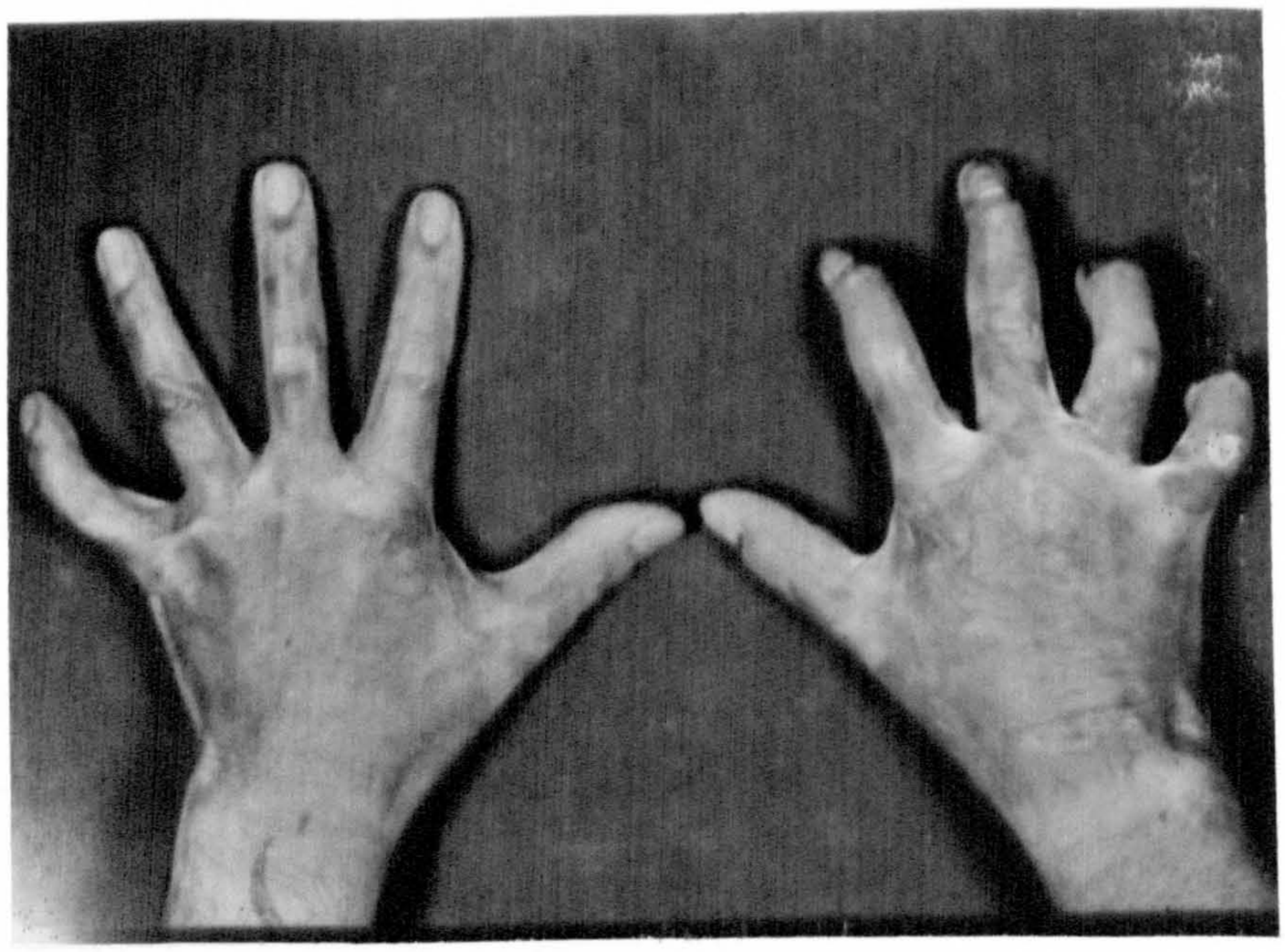

FIGURE 5.26. BOTH HANDS AFTER 10 WEEKS ON PRESSURE THERAPY SHOWING MARKED COSMETIC IMPROVEMENT

FIGURE 5.27. BOTH HANDS AFTER 12 MONTHS PRESSURE THERAPY SHOWING "WRINKLED" SKIN TEXTURE

3,4 and 5 exceeded 100mmHg in this position, and at sites 1 and 3 increased to 40mmHg and 60 - 70mmHg respectively. There was no apparent change in the radius of curvature at any site which could have resulted in artificially high pressures; the mechanical tissue underlying the transducers became more rigid with the hand fixed and the garment was stretched. A combination of these two factors was thought to produce the high pressures measured.

In addition, when the gloves were removed in the first 3 - 6 months of pressure therapy the patient complained of pain and 'throbbing' in both hands. These symptoms disappeared when the gloves were reworn even when the glove had been worn for several weeks and the average pressure applied to the tissue were lower than at the initial fitting.

5.4.3.1. Discussion and Conclusions The pressures measured at the scar/dressing interface varied from site to site, the variations were small presumably because of the similar anatomical location of the transducers and the curvature at these sites. The average pressure applied to each site over 12 months was at least 15mmHg and remodelling occurred at each site. There was, however, no control site. The pressure produced by the Lycra gloves was reduced by about 50% of from original levels after about 4 - 5 weeks wear, however the gloves were not replaced at this time as the pressures produced were still greater than 14 - 15mmHg. The average pressure applied over the scar surfaces was thought to be about 18 - 28mmHg and the degree of scar remodelling achieved was good even after 12 weeks pressure, in terms of elevation, although it remained somewhat erythemic. The rapid flattening of the scar was thought to be due to either accelerated remodelling of the natural remodelling process or to expulsion of extravascular fluid in the scar; the latter reason being discussed in more detail in section 5.5. The pressures reported must have had some effect on blood flow, since the patient reported an absence

of pain and pruritis when the gloves were worn. How these pressures would affect the blood flow is unclear, the most probable reason being that the pressure augmented venous and lymphatic drainage.

The average pressures measured in this case resulted in inducing remodelling at each site investigated, and although significant remodelling occurred after 12 weeks pressure the scar seemed more completely remodelled at 12 months, the texture and appearance of the scar being more similar in appearance to normal scar and normal skin.

5.5. GENERAL DISCUSSION AND CONCLUSIONS

As a preliminary point, the way in which the average pressure values were obtained for each patient was not wholly satisfactory; it would have been better to monitor pressures continuously instead of 'sampling' pressures at irregular intervals and integrating these sampled values to provide an 'average' value of pressure. However continuous monitoring was impractical since the instrumentation was not designed for being worn or used 24 hours a day and, in any event, the development of such an instrumentation system would have unduly delayed clinical investigations.

The 'sampled' values of pressures measured are assumed to be representative of the 'continuous' pressure although obviously, the more 'samples' taken the greater the accuracy between the calculated averaged pressures and the true average pressure. This assumption was thought to be valid since the 6 hour 'quasi long-term' study in case study No. 1 showed that the pressure is sensibly constant at any particular site, apparently varying slightly about a mean value. The observed variations may be due to changes in the arm volume (vide 5.4.1) rather than changes in the mechanical properties of the garments.

Initially 'static' pressure measurements were made however these were generally time-consuming to set up and measurements were restricted to a few sites. Therefore most of the measurements were taken with the transducers being moved to different locations beneath the garments

(vide 5.4.1 and 5.4.2).

The pressures measured were found, as expected, to vary considerably from site to site, the absolute value of pressure depending principally on the anatomical location of the scar which, in turn, defines the radius of curvature the mechanical properties of the tissue and, to a certain extent, the mechanical properties of the pressure garment.

The anatomical sites chosen did not have a small radius of curvature (i.e. less than 100mm) so the pressures measured were thought to be generally independent of curvature. As the transducers were located beneath the pressure garments for a few minutes only, the effects of creep were thought to be very small (vide 4.5.6). The effect of physical parameters on the transducers response was therefore considered almost negligible.

Hypertrophic scars at anatomical sites with a convex curvature, and located over rigid underlying tissue, such as bone, were treated with high pressures, in general, and the cosmetic result of remodelling was good (Case No. 6, site 2). Conversely, with scars at sites where the surface was concave, such as the back between the scapulae or the anterior thorax at the sternum, it was very difficult to apply pressure since the pressure garments 'bridged' the concave surface. This problem was also noted by Larson et al (1971). One way in which this problem was overcome was by inserting 'pressure pads' beneath the elastic garments at the concave surface to present a convex surface to the pressure garment. This technique though successful, was not popular since it introduced some discomfort due to the shape and size of the pads used; and the pads were frequently removed by the patients.

In addition, at sites where the underlying tissue was very compliant, and the effective radius of curvature very large, i.e. at the abdomen or buttocks, pressures greater than 10mmHg were difficult to achieve. Hypertrophic scars on the extremites appeared to be best suited to pressure treatment since they are accessible to garment fitting and

compatible with continuous garment wear. In contrast, scars on the abdomen and hips which required a Lycra 'body-suit' usually affected hygiene and toilet functions inter alia, especially in children.

Permanent remodelling was found to occur at sites which had average pressures of 14 - 15mmHg. This is in contrast to previous reports (Larson et al, 1971, Larson et al, 1974) which state that for permanent remodelling pressure should be greater than mean capillary pressure (24 - 25mmHg). Remodelling was found not to occur at sites which had average pressures of the order of 12mmHg and less, although an average pressure of 15mmHg also did not result in remodelling in one instance (Case No. 11, Table 5.5.).

It is unclear whether a critical threshold level exists for applied pressure which, when exceeded, results in scar remodelling. From the results obtained, this appears to be true although such a threshold level may vary between patients and also between different sites on each patient.

The cosmetic result of remodelling was thought to be dependent on the magnitude of applied pressure; scars which had pressure applied considerably in excess of 14 - 15mmHg, appeared flatter amd smoother, in general, than scars with lower average pressures applied. However, the applied pressure may also have an upper threshold level; on several instances pressure greater than 40mmHg resulted in effects such as ulceration and maceration (Cases No. 3, 11 and 15) and in Case No. 11 when average pressures about 45mmHg were applied, paresthesia occurred within 40 - 50 minutes of application and sooner with higher pressures.

It appears from the results that the magnitude of pressure required to induce remodelling has a lower value of 14 - 15mmHg and an upper value of 40 - 45mmHg. Within this range, better remodelling was achieved with increasing magnitude of pressure. In general, scar remodelling, in terms of reduction in elevation and increasing smoothness in the texture of the scars, occurred rapidly (Case No. 1, Figure) however erythema remained present

in some scars a considerable time after the application of pressure (Case No. 6, Figure 5.14). It has been reported that discontinuing pressure before permanent remodelling of the scar has occurred can result in a recurrance of hypertrophy (Larson et al, 1971, Larson et al, 1974). The only practical method to date of determining whether remodelling is complete is by inspecting the scar; flat scars without erythema have been used as a diagnosis of remodelling (Larson et al, 1974). It was also stated the duration of pressure to achieve maturation or permanent remodelling is on average 6 to 12 months.

In this study, satisfactory remodelling was achieved in general, with 6 months of the application of pressure, with most scars appearing much paler than before pressure was applied, although exceptions (Figure 5.14) occurred. In no case was pressure discontinued once remodelling had been achieved, principally for ethical reasons. It is therefore not possible to comment the duration of pressure with regard to recurrence of scars although it is felt that a minimum period of 6 - 12 months pressure is required to effect permanent remodelling as evidenced by a reduction in erythema.

Clearly a more objective assessment of the appearance of the scar, or of some other parameter, is required in order to specify more accurately the duration of pressure required to induce permanent remodelling.

The reason for the occurrence of rapid scar remodelling was unclear; it was not known whether this was genuine remodelling or was due to extravascular fluid being 'squeezed' out of the tissue. Psillakis et al (1971) reported that the water content in hypertrophic scars is greater than in normal scars, therefore if pressure did 'squeeze' out fluid it was thought that the value of the water content of the pressure treated scars may indicate the degree of maturation achieved by pressure.

A brief investigation was carried out in which biopsies from pressure treated and untreated hypertrophic scars were analysed for % water content. A description of the procedure

and results are given in Appendix B. The results indicate that there is no significant difference between the water content of the pressure treated and untreated hypertrophic scars which prima facie indicates that genuine remodelling has occurred. However, it was thought that the technique employed in obtaining the biopsies was suspect; injections of either 1% or 2% Lignocaine anaesthetic were given near to the areas of which biopsies were obtained. The injecting medium is principally a water carrier and could have significantly modified the water content of the tissues from which samples were taken. The author does not express any great degree of confidence in the results, which are provided principally for completeness of the study.

Of the two materials used to apply pressure Tubigrip retained its elastic properties longer than Lycra, although there was not much difference between the pressures developed when the garments were initially fitted (Case No. 9, Measurement Sessions No. 1 and 2). Both types of garment intially developed pressures at the upper end of the range found to induce remodelling.

Lycra garments exhibited different elastic properties to Tubigrip garments; Lycra having a similar value of stiffness in two orthogonal directions whereas Tubigrip has only one principal direction of stiffness (Appendix B). From the results of the mechanical tests a theoretical calculation of pressures developed at a scar/dressing interface for an identical strain (20%*) imposed on both types of materials resulted in higher pressures being produced by the Tubigrip garment, despite both stiffness loads being included in the calculation of pressure developed by Lycra garments (Appendix B). From this theoretical calculation it appears that the elastic properties of Tubigrip are inherently suited to providing higher interface pressures. Nevertheless, in practice, as shown in cases No. 1 and 6, Lycra garments provided pressures which resulted in good scar remodelling.

---

* 20% strain was a common value of strain when both Lycra and Tubigrip garments were in-situ.

In addition, Lycra garments with a body portion produced frequent complaints of discomfort, especially in children, due to inadequate ventilation of the skin although Lycra is a woven material (vide 5.2.1). In 5 out of 16 cases examined the results were disregarded because patients did not wear the garments continuously, principally due to the discomfort factor (vide 5.4). Of course, no remodelling was achieved with these patients despite high pressures measured. No discomfort was reported with Tubigrip garments, although as the garments were used only on the extremities any comparison with Lycra body garments is unfair.

A further disadvantage of the Lycra garments used in this study was the 'turn around' time from measurement to fitting; 3 weeks was not uncommon and if poor fitting occurred, which was common, the patient did not receive the garment for at least 6 weeks. In contrast, as Tubigrip garments are available in a range of sized which are suitable for most people, fitting and refitting of Tubigrip garments was achieved in minutes.

Lycra garments were expensive compared to Tubigrip (Case No. 9, Lycra sleeve £29.78 and Tubigrip sleeve, < £1). Thus, as patients required at least two pressure garments (one to change with when other was being washed) the total cost of garments per patient was considerable especially when body suits were required (e.g. Case No. 11, circa £1100/annum).

Despite claims by the manufacturer (Jobst Inc. U.S.A.) and various reports (Larson et al, 1974) testifying to the efficiency of pressure garments the author has, in this study, been unable to confirm these claims. On the contrary, the rapid loss of elastic properties, discomfort produced by certain types of garments, and very high cost relative to Tubigrip mitigated against the continued use of Lycra garments in the investigation.

Tubigrip whilst having elastic properties in one direction only provided pressures which produced scar remodelling as good as was achieved by Lycra and it also

retained its initial elastic properties for a considerably longer time. Custom-made Tubigrip garments were not available at the time of the investigation and consequently the use of Tubigrip garments was restricted to scarring on the extremities. Custom-made Tubigrip garments have since become available since the completion of study.

Although Tubigrip and Lycra garments both induce scar remodelling the disadvantages associated with the Lycra material, rather than the advantages of Tubigrip render the latter more suitable for use as pressure garments.

5.6. SUMMARY

Pressure applied to hypertrophic scars from two materials with elastic properties, Lycra and Tubigrip, induced scar remodelling. A comparison of the Tubigrip and Lycra pressure garments in terms of effectiveness and efficiency showed Tubigrip to be the garment of choice for applying pressure. A pressure of at least 14 - 15mmHg was found to be necessary, in general, to induce scar remodelling. The appearance of the remodelled scars was better with higher average pressures applied although pressures above 40 - 50mmHg frequently resulted in some form of adverse tissue reaction. The duration of pressure should be at least 6 - 9 months or until the scar does not appear erythemic. An investigation of the optimum duration pressure application using the % water content of pressure-treated and untreated hypertrophic scars was thought to be inconclusive due to a discrepency in the experimental technique.

The need for a more objective assessment of the minimum duration of pressure required to produce 'maturation' of the scar or non-recurrence of hypertrophy after pressure is discontinued is emphasised. This in turn would assist in optimising pressure therapy.

CHAPTER 6

COLLAGEN BIOSYNTHESIS INVESTIGATIONS IN PRESSURE TREATED AND UNTREATED HYPERTROPHIC SCARS

6.1. Introduction

6.2. Selection of the Method of Determining Collagen Biosynthesis

- 6.2.1. Enzyme-Based Assays of Collagen Synthesis
- 6.2.2. Non-Enzyme Based Assays of Collagen Synthesis

6.3. Materials and Methods

- 6.3.1. Tissue Preparation
- 6.3.2. Incubation Conditions
- 6.3.3. Assay of Total Radioactivity and Hydroxy-Proline Radioactivity

6.4. Experimental Design

- 6.4.1. Patient Population
- 6.4.2. Verification of Incubation System
- 6.4.3. Calibration and Verification of the Assay Procedure

6.5. Experimental Results

- 6.5.1. Collagen Biosynthesis in Normal Skin and Normal Scar.
- 6.5.2. Collagen Biosynthesis in Pressure Treated and Untreated Hypertrophic Scars
- 6.5.3. Discussion and Conclusions

6.6. Summary

CHAPTER 6

6.1. INTRODUCTION

The remodelling of hypertrophic scar tissue has been thought to be due principally to a collagen-based process (vide 3.4); it has been suggested that serum proteins in blood inhibit the enzyme collagenase which results in excess collagen being produced and that applied pressure reduces the blood flow, and consequently the serum proteins. When this happens, the activity of the collagenase is no longer inhibited and the natural remodelling process is initiated or maintained (Baur et al, 1976). However Milsom and Craig (1973) examined collagenase enzymes cultured from normal skin and from hypertrophic scar tissue and found no substantial difference between the nature or the amount of the collagenase enzymes from each tissue type although normal scar was not included in the study. Conversely, the enzyme prolyhydroxylase has been shown to be significantly higher in hypertrophic scars than in normal skin in-vitro (Eisen, Bauer and Jeffrey, 1971) which suggests that collagen biosynthesis in hypertrophic scars may be increased above 'normal' levels in-vivo. A comparative study between the rates of collagen synthesis in normal skin, hypertrophic scars and normal scar using the rate of incorporation of labelled ^{14}C-proline into peptide-bound hydroxy (^{14}C) proline in-vitro showed that although the rates of collagen synthesis were similar in hypertrophic scar and normal skin they were significantly higher in both these tissues than the rate of collagen synthesis in normal scar (Craig et al, 1975a). Craig et al (1975b) in a study of collagen biosynthesis as a function of duration of the scar found that the rate of collagen biosynthesis of a 'normal' scar remained approximately constant in the period 6 months to 20 years after injury. It was also found that the rate of collagen biosynthesis in active hypertrophic scars was about twice that of normal scars for up to 3 years after wounding then fell to about the same level as normal

scars after a subsequent period of two to five years. This result indicated that natural resorption of hypertrophic scars towards 'normal scars' is also accompanied by concomitant biochemical changes.

In order to investigate the hypothesis that the remodelling of hypertrophic scar is due to a collagen-based mechanism which is principally reflected by changes in collagen biosynthesis it is necessary to relate collagen biosynthesis parameters, such as rate, in pressure treated and untreated scars to the magnitude and duration of pressure applied. Furthermore, the collagen biosynthesis studies may indicate whether there is a critical duration of pressure which reduces collagen biosynthesis such that hypertrophy will not recur following discontinuing of pressure therapy. As mentioned in Chapter 5 (vide 5.5) this may assist in determining optimum regimes of pressure therapy.

6.2. SELECTION OF THE METHOD OF DETERMINING COLLAGEN BIOSYNTHESIS

Collagen biosynthesis can be determined by any one of several methods, however techniques using radioactive-labelled materials are the most obvious choice since they produce results from which the absolute rate of synthesis can be determined thereby providing a good indication of what the metabolism or activity of the parent tissue is likely to be in-vivo.

Two principal techniques exist: those which involves enzymes and those which do not. The enzymes usually involved are collagenase and prolyhydroxylase.

6.2.1. Enzyme-Based Assays of Collagen Synthesis

In the case of using the enzyme collagenase, collagen biosynthesis has been estimated by labelling cells with radioactive proline then extracting the protein fraction followed by digestion of the collagen fraction by a collagenase enzyme (Diegelmann, 1975). Analysis of the radioactivity of the respective fractions enables the percentage of collagen and also the percentage of non-collagen proteins to be calculated. This technique is, in biochemical terms, relative simple but a limiting factor in the accuracy of

the results has been the requirement to have an extremely purified form of collagenase. In addition, instability of the enzyme itself can produce widely varying and inaccurate results.

Prolyhydroxylase is the enzyme which converts peptide-bound proline to hydroxyproline (Peacock and Van Winkle, 1971) and has been used in several studies to determine collagen biosynthesis. (Madden and Peacock, 1968, Jeffrey and Eisen, 1971). However this enzyme requires 'catalysts' in the form of oxygen and several other cofactors such as ferrous iron, α-ketoglutarate and ascorbate in order for optimum reaction conditions to be obtained (Hutton et al, 1966). In addition, studies have been reported in which the increase in the prolyhydroxylase activity occurs before the collagen content of the tissue increases (Mussini et al, 1967). That is, the level of collagen synthesis reflected by this enzyme assay and the actual or true level of collagen synthesis may be 'out of phase' and consequently different. Therefore measurement of prolyhydroxylase activity may not accurately reflect the rate of collagen synthesis.

6.2.2. Non-Enzyme Based Assay of Collagen Biosynthesis

Measurement of collagen synthesis by isolating the imino-acid hydroxyproline and then using a radioactive hydroxyproline assay is a well documented technique with consistent and accurate results being reported (Uitto, 1970, Craig et al, 1975a).

Hydroxyproline is found almost exclusively in collagen, constituting about 14% dry weight thereof and therefore the rate of incorporation of proline into peptide-bound hydroxyproline is considered to reflect the rate of collagen biosynthesis. Hydroxyproline *per se* is not incorporated into peptides but proline is incorporated and is then enzymatically hydroxylated into hydroxyproline. This is the reason for incubating tissues with radio-labelled proline. Although hydroxyproline *per se* is not a specific index of collagen content or rate of synthesis, as it is also present in elastin

in very small amounts, the assay is straightforward if somewhat lengthy, and reliable with no tempremental enzymes present. In addition, basic biochemical analyses permits a reasonable estimate of the concentration of hydroxyproline in both elastin and collagen and this analyses can be used to correct the results of the assay if required.

The author thought that the use of a non-enzyme assay would be most suitable for measuring collagen biosynthesis for two principal reasons; available published and well documented results relating to comparisons of collagen biosynthesis between hypertrophic and normal scar tissues and normal skin which would confirm the repeatability of the assay, and the reliability and straightforwardness of the assay procedure. In addition, any errors due to the presence of hydroxyproline in elastin were expected to be low because of the widely reported low levels of elastin in scar tissue (Linares et al, 1974).

The actual assay technique selected to investigate the effect of pressure on collagen biosynthesis in hypertrophic scar tissue in-vitro was based on the method of Uitto (1970) as modified by Craig et al (1975a) in which collagen biosynthesis was estimated by measuring the incorporation of radioactive uniformly labelled (^{14}C)-proline into non-dialysable peptide-bound hydroxy (^{14}C)-proline by tissue samples incubated in-vitro (Appendix C).

6.3. MATERIALS AND METHODS

The major procedures involved during the assay and the apparatus and techniques used therein, are described under the following headings.

6.3.1. Tissue Preparation

Normal skin and hypertrophic and normal scar samples were obtained either during surgery or from the out-patient clinic using a Stiefel* biopsy punch technique. The Biopsy punch technique is dealt with in detail by Tully (1980) and the reader is referred to the associated thesis thereof for a description of the technique employed. The average

---

* Stiefel Laboratorium GmbH, Offenbach, Main, West Germany

weight of tissue samples obtained with the biopsy punch was about 20 - 40mg and from surgery considerably higher.

Biopsies from 13 subjects, 12 of whom were male, receiving pressure therapy were used in the assay. Biopsies were taken from both pressure treated and untreated sites of the same individual where possible although this occurred with only 4 subjects. Normal skin and normal scar samples were obtained from tissue excised during surgery. In the case of normal skin samples from 6 individuals were obtained of which 3 were male, and in the case of normal scar three samples were obtained, of which two were male.

Each tissue sample was transferred, as soon as possible, after removal from the donor to the laboratory, in a vacuum flask of ice cold normal saline. Once in the laboratory, each tissue sample was placed in sterile laminar flow cabinet and the subcutaneous fat and the epidermis were trimmed off with fine springbow scissors or a scalpel and the remaining dermis was then minced, as finely as possible, with scissors. The minced tissue was then added to a flask containing incubation medium, the total weight of which was known, and weighed. The weight of the tissue was obtained by simple subtraction, and was termed 'wet weight', the units of weight being grams.

6.3.2. Incubation Conditions

The minced tissue samples were incubated in a medium of 3.3ml total volume containing N- 2-hydroxyethylpiperazine-N^1-Z ethanesulphonic acid (HEPES) in a 20ml concentration at pH 7.4, glucose at 20mM concentation of 0.05mg/ml and 1μCi of uniformly labelled L-$\left[U-{}^{14}C\right]$-proline (Radiochemical Centre, Amersham). The medium volume was made up to 3.3ml in a phosphate free Krebs-Ringer balanced salt solution to provide the above concentrations (Appendix C). Each sample was incubated in the above medium in a 10ml flask under an air atmosphere at 37°C for the times indicated below. The incubation was stopped by rapidly cooling the flask contents

to $0^{o}C$ with a solution of ice and water and then homogenising the tissue sample in the presence of $2,2^{1}$-bipyridine* (1mM final concentration) in solution together with 100mg of L-proline as a carrier. The blades of the homogeniser (Polytron, U.K.) were rinsed with 2ml Krebs-Ringer solution between samples into the respective sample flasks containing the homogenate to prevent cross-contamination.

6.3.3. Assay of Total Radioactivity and Hydroxyproline Radioactivity

After homogenisation, each sample was placed in dialysis tubing (Visking, 14mm O.D.) and the tubes were sealed by tieing the tubing at either end with surgical suture material (Mersilk grade 3.0), which did not slip. The contents of each tube was approximately 5ml and the samples were suspended in a water bath and dialysed against running tap water for 24 hours. After dialysis the contents of each tube were placed in a 50ml test tube (Quickfit, U.K.) and an equal volume of concentrated (12N) HCl was added giving a resulting concentration of 6N. The test tube was then sealed under nitrogen (N_2) gas with P.T.F.E. tape and stoppered and hydrolysed for 6 hours at $135^{o}C$ in a dry heat oven. Minimum oxygen concentration in each tube was obtained by using a flow and vent system and the minimum concentration was confirmed by using a gas analyser (Radiometer, U.K.). It was found that 1 minute per test tube in the flow and vent system was sufficient to reduce the oxygen concentration in the test tube to around 1% of its original value.

Humin pigments present in the solution were removed by adding 10mg activated charcoal (Norit A) to each sample while they were still warm. After 30 minutes the charcoal was removed by filtering the sample through filter paper (Whatman, grade 1) and then washing through with distilled water (2 x 5ml).

The filtrate and washes were combined and were taken to dryness on a rotary evaporator at $90^{o}C$. The filter paper

* $2,2^{1}$-bipyridine is an iron chelating agent which inhibits the activity of the enzyme prolyhydroxylase.

was kept for noting any radioactive counts lost during the filtration and a 5ml sample of the distillate was also retained for the same reason. The residue of each sample was redissolved in 4ml distilled water. 1mg (100 μl) of carrier L-proline and 2mg (1ml) carrier hydroxyproline were added from appropriate refrigerated standards (Proline 10mg/ml, hydroxyproline 2mg/ml).

100 μl aliquots from each sample were then taken for the determination of total radioactivity (Appendix C). Scintillation counting was carried out in a Packard 3255 liquid scintillation spectrometer.

Aliquots were also taken for determination of the hydroxyproline radioactivity by a modification of the procedure of Craig et al (1975a) (Appendix C).

6.4. EXPERIMENTAL DESIGN

The design of experiments to manifest differences existing between pressure treated and untreated hypertrophic scar is controlled by many factors. The major factors influencing experimental design are considered under the following headings.

6.4.1. Patient Population

Although the patient population is given in 6.3.1. initially it was thought to exclude subjects under 20 years of age frcm the study following a report on the variability of collagen biosynthesis in normal skin with age (Uitto, 1970). In particular, collagen biosynthesis was found to increase rapidly with decreasing age of sample from about 20 years of age. However as the rates of collagen biosynthesis were not averaged in pressure treated and untreated hypertrophic scars it was deemed unnecessary to apply this restriction, although only 2 subjects would have been excluded from the group of subjects from which normal skin samples were obtained.

It was also decided to use duplicates of samples for reproduceability. There was no limit, in theory, to the

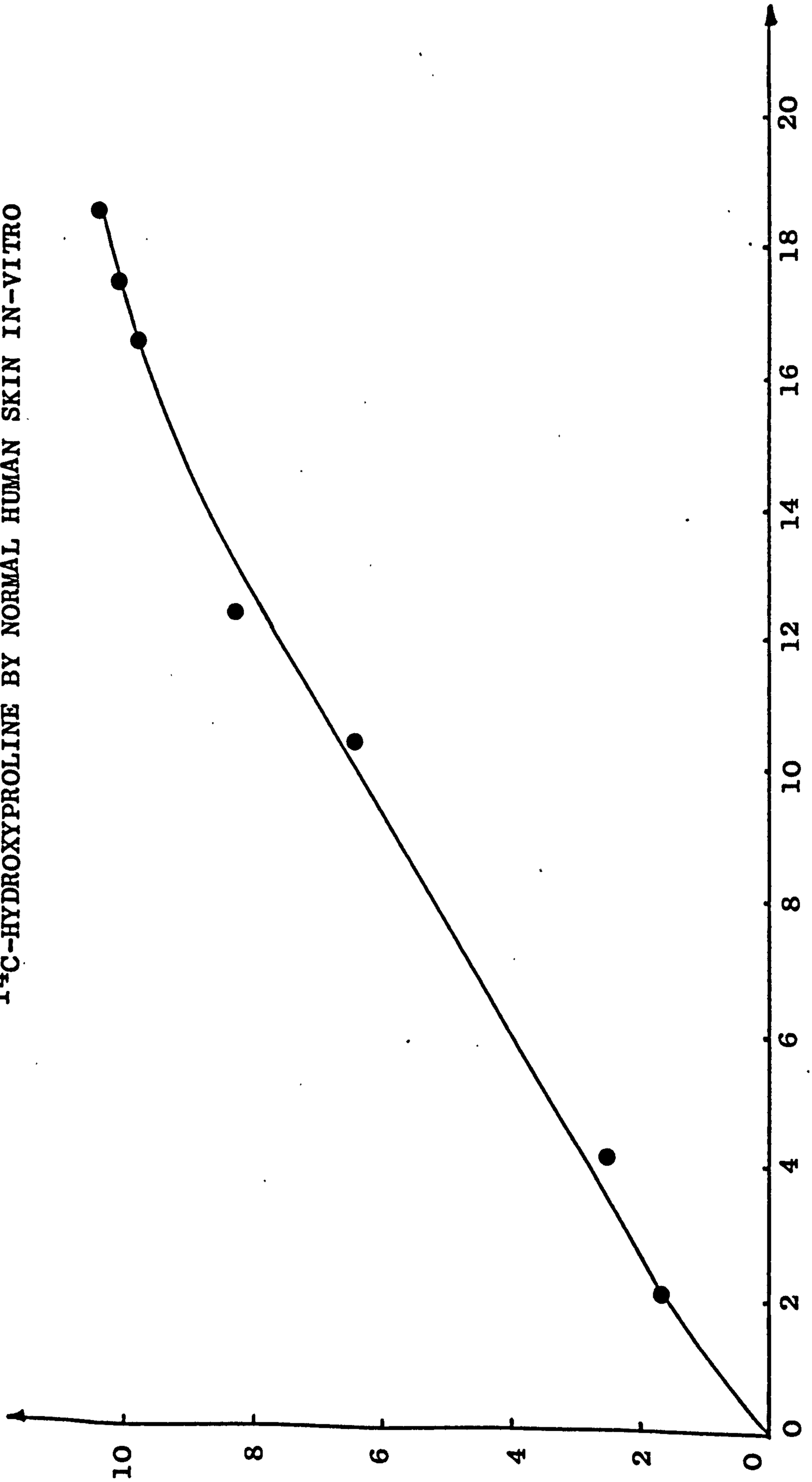

FIGURE 6.1. TIME DEPENDENCE OF THE FORMATION OF PEPTIDE-BOUND ^{14}C-HYDROXYPROLINE BY NORMAL HUMAN SKIN IN-VITRO

number of samples which could be assayed simultaneously. In practice, limitations were imposed by the materials available. However, eight (7 test samples and 1 control) was the most frequent number of samples as there were only eight fractionating columns available.

6.4.2. Verification of Incubation System

Uitto (1970) and Craig et al (1975a) established that before performing an assay of collagen biosynthesis using the aforementioned method a time-course of collagen biosynthesis was essential in order to ensure that the incubation procedure was being operated satisfactorily. Normal skin from the same site on the same individual was examined and prepared as described (vide 6.3.1.). The incubation was continued for 20 hours and samples were removed for investigation after incubation intervals of 2, 4, 10, 12, 16, 17 and 18 hours respectively.

Hydroxyproline radioactivity was determined as described in Appendix C. The results of the time-course experiment are shown graphically in Figure 6.1 and are expressed in disintegrations per minute/100mg wet weight of tissue against incubation time. As shown in the graph, the radioactivity appears to have been incorporated sensibly linearly, over the period of incubation. A slight reduction in the rate of incorporation of radioactivity, as was obtained by Craig et al, 1975a, was observed after about 17 hours of incubation. It was also observed that the counts obtained in this experiment were less than were obtained by Craig et al (1975a) however no reason could be found for this discrepency. It was concluded that the incubation time of 16 hours was suitable since the incorporation of radioactivity was still linear at this time.

6.4.3. Calibration and Verification of the Assay Procedure

In order that the results obtained from the assay were accurate, without undue loss of counts occurring, several preliminary or test assays were performed in order to "de-bug"

the system. Each of these test assays used multiple samples from the same area of tissue, which was normal skin, from the same individual. However in the first test assay both total counts and hydroxyproline counts obtained were not substantially different from the background radiation. On subsequent examination it was found that the autoclave sterilising procedure caused the medium salts to precipitate resulting in the Krebs-Ringer medium having an osmolarity of 3,000 milliosmoles. This resulted in intracellular water being drawn from the cells causing the cells to shrink and die and very little, if any, proline was formed into peptides. Consequently, prior to each incubation the osmolarity of the medium was measured and any deviation from a value of 294 milliosmoles was noted*.

The dialysis procedure was also analysed to determine the loss of counts with time. At various stages of the dialysis 100μl samples of the retentate were taken from the dialysis tubes by inserting a 40mm 9/10 Gillette Syringe through the tubing above the dialysate level therein. The volume of the syringe tip was calibrated by weighing a tip volume of distilled water and the sample volumes were modified by a correction factor (0.7) to obtain accurate results. An initial large rate of reduction due to the large concentration differences gave way to a much lower rate of reduction as the concentration difference between the tube contents and the water bath decreased, which was expected. The radioactivity in non-dialysable peptides was at an approximately constant level after 20 hours, and is equivalent to about 80,000 dpm per 100mg wet tissue. Consequently, 24 hours was selected as the minimum dialysis time. Another reason for selection of this dialysis time and counts is that a value of 80,000 dpm reduces interference from (^{14}C)-proline. This value of counts was found to be in reasonable agreement with a theoretical value for the radioactivity after dialysis (Appendix C).

A control sample of hydroxyproline in the same concentration as (^{14}C)-proline was included in each assay to test

---

* 294 milliosmoles was chosen as it was the optimum value of osmolarity for fibroblast activity.

the efficiency and integrity of the technique.

In addition, counts were measured at various stages of the assay and used to determine the loss of counts at each stage, however the loss of counts was very small in comparison to the counts for hydroxyproline radioactivity. This ensured that the amount of final counts were not low due to unforeseen losses.

The results from the scintillation counter were in counts per minute which were unsuitable for comparisons since they do not reflect the sample weight or the amount of hydroxyproline present. What was required was an indication of the collagen biosynthesis in terms of the weight or original tissue present before the incubation or in terms of the hydroxyproline content of the tissue. In addition, several steps in the assay procedure resulted in a reduction of counts.

The observed counts used to represent collagen biosynthesis recorded by the liquid scintillation counter were corrected to compensate for loss of counts using the formula:-

$$\text{Actual counts (DPM)} = \frac{100}{E} \times \frac{25}{20} \times \frac{5}{4} \times \frac{6}{5} \times \frac{100}{R} \times \text{observed counts (cpm)}$$

where DPM is disintegrations per minute,

$\frac{100}{E}$ is the correction factor the the counter efficiency (Appendix C)

$\frac{25}{20}$ is the correction factor for step 28 of the assay (Appendix C)

5/4 is the correction factor for step 7 of the assay when 1 carbon atom is lost during oxidation procedures

6/5 is the correction factor for step 26 of the assay when only 10ml of the 12ml sample is used

$\frac{100}{R}$ is the correction factor in terms of the amount of hydroxyproline synthesised where R is the (%) percentage recovery of hydroxyproline as pyrrole in μ moles

$$\text{and } \%\ R = \frac{ODsa}{ODps} \times \mu\text{moles}_{ps} \frac{25}{0.1} \times \frac{1}{15.2\ \mu\text{moles HYP}} \times 100$$

Subject		Tissue type	Total Protein Radioactivity x 10^3 (DPM/100mg wet tissue)	Hydroxyproline Radioactivity x 10^3 (DPM/100mg wet tissue)	Ratio $\frac{\text{Hydroxyproline}}{\text{Total Protein}} \times 100$
Age	Sex				
24	M	N	51.4	10.64	20.7
57	M	N	43.3	9.76	22.5
35	M	N	53.3	10.61	19.9
23	F	N	52.57	11.04	21.0
18	F	N	55.9	11.92	21.3
41	F	N	54.05	10.04	18.5
28	M	S	39.5	4.82	12.42
26	F	S	38.3	4.83	12.6
34	F	S	34.9	4.85	13.9

N Normal Skin
S Normal Scar

FIGURE 6.2. TOTAL PROTEIN AND HYDROXYPROLINE SYNTHESIS IN NORMAL SKIN AND NORMAL SCAR.

where ODsa is the absorbance of pyrrole from the sample;
ODps is the absorbance factor of the 0.04μM/ml pyrrole standard, and μmoles HYP is the amount in the assay (15.2 μmoles).

The assay of collagen biosynthesis in normal skin and normal scar were carried out first to compare with the results of Craig (1975a and 1975b) and Uitto (1970) and would also permit a check as to whether the results obtained were sensible.

6.5. EXPERIMENTAL RESULTS

The experimental results are divided into the following subsections for convenience and to facilitate interpretation.

6.5.1. Collagen Biosynthesis in Normal Skin and Normal Scar

The results of the assay for normal skin and normal scar are tabulated in Figure 6.2. The results are expressed in disintegrations per minute (DPM)/100mg wet tissue. Values of the total protein radioactivity and the hydroxyproline radioactivity are given and values of the ratio of hydroxy-proline activity to total protein radioactivity are presented in the table as percentages. The results are also shown graphically in Figure 6.3. The collagen biosynthesis is expressed as DPM/100mg wet tissue and value of each point plotted is the mean of no less than three samples. The mean value of collagen synthesis for normal skin is 10.7 x 10^3 DPM/100mg wet tissue, which is comparable with that obtained by Craig et al (1975a). The value of collagen synthesis for normal scar was considerably lower and was obtained from three different patients. The mean value was 4.83 x 10^3 DPM/100mg wet weight which was somewhat less than that of Craig (1975a and 1975b) however it was still within the same range of results. The age of the normal scars varied from 9 months to 41 months over which the collagen biosynthesis appeared relatively constant. The percentage ratio of collagen biosynthesis to total protein synthesis is obtained by dividing the hydroxyproline radioactivity values by the total protein radioactivity values. These figures show that collagen accounts for a

FIGURE 6.4. RATIO OF COLLAGEN BIOSYNTHESIS TO TOTAL PROTEIN BIOSYNTHESIS IN NORMAL SKIN, NORMAL SCAR AND PRESSURE-TREATED AND UNTREATED HYPERTROPHIC SCAR

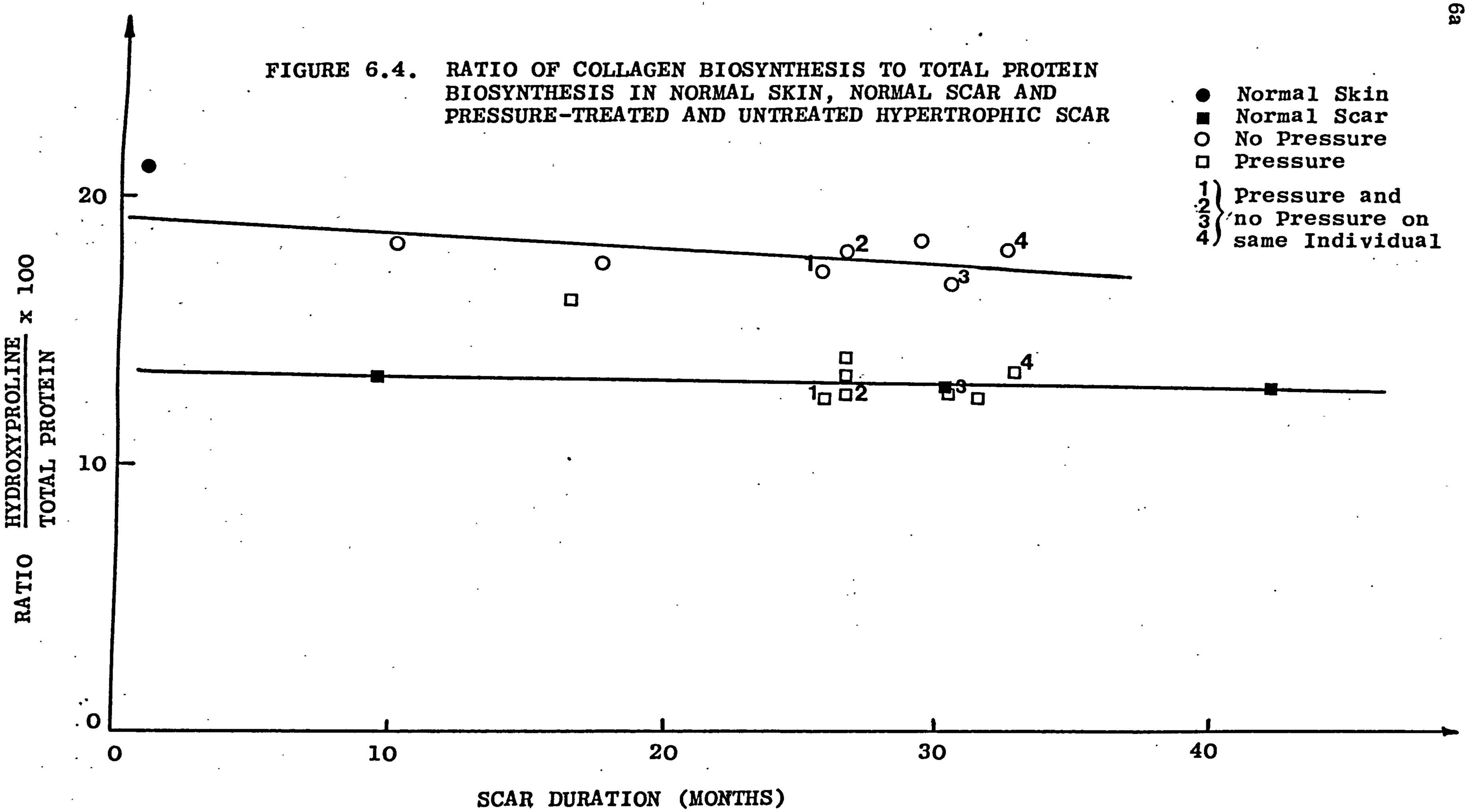

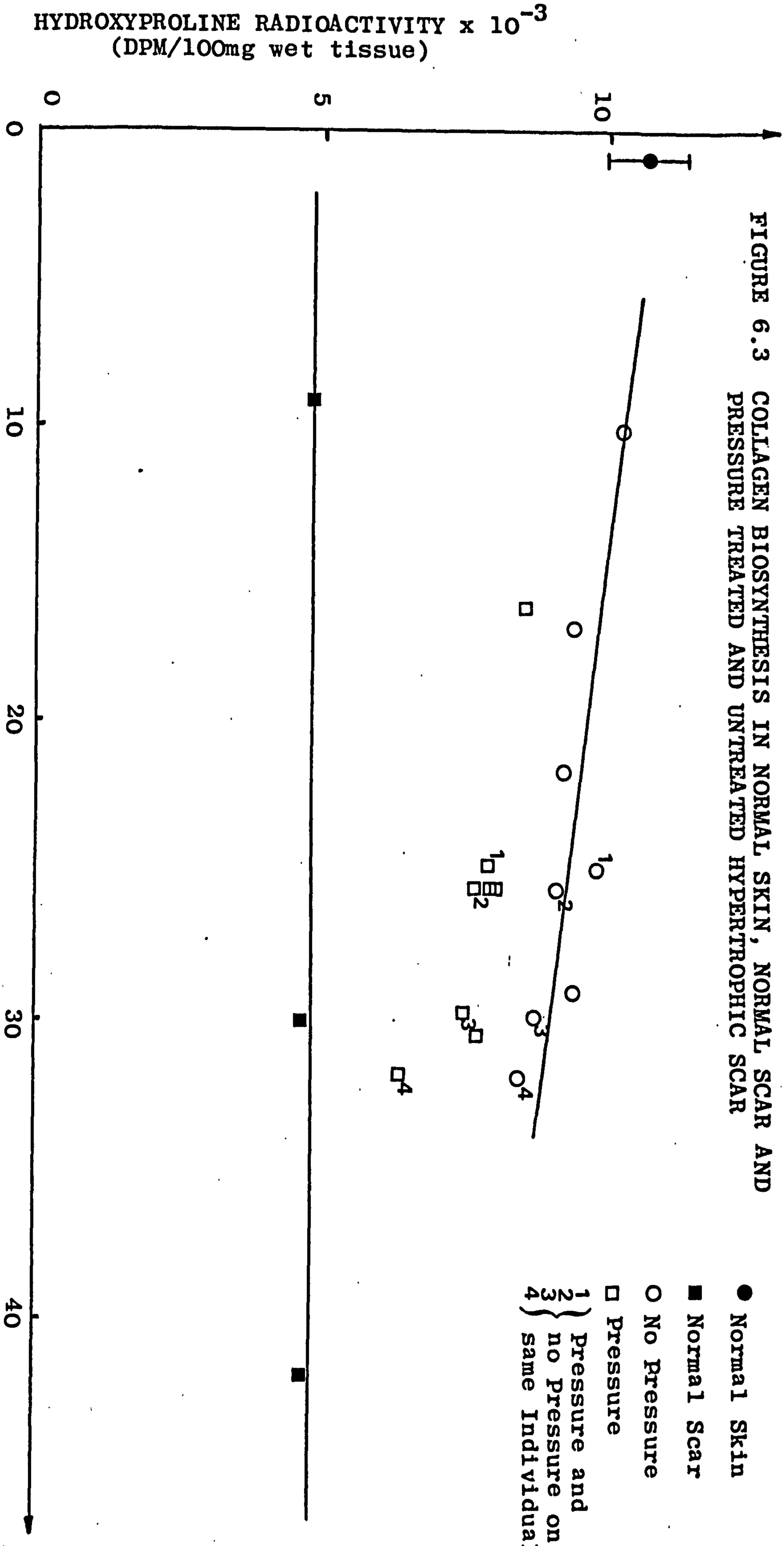

FIGURE 6.3 COLLAGEN BIOSYNTHESIS IN NORMAL SKIN, NORMAL SCAR AND PRESSURE TREATED AND UNTREATED HYPERTROPHIC SCAR

FIGURE 6.5. TOTAL PROTEIN AND HYDROXYPROLINE SYNTHESIS IN PRESSURE TREATED AND UNTREATED HYPERTROPHIC SCAR

Subject			Scar Age (months)	Duration of Pressure (months)	Total Radioactivity DPM/100mg wet tissue $\times 10^3$		Hydroxyproline Activity DPM/100mg wet tissue $\times 10^3$		Ratio $\frac{\text{Hypro}}{\text{Total}} \times 100$	
Case	Age	Sex			No Pressure	Pressure	No Pressure	Pressure	No Pressure	Pressure
-	32	M	10	NIL	55.4	-	10.2	-	18.4	-
10	65	M	16	12*(13)	-	51.27	-	8.46	-	16.5
-	69	M	17	NIL	52.51	-	9.4	-	17.9	-
9	35	M	25	16*(21)	55.11	61.7	9.7	7.90	17.6	12.8
6	45	M	26	22*(28)	50.0	53.78	9.1	7.42	18.2	13.3
2	43	F	26	22*(6)	-	51.88	-	7.57	-	14.0
7	49	M	26	15*(31)	-	53.53	-	7.96	-	12.9
4	6	M	29	NIL	49.73	-	9.3	-	18.7	-
12	28	M	30	16*(28)	48.78	49.04	8.4	6.18	17.3	12.6
1	36	M	31	9*(28)	-	55.52	-	7.44	-	12.4
11	15	M	32	16*(13)	46.99	52.6	8.6	7.20	18.3	13.7

*( ) Average Pressure in mmHg over Duration (vide Figure 5.5)

higher proportion of total proteins synthesised in normal skin than in normal scar, which is in agreement with the results of Craig (1975a) although the values are again lower. The ratio of collagen biosynthesis to total protein synthesis is shown in Figure 6.4.

The results have been expressed in disintegrations per minute/100mg wet tissue for both total protein synthesis and hydroxyproline synthesis. Craig et al (1975a) also expressed the results terms of specific activity in disintegrations per minute/μmole hydroxyproline synthesised. The author has not expressed the results in this form since the ratio of the results, when expressed by either of the above methods, is virtually indistinguisable from the other (Craig et al, 1975a). Consequently, the former method was selected for its simplicity without compromising the accuracy of the results.

It appeared that, from the time-course for incubation together with the preliminary assays of normal skin and normal scar, the results were in the same range, with the similar differences displayed between values from different tissues, as was found by Craig et al (1975a and 1975b).

Therefore, the author felt that the incubation system and assay technique was being operated properly with reliable results being obtained and that samples of pressure treated and untreated hypertrophic scar tissue could be assayed for collagen biosynthesis.

6.5.2. Collagen Biosynthesis in Pressure Treated and Untreated Hypertrophic Scars

The results are tabulated in Figure 6.5. For each subject, details of the subject's age, scar age, duration of pressure, average pressure at biopsy site and whether the sample biopsies were obtained from a pressure treated area or not are given. The results of the collagen biosynthesis in pressure treated and untreated scars are graphically displayed in Figures 6.3 and 6.4 as a function of scar duration in terms of DPM/100mg wet tissue and as a fraction of total protein synthesis respectively.

The values of untreated hypertrophic scar in DPM/100mg wet tissue indicate that the rate of collagen biosynthesis is slightly less than in normal skin initially (10 months post-wounding) but greater than therate of collagen biosynthesis in normal scar, whatever the age of the scar. The results are similar to those of Craig et al (1975a and 1975b) in relative terms but not in absolute terms. The rate of collagen synthesis in untreated scars decreases gradually with increasing scar age which implies a natural resorption process. Each data point plotted is the average of at least two samples, however only 7 data points were obtained for non-pressure treated hypertrophic scars. From Figures 6.3 and 6.4, if the rate of decrease of collagen biosynthesis in untreated hypertrophic scar tissue is assumed to be sensibly constant, then by extrapolation of the curves shown, the value of collagen biosynthesis would not be expected to be significantly different from normal scar levels with scars of about 70 months old.

The collagen biosynthesis results from pressure treated scar biopsies are also displayed in Figures 6.3 and 6.4 The pressure treated scar collagen biosynthesis values are lower than the untreated scar values whatever the age of the scar however no duration of the pressure or magnitude is given. From Figure 6.3 it is evident that pressure reduces the collagen biosynthesis levels compared to non-treated hypertrophic scars of the same age, in general, This is particularly evident in the same individual. Collagen biosynthesis levels in pressure treated scars appeared to stop approaching normal scar levels after about 30 months remaining substantially constant thereafter.

Figure 6.4 is a graph of the ratio of collagen biosynthesis to total protein biosynthesis against age of scar and enables the relative collagen biosynthesis of pressure treated and untreated hypertrophic scar tissue to be compared. This, in the author's opinion, is a more useful way of representing the results of the pressure therapy, as the absolute results have no meaning <u>per se</u>. The results clearly show that collagen biosynthesis in pressure

FIGURE 6.6. COLLAGEN BIOSYNTHESIS IN PRESSURE TREATED SCARS AS A FUNCTION OF SCAR DURATION

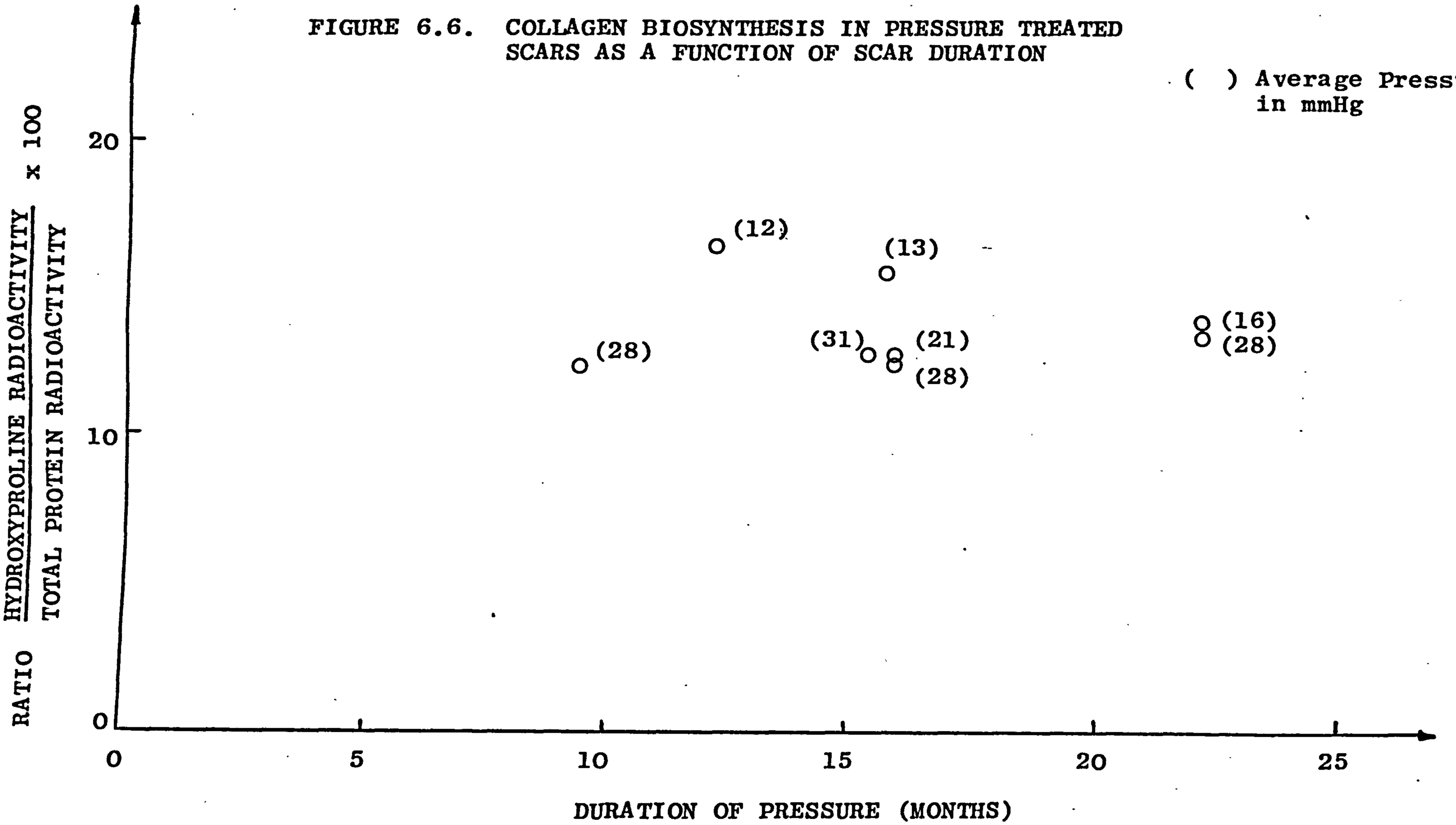

treated scars is reduced, relative to the level of total proteins synthesised in the scar, to a similar level as in normal scar after 30 months scar duration, and that in untreated hypertrophic scars normal levels are not approached until after 60 or 70 months. That is, pressure appears to half the time for collagen biosynthesis in hypertrophic scar to be reduced to normal scar levels by the natural resorption process.

The results, when expressed as above, only state whether pressure was applied but do not include details of the pressure magnitude or duration thereof. Figure 6.6. is a graph of the ratio of collagen to total protein biosynthesis against the duration of applied pressure with average pressure applied (in mmHg) shown in brackets. From Figure 6.6. increasing duration of pressure appears to reduce collagen biosynthesis and it is also evident from the graph, that the greatest reduction in biosynthesis occurs in the first months of pressure application. In addition, pressures considerably greater than the minimum threshold pressure of 14 - 15mmHg (vide 5.5) i.e. (28 or 31mmHg) result, in general, in reducing collagen biosynthesis to lower levels in comparison to scars with lower pressures for the same duration of pressure. These results are construed conservatively since there are, in the author's opinion, perhaps too few data points (eight) to permit definite conclusions to be drawn.

Furthermore, it appears that after about 15 months duration of pressure the effect of varying pressures on the scar has no observable effect; higher pressure does not appear to reduce collagen biosynthesis to levels lower than is achieved by 'low' pressures. However the maximum duration of pressure of the samples examined was 22 months and further changes may be possible after this period.

The values of patient age and collagen biosynthesis for non-pressure treated scars is given in Figure 6.5. It was not thought that a relationship between these variables was present.

6.5.3. Discussion and Conclusions

The results of the assay have been expressed in disintegrations per minute/100mg wet tissue in order to be compared with the results of Craig (1975a, 1975b). 100mg wet tissue was frequently impossible to obtain with the biopsy punch technique and the sample weights were normalised to 100mg wet tissue for comparison purposes. However this procedure may not be strictly accurate as it assumes that there is a uniform uptake of radioactivity per unit sample weight which, in fact, may not be the case. A further error is evident, in theory, in that not all of the proline incorporated into polypeptides is labelled (Appendix C). For accurate results hydroxyproline radioactivity should be expressed in terms of μmoles of labelled proline synthesised, however in practice it has been demonstrated that little difference exists when the results are expressed in terms of wet weight and as a fraction of total protein synthesis (Craig et al, 1975a).

The results of the normal skin and normal scar assays are similar to those obtained by Craig et al (1975a) and although differences between the results may be partially explained by use, in this case, of radiolabelled proline of a higher specific activity, errors due to different techniques of performing the assay are unaccountable. Untreated hypertrophic scars showed a gradual decrease in collagen biosynthesis with increasing scar age, unlike the sharp decrease in biosynthesis about the third year after wounding observed by Craig et al (1975b). One explanation that the author offers regarding this discrepancy is that there was insufficient data obtained to discriminate such a biochemical change. The expression of collagen biosynthesis in terms of the hydroxyproline radioactivity as a fraction of the total protein radioactivity presents a clearer description of the biochemical events.

In the pressure-treated hypertrophic scar samples the rate of collagen biosynthesis falls more rapidly with

increasing scar age than the untreated hypertrophic scar samples. This observation appears to hold in general, however it is also evident that in each case where biopsies were examined from pressure-treated and untreated sites on the same individual, collagen biosynthesis levels were always much lower in the pressure-treated scars. This would seem to confirm that the pressure accelerates natural remodelling of hypertrophic scar tissue.

Collagen biosynthesis in pressure-treated hypertrophic scars is reduced to about the level of normal scar biosynthesis around thirty months post-injury. Further analysis of the results showed that the level of collagen synthesis was dependent on the duration and magnitude of pressure; up to about 15 months duration higher pressures resulted in an acceleration of the remodelling process as evidenced by the reduction in collagen synthesis and after 15 months the remodelling appeared generally independent of the magnitude of the applied pressure. This interpretation of the results makes the 6 - 9 months pressure duration period seem rather optimistic. However the interpretation of the results is consistent with the clinical observations of Larson et al (1971) and Larson et al (1974) that pressure should be applied for at least 9 - 12 months to effect complete remodelling, and that significant cosmetic and functional improvement after 12 months duration of constant pressure was not very noticable.

Pressure-induced remodelling of the hypertrophic scar may occur in two identifiable, and perhaps distinct, phases. This is analogous to the two-phase scar production theory, (Craig et al, 1975b). The first or 'primary' phase being characterised by accelerated remodelling and biochemical changes (e.g. collagen biosynthesis) in which the prolonged application of pressure, even of high magnitudes, provides no increased short term clinical improvement or reduction in collagen biosynthesis; the secondary phase being dominated by the natural remodelling phase in which the collagen biosynthesis levels gradually tends to approach the levels

in normal scars. The accelerated reduction in collagen biosynthesis is reflected by significant cosmetic improvement; pressure-treated scars demonstrating, in general, a superior clinical result than was achieved by the natural remodelling process per se, even after only several months pressure (case study No. 6, Figure 5.14).

The results are in the author's opinion incomplete since biopsies were only obtained from the scars undergoing pressure therapy after at least 10 months pressure treatment. More data is required in the first 12 months of pressure therapy as it has been proposed that the earlier the application of pressure after wounding the quicker and the better the clinical result (Larson et al, 1971). This may be, in turn, reflected by changes in collagen biosynthesis which could be used as a diagnosis of the effectiveness of the pressure therapy. In addition, the effect of pressure should be monitored by the assay after twenty-two months pressure. This would test the hypothesis of the 'secondary phase' of the remodelling process. Although this series of experiments has shown that the rate of collagen biosynthesis in pressure-treated scars is reduced in comparison to the rate of collagen biosynthesis in untreated scars, the nature of the remodelling mechanism is still not completely understood. The reduction in the rate of collagen biosynthesis may, in fact, be due to pressure-induced changes in the scar microcirculation; a reduced blood flow could reduce the availability of serum proteins or it could alter the pO_2 levels so that the rate of collagen biosynthesis was reduced. Clearly, there is a requirement for investigating the response of the scar microcirculation to pressure if it is desired to obtain a fuller understanding of the remodelling mechanism.

It is thought that knowledge of the rate of collagen biosynthesis may prove useful in determining whether pressure is likely to prove more successful than natural remodelling in some cases, and if so, what duration of pressure should be applied to each individual. It is

realised by the author that this assay is not routine in many hospitals, nevertheless, where a such facility for performing the assay exists, its use could assist in providing superior pressure therapy.

6.6. SUMMARY

Collagen biosynthesis in pressure-treated and untreated human hypertrophic scars and normal scars were examined with regard to the age and duration of the scar, to the duration of, and to the magnitude of, the pressure applied. The rate of collagen synthesis was determined using a biochemical assay by measuring the amount of radioactivity from a standard radioactive dose of ^{14}C-proline incorporated into non-dialysable hydroxyproline by samples or biopsies of excised tissues in-vitro. The assay used was selected in preference to others principally because enzymes were not required. The assay was checked for repeatability against the results of Craig et al (1975a and 1975b) using samples of normal skin and normal scar. The results compared reasonably well and possible sources of error were discussed.

The rate of collagen biosynthesis in pressure-treated hypertrophic scars was found to be reduced in comparison to untreated scars of the same age; the rate of collagen biosynthesis in pressure-treated scars being similar to the rate in normal scar tissue at around 30 months scar duration compared to 60 - 70 months in the case of untreated hypertrophic scar tissue. The reduction in rate of collagen biosynthesis was found to be a function of the duration of pressure applied; greater reduction in rate of collagen biosynthesis occurring within the first 12 - 15 months of pressure therapy whereas after about 15 months the effect of continued pressure on the rate of collagen biosynthesis was not noticable. Within the first 12 - 15 months of applied pressure the reduction in the rate of collagen biosynthesis was increased with increasing pressure magnitude. The rate of remodelling of hypertrophic scar tissue, according to collagen biosynthesis levels, is doubled in the case of pressure-treated

scars as compared to untreated scars and the cosmetic result achieved is usually superior.

The remodelling process appears to occur in two distinct phases: a 'primary' phase in which pressure rapidly reduces the rate of collagen biosynthesis to levels approaching those in normal scar and a 'secondary' phase in which continued pressure does not appear to result in any significant reduction in the rate of collagen biosynthesis or further cosmetic improvement; the secondary phase collagen biosynthesis levels being gradually reduced to normal scar levels by the natural remodelling process.

The need for investigation of the response of the scar microcirculation to pressure, and for correlation with rates of collagen biosynthesis is emphasised.

CHAPTER 7

AN INVESTIGATION OF THE EFFECT OF CONSTANT PRESSURE AND PRESSURE GRADIENTS ON THE MICROCIRCULATION

7.1 Introduction

7.2 Microvascular Assessment Techniques: A Review

7.2.1 Angiography

7.2.2 Radioisotope Clearance Techniques

7.2.3 Doppler Ultrasound Blood Flow Monitoring

7.2.4 Laser Doppler Anemometry

7.2.5 Transcutaneous Optical Blood Content and Oxygenation Assessment Device

7.2.6 Development of the Transcutaneous Optical Device

7.2.7 Intravital Microscopy

7.3 The Effect of Pressure Distributions on the Microcirculation using a Hamster Cheek Pouch Model

7.3.1 Materials and Methods

7.3.2 Cheek Pouch Preparation

7.3.3 Microvascular Response Assessment Criteria

7.4 Experimental Design

7.4.1 Uniform Pressure Distributions

7.4.2 Non-Uniform Pressure Distributions

7.5 Experimental Results

7.5.1 Microcirculatory Response to "Low" Uniform Pressure Distributions

7.5.1.1 40mmHg Applied for 20mins.

7.5.1.2 40mmHg Applied for 60mins.

7.5.1.3 Discussion

7.5.2 Microcirculatory Response to "High" Uniform Pressure Distributions

7.5.2.1 400mmHg Applied for 15mins.

7.5.2.2 Discussion

7.5.3 Microcirculatory Response to Non-Uniform Pressure Distributions

7.5.3.1. 20mmHg Pressure
7.5.3.2 40mmHg Pressure
7.5.3.3. Discussion
7.6. Summary

CHAPTER 7

7.1. INTRODUCTION

It has been proposed that the mechanism responsible for pressure-induced scar remodelling is due to ischaemia of the scar in response to applied mechanical pressure, resulting in necrosis of the tissue and consequent flattening of the scar (vide 3.4). Sloan et al (1978), from experimental evidence, disputed this hypothesis and suggested that externally applied pressure reduced an already present degree of hypoxia in the hypertrophic scar tissue to such a level that a critical percentage of its fibroblast population could no longer function normally, leading to an imbalance between collagen synthesis and degradation in favour of the latter, favouring scar resorption. Furthermore, the results of the rates of the collagen biosynthesis studies performed (Chapter 6) lead to the conclusion that for a fuller understanding of the pressure induced scar remodelling mechanism an investigation of the response of the scar microcirculation to pressure is necessary.

In order to investigate the hypothesis for direct or indirect vascularly mediated remodelling it is necessary to monitor the microvascular response of hypertrophic scars to controlled pressures. This, in turn, should permit the vascular responses to be quantified.

7.2. MICROVASCULAR ASSESSMENT TECHNIQUES: A REVIEW

There are several relevant methods of monitoring the microvascular response of skin and each of these methods, in turn, was considered and evaluated for its suitability of use with hypertrophic scar tissue.

7.2.1. Angiography

The roentgenographic visualisation of blood vessels by injecting a radio-opaque material into the circulation is called angiography. It provides a clear indication of blood when vessels are large but its usefulness in monitoring flow in small vessels is limited by the photoreproduction process and the lack of contrast between vessels containing radio-

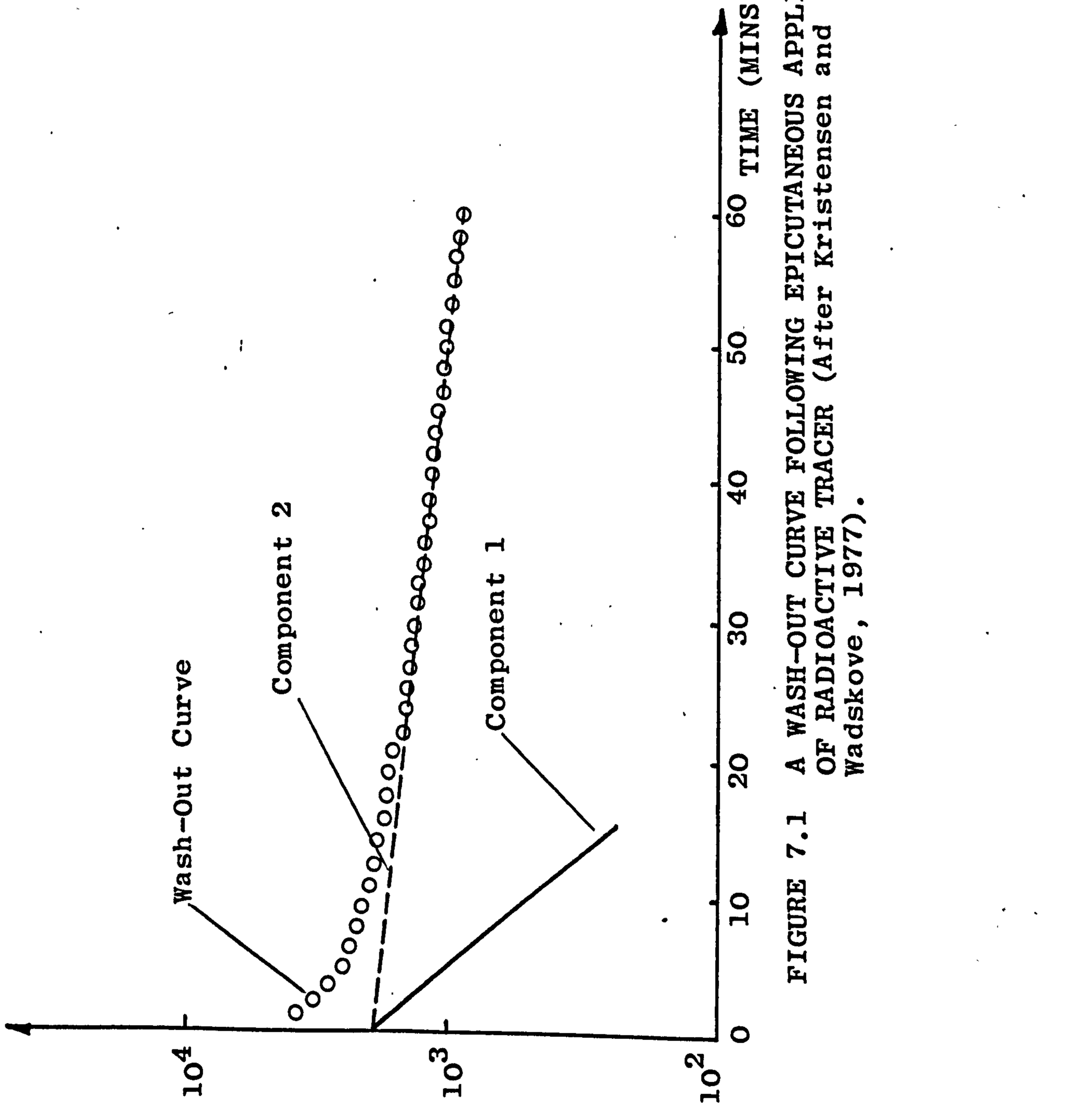

FIGURE 7.1 A WASH-OUT CURVE FOLLOWING EPICUTANEOUS APPLICATION OF RADIOACTIVE TRACER (After Kristensen & Wadskove, 1977).

opaque material and adjacent tissues such as bone.

7.2.2. Radioisotope Clearance Techniques

The use of clearance rates of radioactive materials deposited in skin to measure blood flow was introduced by Sjersen (1961) using Xe^{133}. A bolus of radioactive material is inserted into, or deposited on, the skin at a selected site and the radioactivity at the site recorded over a period of time. The variation of radioactivity with blood flow or "wash-out" over this period of time can be used to provide a quantitative evaulation of the blood flow rate. Figure 7.1. shows a typical wash-out curve where the blood flow can be calculated using component I and the tissue to blood partition coefficient for the radioisotope, in this case Xe^{133}, according to the formula:

$$F = \frac{\ell n\, 2 \times \lambda \times 100}{T_{\frac{1}{2}}}$$

where F = skin blood flow expressed in ml/100 gm. min

λ = skin to blood partition coefficient in ml/gm

$T_{\frac{1}{2}}$ = the half-life* of component I

Hickman and Lindan (1966) used an injected Na^{24} (Sodium 24) technique to study the effect of external pressure on blood flow, on the volar surface of human forearms and on the backs of rats. It was found, in human subjects, that at pressures approaching mean capillary pressure, (taken as 25mmHg) the measured clearance rates indicated that blood flow was about 80% of normal uncompressed tissue blood flow. It was also found that cyclic loading produced different effects on the blood flow during the loading and unloading phases.

Daly et al (1976), using the clearance rate of Xe^{133} to study skin blood flow found that pressures up to 10mmHg

---

* The term half-life is the time in which the activity of a radioactive isotope decays to half its value.

greatly reduced blood flow from normal uncompressed blood flow levels. Above 10mmHg pressure, evidence of an auto-regulatory mechanism of skin blood flow was demonstrated (vide 3.2.1).

Such clearance studies have to be performed rapidly since the level of background radioactivity increases systemically and Xe^{133} is also reported as accumulating in adipose tissue, (Daly et al, 1976). Another disadvantage of clearance techniques is that a finite time is required to produce clearance curves therefore instantaneous values of blood flow are not possible. Therefore, changes occuring during the loading and unloading of the tissue, which may be of clinical significance, cannot be accurately recorded.

Inserting a bolus of radioactivity by injection leads to local vascular disruption which produces hyperaemia further affecting the accuracy of results, and "backtracking" of radioactive material in the lumen of the injecting needle can lead to wrong amounts of the radioactive material being dispensed.

It is known that skin and the subcutaneous tissues exhibit time-dependent mechanical properties (Kenedi et al, 1975), as does hypertrophic scar tissue (Tully , 1980). The results of Hickman and Lindan (1966) also suggested that the response of the local circulation may be time-dependent. Determination of how these time-dependent properties affect blood flow phenomena requires a rapid response technique.

In view of the above disadvantages it was thought radioactive clearance techniques would not reflect or resolve small changes in local scar blood flow in response to external pressures.

7.2.3. Doppler Ultrasound Blood Flow Monitoring

This technique involves placing an ultrasonic transducer onto the surface of the skin superficial to a vessel, which can be either arterial or venous, in

which measurement is desired. An incident ultrasonic signal is compared with a reflected signal from the tissue. The reflected signal is phase-shifted from the incident signal due to the flow of blood in the vessel; this is the Doppler effect. The difference in phase between the incident and the reflected signals is a function of the blood flow rate in the vessel.

This technique has been shown to be suitable for the assessment of perfusion in limbs by monitoring blood flow in large vessels, such as the popiliteal and femoral vessels in the leg (Sigel et al, 1973, Sigel et al, 1975). However, the Doppler ultrasound technique is difficult to use with small diameter blood vessels of the order of 1mm, and use with blood vessels of 100μm diameter and less is limited by spurious signals and artefacts due to "motion" of the tissues. These spurious signals are oftengreater than the measurand and the resulting signal from micro-vessels is generally meaningless.

Consequently,, as the majority of the superficial vessels are microvessels, investigation of the pressure induced microvascular response using Doppler ultrasound is considered unsuitable.

7.2.4. Laser Doppler Anemometry

The principle of the Doppler effect (vide 7.2.3.) is applied to blood flow measurement using a Laser beam. Laser beam radiation is coherent (of a single frequency), in phase, collimated, and is well suited to measuring the flow of single red blood cells (RBC's) which have a maximum dimension of about 8μm. That is, it is capable of measuring blood flow in a capillary. The Laser Doppler has only recently been used experimentally (Daly et al, 1976) although preliminary studies report good correlation with more established radioisotope clearance techniques using Xe^{133} (Xenon 133) (Lappe et al, 1975). The principle of a Laser Doppler appeared to be satisfactory in theory for measuring blood flow in hypertrophic scars but

instrumentation was not commercially available and the technique was not wholly established as a routine research tool at the time of this investigation. In addition, focusing of the Laser beam is made difficult by tissue motion.

7.2.5. Transcutaneous Optical Blood Content and Blood Oxygenation Assessment Device.

Turnbull (1977) developed and constructed a device which measured the blood content and oxygenation of skin from the amount of incident radiation absorbed by blood. A probe containing a fibre optic light source and an array of photodetectors radially disposed about the source was placed on the skin surface. Light,"chopped" at 800 Hz and "phase lock" detected to provide an optimum signal to noise (S/N) ratio, was conducted onto the surface of the skin by light source and the detected backscattered radiation was then filtered to pass only reflected light at either 630nm or 802nm. 630nm is the wavelength at which there is the greatest difference of absorption between oxygenated and reduced blood. 902nm is a wavelength at which the absorption of oxygenated and reduced blood is the same i.e. it is an isobestic wavelength. The amount of backscattered radiation was found to be dependent on the blood content and oxygenation of the tissue being investigated, and it was also shown to be dependent on the mechanical time-dependent properties of the tissue. Turnbull obtained a good correlation between in-vitro experimental results and a mathematical photodiffusion theory model which, it should be noted, was exceedingly complex.

Although the device was claimed to determine absolute values of the blood content and degree of oxygenation it should be understood that with in-vivo studies, the device was used for crude "Yes - No" indications of blood content. This was achieved by firstly occluding and exsanguinating a limb then releasing the occlusion and allowing the limb to reperfuse. Hyperaemia always accompanied reperfusion. These experiments were highly artificial with regard to

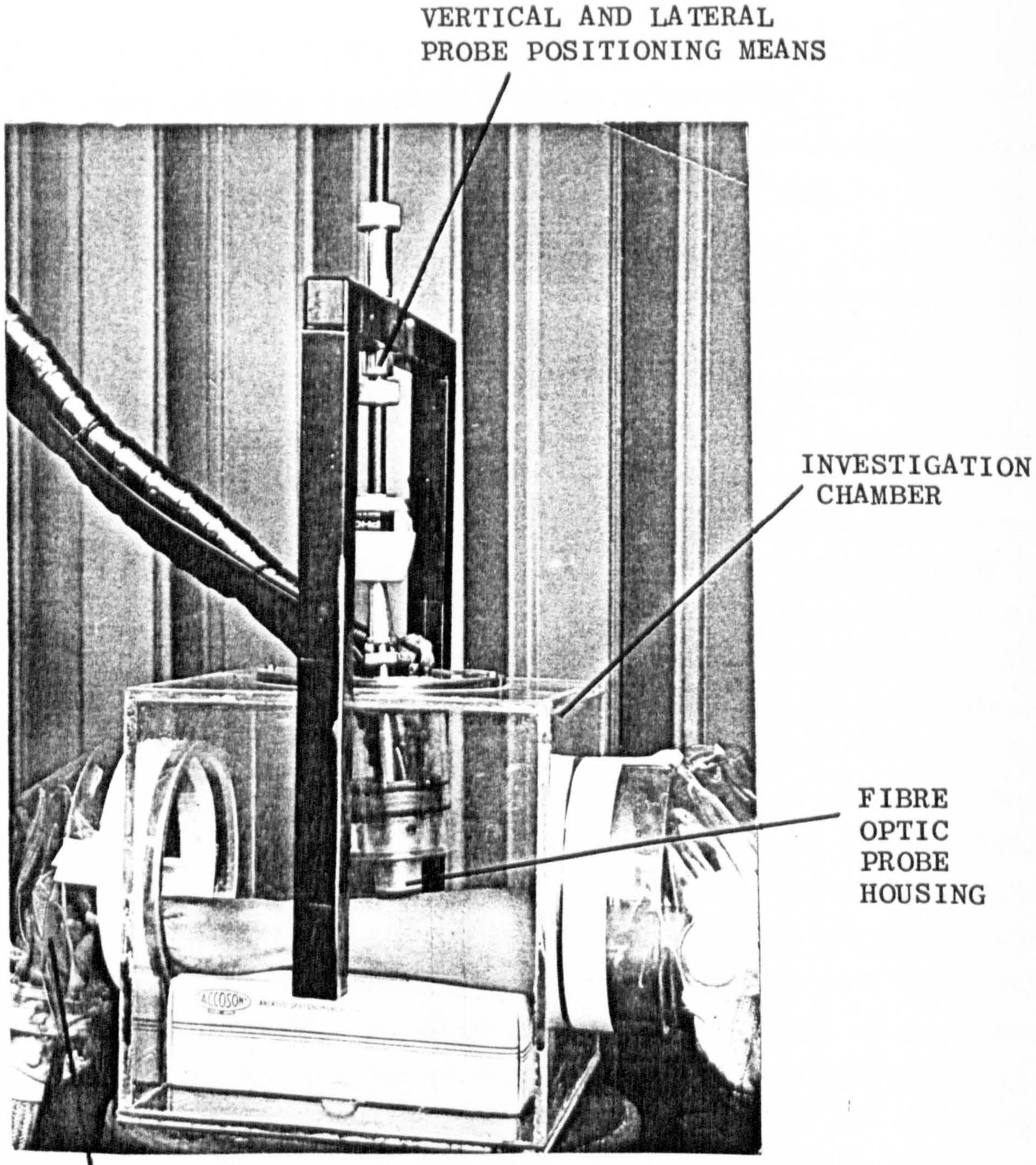

FIGURE 7.2. PNEUMATIC PRESSURE CHAMBER FOR INVESTIGATING BLOOD CONTENT AND OXYGENATION

normal clinical requirements and were primarily used to evaluate the instrumentation.

The transcutaneous optical assessment device was still under development at the time of the investigation. As the preliminary in-vivo results were promising and showed that the instrumentation could be used on human subjects, the author therefore undertook to determine the potential of the device with regard to assessing changes in hypertrophic scar vascularity.

7.2.6. Development of the Transcutaneous Optical Device

The author developed and constructed an investigation chamber for use with the aforementioned apparatus of Turnbull(1977) in which the vascular response to controllable pressure applications could be observed (Figure 7.2.). Pneumatically produced hydrostatic pressures between 10mmHg and 50mmHg were applied to human forearms for varying periods of time using a controlled environment treatment (C.E.T.) device, manufactured by Cape Engineering Ltd.*

The few results obtained were virtually unanalysable and indicated that the optical apparatus was totally unsuitable for investigating the microvascular response of hypertrophic scar tissue to external pressure. For example, if the fibre optic probe was positioned on the skin with minimal pressure involuntary tissue movements resulted in the production of spurious signals and artefacts of about two orders of magnitude greater than the maximum signal arising from a 40mmHg hydrostatic pressure change. In addition, the pressure required to be applied to the skin by the probe to ensure good contact and to obtain consistent readings invariably resulted in arresting local blood flow which, of course, gave either very low or null readings. Although this instrumentation system has recently provided in-vitro experimental results which correlate well with the theory over a wide range of haematocrit suspensions (Barbenel et al, 1979) the practical difficulties involved in adapting this technique for routine clinical use, by the author,

---

* Cape Engineering Company Limited,
Cape Road, Warwick, CV34 5DL, England

were reflected in widely varying and generally incomprehensible in-vivo results from volunteer subjects. In the short term, the author believed that these limitations were unlikely to be overcome.

7.2.7. Intravital Microscopy

This is a technique in which the microcirculation is observed with a microscope. It permits the investigator to readily evaluate the microcirculatory response to various influences such as temperature, drugs, pressure etc. Tissues investigated by this technique must be very thin and flat to permit the transmission of light consequently microcirculation investigations have been mainly limited to animal models such as the frog web (Roy and Brown, 1879) the the hamster cheek pouch (Lutz et al, 1951, Romanus, 1977).

Brånemark (1971) successfully adapted this technique for use in human beings; a tube pedicle was raised on the volar arm surface and a titanium chamber was inserted therein. The titanium chamber has two light transmissible lenses spaced apart in parallel. When the wound healed scar tissue successfully grew between the lenses. The chamber was then attached to a high resolution light microscope and the response of the microcirculation to occlusions over various durations was investigated.

Romanus (1977) used a hamster cheek pouch model to investigate the microcirculatory response to pressure induced ischaemia and demonstrated that the microcirculatory response to controlled pressures could be monitored continuously thus enabling time-dependent effects to be evaluated. Another important feature of Romanus' instrumentation was that the magnitude of applied pressure could be finely controlled.

Although observations of the microcirculation are primarily qualitative, continual recordings of several parameters such as the proportion of capillaries reperfused after pressure provides semi-quantitative data and has been used to provide an "accurate" assessment of the response of the tissue.

The author thought, from the various reports, that vital microscopy was a suitable technique with which to assess the microvascular response to mechanical stimuli. However, to investigate the effect of pressure on hypertrophic scar tissue using vital microscopy, the experimental techniques of both Brånemark (1968, 1971) and Romanus (1977) required to be combined. However, this had never been attempted and initial attempts by the author proved frivolous since both sets of equipment had been designed for entirely different purposes. The shape and size of the hamster cheek pouch is comparable in many cases to the physical dimensions of a hypertrophic scar vascular bed, that is about 5 - 10cm^2 by 100 - 150μm thick.

In addition, the parenchymal cell content is relatively low, which means that the response of the tissue to external trauma is primarily vascular and not cellular. Consequently, the author thought that the hamster cheek pouch could be used as a model for investigating response of hypertrophic scar tissue to the effects of external mechanical stimuli, in the form of pressure distributions.

7.3. THE EFFECT OF PRESSURE DISTRIBUTIONS ON THE MICRICIRCULATION USING A HAMSTER CHEEK POUCH MODEL

7.3.1. Materials and Methods

Hamsters (Mesocricetus auratus) of both sexes were used. The total number of experiments performed was 34 and the total number of animals used was 27. The animals were fed ad libitum with water and pellets and were kept in an airconditioned room at 17°C.

Anesthesia was induced with sodium pentobarbital (6 mg/100 g body weight) intramuscularly and supplemented with Diazepam (2.5 mg/100 g body weight) intraperitoneally. Additional sodium pentobarbital was given when needed.

At the end of the experiments the animals were sacrificed by an excessive dose of pentobarbital.

7.3.2. Cheek Pouch Preparation

A hamster was placed on a Perspex plate and the cheek

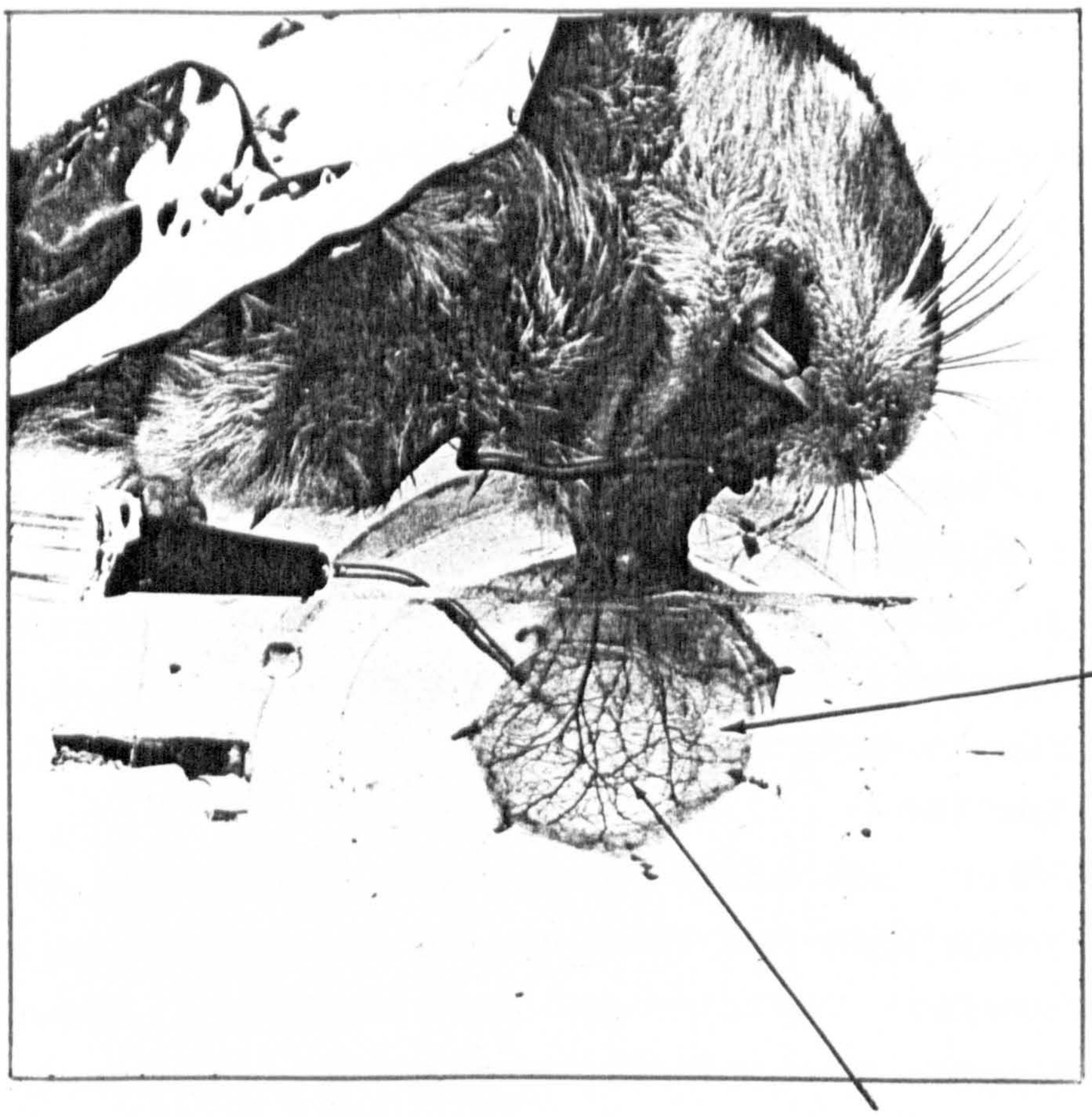

FIGURE 7.3. HAMSTER CHEEK POUCH MOUNTED OVER PRESSURE CHAMBER

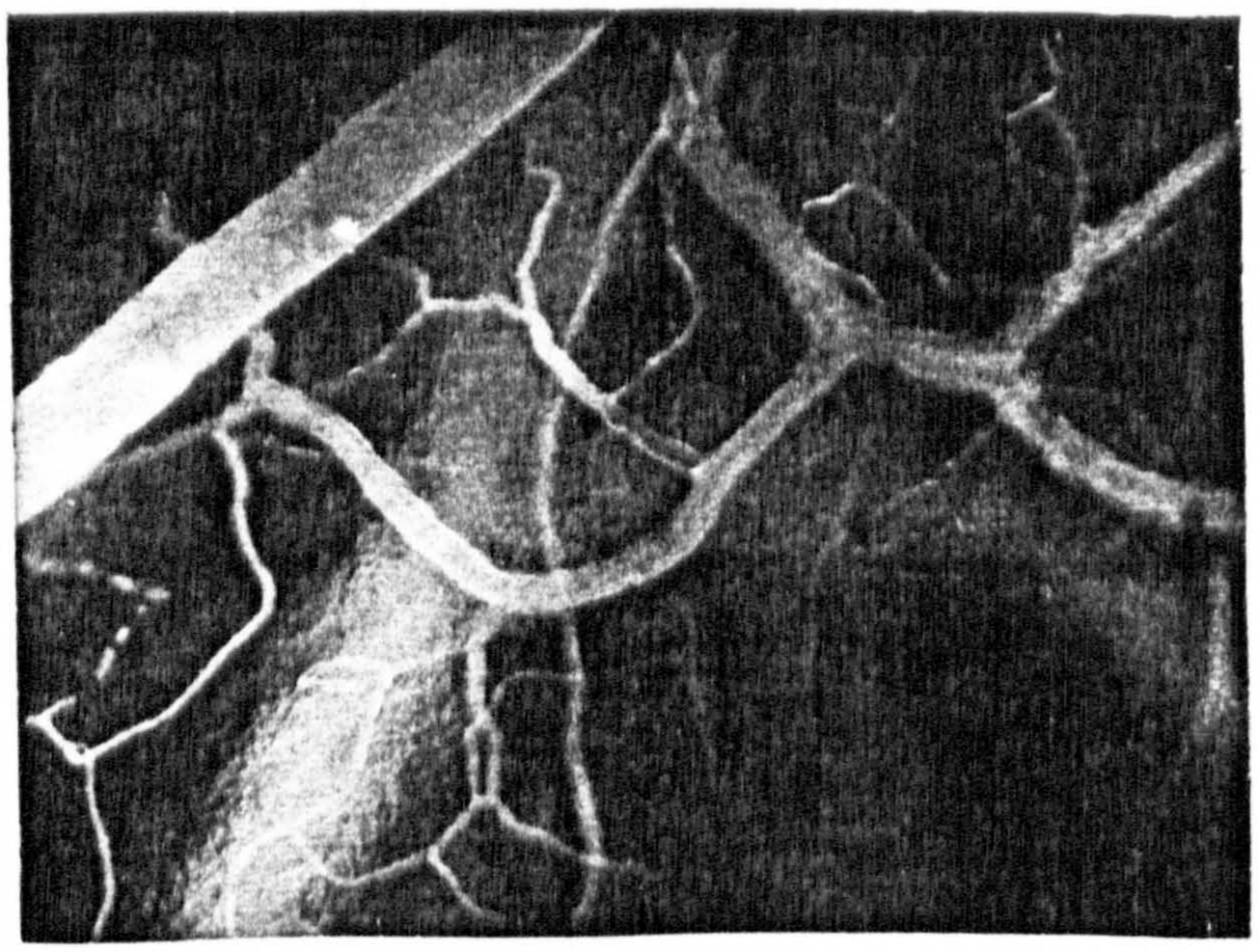

FIGURE 7.4. POLAROID PHOTOGRAPH OF A PART OF CHEEK POUCH ILLUMINATED WITH U-V LIGHT AFTER INFUSION OF FITC DEXTRAN

pouch everted, and stretched over the plate to form an essentially two-dimensional network of vessels (Figure 7.3). This mounting procedure was carried out with the microscope to ensure that blood flow within the vessels was not disrupted due to the production of strains. A Perspex cover plate was then placed on top of the pouch.

FITC Dextran or 5% Evans Blue with Albumin (EBA) was injected intravenously into the hind limb of each hamster at least 30mins. prior to investigations. FITC Dextran (Mw 70,000) does not leak through blood vessels walls and also fluoresces under ultra-violet light which results in blood vessels being highly contrasted against the surrounding tissue (Figure 7.4.).

Pressure was applied to the cheek pouch via a 10μm thick latex membrane having a maximum pressure applying area of about 35mm^2. Pressure, up to 60mmHg, was provided by a column of water and, greater than 60mmHg, pneumatically. The apparatus used is shown schematically in Figure 7.5.

A Leitz Biomed intravital microscope having an NA 0.60 condenser and a green filter with maximum transmission at 5500Å was used to observe the pressure treated and the untreated areas. Recordings were made using a Polaroid camera with 3000ASA polaroid film (Polaroid,USA). Polaroid recordings were also supplemented by white light recordings using 35mm black and white film (Ilford U.K.).

Viewing fields inside and outside the pressure treated area, (the area of each field being about 0.5mm^2), were selected for observation. The fields outside the pressure treated area served as control in each experiment.

During preparation and throughout each experiment the cheek pouch was suffused with a heated, temperature regulated modified Krebs-Ringer Solution which maintained the cheek pouch at a temperature of 36.5 $\pm$ 1.0^{o}C.(Romanus, 1977).

The frequency of recording data was a function of the duration of each experiment and of the number of viewing fields selected. The frequency of recording was restricted

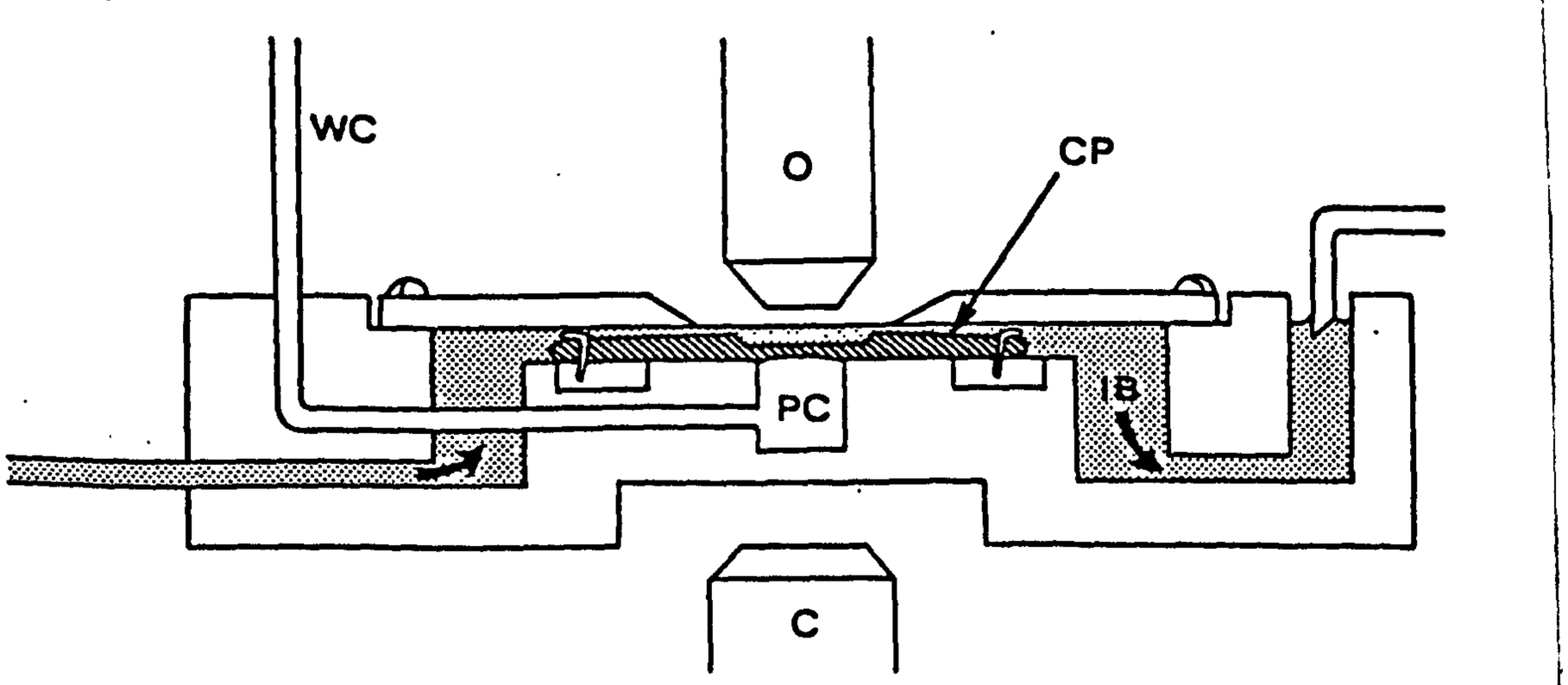

FIGURE 7.5. MOUNTING PLATFORM FOR CHEEK POUCH (CP) WITH PRESSURE CHAMBER (PC), IRRIGATION BATH (IB), WATER COLUMN (WC), OBJECTIVE (O) AND CONDENSER (C)

(AFTER ROMANUS, 1977)

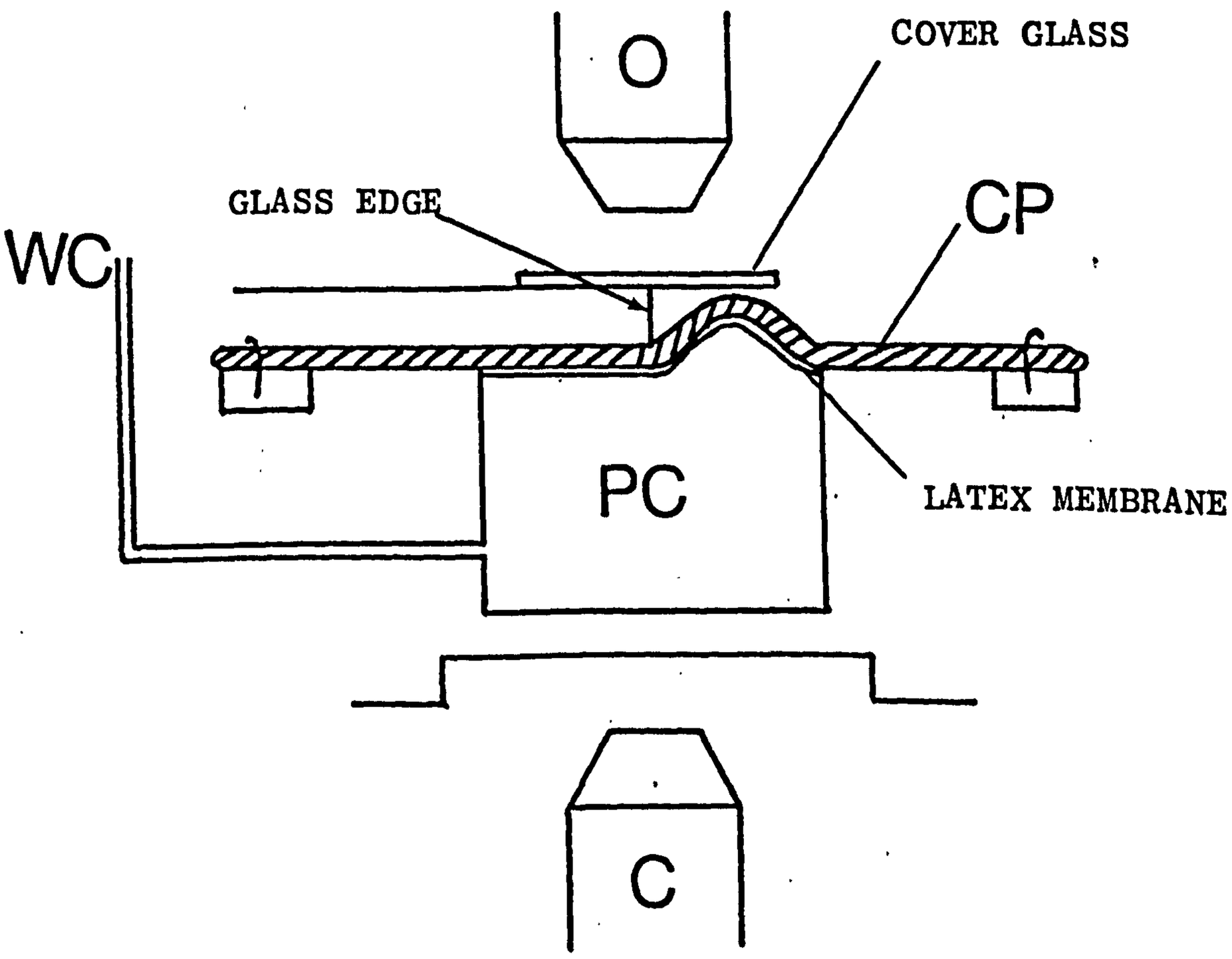

FIGURE 7.6. APPARATUS FOR PRODUCING PRESSURE GRADIENTS BY COMPRESSING THE CHEEK POUCH (CP) AGAINST THE GLASS EDGE BY THE LATEX MEMBRANE

as the Polaroid film required 90 seconds exposure due to the low intensity of light. Where a large area of pouch was being observed, which meant that as many as 8 viewing fields were present, the frequency of recording data was low i.e. it took about 12 mins. to obtain a complete photographic recording of 1 field.

7.3.3. Microvascular Response Assessment Criteria

The following parameters were recorded in each selected viewing field in each experiment as frequently as possible and were used as criteria to assess the microvascular response.

Hyperaemia Flow velocities in arterioles, venules and capillaries were estimated during, and after release of, pressure by comparison with pre-pressure velocities. The flow velocity was estimated as no flow, slow flow, or flow equal to or higher than pre-pressure flow velocity.

Inflammatory Response The number of white blood cells (WBC's) sticking to the walls of vessels were recorded either as nil (nil or single WBC's in few vessels); few (single WBC's/vessel in several vessels) or many (several WBC's/vessel in several vessels).

Microvascular Damage This was simply estimated by counting the number of leakages of FITC Dextran in the extravascular compartment. These leakages showed up as bright fluorescent patches contrasted against the dark background in comparison with the recordings of the undamaged tissue.

Vessel Strains Pressure-induced strain was estimated for each type of vessel and was obtained by comparing pre-pressure vessel lengths with the post-pressure lengths and calculating the vessel strain therefrom.

Selected Area Observations Within each of the selected fields a smaller area was examined with regard to the number of microvessels reperfused, the number of microthrombi (which are composed mainly of platelets, fibrin and WBC's) and the number of microbleedings (which was estimated by

extravasated RBC's).

7.4. EXPERIMENTAL DESIGN

The design of experiments was mainly influenced by the results of three studies; clinical studies performed by the author (Chapter 5); a study of pressure induced ischaemia (Romanus, 1977); and a series of in-vivo experiments on the effects of pressure on the conduction velocity of neural transmission signals (Rydevik and Lundborg, 1977).

In particular, Rydevik and Lundborg (1977) found that in sections of rabbit tibial nerve which were compressed by distributions of up to 400mmHg, the greatest damage, as evidenced by leakage of Evans blue dye (EBA) from blood vessels, occured at the boundary between the compressed and the uncompressed tissue where the pressure gradient was highest. Rydevik thought that this was due to increased shear forces being produced at the boundary.

Extrapolation of the results of Rydevik and Lundborg to hypertrophic scars receiving pressure therapy from elasticated garments is important since the pressures applied to scars by the elasticated garments are also due to a combination of forces; forces "normal" to the scar surface and forces in the plane of the scar surface, "in-plane" forces (vide 4.3.1.4).In order to define the micro-circulatory response to pressure it is necessary to differentiate between uniform and non-uniform pressure distributions.

Since the pressure chamber of the apparatus shown in Figure 7.5. is either pneumatically or hydraulically pressurised, the pressure distribution applied via the latex membrane is uniform and only the magnitude can be varied.

In order to apply a non-uniform pressure distribution using the apparatus shown in Figure 7.5., it was necessary to modify the interface between the latex membrane and the cheek pouch to produce a discontinuity in a uniform pressure distribution which would result in pressure gradients being produced within the cheek pouch.

7.4.1. Uniform Pressure Distribution

Uniform pressures of different magnitudes were applied to the cheek pouch for varying durations as described in 7.3.2.

In particular, pressures of two distinct magnitudes were applied; high pressures of an order of magnitude greater than capillary pressure, and 'low' pressures within the normal range of capillary pressure.

'Low' Uniform Pressures A 'low' uniform pressure of 40mmHg was selected for application. This magnitude had been found, clinically, to an upper limit of pressures measured under elasticated garments which had induced scar remodelling. (vide 5.5). Two series of experiments were performed. In the first series, each experiment lasted for about 20mins. and, in the second series, for about 60mins.

'High' Uniform Pressures were selected to repeat the experiments of Rydevik and Lundborg (1977). A pressure magnitude of 400mmHg was applied for about 15mins. The microcirculatory response was monitored until 30mins. after release of pressure. Particular attention was given to the response near the boundary region of the cheek pouch which delineates compressed tissue and non-compressed tissue.

7.4.2. Non-Uniform Pressure Distributions

The apparatus used was basically identical to that described in 7.3.2. and is shown in Figure 7.6. In addition, the Perspex cover plate was removed and a glass slide was secured in place over the cheek pouch such that one half of the cheek pouch was covered by the glass slide whereas the other half of the cheek pouch remained uncovered. When pressure was applied, the latex membrane was inflated and the half of the cheek pouch beneath the glass slide was compressed against the glass slide by the latex membrane, whereas the other half of the cheek pouch remained relatively uncompressed. (Figure 7.6.). A pressure gradient was thus

Experiment No.	Pressure Duration (mins)	FITC Dextran Admin. (mins)	MICROVASCULAR RESPONSE			Status 30mins. after pressure
			Hyperaemia	Inflammatory Response	Leakages	
1	9	-28	-	-	-	NORMAL
2	18	-30	-	-	-	NORMAL
3	15	-33	-	-	-	NORMAL
4	27	-30	-	-	-	NORMAL
5	25	-40	-	-	-	NORMAL
6	65	-30	-	YES	-	REDUCED FLOW IN CAP.$_s$, Vs.
7	61	-30	YES	YES	-	NORMAL
8	← DISREGARDED : No Ca^{2+} ions in Suffusion Solution →					
9	60	-32	YES	YES	-	Reduced flow in venules: Oedema
10	60	-31	YES	YES	-	NORMAL

FIGURE 7.7. RESULTS OF MICROVASCULAR RESPONSE TO UNIFORM PRESSURE DISTRIBUTION OF 40mmHg.

produced within the cheek pouch tissue, extending from the compressed area to the uncompressed area.

It was necessary to position a thin cover glass on top of the slide to prevent vapour from the suffusion solution condensing on the objective lens and obscuring the field of view.

Two magnitudes of pressure were applied, 20mmHg and 40mmHg, each magnitude being maintained for about 15mins. duration.

In order to obtain the maximum amount of data from the animals the two magnitudes of pressure were applied to each hamster cheek pouch with a period of no-pressure between pressure applications. 20mmHg was first applied followed by a period of no-pressure during which time the blood flow in the cheek pouch returned to normal whereupon 40mmHg was applied. Following application of 40mmHg pressure the microcirculatory response was monitored up to 30mins. after release of pressure using the criteria of 7.3.3.

7.5. EXPERIMENTAL RESULTS

7.5.1. Microcirculatory Response to "Low" Uniform Pressure Distributions

The response to 'Low' Uniform Pressure Distributions is described under the following sections 7.5.1.1. and 7.5.1.2.

7.5.1.1. 40mmHg Applied for 20mins. The results of 'low' pressure experiments of 7.4.1 are tabulated in Figure 7.7. Five experiments, (1 - 5), were performed with pressure being applied for periods between 9mins. and 27mins., the mean period being 18.8mins. FITC Dextran was infused into the tibial vein between 28mins. and 40mins. before the application of pressure, the mean time of infusion being 32.2mins. Blood flow appeared to be stopped in all vessels within 10mins. after the application of pressure. Blood flow ceased firstly within venules and capillaries then large venules and arterioles. No microvascular

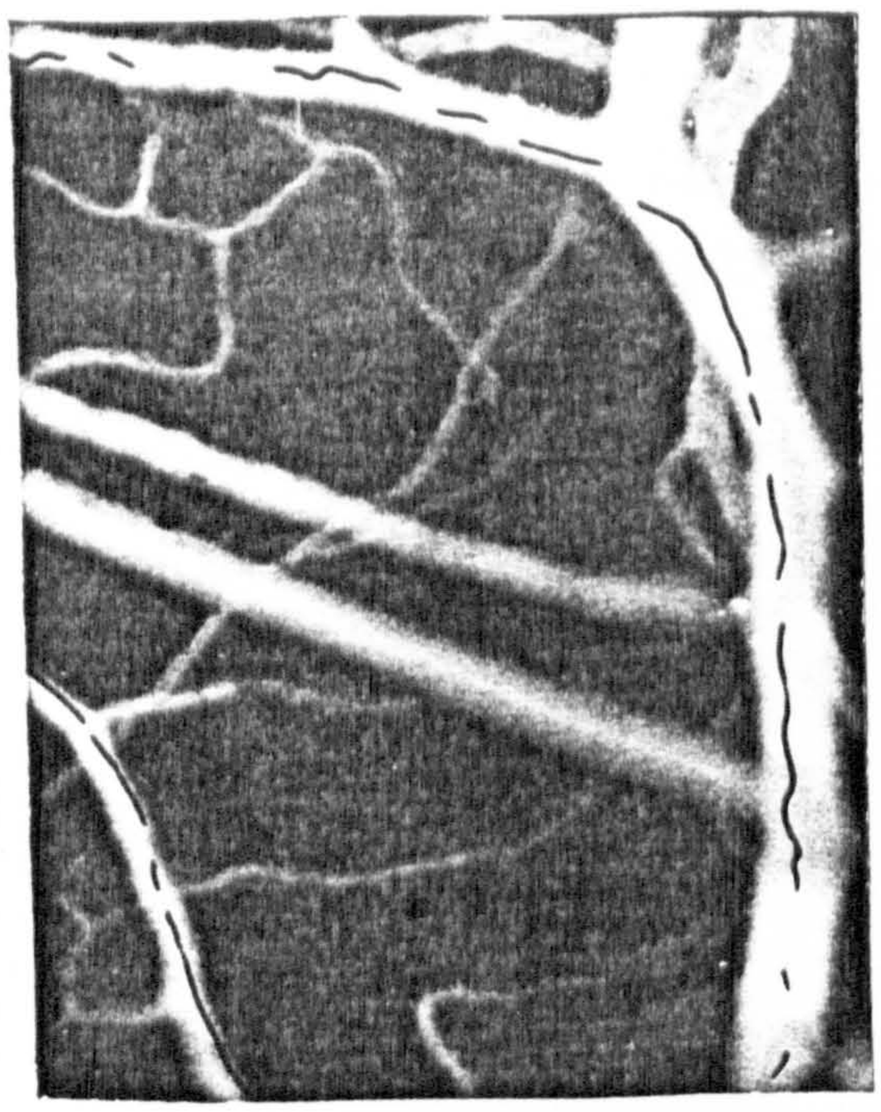

FIGURE 7.8a BEFORE PRESSURE

FIGURE 7.8b 22-24MINS AT 40mmHg

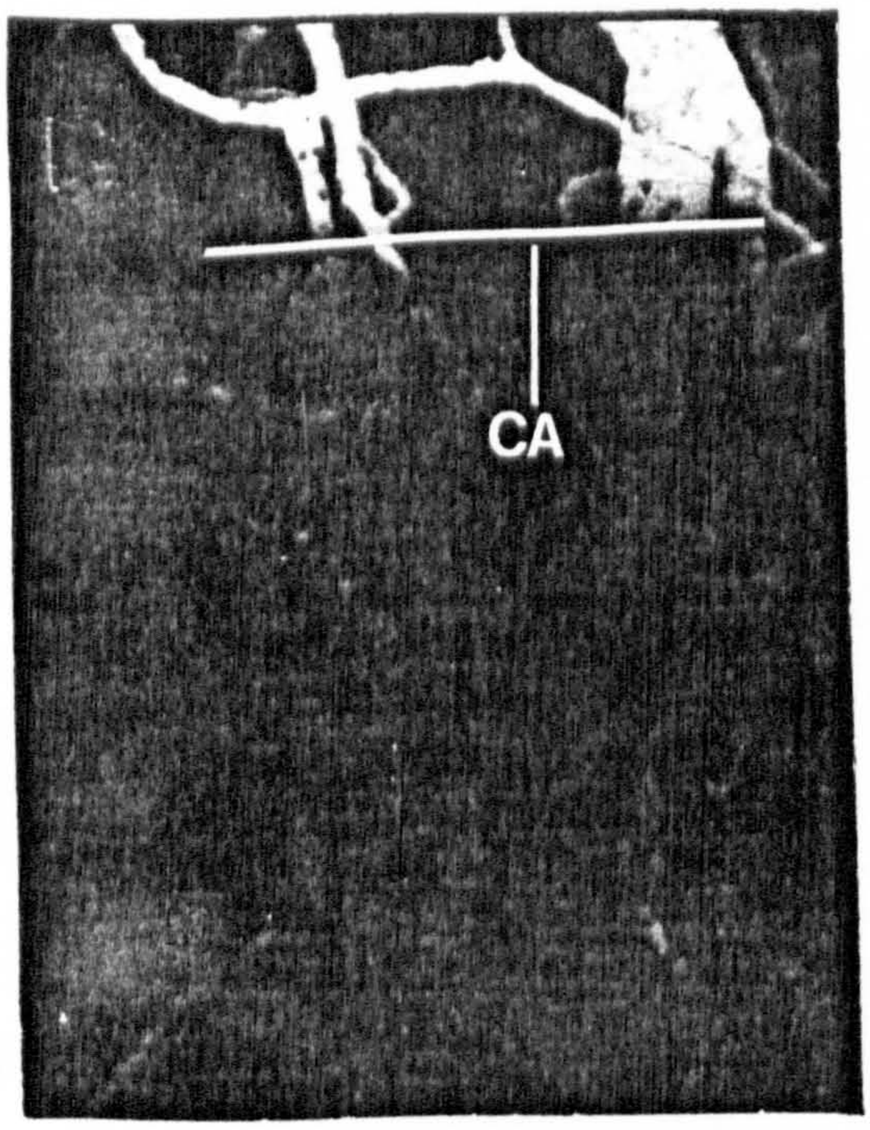

FIGURE 7.8c 59-61MINS AT 40mmHg

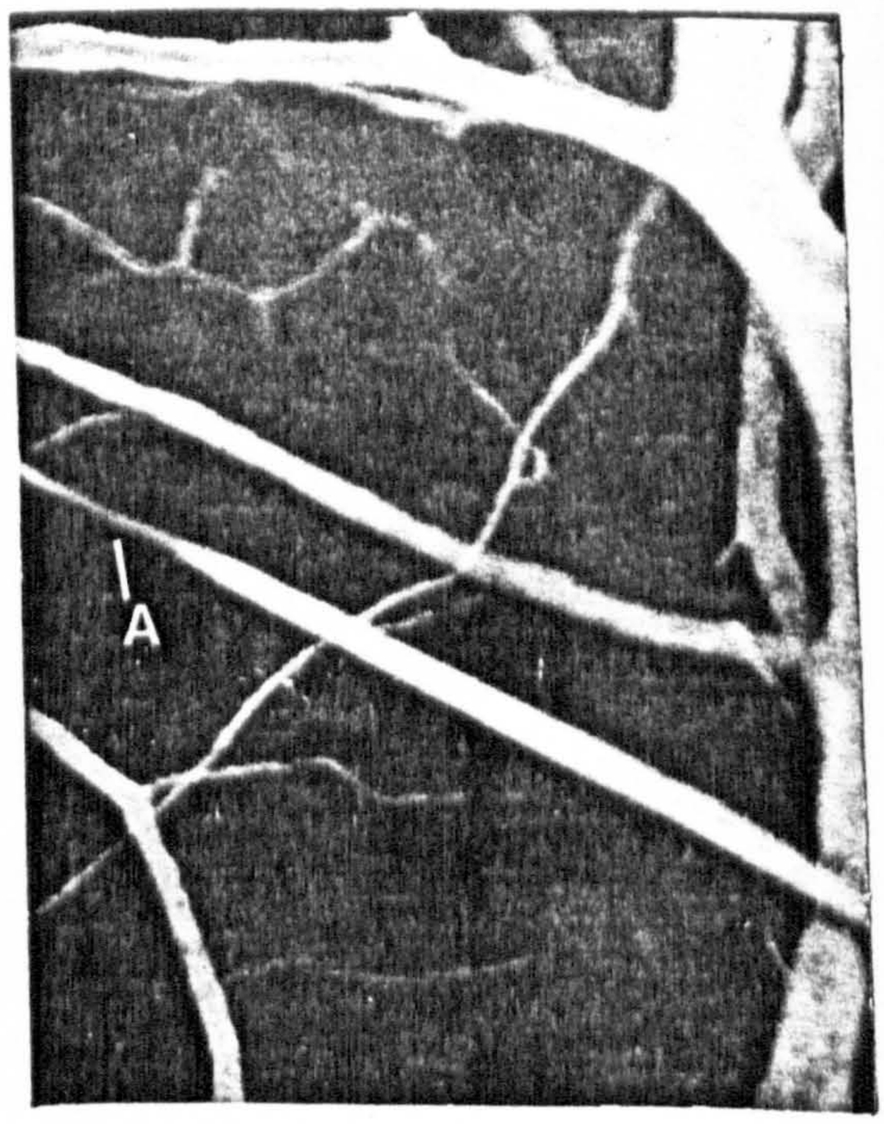

200μm

FIGURE 7.8d 15MINS. AFTER PRESSURE RELEASE

FIGURE 7.8. MICROVASCULAR RESPONSE TO UNIFORM PRESSURE DISTRIBUTION OF 40mmHg SHOWING EXTENT OF COMPRESSED AREA (CA) AND "PINCHED" ARTERIOLE (A)

reactions were observed on release of pressure. 10mins. after pressure was released normal flow was reported in all vessels within the selected areas. There were no leakages observed, either at the boundary zone or within the compressed zone. Vessel strains were not estimated since the changes in length were too small to be accurately measured.

40mmHg Applied for 60mins. 5 experiments, (5 - 10) were performed, with the results shown in Figure 7.7, for periods varying between 60 and 65mins., the mean duration of pressure being 62mins. FITC Dextran was infused between 30 and 32mins. prior to the application of pressure, the average time of infusion being 30.8mins. Blood flow stopped in all vessels within 5 - 15mins. after the onset of pressure, depending on the type of vessel. Thereafter, as the duration of pressure increased, the vessels in the compressed zone became increasingly exsanguinated.

Figures 7.8a, 7.8b, 7.8c and 7.8d are sequential polaroid photographs showing an area of the hamster cheek pouch near the boundary zone (experiment 6) before pressure, after 22 - 24mins. pressure, after 59 - 61mins. pressure and 15mins. after release of pressure respectively. Figure 7.8c demonstrates a marked increase in occlusion compared to 7.8b and also clearly delineates the extent of the compressed area (CA). Figure 7.8d demonstrates extensive reflow in most vessels although a large arteriole (A) clearly remains "pinched".

Only recordings from experiments 7, 9, 10 were suitable for analysis of vessel deformations. In the majority of vessels examined within the selected areas, no differences were observed between the lengths of vessels before the application, and after the release, of pressure. Reflow occured in all vessels, in the selected areas within 30mins. of pressure being released. Hyperaemia and an inflammatory response were observed in each experiment. Oedema was observed (expt. 9) and flow in arterioles and capillaries

was still reduced 30mins. after release of pressure (Figure 7.8d.).

In experiment 8, calcium (Ca^{2+}) ions had been erroneously omitted from the suffusion solution. This meant that the integrity of the endothelial membrane disappeared whereby vessel permeability increased and FITC Dextran leaked into the extravascular compartment producing numerous leakages. Experiment 8 was not included in the subsequent analysis or discussion of the results.

7.5.1.3. Discussion In the nine relevant experiments, blood flow was stopped in all vessels in the selected areas, within 15mins. of the pressure being applied. This finding is somewhat inconsistent with that of Romanus (1977) who found that a pressure of 60mmHg was just enough to completely arrest the cheek pouch circulation. The microvascular response to lower pressure magnitudes were not reported. Kosiak (1959), from routine histology techniques, reported an absence of microvascular changes following the application of 35mmHg pressure for up to 72 hours to the trochanteric region of dogs. However, this relatively high tolerance threshold may be due to the presence of a significantly higher amount of adipose tissue and muscle in canine tissue.

In this series of experiments no tissue reactions were observed when the average pressure duration was 19mins. however when the mean duration was extended to 62mins., tissue reactions in the form of hyperaemia and an inflammatory response were observed in each experiment following release of pressure.

The tissue reactions observed following the 60mins. pressure duration may be due to the fact that metabolic degradation products, which include vasoactive substances, have time to accumulate and induce hyperaemia, (Brånemark, 1971, Karpf et al, 1974, Larssonet al, 1977, Romanus et al, 1977). Hyperaemia is, however, also accompanied by restoration of tissue metabolism (Romanus, 1977). It would seem reasonable, with these experiments, to assume that tissue metabolism had returned to near normal values 30mins. after

Experiment No.	Pressure Duration (mins)	EBA/ FITC Dextran Admin.(mins)	MICROVASCULAR RESPONSE			Flow Status 30mins. After Pressure
			Hyperaemia	Inflammatory Response	Leakages	
1	15	+8	-	-	-	NORMAL
2	15	-26	-	-	-	NORMAL
3	15	-20	-	-	-	NORMAL
4	16	+12	YES	-	-	NORMAL
5	15	-28	-	YES	-	REDUCED
6	21	-30	-	YES	-	NORMAL
7	20	-33	-	YES	-	REDUCED
8	17	-30	-	YES	-	REDUCED
9	22	-40	-	YES	-	REDUCED
10	← DISREGARDED:ANIMAL DIED DURING EXPERIMENT →					

FIGURE 7.9 RESULTS OF MICROVASCULAR RESPONSE TO UNIFORM PRESSURE DISTRIBUTION OF 400mmHg

release of pressure.

The vessel strains measured in the 60mins. duration experiments were not more than a few percent and could easily have been due to measurement error. This appeared to have no significance on the restoration of blood flow. Theoretically, for a 5% increase in the length of a vessel (assuming laminar flow) there is a reduction of 12% in the blood flow rate (Appendix D). However, a 12% reduction in blood flow rate is unlikely to produce any significant metabolic changes which will induce tissue damage (Daly et al, 1976).

With the 40mmHg uniform pressure distribution it appears that the microvascular reaction is principally dependent on the duration of pressure. Therefore, it is reasonable to infer that 40mmHg is above the critical pressure necessary to reduce blood flow to a level which cannot support normal tissue function although it should be understood that this critical pressure may vary with the mean arteriolar pressure. This explanation of the results is consistent with previous reports which state that once the critical threshold pressure has been overcome, time is the predominant factor in determining tissue viability (Kosiak, 1959, Ferguson-Pell, 1977).

7.5.2. Microvascular Response to "High" Uniform Pressure Distributions

The microcirculatory response to 'high' uniform pressures is reported under the following sections 7.5.2.1. and 7.5.2.2.

7.5.2.1. 400mmHg Applied for~15mins. The results of these experiments are shown in Figure 5.9. Ten experiments were performed, one of which was disregarded, (experiment 10). 400mmHg was applied in each experiment, the average period being 17.3mins. EBA dye was used in experiments 1 - 4 and FITC Dextran was used in experiments 5 - 10. It was attempted to infuse each dye at least 30mins. prior to the application of pressure. However, this was not always possible but it appeared to have no effect on the blood flow

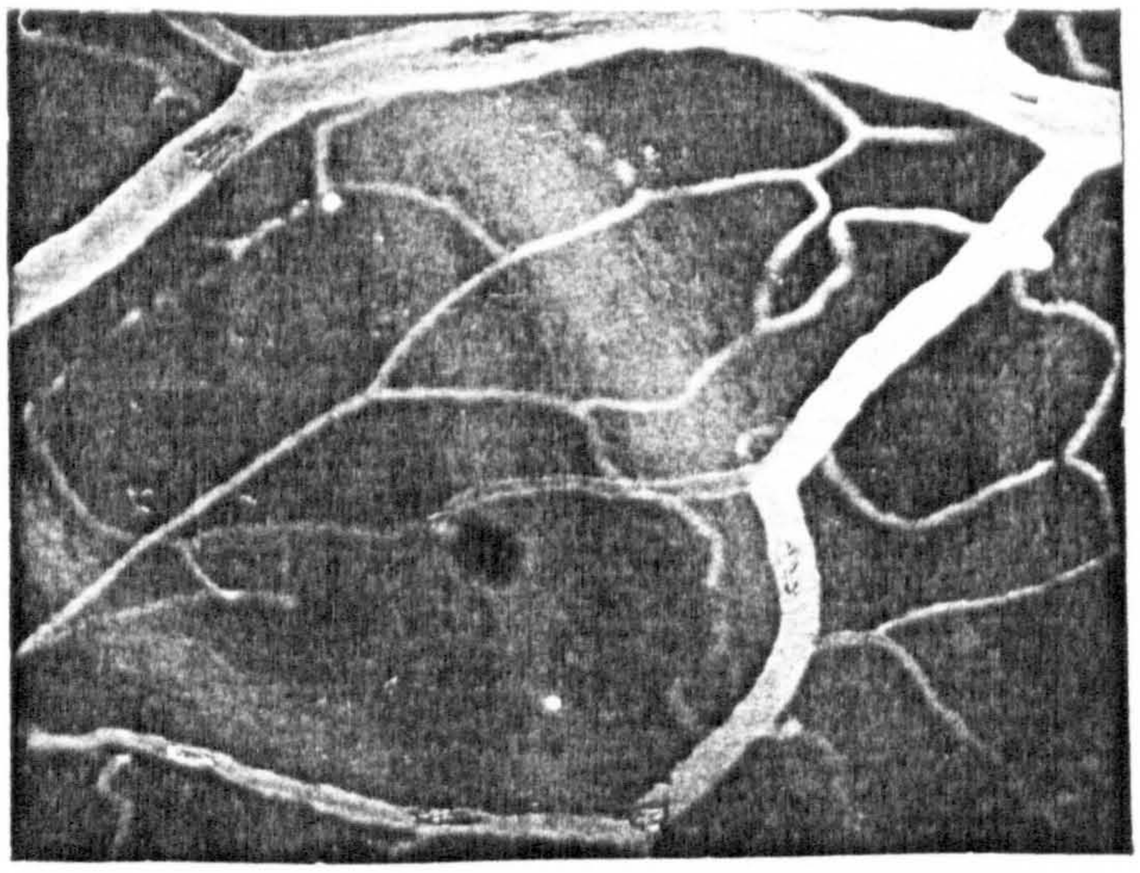

FIGURE 7.10a BEFORE PRESSURE

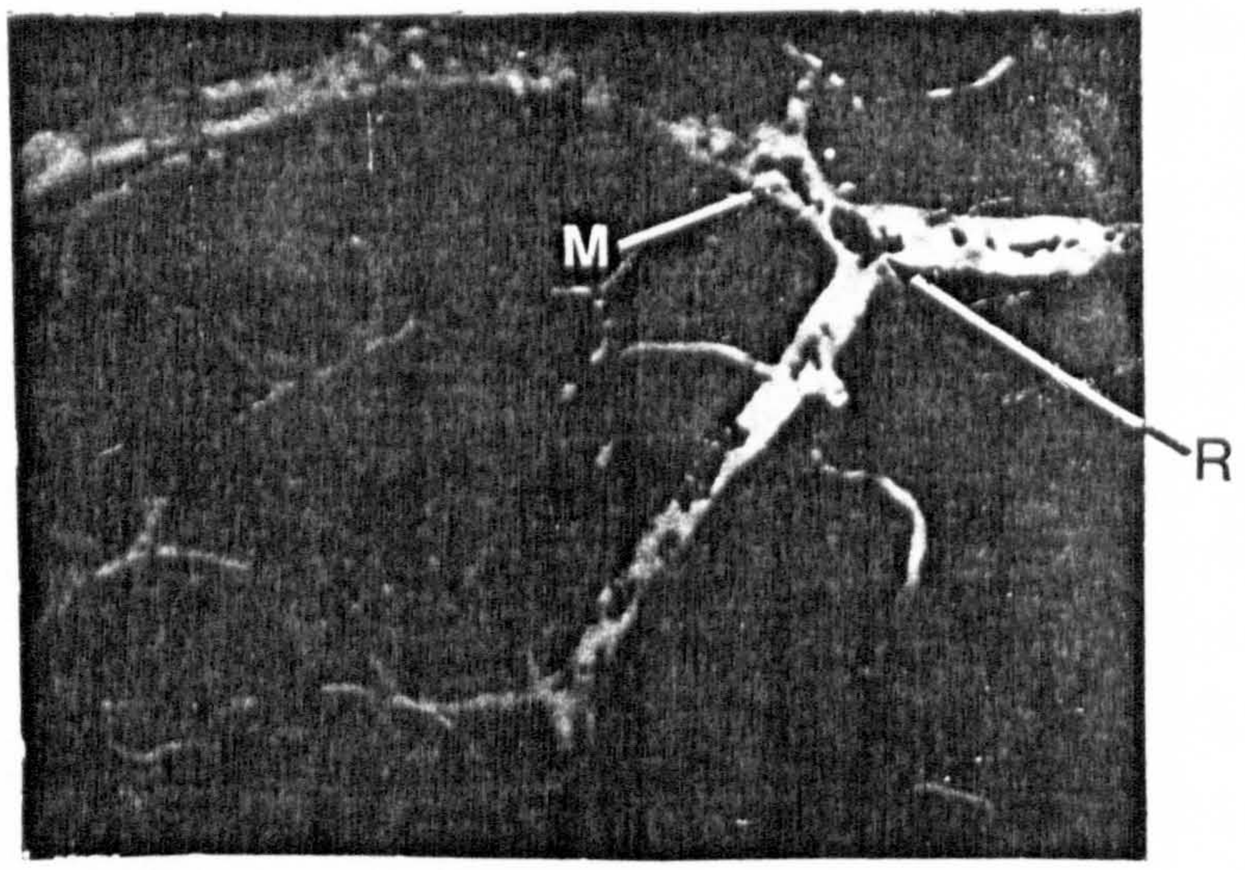

FIGURE 7.10b 12MINS. AT 400mmHg

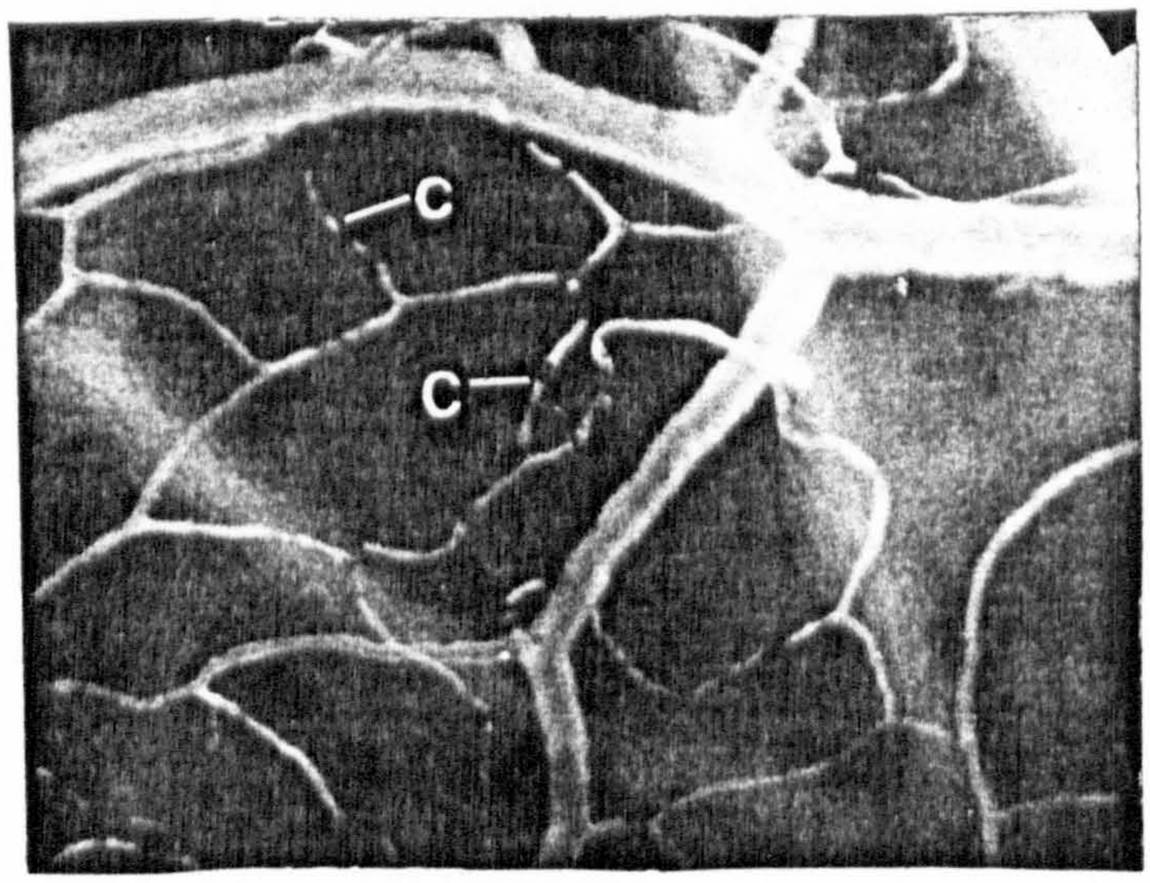

200μm

FIGURE 7.10c 20-21MINS. AFTER RELEASE OF PRESSURE

FIGURE 7.10 MICROVASCULAR RESPONSE TO UNIFORM PRESSURE DISTRIBUTION OF 400mmHg SHOWING MICROTHROMBI (M) AND ROULEAUX (R)

before pressure was applied.

Following the application of pressure, blood flow immediately stopped in all vessels within the selected area in each experiment.

Figures 7.10a, 7.10b, 7.10c are sequential polaroid photographs which show a compressed area of hamster cheek pouch in experiment 8, before the application of pressure, 11 - 12mins. after the application of 400mmHg pressure and 20 - 21mins. after release of pressure respectively. Figure 7.10b demonstrates a complete blood flow arrest with aggregations of red blood cells (rouleaux - (R)) evident in a large venule, together with micro-thrombi formation (M). 20 - 21mins. after release of pressure reflow superficially appears extensive and complete, however a closer inspection of Figure 7.10c shows that reflow did not occur in some capillaries (C).

Following release of pressure blood flow was gradually re-established. Hyperaemia was observed in one experiment (4) and inflammatory responses were recorded in each of experiments 5 - 9. Only the polaroid photographic recordings in experiments 5 - 9 were of suitable quality to permit quantitative evaluation of pressure induced changes, such as vessel strains. 30mins. after release of pressure inflammatory responses persisted in experiments 6, 7 and 9. No leakages were observed. 30mins. after release of pressure, flow was observed to be approximately normal in all experiments, although in some vessels within selected observation zones reduced flow was noted (experiment 8, Figure 7.10c).

Vessel strains were calculated in experiments 5 to 9 using the formula

$$\epsilon = \frac{\delta l}{l_o} = \frac{l_e - l_o}{l_o}$$

where ϵ = vessel strain

l_o = original vessel length

δl = change in length

l_e = length after release of pressure

Experiment No.	Vessel Type	Vessel location	Length Before Pressure	Length After Pressure	Strain (%)	FLOW AFTER RELEASE
5	Venules (large)	CA	119.35	161.7	34.48	N (NORMAL)
			492.8	531.3	7.8	N
6	Capillaries	CA	23	26	13	N
			15	17	13.3	N
			13	15	5.3	N
			32	35	9.4	N
			12	12.5	4.2	N
			23	23	0	N
	Venules	CA	19	20	5	N
			19	24	25	R
7	Venules (large)	CA	49	49	0	N
			31.5	37	17.5	N
			25	25	0	N
			34	36	5.9	N
	Venules (small)	CA	19	20	5.3	N
			10	11.5	15	N
			23	26	18.3	N
	Arterioles	CA	71	84	2.8	N
			36	37	11	N
	Capillaries	CA	18	20	11	N
			15	11	0	N
			18	16	6.7	N
			9	19	5.6	N
			20	20	0	N
8	Venule (large)	CA	35	42	20	N
	Venule (small)	CA	18	20	0	N
			12	12	0	N
			25	25	0	N
	Venule (large)		19	22	15.8	N
			27	27	0	N

FIGURE 7.11 PRESSURE INDUCED STRAINS IN DIFFERENT VESSEL TYPES.

The strain calculations for vessels of different types are tabulated in Figure 7.11.

The length of each vessel was measured by a metric caliper which had a resolution of 0.1mm.

The measurement error for a single person reading the caliper could be assumed to be to be a maximum of ± 0.1mm, which is less than 1% in the case of the average vessel length measured, the average length being about 120 - 150mm. Other errors, due to optical artefacts between photographs are assumed to be negligible.

Therefore the accuracy of the majority of vessel strains measured is within ± 1% of the true strain value.

As the number of vessels of a particular vessel type, for example capillaries, investigated in one experiment is small of necessity, to obtain a more comprehensive quantification of the response, strains of like kinds of vessels were averaged, with the results shown in Figure 7.12.

Comparing the vessel types, venules (large and small) exhibited the greatest strain following removal of pressure, followed by capillaries then arterioles.

Reflow occured in almost all vessels within 30mins. after release of pressure (Figure 7.9). However, in experiment 6, no reflow occured in a venule which exhibited a strain of 25%, but in experiment 7, reflow occured within 16 - 18 and in 19 - 21mins. in two venules which exhibited strains of 15% and 13.5% respectively after release of pressure.

There was no measurable difference observed between strains recorded from vessels near boundary zone and strains recorded from vessels within the compressed zone.

7.5.2.2. Discussion Reflow was reported in almost all vessels within the selected areas 30mins. after release of pressure indicating that whatever the values of induced strains, they did not permanently occlude blood flow. In some cases, however, the flow was estimated to be reduced below "normal" levels. A reason for the difference between

VESSEL TYPE	Number of Vessels	Average Strain (%)
Capillary	15	7
Small Venule	11	8.5
Large Venule	7	11.3
Arteriole	2	2.8 and 18.3

Figure 7.12 AVERAGE PRESSURE INDUCED STRAIN IN DIFFERENT VESSEL TYPES.

average strain values of different vessel types may be due to the structure of the vessels: It is well known that venules, and arterioles have differing amounts of elastic tissue and it may be that the average vessel strains reflect the elastic recoil or "recoverability capacity" of the respective vessel types. In particular, vessels such as arterioles have much more elastin than small venules thereby possessing a greater capacity of recovery in response to pressure induced strains.

A theoretical prediction, derived from a Poiseulles Law laminar flow model (Appendix D) relates the flow rate within a thin-walled tube to the vessel strain for a homogeneous fluid medium as

$$\frac{Q_2}{Q_1} = \frac{(1-4\ \delta r/r)}{(1+\ \delta x/x)}$$

where Q_2 = flow in a strained vessel
Q_1 = flow in an unstrained vessel
δx = increase in length
x = original length
r = original radius
δr = increase in radius

The limiting value occurs when $Q_2 = 0$ i.e. there is no flow in the strained vessel.

This occurs when $1 - 4(\delta r/r) = 0$ or when the radial strain is 25%. For an isovolumetric material the corresponding axial or longitudinal strain is $\approx 26.3\%$.

Experimentally, this theoretical prediction appeared to be confirmed in the case of the venule which remained strained by 25% after removal of pressure, and in which reflow did not occur 30mins. after release of pressure (Figure 7.11). Although much more data would be required to substantiate this apparent confirmation it is possible, therefore, that applied uniform pressure distributions, of a sufficiently high magnitude can result in vessels being strained beyond a critical value, the effect of which is a reduction and eventual cessation of blood flow within the vessel. However, with the magnitudes of pressure measured at scar/dressing interface it appears highly

Experiment No.	Pressure Duration (mins)	FITC Dextran Admin (mins)	MICROVASCULAR REACTION			WIDTH OF OCCLUDED AREA (μm)	FLOW STATUS 30Mins After Pressure
			Hyperaemia	Inflammatory Response	Leakages		
1	20	-30	YES	-	YES	380	Normal
2	17	-35	YES	-	-	352	Normal
3	15	-40	-	YES	-	364	Normal
4	15	-25	YES	YES	-	346	Normal
5	15	-50	YES	-	-	348	Normal
6	15	-25	YES	-	-	342	Normal
7	18	-90	YES	-	-	364	Normal

FIGURE 7.13 RESULTS OF MICROVASCULAR RESPONSE TO 20mmHg NON-UNIFORM PRESSURE DISTRIBUTION

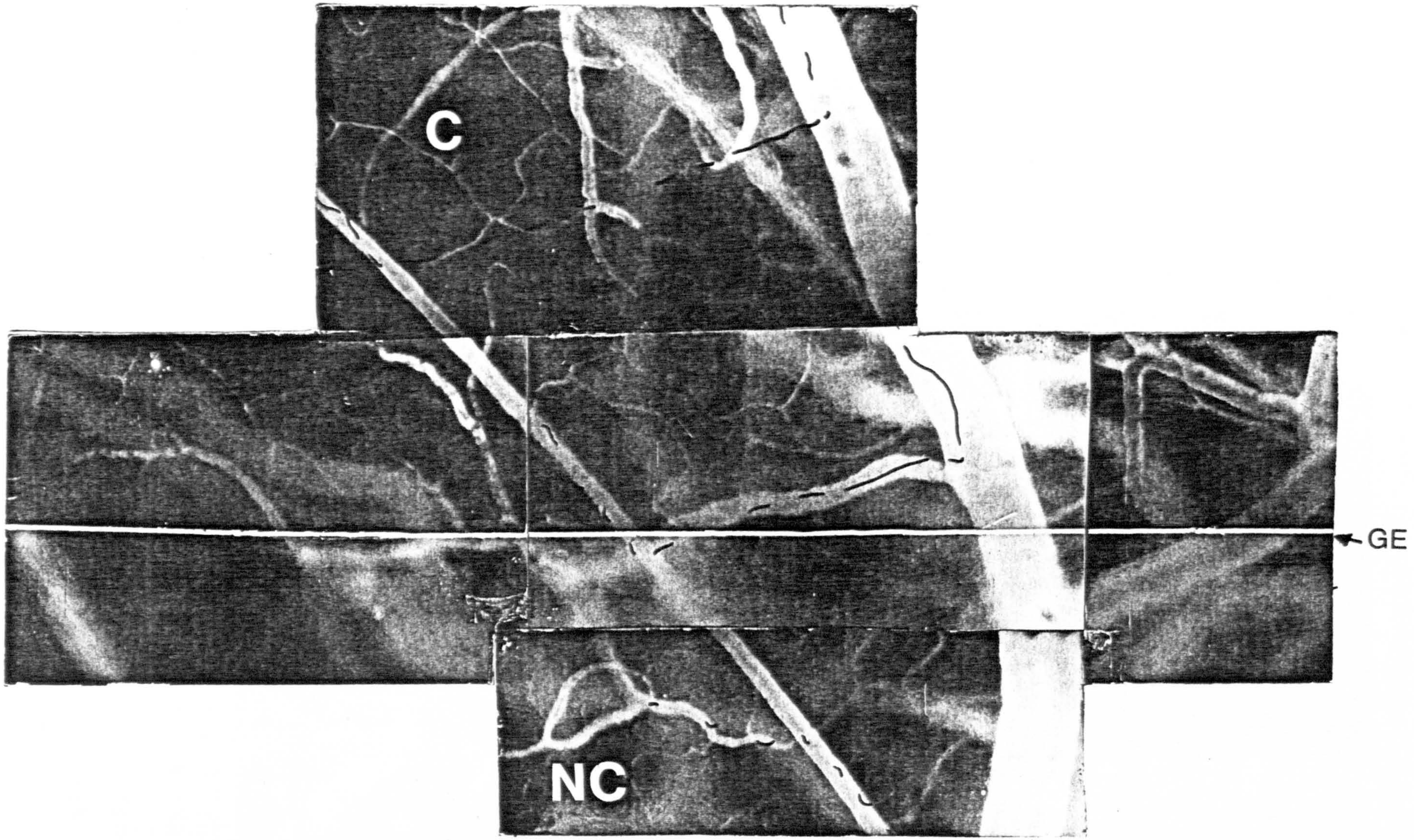

FIGURE 7.14a BEFORE THE APPLICATION OF PRESSURE SHOWING GLASS EDGE (GE) DELINEATING COMPRESSED (C) AND UNCOMPRESSED (UC) ZONES

FIGURE 7.14b MICROVASCULAR RESPONSE TO 20mmHg INDUCED PRESSURE DISTRIBUTION SHOWING THE WIDTH (W_1) OF THE OCCLUDED AREA (OA_1) BETWEEN THE COMPRESSED (C) AND UNCOMPRESSED (NC) AREAS

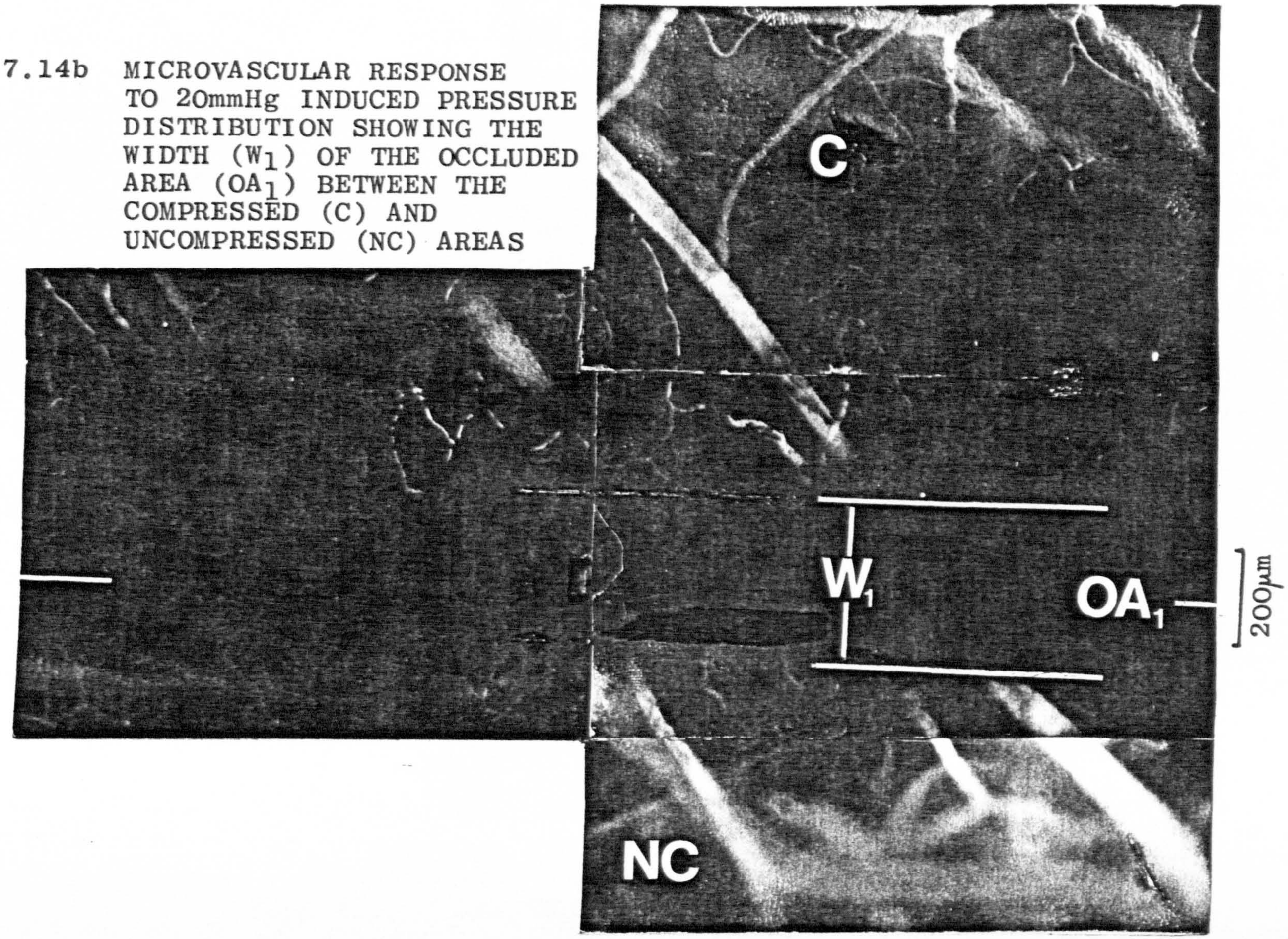

unlikely that the response to pressure would be reflected in this way.

7.5.3. The Microcirculatory Response to Non-Uniform Pressure Distributions.

7.5.3.1. 20mmHg Pressure Seven experiments were performed in this series the results of which are shown in tabulated form in Figure 7.13. Pressure was applied for periods between 15mins. and 20mins., the mean duration being 16.5mins. FITC Dextran was administered at least 25mins. before the application of pressure in each case.

Immediately following the application of pressure, vessels on either side of the glass slide edge were completely occluded (Figure 7.14b). A typical example is experiment 1, with the tissue response shown in Figures 7.14a and 7.14b which are composite Polaroid photographs of the same area of cheek pouch at the boundary between the compressed area (C) and the uncompressed area (NC) taken before, and during, the application of pressure respectively.

The width (W_1) of the occluded area (OA_1) appeared to be constant across the length of the glass slide edge and was calculated as 380μm* from a calibrated grid. The average pressure gradient from the compressed to the non-compressed area was estimated as -52.5mmHg/mm in the present case. The overall mean width for the seven experiments was 356μm resulting in an overall mean pressure gradient of -56.08mmHg/mm.

---

* This figure is only approximate since the difference in elevation between the compressed and uncompressed tissues (Figure 7.6.) is such that all parts of the viewed area cannot be in focus simultaneously. Consequently, parts of each area were rephotographed "in-focus" and the resulting prints were spliced together to form a composite "in-focus picture" of the investigated area. No matter how much care is taken during this procedure photographic detail is inevitably lost.

Experiment No.	Pressure Duration (mins)	Duration of No-Pressure (mins)	MICROVASCULAR RESPONSE			WIDTH OF OCCLUDED AREA (μm)	FLOW STATUS 30mins After Pressure
			Hyperaemia	Inflammatory Response	Leakages		
1	20	-15	YES	YES	YES	396	Reduced
2	17	-22	YES	YES	YES	384	Reduced
3	15	-18	-	YES	YES	380	Normal
4	15	-15	YES	YES	YES	397	Normal
5	15	-15	YES	YES	YES	408	Reduced
6	15	-25	YES	YES	-	384	Normal
7	18	-20	-	YES	-	398	* Reduced

* Age of Pouch Suspected as being responsible

FIGURE 7.15 RESULTS OF MICROVASCULAR RESPONSE TO 40mmHg INDUCED NON-UNIFORM PRESSURE DISTRIBUTION

In the compressed area the blood flow in most vessels appeared to remain unaltered throughout the duration of pressure in each experiment (Figure 7.14b). In the uncompressed areas no changes in the microvascular flow were observed except in vessels near to the occluded area in which flow appeared to be slightly reduced.

On release of pressure, the vessels within the occluded zone were immediately reperfused. Hyperaemia was observed in six experiments and inflammatory responses in two experiments. One leakage was observed (experiment 2) in the compressed area, but it was not located near to the boundary.

The time for apparently normal blood flow to return to the vessels varied between 15mins. and 25mins., the average period being 18.5mins.

7.5.3.2. 40mmHg Pressure 7 experiments were performed in this series, the results of which are shown in tabulated form in Figure 7.15. Pressure was applied for a period between 15mins. and 22mins., with a mean duration of 16.1mins., after the microcirculation had returned to normal.

The response is illustrated by example in which Figure 7.16a and Figure 7.16b are composite Polaroid photographs of the same cheek pouch area of experiment 1 taken during pressure application and after release of pressure respectively.

When pressure was applied, all vessels on either side of the glass slide were immediately and completely occluded. The width (W_2) of the occluded area (OA_2) appeared constant across the length of the glass edge and was measured as 396 μm. The average pressure gradient from the compressed to the uncompressed area is -101mmHg/mm, and the overall mean pressure gradient is -102mmHg/mm.

During pressure, the blood flow in the compressed area in each experiment gradually ceased in all vessels within the

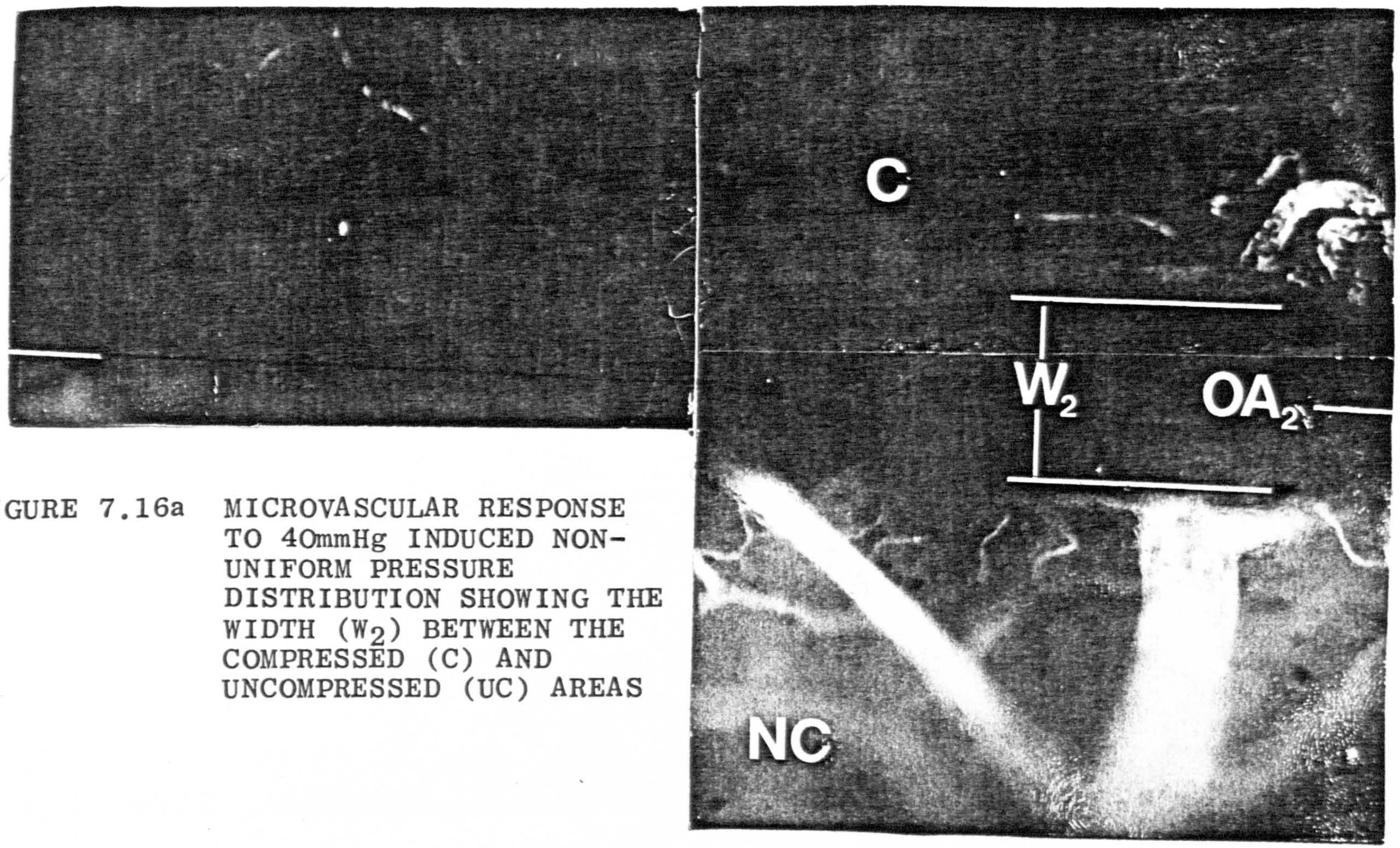

FIGURE 7.16a MICROVASCULAR RESPONSE TO 40mmHg INDUCED NON-UNIFORM PRESSURE DISTRIBUTION SHOWING THE WIDTH (W_2) BETWEEN THE COMPRESSED (C) AND UNCOMPRESSED (UC) AREAS

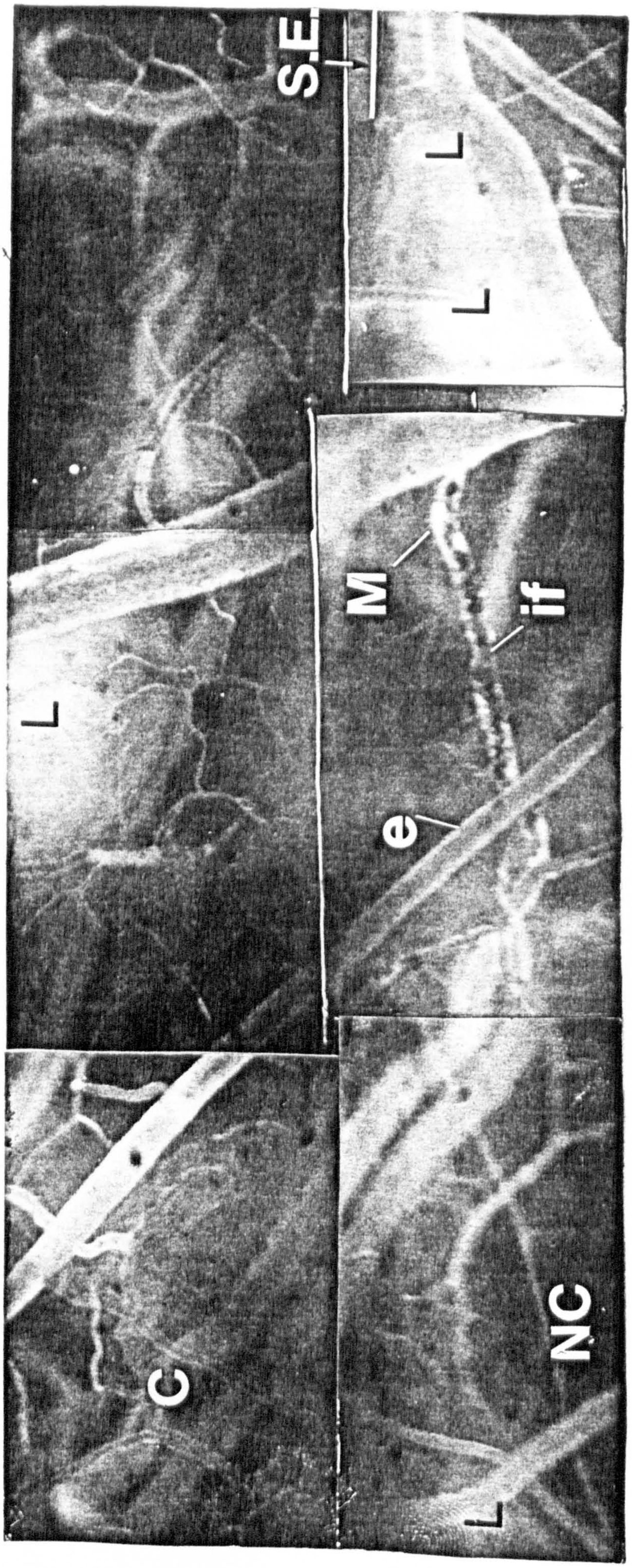

FIGURE 7.16b MICROVASCULAR RESPONSE FOLLOWING RELEASE OF 40mmHg PRESSURE
SHOWING LEAKAGES (L), MICROTHROMBI (M), INFLAMMATORY RESPONSE (if),
HYPERAEMIA(e) THE COMPRESSED (C) AND UNCOMPRESSED (NC) AREAS

compressed area, until 10 - 12mins. after the application of pressure when blood flow appeared to be completely arrested. This result is consistent with results obtained from experiments of sections 7.5.1.1. and 7.5.1.2.

Blood flow appeared normal in all vessels in the uncompressed area in each experiment.

Immediately after release of pressure (Figure 7.16b), microcirculatory reactions were observed in each experiment; hyperaemia in six experiments and inflammatory responses in all seven experiments. Numerous leakages of blood into the extravascular compartment were observed in six experiments, indicating damaged vessels. The leakages were located mainly outwith the occluded area but occurred in both the compressed and uncompressed areas near to, and in a direction parallel to, the glass slide edge (G.E.) Figure 7.16b shows leakages (L) and an inflammatory response (If). Microthrombi (M) are also observed.

Flow was considerably reduced in most vessels within, or in the immediate vicinity of, the compressed area (C), 15mins. after the release of pressure, and 30mins. after release of pressure a marked reduction in flow remained in four cases (Experiments 1, 2, 5 and 7).

7.5.3.3. Discussion The discussion of effect of forces, other than normal or uniform forces, on tissue is notably absent from the most pertinent literature in tissue mechanics. This is probably due to the fact that no satisfactory method or apparatus for measuring such forces has been developed. Clinically, the importance of non-uniform force and pressure distributions has long been recognised as a contributory, and perhaps predominant factor in the development of tissue damage. Reichel (1958) suggested that friction-induced shear forces could be a major cause of decubitus ulceration in paraplegics. Chow et al (1976) stated that in-plane forces resulting from normal or hydrostatic loading were the major source of restricting circulation.

The maximum value of pressure gradient which the author found reported in the literature was calculated from normal pressure measurements on sitting human subjects (Kosiak, 1959). Kosiak calculated that the maximum gradient for a peak pressure of 259mmHg (34.6 kPa) was 3.67mmHg/mm at the ischial tuberosities. This calculation however does not take into account the thickness of the tissue, therefore the values are applicable to the skin surface only. The thickness of the tissue may modify the distribution of pressure and consequently, the pressure gradients within the tissue considerably. Therefore the actual pressure gradients acting on the tissue containing the circulation and microcirculation is unknown, although since the ischial tuberosities are sharp bony prominences, which support nearly the full weight of the body when sitting, it is reasonable to assume that the pressures measured thereunder are possibly the highest naturally occurring constant values of pressure at tissue/external environment interfaces. The pressure gradients calculated therefrom may also be amongst the highest naturally occurring values of this parameter and 3.67mmHg/mm measured at the skin surface thus appears to be a value which the body can tolerate without evident tissue damage.

In this series of experiments 7.5.31, a mean pressure gradient magnitude of 56mmHg/mm applied for 15mins., did not produce any observable acute microvascular damage, and 30mins. after release of pressure blood flow had returned to normal in all parts of the pouch including the occluded area. When the mean value of the pressure gradient magnitude was increased to 102mmHg/mm and maintained for the same period of time it was found that on release of pressure, acute damage had occurred to vessels near, or within, the occluded zone parallel to the glass edge. Damage was still evident 30mins. after release of pressure. As the thickness of epithelial tissue between the pressure membrane and the vasculature was about 25μm it is reasonable to assume that the distribution of pressure was not

significantly modified and that the pressure gradients measured were applied to the microcirculation.

Although with these results it appears that there may be a critical value of pressure gradient which, when exceeded, results in acute microvascular damage, the values of these results cannot be taken as absolute, as their calculation involves assumptions which may be invalid. For example, it is assumed, in the measurements of the occluded area, that the pressure drop from the compressed area to the uncompressed area is equal to the total value of the applied uniform pressure and occurred only across the width of the occluded area. In fact, the actual distance over which the pressure drop occurred may have been several millimeters and the pressure drop may not have been 100% of the total applied pressure due to the ballooning effect of the membrane (Figure 7.6). However, as the difference between the width of the occluded zones, in the case of the 20mmHg and 40mmHg non-uniform pressure distributions was only 16 μm or about 5% of the width of the 20mmHg occluded zone, it was thought that most of the pressure drop did occur across the occluded zone. Therefore although the calculated values of pressure gradients were probably slightly higher than the true pressure gradients, they were in the same order of magnitude. Therefore it was thought that the assumption used in the calculation of the pressure gradients was valid.

A reason for these artificially high values may be the manner in which the non-uniform pressure distributions are produced; by the membrane acting on a sharp glass edge. Theoretically the pressure profile from the compressed to the uncompressed area does not result in a constant gradient but has a 'quasi-infinite' pressure spike at the glass edge. It is possible that such very high peak pressures could produce tissue damage <u>per se</u> without inducing strains sufficient to pull the endothelial cells, lining vessels walls, apart. However, the leakages observed (Figure 7.16b) occurred only the edge of the occluded

zone where there was in one case no pressure, and in the other case 40mmHg. Since 40mmHg was found not to cause leakages from the vessels it is concluded that the postulated peak pressures did not produce any tissue damage, as evidenced by no leakages of FITC Dextran.

If the results of these experiments are to be sensibly construed with regard to the response of hypertrophic scar tissue to pressure, the experiments performed on the model should be representative of the manner in which pressure is applied to the scar by the elasticated pressure garments (vide 4.3.1.2).

Since the mechanical properties of the tissue, inter alia, affect pressure distributions variation of pressure over the skin surface produces pressure gradients on the skin surface, in addition to local constant pressures being applied (Figures 5.9, 5.10). Therefore it was thought that the experiments performed on the model were representative of the actual pressure applied by pressure garments.

In the clinical measurement situation, a pressure difference of 20 - 30mmHg occurred over a distance of about 10 - 20mm (Case study No. 6, Figure 5.8), which implies a pressure gradient of about 1 - 3mmHg/mm. At the site at which this pressure gradient was present, remodelling was achieved rapidly and the cosmetic result achieved was good. Satisfactory remodelling was, however, also achieved at other sites where the pressure gradient was very much lower, therefore, remodelling would seem to be due to a combination of normal pressures and pressure gradients. It is difficult to assess the relative influence of normal pressure and pressure gradients on the microcirculation of scar tissue, although the results of this chapter tend to indicate that pressure gradient is predominant.

Furthermore, as the average values of pressure measured beneath the garment were, in general, less than 25 - 30mmHg it seems likely that pressure garments do not have a

direct and significant effect on the microcirculation. Therefore the hypothesis that hypertrophic scar remodelling is achieved as a direct result of a microcirculation leading to ischaemic necrosis is thought unlikely to be correct.

7.6. SUMMARY

Vital microscopy was selected as the most suitable technique with which to assess the response of the microcirculation to local applied pressure. It was not possible to investigate the response of hypertrophic scar microcirculation to pressure due to limitations of the available instrumentation. A hamster cheek pouch model was used to investigate the response of the microcirculation to normal pressure levels found to induce hypertrophic scar remodelling and to other pressure distributions.

Pressures were applied to the cheek pouch by a column of water via an inflated rubber membrane. A fluorescent dye, FITC Dextran was infused into the hamster's circulation prior to the application of pressure and recordings of the microvascular response were made on black and white Polaroid film.

The microvascular response to the following applied pressure distributions was investigated:

(i) 40mmHg applied for 20 minutes and 40 minutes respectively,

(ii) 400mmHg uniform pressure applied for ≃ 15 minutes,

(iii) 20mmHg and 40mmHg uniform pressure applied for 20 minutes respectively, to a 'discontinuity', to provide non-uniform pressure distributions.

The results of investigations (i) and (ii) indicated that normal flow was nearly always re-established within 30 minutes post release of pressure, and that no apparent microvascular damage was present, judged by the absence of FITC Dextran in the extravascular compartment.

The results of investigation (iii), in contrast to (i) and (ii) demonstrated significant damage to the microvascular system occured in the region where the

pressure gradient was greatest, i.e., at the edge of the discontinuity, as evidenced by the leakage of FITC Dextran into the extravascular compartment at several locations thereat. In addition normal flow was not re-established at 30 mins. post-release of pressure and hyperaemia and inflammatory response were also observed.

Uniformly applied pressures of 30-40mmHg for 20 mins. produced pressure gradients which caused significantly more damage to the microcirculation than was achieved by the application of average pressures of an order of magnitude greater for an equivalent time, and longer.

Pressure magnitudes which induced scar remodelling, 20mmHg-40mmHg, did not produce any damage to the microcirculation, as evidenced by no FITC Dextran leakages. The hypothesis that remodelling occurs due to pressure-induced ischaemic necrosis is thought not to be correct.

CHAPTER 8

SYNOPSIS

The investigation reported in this thesis has been presented as a natural progression of activities. At various stages, arguments were developed and conclusions reached on which were based the continuing experimental design. Following each stage of the investigation the significance of the results was discussed. It now remains to evaluate the level of achievement in relation to the initial objectives.

I set out with three objectives:

(i) To develop and construct an instrumentation system to obtain quantitative values of the magnitude of pressure at the scar/dressing interface.

(ii) To investigate the relationship between pressure magnitude, duration of pressure and the scar remodelling results, and

(iii) To investigate the nature of remodelling mechanism induced by the effect of mechanical pressure on scar tissue.

The design criteria for an interface pressure sensor is described in section 4.2 and the selection of the parallel-plate capacitive transducer is discussed in section 4.3. The construction and design of signal recovery and processing circuitry is discussed in section 4.6. The thin, flexible capacitive pressure transducer is the sensor of choice, it produces minimal pertubation of the measurement site due to its high 'aspect ratio' and its small sensing area permits high spatial resolution. The complete system offers portability together with the advantages of high accuracy. My interpretation of the results of the laboratory experiments and evaluation of the transducer were subsequently confirmed by the results of the clinical investigations. The response of the transducer to physical parameters other than pressure was found to be small, except in the case of curvature, sensitivity to which is an intrinsic physical property of this type of transducer. A technique of recording pressures at the scar/pressure garment interface was developed. Typical signals are illustrated in Chapter 5.

Pressures developed at the scar or skin/pressure garment interface were found to be dependent on the mechanical properties of the underlying tissue, on the radius of curvature at the location of the transducer and on the elastic properties of the pressure garment.

The pressure magnitudes and duration of pressures found to induce remodelling are described in section 5.5 and

section 6.5.3.

Both Tubigrip and Lycra garments accelerated scar remodelling; Tubigrip however maintained its initial pressures, when first fitted, for a longer time and was considerably cheaper.

The requirements of the first two objectives are therefore satisfied.

A review of the literature revealed two salient hypotheses for the pressure-induced remodelling mechanism; one hypothesis stated that pressure-induced remodelling occurred by ischaemic necrosis, however in view of the results of Chapter 7 this hypothesis was thought unlikely to be correct. The other hypothesis that pressure reduces the blood supply to the scar such that the collagen biosynthesis-degradation balance was shifted in favour of the latter, implying removal of accumulation of collagen and consequently scar remodelling, is thought more likely to be correct.

I cannot state that the second hypothesis is correct as other factors may be implicated as discussed in section 6.5.3. The complexity of the pressure-induced remodelling mechanism is described.

It is also clear that an assay of collagen biosynthesis in pressure-treated scars could prove a useful index of determining whether permanent scar remodelling had occurred.

The need for further investigation, particularly of the relationship of the vascular response of the scar and the collagen biosynthesis response to pressure <u>in-vivo</u> is clearly indicated.

Further studies are presently being carried out using oxygen-sensitive microelectrodes to correlate pO_2 tensions with pressure magnitudes in pressure-treated and untreated scars to provide fuller understanding of the remodelling mechanism.

The investigations of the remodelling mechanism included in this thesis may lead to understanding of the mechanism of hypertrophy, which has considerable prophylatic implications. In addition, the investigations described in Chapter 7 provide further knowledge of tissue behaviour in response to non-uniform pressure distributions.

BIBLIOGRAPHY

BARBENEL, J.C. (1978)
Research, development and evaluation on improved hospital bed support surfaces and materials. First Annual Report to Scottish Home and Health Department, University of Strathclyde, Glasgow

BARBENEL, J.C., Turnbull, F.W. and Nisbet, R.M. (1979)
Backscattering of light by red cell suspensions. Med. Biol. Eng. & Comp: 17: 763 - 768

BAUR, P.S., Larson, D.L. and Stacey, T.R. (1975)
The observations of myofibroblasts in hypertrophic scars. Surg. Gynec. and Obstet. 141: 22 - 26

BAUR, P.S., Larson, D.L., Stacey, T.R., Barrat, G.F., Dobrkovsky, M. (1976)
Ultrastructural analysis of pressure treated human hypertrophic scars. J. Trauma 16: 958 - 967

BAZIN, S., Nicoletis, C., Delbet, J.P., Delauney, A. (1970)
Comparitive study of water, collagen and mucopolysaccharide content of normal human skin and of normal and keloid scar tissue. C.R. Acad. Sci. (Paris) 270: 1532

BAZIN, S., Bailey, A.J., Nicoletis, C., Delauney, A. (1975)
Biochemical composition and molecular structure of the intercellular matrix in human hypertrophic scars. International Plastic Surg. Congress

BED Sore Biomechanics (1976)
Eds. R.M. Kenedi, J.M. Cowden and J.T. Scales
Pub. London MacMillan

BHANGOO, K.S., Quinlivian, J.K., Connelly, J.R. (1976)
Elastin fibres in scar tissue. Plast. Reconst. Surg. 57: 308 - 313

BIOMECHANICAL Research and Development Unit (1977)
Effect of continuous pneumatic pressure on lymphoedema. Internal Report, Queen Mary's College, Roehampton, London.

BLACKBURN, W.R. and Cosman, B. (1966)
Histologic basis of keloid and hypertrophic scar differentiation. Arch. Path 82: 65 - 71

BLAIR, V.P. (1924)
The influence of mechanical pressure on would healing. Ill. Med. J., 46: 249 - 252

BLOOM, W. and Fawcett, D.W. (1969)
A textbook of histology. Pub. Saunders 9th Edn.

BRÅNEMARK, P.I., Ekholm, R., and Lindhe, J. (1968)
Colloidal carbon used for identification of vascular permeability. Med. Exp. 18: 139 - 150

BRÅNEMARK, P.I. (1971)
Intravascular anatomy of blood cells in man.
Pub. Basle. Karger.

BROWN, I.A. (1971)
Structural aspects of the biomechanical properties of human skin. Ph.D. Thesis University of Strathclyde, Glasgow.

CAMPION, E.C., Hoffman, D.C. and Jepson, R.P. (1968)
Australia and New Zealand Journal of Surgery
38: 154

CHOW, W.W., Juvinell, R.C., and Cockrell, J.L. (1976)
Effects and characteristics of cushion covering membranes. In "Bed Sore Biomechanics" Eds. R.M. Kenedi, J.M. Cowden, and J.T. Scales. Pub. London. MacMillan: 301 - 310

COHEN, I.K., Keiser, H.R. and Sjoerdsma, A. (1971)
Collagen synthesis in human keloid and hypertrophic scar. Surg. Forum. 22: 488

CRAIG, R.D.P., and Schofield, J.D. (c. 1973)
The role of mucopolysaccharides in scar tissue.
Internal Report, University Hospital of South Manchester, U.K.

CRAIG, R.D.P., Schofield, J.D., and Jackson, D.S. (1975a)
Collagen biosynthesis in normal human skin, normal and hypertrophic scar and keloid, Europ. J. Clin. Invest. 5: 69 - 74

CRAIG, R.D.P., Schofield, J.D. and Jackson, D.S. (1975b)
Collagen biosynthesis in normal and hypertrophic scars and keloid as a function of the duration of the scar. Brit. J. Surg. 62: 741 - 744

CRONIN, T.D. (1961)
The use of a moulded splint to prevent contracture after split-skin grafting on the neck. Plast. Reconst. Surg. 27: 7 - 18

DALY, C.H. (1968)
Viscoelastic properties of human skin in-vivo.
21st Annual Conference on Engineering in Medicine and Biology

DALY, C.H., Chimoskey, J.E., Holloway, G.A. et al (1976)
The effect of pressure loading on the blood flow rate in human skin. In "Bed Sore Biomechanics" Eds. R.M. Kenedi, J.M. Cowden and J.T. Scales. Pub. London MacMillan, 69 - 77

DE BRUYNE, P., and Dvořak, T. (1976)
The pressure exerted by an elastic stocking and its measurement. Med. Biol. Eng. Jan: 94 - 96

DIANA, J.N. and Laughlin, M.H. (1974)
Effect of ischaemia on capillary pressure and equivalent pore radius in capillaries of the isolated dog hind limb. Circulat. Res. 35: 77 - 101

DIEGELMANN, R.F., Rothkopf, L.C. and Cohen, I.K. (1975)
Measurement of collagen biosynthesis during would healing. J. Surg. Res. 19: 238 - 243

DINSDALE, S.M. (1974)
Decubitus ulcers: Role of pressure and friction in causation. Arch. Phys. Med. 55: 147 - 152

EISEN, A.Z., Bauer, E.A. and Jeffrey, J.J. (1971)
Human skin collagenase. The role of serum alpha-globulins in the control activity in-vivo and in-vitro. Proc. Nat. Acad. Sci. 68: 248 - 251

FERGUSON-PELL, M. (1977)
Critical assessment of the effects of pressure with special reference to the development of pressure sores. Ph.D. Thesis, University of Strathclyde, Glasgow.

FERNIE, G.R. (1973)
Biomechanical aspects of the aetiology of decubitus ulcers on human patients. Ph.D. Thesis, University of Strathclyde, Glasgow.

FRANK, W.E. and Gibson, R.J. (1954)
A new pressure-sensing instrument. J. Franklin Institute. 258: 21 - 30

FUJIMORI, R., Hiramoto, M. and Ofuji, S., (1968)
Sponge fixation method for the treatment of early scars. Plast. Reconst. Surg. 42: 322 - 327

GABBIANI, G., and Majno, G. (1971)
Dupuytrens Contracture: Fibroblast Contraction? Am. J. Path. 66: 131 - 146

GARDNER, W.J. (1966)
Circumferential pneumatic compression effect of the "G-Splint" on blood flow.
J.A.M.A.. 196: 491 - 493

GUTTMAN, L., (1976)
The prevention and treatment of pressure sores. In "Bed Sore Biomechanics" Eds. R.M. Kenedi, J.M., Cowden and J.T. Scales Pub. London. MacMillan

HICKMAN, K.E. (1965)
Rheological behaviour of tissues subjected to external pressure. Ph.D. Thesis, Western Reserve University Medical School, Cleveland, Ohio.

HICKMAN, K.E., Lindan, O., Reswick, J.B., Scanlam, R.H., (1966)
Deformation and flow in compressed skin tissues. Proc. Symp. Bio-Mech. Fluid. Mech. A.S.M.E.: 127:

HUSAIN, T. (1953)
Experimental study of some pressure effects on tissue with respect to the bedsore problem. J. Path. Bact. 66: 347 - 358

HUTTON, J.J. Jnr., Tappel, A.L., and Udenfriend, S. (1966)
Requirements for alpha-ketoglutarate, ferrous iron and ascorbate by collagen proline hydroxylase. Biochem., Biophys. Res. Commun 24: 179

JEFFREY, J.J., Eisen, A.Z. and Fleckmann, P.H. (1973)
A sensitive microassay for prolyl hydroxylase activity in normal and psoriatic skin. J. Invest. Derm. 60: 46

KARPF, M., Stock, W., Gebert, E., Kruse,Jaires (J.D.) and Zimmermann, W. (1974)
Stoffwechselveranderungen und restitution nach temporaer tourniquet - ischamie beim menschen. Langenbeeks Arch. Chir. Suppl. Chir. Forum.

KENEDI, R.M., Gibson, T., Evans, J.H. and Barbenal, J.C. (1975)
Tissue mechanics (Review Article) Phys. Med. Biol. 20: 699 - 717

KISCHER, C.W. and Bailley, J.F. (1972)
The mast cell in hypertrophic scars. Tex. Rpts. Biol. Med. 30: 327 - 338

KISCHER, C.W. (1975a)
Predictability of resolution of hypertrophic scars by S.E.M. J. Trauma 13: 205 - 208

KISCHER, C.W. (1975b)
Alteration of hypertrophic scars induced by mechanical pressure. Arch. Dermat 111: 60 - 64

KOSIAK, M. (1959)
Etiology and pathology of ischaemic ulcers Arch. Phys. Med. Rehad. 40: 62 - 69

KRISTENSEN, J.K., and Wadskove, S. (1977)
Studies of ^{133}Xe wash-out from normal human skin: quantitative measurements of blood in normal and corticosteriod-treated skin. J. Invest. Derm. 68: 196 - 200.

KROGH, A. (1929)
The anatomy and physiology of capillaries. Revised Edition. New Haven.

LANDAU, J.V. and McAlear, J.H. (1961)
The micromorphology of Fl and primary human amniotic cells following exposure to high hydrostatic pressure. Can. Res. 21: 812 - 814

LANDIS, E.M. (1930)
Micro-injection studies of capillary blood pressure in human skin. Heart 15: 209 - 228

LAPPE ET AL (1975)
Measurement of cutaneous blood flow by laser doppler. Circulation Res. Reported in Session B Discussion "Bed Sore Biomechanics" Eds. R.M. Kenedi, J.M. Cowden, and J.T. Scales, Pub. London, MacMillan.

LARSON, D.L. (1978)
Personal Communication. Shriners Burns Institute Galveston, Texas.

LARSON, D.L., Abston, S.,Evans, E.B., Dobrkovsky, M., and Linares, H.A. (1971)
Techniques for decreasing scar formation and contractures in the burned patient. J. Trauma 11: 807 - 823

LARSON, D.L., Linares, H.A., Baur, P., Willis, B., Abston, S. and Lewis, S.R. (1974)
Pathological aspects of skin healing in burns, International Symposum on Wound Healing. Amsterdam. Pub. Montreaux: Foundation International Cooperation in Medical Sciences.

LARSSON, J., and Risberg, B. (1977)
Fibrinolytic activity in human legs in tourniquet ischaemia. J. Throm. Res.

LAURITZEN, K. (1978)
Personal Communication, laboratory of experimental biology. Department of Anatomy, University of Göteborg, Sweden.

LEAF, A. (1973)
Cell swelling. A factor in Ischaemic Tissue Injury, Circulation 48: 455 - 458

LEWIS, D.W. and Nourse, N.B. (1978)
A device designed to approximate shear forces on human skin (a preliminary study) Bull. Pros. Res. (Aug. - Sept.): 36 - 46

LINARES, H.A., Kischer, C.W., Dobrkovsky, M. and Larson, D.K. (1972)
The histotypic organisation of the hypertrophic scar in humans. J. Invest. Dermat 59: 4, 323 - 331

LINARES, H.A. (1973)
On the origin of the hypertrophic scar. J. Trauma 13: 70 - 75

LINARES, H.A. and Larson, D.L. (1974)
Elastic tissue and hypertrophic scars. In 4th International Congress on Burn Injuries. Bueno Aires, Argentina.

LUTZ, B.R., Fulton, G.P. and Akers, R.P. (1951)
White thromboembolism in the hamster cheek pouch after trauma, infection and neoplasia. Circulation 3: 339 - 351

MADDEN, J.W. and Peacock, E.E. Jr. (1968)
Studies on the biology of collagen during wound healing. 1. Rate of Collagen Synthesis and Deposition in Cutaneous Wounds of the Rat. Surgery 64: 288 - 294

MADDEN, J.W., Norton, D. and Peacock, E.E. (1974)
Contraction of experimental wounds. I, Inhibiting Wound Contraction by using a Topical Smooth Muscle Antagonist. Surgery 76: 8 - 15

MAJNO, G., Gabbiani, G. and Hirshel, B.J. (1971)
Contraction of granulation tissue in-vitro; similarity to smooth muscle, Science 173: 548

MANCINI, R.E. and Quaife, J.V. (1961)
Histogenesis of experimentally produced keloids. J. Invest. Derm. 38: 143 - 150

MEDICAL Research Council Annual Report (1977)
A report submitted to the Secretary of State for Education and Science on Activities from 1st April, 1976 to 31st March, 1977.

MILSOM, J.P. and Craig, R.P.D. (1973)
Collagen degradation in cultured keloid and hypertrophic scar tissue. Brit. J. Derm. 89: 635

MOWLEM, R (1951)
Hypertrophic scars, British J. Plast. Surg. 4: 113 - 120

MUREN, A., and Zederfeldt, B. (1966)
Delayed effect of denervation on the healing of superficial skin defects in rabbits. Acta. Chir. Scand. 132: 618 - 620

MUSSINI, E., Hutton, J.J. and Udenfriend, S. (1967)
Collagen proline hydroxylase in wound healing. Granuloma Formation, Scurvy and Growth. Science 157: 927

NACHEMSON, A.L. and Evans, J.H. (1968)
Some mechanical properties of the third human lumbar interlaminar ligament (Ligamentam Flavum) J. Biomechs. 52: 149 - 156

NAISMITH, R.S. and Evans, J.H. (1977)
Unpublished results: Study of the variation in thermal emissivity of hypertrophic scars and normal skin, University of Strathclyde, Glasgow.

NATIONAL Academy of Science Workshop.
Pressure and force measurement (1968). A report of a Workship Sponsored by the Committee on Proshtetics Research and Development, held at Veterans' Administration Prosthetic Centre, New York (May 27 - 29)

PEACOCK, E. and Van Winkle, W. (1976)
Wound repair. W.B. Saunders, New York.

PSILLAKIS, J.M. Francisco, B de J., Sugena, R.C., Mariana, U., and Spina, V. (1971)
Water and electrolyte content of normal skin normal and hypertrophic scars and keloid. Plast. Reconst. Surg. 47: 272 - 274

REICHEL, S. (1958)
Shearing force as a factor in decubitus ulcers in paraplegics J. Amer. Med. Ass. 166: 762

RESWICK, J.B. and Rodgers, J.E. (1976)
Experience at Rancho Los Amigos Hospital with devices and techniques to prevent pressure sores. In "Bed Sore Biomechanics" Eds. R.M. Kenedi, J.M., Cowden and J.T. Scales Pub. London. MacMillan

RITZMANN, S.E., Daniels, J.C., Larson, D.L. (1973)
Diagnostic interpretation of serum protein abnormalism in thermal burns. Am. J. Clin. Pathol. 60: 135 - 144

ROMANUS, E.M. (1977)
Microcirculatory reactions to local pressure induced ischaemia. Ph.D. Thesis, University of Goteborg, Sweden.

ROSS, R. (1969)
Wound healing. Sci. Am., 220: 40

ROY, C., and Brown, G. (1879 - 1880)
The blood pressure and its variations in the arterioles, capillaries and smaller veins. J. Physiol., London 2: 323 - 359

RUDD, T.N. (1962)
The pathogenesis of decubitus ulcers. J. Am. Geriat. soc. 10: 48 - 53

RYDEVIK, B. and Lundborg, G. (1977)
Permeability of intraneural microvessels and perineurium following actute, graded experimental nerve compression. Scand. J. Plast. Reconst. Surg. 11: 179 - 187

SABRI, S., Roberts, V.C. and Cotton, L.T. (1971)
Effects of externally applied pressure on the haemodynamics of the lower limb. Brit. Med. J. 3: 503 - 508

SACHS, M.L., Miller, M.E. and Williams, G.T. (1974)
An electropneumatic sensor for direct measurement of spot pressures between a soft surface in contact with a rigid or conforming surface. Proc. 27th A.C.E.M.B. 11: 90

SACHS, M.L. and Miller, M. (1976)
Contribution to session a discussion in "Bed Sore Biomechanics" Eds. R.M. Kenedi, J.M. Cowden, and J.T. Scales, Pub. London. MacMillan 33 - 34

SELYE, H. (1967)
Ischaemic neurosis: Prevention by stress. Science 156: 1262 - 1263

SEWELL, I.A. (1974)
Circulation in the tissues. In: "Scientific Foundations of Anaesthesia" Eds. C. Scuir and S. Feldman. Year Book of Medicine, 2nd Edition.

SHETLAR, M.R., Dobrkovsky, M., Linares, H., Villarante, V.R., Shetlar, C.L. and Larson, D.L. (1971)
The hypertrophic Scar: Glycoprotein and collagen components of burn scars. Proc. Soc. Exp. Biol. 138: 298 - 300

SHETLAR, M.R., Shetlar, C.L., Chein, S., Linares, H.A., and Larson, D.L. (1972)
The hypertrophic scar. Hexosamine containing components of burn scars. Proc. Soc. Exp. Biol. Med. 139: 544 - 547

SHETLAR, M.R., Shetlar, C.L. and Linares, H.A. (1977)
The hypertrophic scar: Location of glycosaminoglycans within scars. Burns 4: 14 - 19

SIGEL, B., Edelsten, A.L. and Savitch, L. (1973)
Compression of the deep venous system of the lower leg during inactive recumbency. Arch. Surg. 106: 38 - 43

SIGEL, B., Edelsten, A.L., Savitch, L., Hasty, J.H. and Felix, R. (1975)
Type of compression for reducing venous stasis. Arch. Surg. 110: 171 - 175

SJERSEN, P. (1961)
Blood flow in cutaneous tissue in main studied by washout of radioactive Xenon circulation. Res. 25: 215

SLOAN, D.F., Brown, R.D., Wells, C.H., Hutton, T.G. (1978)
Tissue gases in human hypertrophic burn scars. Plast. and Reconst. Surg. 61: 431 - 436

STROCK, P.E. and Majuo, G. (1969)
Vascular responses to experimental tourniquet ischaemia. Surg. Gynec. Obstet. 129: 309 - 318

TOLHURST, D.E. (1977)
Hypertrophic scarring prevented by pressure: a case report. Brit. J. Plast. Surg. 30: 218 - 219

TULLY, A.E., (1980)
Hypertrophic scar tissue. Ph.D. Thesis University of Strathclyde, Glasgow.

TURNBULL, F. (1977)
The optical measurement of blood content and blood oxygen saturation in superficial tissue. Ph.D. Thesis, University of Strathclyde, Glasgow.

UITTO, J. (1970)
A method for studying collagen biosynthesis in human skin biopsies in-vitro. Biochem. Biophys. Acta. 201: 438 - 445

WEBER, L., Meigel, N.N. and Spier, W. (1978)
Collagen polymorphism in human hypertrophic scars. Arch. Derm. Res. 261: 63 - 71

WHIMSTER, I.W. (1976)
The trophic effects of nerves on skin. Contribution to Session A Discussion. In "Bed Sore Biomechanics" Eds. R.M. Kenedi, J.M. Cowden, and J.T. Scales. Pub. London, MacMillan 31 - 33

APPENDIX A

This Appendix contains the theory for the derivation of capacitance Bridge sensitivity, and the circuit diagrams used for processing the transducer signal referred to in Chapter 4.

DERIVATION OF CAPACITANCE BRIDGE SENSITIVITY

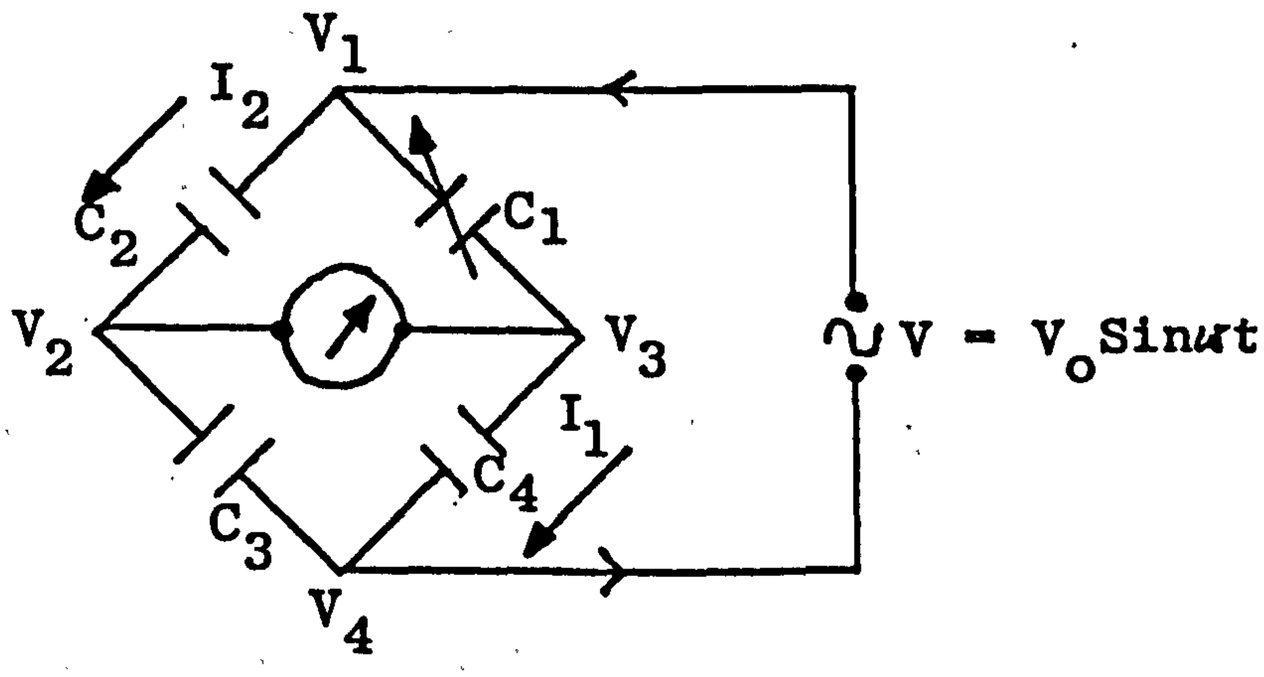

In the capacitance bridge represented above assume that an a.c. signal is applied to two arms of the bridge. Let the voltage of this signal be given by $V = V_o \sin\omega t$ where V_o is the peak to peak amplitude, ω the angular frequency of oscillation, and t time. I_1, I_2, I_3, I_4, represent the current flowing in the arms of the bridge. C_2, C_3, C_4, are the fixed capacitors in the bridge and C_1 the variable capacitance of the pressure transducer.

Applying the laws of Kirchoff:

$$V_1 - V_2 = \frac{I_2}{j\omega C_2} \qquad \ldots.(1)$$

$$V_1 - V_3 = \frac{I_1}{j\omega C_1} \qquad \ldots.(2)$$

$$V_2 - V_4 = \frac{I_2}{j\omega C_3} \qquad \ldots.(3)$$

$$V_3 - V_4 = \frac{I_1}{j\omega C_4} \qquad \ldots.(4)$$

Eliminating 1_1 (1) and (3)

$$(V_1 - V_2) = (V_2 - V_4)\, C_3$$

$$(V_1 - V_3)\, C_1 = (V_3 - V_4)\, C_4$$

Note that j and ω cancel, implying frequency independence and no phase changes with changes in C_1.

$$\text{Hence } V_1 = \frac{V_2\,(C_3 + C_2) - V_4 C_3}{C_2} \qquad \ldots.(5)$$

$$\text{and } V_1 = \frac{V_3\,(C_4 + C_1) - V_4 C_4}{C_1} \qquad \ldots.(6)$$

$$\text{but } V_1 - V_4 = V = V_o \sin\omega t \qquad \ldots.(7)$$

substitute (7) into (5) and (6)

$$V + V_4 = \frac{V_2(C_3 + C_2) - V_4 C_3}{C_2}$$

$$\text{and } V + V_4 = \frac{V_3(C_4 + C_1) - C_4 V_4}{C_1}$$

rearranging

$$V_4 = \frac{V_2(C_3 + C_2) - C_2 V}{C_3 + C_2} \qquad \ldots.(8)$$

$$\text{and} \qquad V_4 = \frac{V_3(C_4 + C_1) - C_1 V}{C_4 + C_1} \qquad \ldots.(9)$$

Eliminating V_4

$$V_3(C_4 + C_1)(C_3+C_2) - C_1(C_3+ C_2)V = V_2(C_3+C_2)(C_4+ C_1) - C_2(C_4+ C_1)V$$

$$V_3 - V_2 = \frac{V(C_1(C_3 + C_2) - C_2(C_4+ C_1))}{(C_4 + C_1)\ (C_3 + C_2)}$$

$$V_3 - V_2 = \frac{V(C_1C_3 - C_2C_4)}{(C_4 + C_1)\ (C_3 + C_2)} \qquad \ldots.(10)$$

If $C_3 = C_4 = C$

$$V_3 - V_4 = \text{OUTPUT} = \frac{VC(C_1 - C_2)}{(C + C_1)(C + C_2)} \quad \ldots\ldots(11)$$

If $C_1 = C_2$, $V_3 - V_2 = 0 = \text{BALANCE}$

For $C_1 \approx C_2$, let $C_1 - C_2 = \Delta C$ and let $C_1 \approx C$

$$\therefore V_1 - V_2 = \Delta V = \frac{V \Delta C}{4C}$$

$$\frac{\Delta V}{\Delta C} = \frac{V}{4C} \quad \ldots\ldots(12)$$

IF $C = 500$ pF

and if ΔC is $< 10\%$ of C

$$\text{then} \quad \frac{\Delta V}{\Delta C} = 0.5\text{mV/V/pF} \quad \ldots\ldots(13)$$

CIRCUIT DIAGRAM FOR PROCESSING THE TRANSDUCER SIGNAL

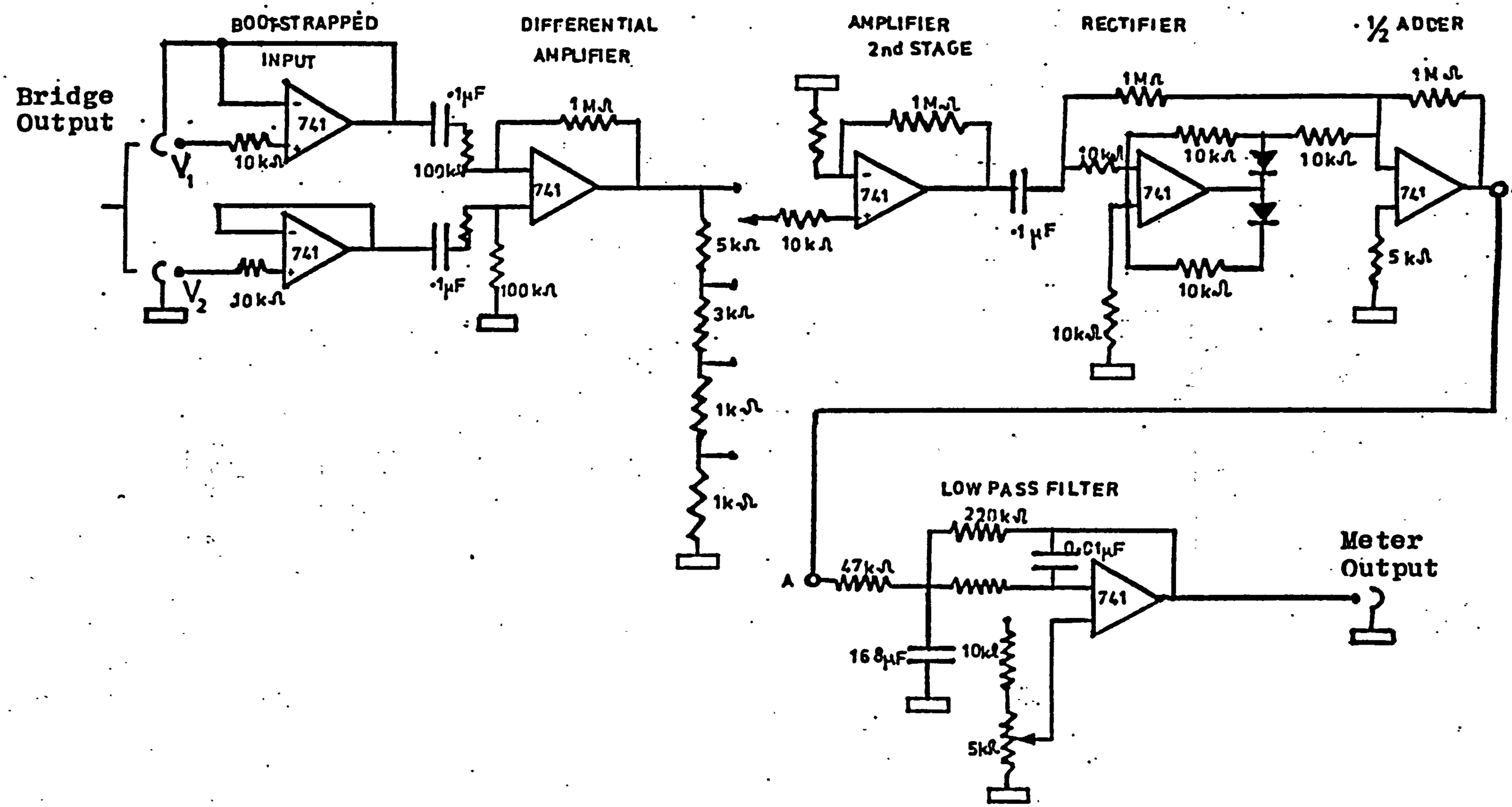

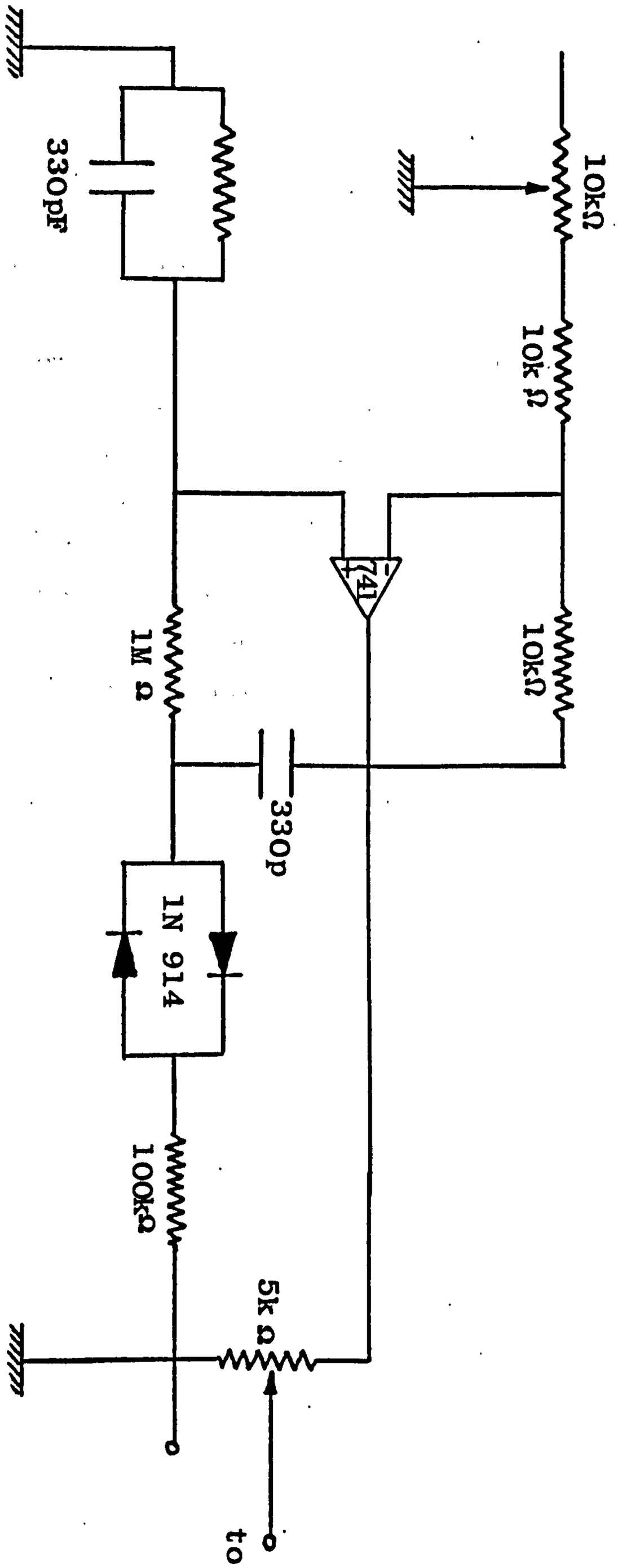

WEIN OSCILLATOR CIRCUIT DIAGRAM

APPENDIX B

This Appendix relates to Chapter 5 and contains the standard sheet used to record data; the results of load-strain mechanical tests carried out on used and unused Tubigrip and Lycra garments; a theoretical derivation of the pressures expected to be produced by Lycra and Tubigrip garments; and the results of a short study on the effect of water content of pressure-treated and untreated scar tissue.

It also contains tables of pressure measurements recorded at each measurement session of Cases No. 1,6 and 9.

PATIENT DATA SHEET

Patient: _____ Calibration Date: _____

Transducer No.	S.S.W. No.	Balance	Zero	Gain/ Range	Remarks	Meter
	1					
	2					
	3					
	4					
	5					
	CAL		CCW (O)	GIR.		

BATTERY: B^+ = V
B^- = V

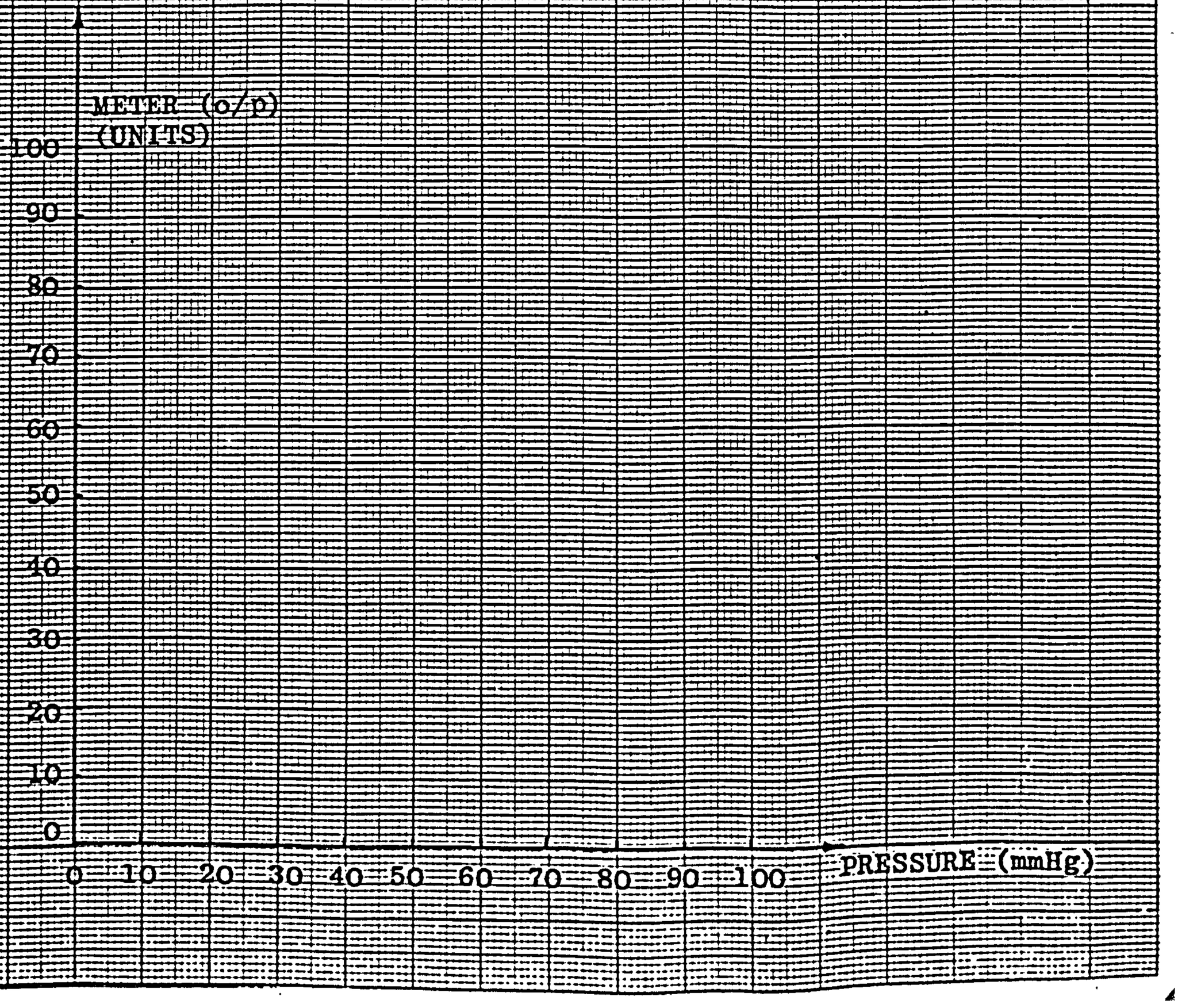

LOAD - STRAIN RESPONSE OF TUBIGRIP MATERIAL OF DIFFERENT SAMPLE WIDTHS

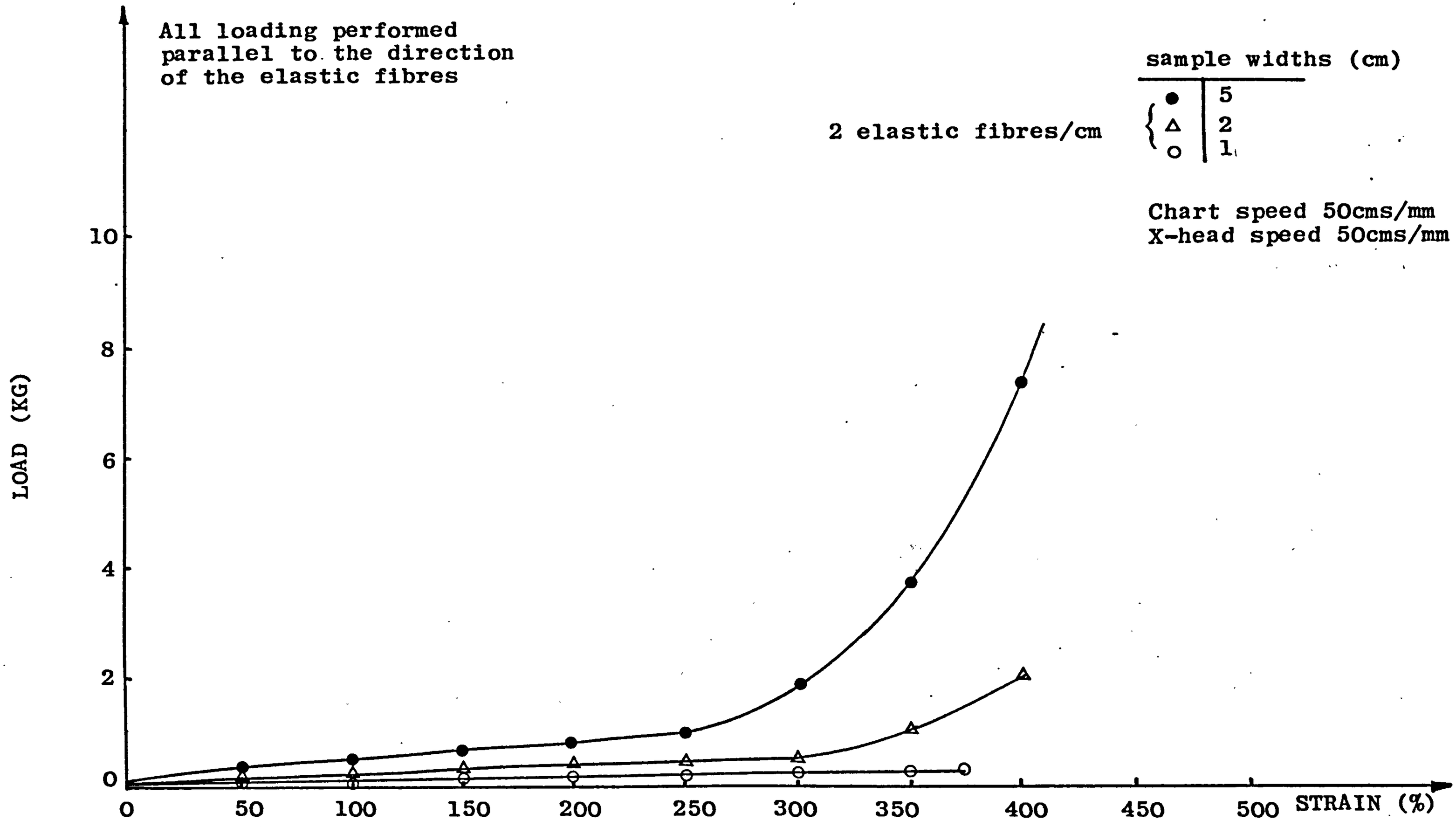

LOAD - STRAIN RESPONSE OF LYCRA MATERIAL OF DIFFERENT SAMPLE WIDTHS

Direction ↑	Direction ←
● used Lycra	▲ used Lycra
○ unused Lycra	△ unused Lycra

THEORETICAL DERIVATION OF PRESSURE DEVELOPED AT AN INTERFACE BETWEEN A SURFACE AND PRESSURE GARMENTS

Supposing that at a point x along the longitudinal axis of an arm, the radius of the arm at the point x is r, and that the arm is assumed to be circular at point x and to have no radius of curvature in the longitudinal direction. Therefore if a pressure garment having elastic properties is placed on the arm the component of force produced by the elastic tension in the garment acting normal to the surface of the arm at point x is given by

$$T_n = 2T\sin \alpha/2 \text{ (vide 4.3.1.4.)}$$

where T = circumferential elastic tension in the garment.

The radial pressure acting on a unit area

$$P_n = \frac{2T\sin(\alpha/2)}{r \cdot \alpha/2}$$

when α is small $\sin \alpha/2 \approx \alpha/2$

therefore $P_n = \frac{T}{r}$ B(1)

(De Bruyne, P., and Dvorak, T., 1978)

From the mechanical tests carried out it is possible to calculate the pressure developed at the scar/pressure garment interface.

Lycra Garments

a) Unused Garments

For a strain of 20% (which is common in practice) the load (in grams) is about 100gms. Since Lycra is stretched in two directions the load is effectively doubled to 200gms.

i.e. from equation B(1) the pressure applied to the unit area, P_n, is given by $\frac{200}{r}$ and if the radius of the

arm is taken as r,cms. then pressure

$$P_n = \frac{200}{5} = 40gm/cm^2$$

which is equivalent to 29.4mmHg.

b) · Used Lycra

After 3 weeks the garment tension is about 50gms for one direction of stretch only giving a pressure value of 14.7mmHg i.e. the pressure predicted from the mechanical tests would fall by about 50% after 3 weeks wear.

Tubigrip Garments

Unused Tubigrip

For a strain of 20% the load (in grams) is about 250gms. which, ,using equation B(1), gives a radial pressure of 36.7mmHg.

This rather crude calculation shows that Tubigrip with elastic properties in only one direction has a better capability than Lycra due to its inherent mechanical properties to produce greater radial pressures acting on a surface.

Used Tubigrip

No tests were performed on used Tubigrip samples

THE EFFECT OF PRESSURE ON THE WATER CONTENT OF SCAR TISSUE

Biopsies from pressure-treated and untreated scars were taken from the out-patient clinic under local anaesthetic. Biopsies were obtained using a Stiefel Biopsy punch technique (Tully, 1980)

The tissue was weighed immediately after removal and was vacuum desicated over $CaCO_3$ and the weight of tissue monitored frequently until a stable weight was recorded. The water content of each biopsy was expressed as a percentage of the weight of wet tissue.

12 samples were obtained from pressure-treated scars

and 10 samples from untreated scars.

The results are given as

% H_2O/wet weight tissue

Pressure Treated Scars	Untreated Scars
78.83	74.07
72.17	72.15
73.77	69.08
68.81	67.15
67.21	73.04
78.14	76.85
77.14	67.52
75.85	70.60
78.88	73.39
72.92	69.15
79.3	-
73.3	-
mean value 74.93	71.3
S.D. ± 4.17	± 3.319

The pressure treated and untreated scars were compared using Student's t-test and an F-test. There was no significant difference found between the results at the 95% confidence levels.

The results were also found not to be signifantly different for normal scars values of 72 - 80% H_2O/wet weight of tissue samples from 27 patients (Psillakis et al, 1971).

No relationship was found between pressure duration or pressure magnitude and % H_2O content in pressure treated scar tissue.

CASE STUDY NO. 1: PRESSURES MEASURED AT INTERFACE

Measurement Session No.	Week No	Interface Pressures Measured (mmHg)				
		Site 1	Site 2	Site 3	Site 4	Site 5
1	1	25	32	42	40	37
2	3	15	24	34	32	29
3	5	10	15	22	21	19
4	7*	6/28	9/34	16/41	15/41	12/38
5	10	16	22	32	31	30
6	12	13	14	22	22	20
7	14*	9/25	7/34	15/43	14/42	14/38
8	17	14	23	32	31	29
9	19	10	17	23	22	20
10	22*	5/27	12/32	16/45	15/43	14/40
11	23	20	22	34	32	31
12	25	15	16	25	24	22
13	28*	9/28	12/33	17/40	16/41	15/37
14	30	18	24	32	31	27
15	33	12	17	22	22	19
16	35*	9/26	12/30	15/44	15/42	13/39
17	37	20	24	34	32	30
18	40	13	18	24	22	19
19	42*	8/26	14/32	15/43	14/42	13/38
20	44	18	25	31	31	31
21	46	12	16	23	21	23
22	49*	4/25	12/31	14/42	13/41	16/40
23	51	19	21	33	32	32
24	54	11	15	23	22	20
25	56	8	10	15	14	14

* Denotes new Lycra garment fitted

CASE STUDY NO. 6: PRESSURES MEASURED AT INTERFACE

Measurement Session No. 1

Week 0 : New Lycra Garment Fitted

Distance From Cuff (inches)	Pressure Measured at Interface (mmHg)			
	Path 1	Path 2	Path 3	Path 4
0	13	14	12	9
1	36	41	18	17
2	30	38	22	22
3	28	33	20	19
4	14	25	17	18
6	22	32	21	18
8	19	10	41	27
10	23	20	32	26
12	22	24	19	16
14	18	20	15	9

Measurement Session No. 2

Week 2

Distance From Cuff (inches)	Pressure Measured at Interface (mmHg)			
	Path 1	Path 2	Path 3	Path 4
0	12	12	10	9
1	34	39	14	14
2	28	36	20	20
3	25	32	17	16
4	12	22	14	16
6	20	30	18	14
8	20	8	38	25
10	17	18	29	23
12	17	20	29	12
14	14	17	13	7

Measurement Session No. 3

Week 4

Distance From Cuff (inches)	Pressure Measured at Interface (mmHg)			
	Path 1	Path 2	Path 3	Path 4
0	11	10	8	8
1	20	19	10	11
2	16	17	10	13
3	15	16	11	13
4	14	15	12	13
6	12	17	13	11
8	7	7	17	14
10	15	13	13	13
12	14	14	9	9
14	7	12	9	7

Measurement Session No. 4

Week 7

Distance From Cuff (inches)	Pressure Measured at Interface (mmHg)			
	Path 1	Path 2	Path 3	Path 4
0	9	8	7	9
1	14	11	8	10
2	11	12	8	11
3	11	13	9	12
4	12	12	11	13
6	9	10	9	10
8	5	7	7	8
10	13	10	7	7
12	14	9	6	7
14	6	8	5	6

Measurement Session No. 5

Week 7: New Lycra Garment Fitted

Distance From Cuff (inches)	Pressure Measured at Interface (mmHg)			
	Path 1	Path 2	Path 3	Path 4
0	15	15	14	11
1	35	40	17	16
2	30	36	20	20
3	27	34	20	19
4	14	23	16	18
6	24	30	23	18
8	21	12	37	25
10	23	24	30	25
12	24	24	16	17
14	19	19	15	11

Measurement Session No. 6

Week 9:

Distance From Cuff (inches)	Pressure Measured at Interface (mmHg)			
	Path 1	Path 2	Path 3	Path 4
0	11	12	10	9
1	31	36	13	15
2	25	32	19	21
3	23	27	17	16
4	14	21	14	15
6	20	27	19	12
8	19	9	34	22
10	16	17	22	21
12	16	17	14	14
14	14	15	12	8

Measurement Session No. 7

Week 12

Distance From Cuff (inches)	Pressure Measured at Interface (mmHg)			
	Path 1	Path 2	Path 3	Path 4
0	11	9	7	7
1	16	17	10	12
2	13	18	12	12
3	12	14	10	10
4	16	13	11	12
6	13	15	10	9
8	10	7	15	8
10	13	11	12	7
12	13	10	8	7
14	9	10	7	6

Measurement Session No. 8

Week 14

Distance From Cuff (inches)	Pressure Measured at Interface (mmHg)			
	Path 1	Path 2	Path 3	Path 4
0	7	8	7	8
1	12	10	7	8
2	10	11	7	9
3	9	10	8	10
4	11	11	9	10
6	9	10	8	7
8	4	6	6	6
10	12	8	6	6
12	11	7	4	6
14	6	6	4	5

Measurement Session No. 9

Week 14: New Lycra Garment Fitted

Distance From Cuff (inches)	Pressure Measured at Interface (mmHg)			
	Path 1	Path 2	Path 3	Path 4
0	15	16	13	10
1	37	42	19	18
2	31	39	24	24
3	30	34	23	23
4	16	27	19	19
6	26	35	23	19
8	23	12	45	29
10	27	23	36	27
12	24	26	20	17
14	19	19	15	12

Measurement Session No. 10

Week 17

Distance From Cuff (inches)	Pressure Measured At Interface (mmHg)			
	Path 1	Path 2	Path 3	Path 4
0	12	11	11	9
1	30	30	14	13
2	26	26	16	17
3	13	15	16	17
4	20	19	13	14
6	19	22	19	14
8	21	10	32	20
10	15	16	24	18
12	13	17	15	15
14	15	14	12	11

Measurement Session No. 11

Week 20

Distance From Cuff (inches)	Pressure Measured at Interface (mmHg)			
	Path 1	Path 2	Path 3	Path 4
0	10	8	8	8
1	17	17	9	9
2	14	14	9	12
3	13	14	10	12
4	12	12	9	11
6	12	14	11	10
8	8	6	11	12
10	13	11	13	10
12	14	11	10	8
14	7	9	8	7

Measurement Session No. 12

Week 22

Distance From Cuff (inches)	Pressure Measured at Interface (mmHg)			
	Path 1	Path 2	Path 3	Path 4
0	9	8	7	8
1	12	10	8	9
2	10	11	8	10
3	10	10	8	11
4	10	10	9	11
6	9	8	7	10
8	5	7	6	7
10	11	10	6	6
12	11	9	6	6
14	6	7	5	5

Measurement Session No. 13

Week 22: New Lycra Garment Fitted

Distance From Cuff (inches)	Pressure Measured at Interface (mmHg)			
	Path 1	Path 2	Path 3	Path 4
0	14	14	12	10
1	35	40	17	16
2	29	37	23	24
3	27	30	20	20
4	13	23	18	19
6	27	30	20	21
8	24	12	40	26
10	24	22	35	26
12	22	23	21	18
14	18	19	16	10

Measurement Session No. 14

Week 24

Distance From Cuff (inches)	Pressure Measured at Interface (mmHg)			
	Path 1	Path 2	Path 3	Path 4
0	12	12	9	10
1	28	32	14	14
2	24	24	16	17
3	22	25	17	15
4	12	21	15	15
6	19	26	16	16
8	19	10	30	20
10	16	19	24	19
12	14	18	16	13
14	14	15	14	9

Measurement Session No. 15

Week 26

Distance From Cuff (inches)	Pressure Measured at Interface (mmHg)			
	Path 1	Path 2	Path 3	Path 4
0	10	10	9	9
1	19	17	11	12
2	15	16	10	12
3	14	15	11	13
4	14	16	13	14
6	11	12	16	11
8	6	8	12	15
10	12	13	10	12
12	11	13	10	8
14	7	11	9	9

Measurement Session No. 16

Week 29

Distance From Cuff (inches	Pressure Measured at Interface (mmHg)			
	Path 1	Path 2	Path 3	Path 4
0	9	8	8	8
1	13	10	8	11
2	10	10	9	11
3	9	10	9	9
4	9	9	10	10
6	8	9	8	10
8	6	8	6	7
10	9	9	7	6
12	7	9	6	6
14	6	7	6	6

Measurement Session No. 17

Week 29: New Lycra Garment Fitted

Distance From Cuff (inches)	Pressure Measured at Interface (mmHg)			
	Path 1	Path 2	Path 3	Path 4
0	13	13	11	10
1	34	37	17	16
2	27	34	23	20
3	25	30	21	19
4	14	22	17	17
6	22	30	22	17
8	21	11	36	26
10	24	22	30	25
12	22	26	20	16
14	19	21	16	10

Measurement Session No. 18

Week 32

Distance From Cuff (inches)	Pressure Measured at Interface (mmHg)			
	Path 1	Path 2	Path 3	Path 4
0	11	11	10	9
1	27	28	14	12
2	21	25	15	14
3	19	22	15	16
4	13	16	13	16
6	17	26	18	13
8	17	10	24	18
10	16	18	23	16
12	15	19	16	14
14	15	17	14	10

Measurement Session No. 19

Week 33

Distance From Cuff (inches)	Pressure Measured at Interface (mmHg)			
	Path 1	Path 2	Path 3	Path 4
0	10	9	8	9
1	20	16	11	12
2	15	14	12	13
3	15	13	12	13
4	13	14	14	12
6	13	16	12	11
8	9	10	14	13
10	14	14	17	14
12	14	13	13	10
14	10	11	10	9

Measurement Session No. 20

Week 36

Distance From Cuff (inches)	Pressure Measured at Interface (mmHg)			
	Path 1	Path 2	Path 3	Path 4
0	9	9	7	7
1	13	9	7	11
2	11	12	10	12
3	11	11	10	11
4	10	8	11	10
6	11	7	9	7
8	7	7	9	6
10	11	9	14	11
12	10	11	11	11
14	7	9	6	8

Measurement Session No. 21

Week 36: New Lycra Garment Fitted

Distance From Cuff (inches)	Pressure Measured at Interface (mmHg)			
	Path 1	Path 2	Path 3	Path 4
0	14	14	13	10
1	36	37	19	16
2	30	36	22	23
3	27	31	20	19
4	13	25	17	18
6	21	30	20	20
8	19	10	36	25
10	23	18	30	25
12	20	22	17	17
14	16	20	16	11

Measurement Session No. 22

Week 38

Distance From Cuff (inches)	Pressure Measured at Interface (mmHg)			
	Path 1	Path 2	Path 3	Path 4
0	12	13	11	10
1	33	35	15	13
2	25	33	20	21
3	11	31	16	15
4	23	22	13	16
6	21	28	17	13
8	16	8	36	22
10	16	17	25	21
12	15	21	15	14
14	14	16	12	10

Measurement Session No. 23

Week 40

Distance From Cuff (inches)	Pressure Measured at Interface (mmHg)			
	Path 1	Path 2	Path 3	Path 4
0	10	10	9	9
1	21	19	10	11
2	17	18	11	12
3	16	18	12	13
4	14	16	14	12
6	11	17	10	10
8	9	6	16	14
10	16	10	14	12
12	15	12	7	10
14	11	11	6	7

Measurement Session No. 24

Week 43

Distance From Cuff (inches)	Pressure Measured at Interface (mmHg)			
	Path 1	Path 2	Path 3	Path 4
0	8	9	8	8
1	13	10	8	9
2	12	11	9	9
3	11	13	10	10
4	11	12	11	11
6	8	10	9	9
8	7	6	8	10
10	6	9	10	9
12	10	9	8	7
14	7	8	6	7

Measurement Session No. 25

Week 43: New Lycra Garment Fitted

Distance From Cuff (inches)	Pressure Measured at Interface (mmHg)			
	Path 1	Path 2	Path 3	Path 4
0	14	15	13	11
1	36	38	16	15
2	28	35	19	19
3	26	34	20	19
4	13	22	15	17
6	25	29	22	17
8	22	11	35	24
10	24	24	28	25
12	23	23	15	17
14	18	18	14	11

Measurement Session No. 26

Week 46

Distance From Cuff (inches)	Pressure Measured at Interface (mmHg)			
	Path 1	Path 2	Path 3	Path 4
0	11	12	10	10
1	22	36	13	14
2	20	24	16	13
3	19	22	16	17
4	12	20	13	16
6	19	24	18	16
8	16	10	25	20
10	16	16	20	21
12	15	14	16	17
14	13	14	12	9

Measurement Session No. 27

Week 48

Distance From Cuff (inches)	Pressure Measured at Interface (mmHg)			
	Path 1	Path 2	Path 3	Path 4
0	10	10	8	9
1	16	17	11	12
2	14	18	12	12
3	14	15	10	11
4	10	13	10	10
6	13	14	10	10
8	10	9	14	9
10	13	11	13	10
12	12	10	13	11
14	9	11	10	9

Measurement Session No. 28

Week 50

Distance From Cuff (inches)	Pressure Measured at Interface (mmHg)			
	Path 1	Path 2	Path 3	Path 4
0	7	9	8	8
1	12	10	8	8
2	11	11	9	9
3	8	10	9	10
4	10	10	8	9
6	9	9	7	7
8	6	9	7	8
10	10	8	10	11
12	11	8	11	11
14	7	7	9	8

Measurement Session No. 29

Week 50: New Lycra Garment Fitted

Distance From Cuff (inches)	Pressure Measured at Interface (mmHg)			
	Path 1	Path 2	Path 3	Path 4
0	11	10	11	9
1	34	39	16	14
2	30	37	21	18
3	25	28	17	17
4	15	20	15	17
6	20	25	18	17
8	8	9	36	24
10	20	18	25	22
12	19	20	14	14
14	13	15	10	8

Measurement Session No. 30

Week 51

Distance From Cuff (inches)	Pressure Measured at Interface (mmHg)			
	Path 1	Path 2	Path 3	Path 4
0	11	10	10	8
1	32	35	15	13
2	28	31	19	16
3	23	26	16	15
4	14	18	14	15
6	18	22	16	22
8	8	9	30	20
10	19	16	23	19
12	16	17	12	12
14	12	13	9	8

Measurement Session No. 31

Week 52

Distance From Cuff (inches)	Pressure Measured at Interface (mmHg)			
	Path 1	Path 2	Path 3	Path 4
0	10	9	9	8
1	30	33	14	13
2	24	29	18	14
3	21	24	16	14
4	13	16	14	14
6	16	20	16	17
8	7	8	30	17
10	17	14	21	15
12	14	15	12	11
14	12	12	8	8

Measurement Session No. 32

Week 53

Distance From Cuff (inches)	Pressure Measured at Interface (mmHg)			
	Path 1	Path 2	Path 3	Path 4
0	10	9	9	8
1	28	30	12	12
2	22	26	14	14
3	19	15	15	13
4	12	19	14	14
6	14	19	12	15
8	7	8	24	15
10	14	13	18	13
12	12	13	11	11
14	11	11	8	9

Measurement Session No. 33

Week 54

Distance From Cuff (inches)	Pressure Measured at Interface (mmHg)			
	Path 1	Path 2	Path 3	Path 4
0	9	8	9	8
1	24	23	11	11
2	20	19	13	14
3	16	13	13	13
4	10	16	12	13
6	12	16	11	13
8	7	8	16	12
10	12	12	14	13
12	10	11	10	10
14	10	9	8	9

Measurement Session No. 34

Week 55

Distance From Cuff (inches)	Pressure Measured at Interface (mmHg)			
	Path 1	Path 2	Path 3	Path 4
0	8	7	8	7
1	16	15	9	9
2	13	15	11	12
3	10	12	11	11
4	9	13	10	11
6	11	11	10	11
8	7	12	11	10
10	12	8	12	10
12	9	11	10	9
14	9	8	7	8

Measurement Session No. 35

Week 56

Distance From Cuff (inches)	Pressure Measured at Interface (mmHg)			
	Path 1	Path 2	Path 3	Path 4
0	8	9	8	7
1	11	11	8	8
2	12	10	10	9
3	10	9	10	9
4	8	11	7	9
6	9	11	8	8
8	7	10	11	8
10	9	8	10	7
12	8	9	9	8
14	7	8	7	6

Measurement Session No. 36

Week 56: New Lycra Garment Fitted

Distance From Cuff (inches)	Pressure Measured at Interface (mmHg)			
	Path 1	Path 2	Path 3	Path 4
0	16	14	14	12
1	37	41	19	17
2	30	37	22	22
3	29	34	23	20
4	13	24	18	19
6	25	30	24	19
8	22	14	37	26
10	22	24	31	26
12	25	25	17	20
14	19	20	16	13

Measurement Session No. 37

Week 59

Distance From Cuff (inches)	Pressure Measured at Interface (mmHg)			
	Path 1	Path 2	Path 3	Path 4
0	12	11	12	10
1	29	29	14	13
2	24	26	15	16
3	11	16	16	14
4	12	17	12	13
6	19	21	16	14
8	16	12	26	18
10	17	16	22	18
12	14	16	14	15
14	14	14	13	11

Measurement Session No. 38

Week 61

Distance From Cuff (inches)	Pressure Measured at Interface (mmHg)			
	Path 1	Path 2	Path 3	Path 4
0	10	9	9	8
1	17	16	12	10
2	15	13	12	11
3	9	11	13	11
4	10	11	9	10
6	13	12	11	10
8	10	8	14	13
10	13	13	13	12
12	11	13	10	9
14	8	11	9	8

Measurement Session No. 39

Week 64

Distance From Cuff (inches)	Pressure Measured at Interface (mmHg)			
	Path 1	Path 2	Path 3	Path 4
0	9	7	7	7
1	12	11	6	6
2	11	9	6	7
3	8	9	7	8
4	7	8	5	8
6	8	6	7	7
8	7	4	8	8
10	6	7	7	8
12	7	7	6	6
14	4	6	5	5

Measurement Session No. 40

Week 64 New Lycra Garment Fitted

Distance From Cuff (inches)	Pressure Measured at Interface (mmHg)			
	Path 1	Path 2	Path 3	Path 4
0	14	14	13	10
1	35	41	17	17
2	29	36	23	22
3	26	31	21	19
4	13	24	18	22
6	26	31	21	20
8	24	13	38	27
10	24	23	36	27
12	23	23	20	19
14	19	19	17	12

Measurement Session No. 41

Week 68

Distance From Cuff (inches)	Pressure Measured at Interface (mmHg)			
	Path 1	Path 2	Path 3	Path 4
0	10	29	10	10
1	11	10	9	9
2	20	17	11	11
3	16	15	10	11
4	12	14	10	12
6	14	15	14	14
8	10	10	12	10
10	12	14	10	14
12	11	15	11	10
14	7	12	9	8

Measurement Session No. 42

Week 71

Distance From Cuff (inches)	Pressure Measured at Interface (mmHg)			
	Path 1	Path 2	Path 3	Path 4
0	8	9	8	7
1	13	9	8	10
2	11	10	7	8
3	10	11	7	9
4	8	12	9	10
6	6	10	9	7
8	9	7	4	6
10	10	8	7	7
12	11	9	8	6
14	7	6	6	5

Measurement Session No. 43

Week 73

Distance From Cuff (inches)	Pressure Measured at Interface (mmHg)			
	Path 1	Path 2	Path 3	Path 4
0	6	6	7	6
1	7	7	6	6
2	6	3	6	6
3	6	3	6	8
4	5	4	5	7
6	5	7	7	5
8	5	6	3	5
10	4	7	6	5
12	5	6	5	6
14	4	5	5	4

Measurement Session No. 44

Week 73 New Lycra Garment Fitted

Distance From Cuff (inches)	Pressure Measured at Interface (mmHg)			
	Path 1	Path 2	Path 3	Path 4
0	14	14	12	10
1	35	39	17	16
2	29	36	23	23
3	29	33	22	21
4	14	24	17	20
6	21	32	20	17
8	19	10	37	28
10	22	20	31	27
12	22	23	19	18
14	18	20	16	12

Measurement Session No. 45

Week 76

Distance From Cuff (inches)	Pressure Measured at Interface (mmHg)			
	Path 1	Path 2	Path 3	Path 4
0	12	11	11	9
1	30	30	15	12
2	24	26	16	17
3	14	15	17	17
4	20	19	13	14
6	18	22	20	15
8	20	10	33	22
10	16	17	24	19
12	14	17	15	16
14	15	15	12	12

Measurement Session No. 46

Week 80

Distance From Cuff (inches)	Pressure Measured at Interface (mmHg)			
	Path 1	Path 2	Path 3	Path 4
0	8	8	7	8
1	9	9	8	9
2	9	7	8	10
3	7	6	8	9
4	6	6	9	11
6	6	7	6	9
8	5	4	6	6
10	7	7	6	7
12	6	6	5	6
14	6	6	5	6

Measurement Session No. 47

Week 80 New Lycra Garment Fitted

Distance From Cuff (inches)	Pressure Measured at Interface (mmHg)			
	Path 1	Path 2	Path 3	Path 4
0	14	14	13	9
1	38	40	19	18
2	28	37	23	21
3	25	31	19	20
4	15	26	18	18
6	23	32	22	18
8	17	11	42	26
10	25	21	30	25
12	22	23	18	16
14	18	20	16	10

Measurement Session No. 48

Week 84

Distance From Cuff (inches)	Pressure Measured at Interface (mmHg)			
	Path 1	Path 2	Path 3	Path 4
0	12	10	8	8
1	21	18	10	11
2	16	17	9	13
3	15	16	9	15
4	13	15	12	13
6	12	15	13	12
8	9	9	16	16
10	14	14	13	13
12	14	13	10	10
14	9	12	9	9

Measurement Session No. 49

Week 86

Distance From Cuff (inches)	Pressure Measured at Interface (mmHg)			
	Path 1	Path 2	Path 3	Path 4
0	9	8	8	9
1	14	11	8	10
2	11	12	9	11
3	10	12	9	11
4	11	10	10	12
6	9	8	9	9
8	6	7	7	8
10	11	9	7	7
12	10	9	6	7
14	8	8	5	6

Measurement Session No. 50

Week 88

Distance From Cuff (inches)	Pressure Measured at Interface (mmHg)			
	Path 1	Path 2	Path 3	Path 4
0	8	7	7	7
1	11	9	6	7
2	8	10	8	8
3	9	10	8	9
4	9	9	8	8
6	8	6	7	8
8	5	6	6	6
10	8	7	6	7
12	9	6	5	6
14	7	6	5	6

Measurement Session No. 51

Week 88: New Lycra Garment Fitted

Distance From Cuff (inches)	Pressure Measured at Interface (mmHg)			
	Path 1	Path 2	Path 3	Path 4
0	15	15	14	11
1	35	38	18	16
2	29	36	20	20
3	26	34	20	19
4	14	24	16	18
6	22	29	23	17
8	20	12	38	25
10	23	24	30	26
12	24	24	16	17
14	20	19	15	13

Measurement Session No. 52

Week 91

Distance From Cuff (inches)	Pressure Measured at Interface (mmHg)			
	Path 1	Path 2	Path 3	Path 4
0	12	11	11	9
1	28	31	14	13
2	24	25	15	15
3	12	16	15	16
4	20	18	13	16
6	19	21	19	12
8	19	9	28	12
10	16	16	21	19
12	14	16	16	15
14	13	13	12	11

Measurement Session No. 53

Week 94

Distance From Cuff (inches)	Pressure Measured at Interface (mmHg)			
	Path 1	Path 2	Path 3	Path 4
0	10	9	8	9
1	17	17	9	9
2	14	14	8	10
3	11	12	10	10
4	12	13	9	10
6	12	13	10	11
8	8	6	10	11
10	13	11	13	9
12	11	10	10	8
14	10	10	9	7

Measurement Session No. 54

Week 96

Distance From Cuff (inches)	Pressure Measured at Interface (mmHg)			
	Path 1	Path 2	Path 3	Path 4
0	9	8	7	7
1	12	9	8	8
2	11	10	7	8
3	10	10	8	7
4	10	10	8	7
6	9	8	7	8
8	5	7	8	7
10	10	10	6	6
12	9	8	7	6
14	6	8	6	7

Measurement Session No. 55

Week 96 New Lycra Garment Fitted

Distance From Cuff (inches)	Pressure Measured at Interface (mmHg)			
	Path 1	Path 2	Path 3	Path 4
0	14	14	13	10
1	34	38	18	16
2	29	35	22	24
3	26	30	20	20
4	14	23	19	19
6	28	29	21	20
8	25	13	38	26
10	25	23	35	26
12	23	23	23	18
14	19	19	17	10

Measurement Session No. 56

Week 99

Distance From Cuff (inches)	Pressure Measured at Interface (mmHg)			
	Path 1	Path 2	Path 3	Path 4
0	12	11	11	IO
1	29	31	13	13
2	23	24	14	15
3	11	17	15	17
4	20	17	13	17
6	18	20	18	14
8	17	10	26	18
10	16	16	22	16
12	15	16	17	15
14	13	14	13	9

Measurement Session No. 57

Week 102

Distance From Cuff (inches)	Pressure Measured at Interface (mmHg)			
	Path 1	Path 2	Path 3	Path 4
0	10	8	9	8
1	17	16	10	9
2	14	13	11	12
3	13	13	11	12
4	12	12	10	10
6	11	13	9	10
8	8	6	10	11
10	10	11	12	10
12	12	12	10	9
14	9	10	9	7

Measurement Session No. 58

Week 104

Distance From Cuff (inches)	Pressure Measured at Interface (mmHg)			
	Path 1	Path 2	Path 3	Path 4
0	9	7	8	7
1	12	12	7	7
2	11	10	10	9
3	9	10	10	10
4	8	9	9	8
6	9	10	8	7
8	86	5	9	7
10	8	8	10	6
12	7	9	8	8
14	7	7	6	6

Measurement Session No. 59

Week 104 New Lycra Garment Fitted

Distance From Cuff (inches)	Pressure Measured at Interface (mmHg)			
	Path 1	Path 2	Path 3	Path 4
0	14	16	13	13
1	37	44	19	19
2	31	41	24	25
3	30	36	23	22
4	16	28	20	21
6	24	33	26	23
8	22	15	45	30
10	25	24	37	29
12	22	28	24	21
14	18	22	17	17

Measurement Session No. 60

Week 107

Distance From Cuff (inches)	Pressure Measured at Interface (mmHg)			
	Path 1	Path 2	Path 3	Path 4
0	12	12	10	11
1	34	39	16	16
2	28	36	20	20
3	25	31	19	18
4	12	24	19	18
6	21	30	22	19
8	21	9	33	23
10	18	16	30	22
12	18	19	20	15
14	15	14	14	13

Measurement Session No. 61

Week 110

Distance From Cuff (inches)	Pressure Measured at Interface (mmHg)			
	Path 1	Path 2	Path 3	Path 4
0	9	10	8	10
1	16	17	11	14
2	13	16	13	15
3	13	14	14	14
4	12	13	14	14
6	10	11	16	15
8	8	8	15	16
10	12	11	12	15
12	14	15	11	11
14	10	11	10	9

CASE STUDY NO. 9: PRESSURE MEASURED AT INTERFACE

Measurement Session No. 1

Week No. 0: Lycra Garment

Distance From Proximal Cuff (inches)	Pressure measured on Pathways		
	Path 1	Path 2	Path 3
0	10	12	14
1	12	14	17
2	14	19	22
3	12	23	19
4	9	19	22
5	9	17	23
6	7	16	18
7	8	16	17
8	7	14	13
9	5	10	11

Measurement Session No. 2

Week 2

Distance From Proximal Cuff (inches)	Pressure measured on Pathways		
	Path 1	Path 2	Path 3
0	7	8	9
1	8	10	12
2	10	11	14
3	8	11	14
4	7	10	13
5	6	9	11
6	5	8	10
7	5	9	9
8	4	8	8
9	3	5	7

Measurement Session No. 3

Week 2: Tubigrip Garment Fitted

Distance from Proximal Cuff (inches)	Pressure measured on Pathways		
	Path 1	Path 2	Path 3
0	8	10	11
1	10	12	12
2	11	16	19
3	12	19	18
4	7	18	23
5	8	16	24
6	7	15	17
7	7	14	16
8	8	13	12
9	4	9	11

Measurement Session No. 4

Week 4

Distance from Proximal Cuff (inches)	Pressure measured on Pathways		
	Path 1	Path 2	Path 3
0	8	10	10
1	10	11	12
2	11	15	18
3	12	18	18
4	8	17	22
5	8	16	22
6	8	14	16
7	7	14	16
8	7	13	12
9	4	9	11

Measurement Session No. 5

Week 6

Distance from Proximal Cuff (inches)	Pressure measured on Pathways		
	Path 1	Path 2	Path 3
0	8	10	10
1	10	10	11
2	11	15	17
3	11	17	17
4	8	17	21
5	9	16	21
6	8	14	16
7	7	13	15
8	7	12	12
9	5	9	10

Measurement Session No. 6

Week 8

Distance from Proximal Cuff (inches)	Pressure measured on Pathways		
	Path 1	Path 2	Path 3
0	8	10	10
1	9	9	11
2	10	4	17
3	10	16	16
4	8	16	20
5	9	15	20
6	8	14	16
7	6	13	14
8	6	11	12
9	5	8	9

Measurement Session No. 7

Week 11

Distance from Proximal Cuff (inches)	Pressure measured on Pathways		
	Path 1	Path 2	Path 3
0	7	9	9
1	8	10	10
2	9	13	16
3	10	15	15
4	9	15	18
5	7	14	18
6	8	13	14
7	5	11	13
8	4	9	11
9	4	6	7

Measurement Session No. 8

Week 14

Distance from Proximal Cuff (inches)	Pressure measured on Pathways		
	Path 1	Path 2	Path 3
0	5	9	8
1	7	9	9
2	8	12	14
3	9	14	14
4	8	14	15
5	7	13	16
6	7	10	13
7	4	9	11
8	4	7	9
9	4	4	5

Measurement Session No. 9

Week 15: New Tubigrip Garment Fitted

Distance from Proximal Cuff (inches)	Pressure measured on Pathways		
	Path 1	Path 2	Path 3
0	9	12	11
1	11	14	12
2	13	16	18
3	12	19	23
4	9	18	25
5	10	17	18
6	11	16	17
7	10	15	16
8	9	13	13
9	7	11	12

Measurement Session No. 10

Week 16

Distance from Proximal Cuff (inches)	Pressure measured at Pathways		
	Path 1	Path 2	Path 3
0	8	12	10
1	10	13	11
2	11	15	17
3	9	17	22
4	9	17	23
5	9	15	18
6	10	14	16
7	9	13	16
8	8	12	13
9	6	11	11

Measurement Session No. 11

Week 17

Distance from Proximal Cuff (inches)	Pressure measured on Pathways		
	Path 1	Path 2	Path 3
0	8	13	11
1	11	14	12
2	11	15	18
3	10	18	22
4	8	17	23
5	9	16	16
6	9	15	17
7	10	14	15
8	9	14	13
9	6	10	10

Measurement Session No. 12

Week 18

Distance from Proximal Cuff (inches)	Pressure measured on Pathways		
	Path 1	Path 2	Path 3
0	8	12	10
1	10	13	12
2	11	13	17
3	9	16	21
4	9	16	22
5	9	15	16
6	10	14	16
7	9	14	14
8	8	13	13
9	6	10	9

Measurement Session No. 13

Week 20

Distance from Proximal Cuff (inches)	Pressure measured on Pathways		
	Path 1	Path 2	Path 3
0	8	11	10
1	10	12	11
2	9	12	16
3	8	15	20
4	9	15	21
5	8	15	16
6	9	13	15
7	8	13	13
8	7	12	12
9	6	10	8

Measurement Session No. 14

Week 21

Distance from Proximal Cuff (inches)	Pressure measured on Pathways		
	Path 1	Path 2	Path 3
0	8	10	10
1	9	12	10
2	8	11	16
3	9	14	20
4	8	15	20
5	8	15	16
6	8	14	14
7	7	13	13
8	7	12	11
9	6	10	8

Measurement Session No. 15

Week 22

Distance from Proximal Cuff (inches)	Pressure measured on Pathways		
	Path 1	Path 2	Path 3
0	8	10	10
1	8	11	11
2	8	11	15
3	9	14	19
4	8	15	20
5	8	14	16
6	7	15	15
7	8	13	13
8	6	11	11
9	6	10	8

Measurement Session No. 16

Week 23

Distance from Proximal Cuff (inches)	Pressure measured on Pathways		
	Path 1	Path 2	Path 3
0	8	9	10
1	7	11	11
2	8	10	15
3	8	14	18
4	7	14	19
5	8	15	15
6	7	13	15
7	7	13	13
8	6	11	10
9	6	10	8

Measurement Session No. 17

Week 25

Distance from Proximal Cuff (inches)	Pressure measured on Pathways		
	Path 1	Path 2	Path 3
0	8	9	9
1	7	10	10
2	7	10	14
3	7	14	16
4	6	14	17
5	7	14	15
6	7	13	15
7	7	12	12
8	6	10	10
9	6	10	8

Measurement Session No. 18

Week 26

Distance from Proximal Cuff (inches)	Pressure measured on Pathways		
	Path 1	Path 2	Path 3
0	7	9	9
1	6	10	10
2	7	9	14
3	7	14	15
4	6	14	15
5	7	14	15
6	7	13	14
7	6	12	12
8	6	10	8
9	6	9	4

Measurement Session No. 19

Week 27

Distance from Proximal Cuff (inches)	Pressure measured on Pathways		
	Path 1	Path 2	Path 3
0	6	9	8
1	6	10	10
2	6	9	13
3	5	13	13
4	6	13	14
5	6	12	14
6	6	12	13
7	5	10	8
8	5	9	6
9	5	8	3

Measurement Session No. 20

Week 27: New Tubigrip Fitted

Distance from Proximal Cuff (inches)	Pressure measured on Pathways		
	Path 1	Path 2	Path 3
0	9	11	11
1	11	13	13
2	12	17	19
3	13	20	19
4	9	19	22
5	8	16	24
6	8	16	18
7	8	15	17
8	9	13	16
9	5	11	13

Measurement Session No. 21

Week 31

Distance from Proximal Cuff (inches)	Pressure measured on Pathways		
	Path 1	Path 2	Path 3
0	9	11	11
1	10	12	13
2	12	16	19
3	12	20	19
4	9	18	22
5	8	16	23
6	8	16	17
7	8	15	17
8	8	12	16
9	5	10	12

Measurement Session No. 22

Week 35

Distance from Proximal Cuff (inches)	Pressure Measured on Pathways		
	Path 1	Path 2	Path 3
0	8	9	9
1	7	11	11
2	8	14	16
3	8	15	16
4	7	14	17
5	7	13	18
6	7	14	16
7	6	14	15
8	7	11	14
9	6	9	10

Measurement Session No. 23

Week 38

Distance from Proximal Cuff (inches)	Pressure measured on Pathways		
	Path 1	Path 2	Path 3
0	6	8	8
1	6	9	10
2	5	8	13
3	6	14	13
4	5	13	14
5	5	12	14
6	6	11	13
7	6	10	10
8	5	9	8
9	5	7	5

Measurement Session No. 24

Week 40

Distance from Proximal Cuff (inches)	Pressure measured on Pathways		
	Path 1	Path 2	Path 3
0	4	8	8
1	4	7	10
2	4	7	12
3	5	12	12
4	4	12	12
5	4	11	12
6	4	10	10
7	3	10	7
8	3	8	4
9	3	7	4

Measurement Session No. 25

Week 40: New Tubigrip Garment Fitted

Distance from Proximal Cuff (inches)	Pressure measured on Pathways		
	Path 1	Path 2	Path 3
0	9	13	11
1	12	15	12
2	13	15	18
3	14	17	24
4	11	20	24
5	12	19	19
6	10	19	17
7	11	17	16
8	10	14	14
9	10	11	13

Measurement Session No. 26

Week 43

Distance from Proximal Cuff (inches)	Pressure measured on Pathways		
	Path 1	Path 2	Path 3
0	9	12	11
1	11	13	11
2	12	14	17
3	12	16	22
4	10	19	22
5	10	18	18
6	9	18	16
7	10	16	15
8	9	13	14
9	9	10	12

Measurement Session No. 27

Week 46

Distance from Proximal Cuff (inches)	Pressure measured on Pathways		
	Path 1	Path 2	Path 3
0	8	11	10
1	10	12	10
2	11	13	15
3	11	15	17
4	9	17	18
5	9	17	17
6	9	17	16
7	8	16	15
8	9	12	12
9	8	10	10

Measurement Session No. 28

Week 49

Distance from Proximal Cuff (inches)	Pressure measured on Pathways		
	Path 1	Path 2	Path 3
0	8	10	9
1	8	12	10
2	9	12	14
3	8	15	16
4	8	15	15
5	7	14	15
6	6	14	14
7	8	14	12
8	7	11	9
9	6	9	6

Measurement Session No. 29

Week 49: New Tubigrip Garment Fitted

Distance from Proximal Cuff (inches)	Pressure measured on Pathways		
	Path 1	Path 2	Path 3
0	10	13	11
1	12	15	12
2	14	16	18
3	14	16	23
4	12	19	25
5	12	20	20
6	11	19	18
7	11	17	16
8	10	15	15
9	10	12	12

Measurement Session No. 30

Week 52

Distance from Proximal Cuff (inches)	Pressure measured on Pathways		
	Path 1	Path 2	Path 3
0	9	12	11
1	11	13	11
2	12	15	16
3	12	15	21
4	11	17	22
5	12	18	19
6	10	18	17
7	9	16	15
8	10	15	15
9	9	11	10

Measurement Session No. 31

Week 56

Distance from Proximal Cuff (inches)	Pressure measured on Pathways		
	Path 1	Path 2	Path 3
0	8	11	9
1	10	12	10
2	11	13	13
3	10	15	17
4	10	16	17
5	9	16	18
6	8	16	15
7	7	15	14
8	8	13	11
9	8	9	8

Measurement Session No. 32

Week 58

Distance from Proximal Cuff(inches)	Pressure measured on Pathways		
	Path 1	Path 2	Path 3
0	8	11	9
1	8	10	10
2	8	12	11
3	8	13	16
4	7	15	15
5	8	14	16
6	7	13	15
7	6	13	13
8	7	12	8
9	8	8	4

Measurement Session No. 33

Week 58: New Tubigrip Garment Fitted

Distance from Proximal Cuff (inches)	Pressure measured on Pathways		
	Path 1	Path 2	Path 3
0	10	11	11
1	11	12	13
2	12	15	17
3	12	18	17
4	10	18	21
5	10	17	21
6	10	16	19
7	11	16	18
8	10	15	17
9	8	14	13

Measurement Session No. 34

Week 61

Distance from Proximal Cuff (inches)	Pressure measured on Pathways		
	Path 1	Path 2	Path 3
0	9	9	9
1	10	11	12
2	11	14	15
3	10	15	16
4	8	16	17
5	10	15	17
6	9	15	16
7	9	14	16
8	8	14	15
9	7	11	12

Measurement Session No. 35

Week 64

Distance from Proximal Cuff (inches)	Pressure measured on Pathways		
	Path 1	Path 2	Path 3
0	9	9	9
1	9	10	12
2	9	10	14
3	9	13	15
4	8	15	15
5	9	15	15
6	8	14	14
7	8	14	15
8	8	12	11
9	7	10	8

Measurement Session No. 36

Week 67

Distance from Proximal Cuff (inches)	Pressure measured on Pathways		
	Path 1	Path 2	Path 3
0	7	8	8
1	8	10	11
2	7	12	13
3	7	12	13
4	7	14	15
5	6	13	14
6	7	13	13
7	6	13	11
8	6	11	7
9	5	9	4

APPENDIX C

This Appendix relates to Chapter 6 and contains the procedure for the hydroxyproline ^{14}C Assay, the procedure for the determination of hydroxyproline and total radioactivity, the reagents used in the assay and their composition. The Appendix also contains a theoretical prediction of collagen biosynthesis and the derivation of an efficiency value for the Packard Counter.

PROCEDURE FOR HYDROXYPROLINE ^{14}C ASSAY

Step Number	Description
1.	A clean, unbroken large tube of 50ml capacity for each sample was selected.
2.	1mg (100µl) carrier proline and 2mg (1ml) carrier hydroxyproline were added to each tube.
3.	A suitable aliquot of each sample (up to about 50,000 cpm) was added and the pH was adjusted to 8.0 (1 drop of phenophthalein to faint pink using 1.0 N and 0.1 N NaOH)
4.	The volume in each tube was adjusted to 5ml by the addition of distilled H_2O.
5.	6ml 0.2M sodium pyrophosphate buffer pH 8.0 was added to each tube and was mixed well, and the solution was then checked to see if it remained pink.
6.	25ml of Chloramine-T in methyl cellosolve (1.4085 gms/25ml) was prepared.
7.	Each sample was oxidised with 1.0ml of freshly prepared chloramine solution; A clock was set for 20mins. at the first addition, and the chloramine solution was added to each tube, and then each tube was mixed.

8. At the end of 20mins. the oxidiation was stopped by the addition of 6ml of 3.6ml sodium thiosulphate to each tube.

9. The sample was adjusted to faint pink with 1.0N and 0.1N NaOH.

10. 4ml Tris buffer pH 8.0 was added to each tube and mixed well.

11. Each tube was saturated with an excess of NaCl (one teaspoonful, 5ml, was sufficient).

12. 10ml scintillation grade toluene was added to each tube and each tube was capped tightly with a P.T.F.E.-lines rubber stopper.

13. The level of the water layer on the outside of each tube was then marked.

14. The tubes were then shaken in an automatic shaker for 5mins.

15. The tubes were centrifuged for 4mins. at about 1400 rpm in a Mistral MSE 61 centrifuge at $0^{o}C$. The level of the water layer in the tube after centrifugation was checked and any decrease was noted.

16. The toluene layer was completely removed using suction and a disposable capillary pipette for each tube. This toluene was discarded.

17. The tubes were capped tightly and placed in a boiling water bath. The water level of the bath was always above the liquid level in the tubes. When the water bath returned to boiling a timer was set fot 25mins.

18. After 25mins. the tubes were removed from the boiling water and cooled to room temperature under running tap water.

19. Additional NaCl was added to saturation, to aid protein precipitation, if necessary.

20. Exactly 12ml of toluene was added to each tube, each tube was sealed and shaken for 5mins. as per step 14.

21. The tubes were centrifuged as per step 15.

22. The samples were then carefully transported to the laboratory.

23. 15 grams of silicic acid (Bio-rad minus 325 mesh) were suspended in 50ml toluene (this was enough for 10 columns, although only eight columns were used).

24. To each column (30cm x 1cm with a glass wool plug) a thin layer of sand ($\frac{1}{4}$" - $\frac{1}{8}$") was added and then 5ml of silicic acid toluene suspension was added. The silicic acid toluene suspension was continuously mixed on a magnitic stirrer.

25. Each column was washed with a small amount of toluene to remove silicic acid from the walls of the column.

26. Once the column had dried exactly 10ml of the clear toluene layer was added from the sample.

27. When the column was again dry it was washed with 5ml toluene (this was added very slowly, so as not to disturb the column). When the column was again dry (which took about 20mins.) 10ml of toluene was added.

28. After the second washing had passed through the column, the volume in each collection flask was checked and if it was less than 25ml, the volume was noted. 20ml of the eluate was removed and placed in a counting vial.

29. 1.0 non-aqueous scintillation fluid was added to each vial containing 20ml of the eluate and placed in the counter for counting (i.e. there was 21ml in each vial). Counts from this vial correspond to the hydroxyproline radioactivity.

Procedure for the Determination of Hydroxyproline

30. Hydroxyproline was oxidised to pyrrole in step 5 of the assay and the pyrrole can be converted to a relatively specific chromophore with p-dimethylaminobenzaldehyde (Ehrlich's reagent). Thus the percentage recovery of hydroxyproline (in μmoles) as pyrrole can be calculated. From the eluate of each sample obtained in step 28, 0.1 ml was removed and placed in a clean spectrophotometer vial and 4.8ml of scintillation grade toluene was added to each vial. In one vial 5ml of toluene was placed to be used as a blank. Pyrrole standards of 0.02 μM/ml and 0.04μM/ml were prepared by taking 1.0ml and 2.0ml respectively of a 0.01mM/l standard and making the volume to 5ml with toluene (the 0.01mM/l was stored at -20^{o}C, warmed to room temperature beforehand).

Procedure for Determination of Total Radioactivity

From the redissolved residue of each sample a 100 μl aliquot was taken and was added to 2.0ml of the aqueous counting solution, made up as described below. The samples were placed in a Packard 3255 liquid scintillation spectrometer and the radioactivity was measured in counts per minute (cpm).

31. 2ml of thawed Ehrlich's reagent was added to each tube and the tube contents were mixed as soon as possible after the addition of the reagents.

32. The tubes were then placed in the dark for 30 - 45mins. and read in a colourimeter at 560 μm.

REAGENTS

Hydroxyproline carrier:	L-hydroxyproline (MW 131.25) was prepared in a concentration of 2mg/ml in 250ml batches and stored refrigerated under toluene.
Proline carrier:	L-Proline (MW 115) was prepared in a concentration of 10mg/ml and stored as above.
Sodium Pyrophosphate:	0.2M prepared in 1 litre batches (dissolved in 800ml hot H_2O and cooled to room temperature the pH was adjusted to 8.0 with concentrated HCl and then diluted to 1 litre and stored in plastic bottles at room temperature).
Sodium Thiosulphate: (Anhydrous)	3.6M prepared in 1 litre batches (to 500ml of water the salt gradually added stirring constantly and each aliqout of salt was allowed to dissolve before adding more; water was added until the final volume was 1 litre) stored under toluene in brown bottles at room temperature. The solution was extracted with a 10ml pipettor.
Pheolphthalein:	A 1% solution in absolute alcohol was prepared.
Tris Buffer:	A 1.0M solution was prepared in 1 litre batches (the molecular weight of the salt was dissolved in 800ml H_2O and the pH was adjusted to 8.0 with concentrated HCl and then diluted to 1 litre and stored in plastic bottles at room temperature).

Pyrrole Standard:

A stock solution was made to a concentration of 0.1 millimoles/litre in toluene - redistilled pyrrole and diluted pyrrole standard stored at -20°C in amber bottles or bottles wrapped in aluminium foil.

Ehrlich's Reagent:

Purification of Crystals:

1. 250 gm p-dimethylaminobenzaldehyde is dissolved in 1.5 l. warm absolute ethanol (50°C) and filtered, while still warm, through coarse filter paper.

2. The solution is placed overnight in the deep freezer.

3. The alcohol is filtered off with suction, and the crystals are washed with 500ml cold absolute ethanol.

4. The crystals are again dissolved in 1:51. warm ethanol, and the solution placed in the deep freezer overnight.

5. The alcohol is filtered off with suction, and the crystals washed with 500ml cold ethanol. The crystals should be allowed to dry with suction for about 20 to 30 minutes.

6. The crystals are dryed in an oven (temperature should be 30 - 35°C- if the temperature should go higher than 40°C, the crystals will melt). They should be allowed to dry for approximately 8 hours or until no odour of ethanol is evident.

Yield: 70 - 80%.

Preparation of Ehrlich's Reagent:

1. 27.4 ml conc. H_2SO_4 is added to 200.0ml cold absolute ethanol.

2. 120.0 gm purified p-dimethylamino-benzaldehyde is added to 200.0ml absolute ethanol in another beaker.

3. The acid-alcohol mixture is placed in the deep freezer, and when it is cold is added slowly to the DMA-BA mixture with stirring.

4. The final solution is stored in brown bottles in the refrigerator. Before use, it is usually necessary to warm and shake the solution in order to redissolve the crystals.

Solution for Total Counts (Aqueous):

200 ml	Non-aqueous fluor (as above)
400 ml	Toluene
240 ml	2-Methoxyethanol (i.e. methyl cellusolve)

Mix well before use stored in brown bottles.

Solution for Hydroxyproline Counts (Non-Aqueous):

30 gm	2,5-diphenyloxazole (PPO)
600 mg	1,4-bis- 2(5-Phenyloxazole)benzene (POPOP)

dilute to 2 litres with toluene; mix well using a magnetic stirrer and store in brown bottles.

INCUBATION MEDIUM

The incubation medium was a phosphate-free Krebs-Ringer balanced salt solution made up according to the following ingredients:-

	Grams/l	Grams/100ml	Parts of Solution (ml)
0.9% NaCl	9	0.9	100
1:15% KCl	11.5	1.15	4
1.22% $CaCl_2$	12.2	1.22	3
2.11% KH_2PO_4	21.1	2.11	1
3.82% $MgSO_4 7H_2O$	38.2	3.82	1
1.30% $NaHCO_3$	13.0	1.3	3

The final volume of each batch of medium was 112ml.

To 96ml of medium 2ml of glucose solution and 2ml of Hepes both sterile was added to give a 20mM concentration of each in the medium. The Krebs-Ringer solution was sterilised using a Millipore filter and syringe.

THEORETICAL PREDICTION OF COLLAGEN BIOSYNTHESIS DURING INCUBATION WITH ^{14}C-PROLINE

At the beginning of the incubation there is, in the tissues, free labelled and unlabelled proline and bound proline and hydroxyproline (unlabelled):-

1.

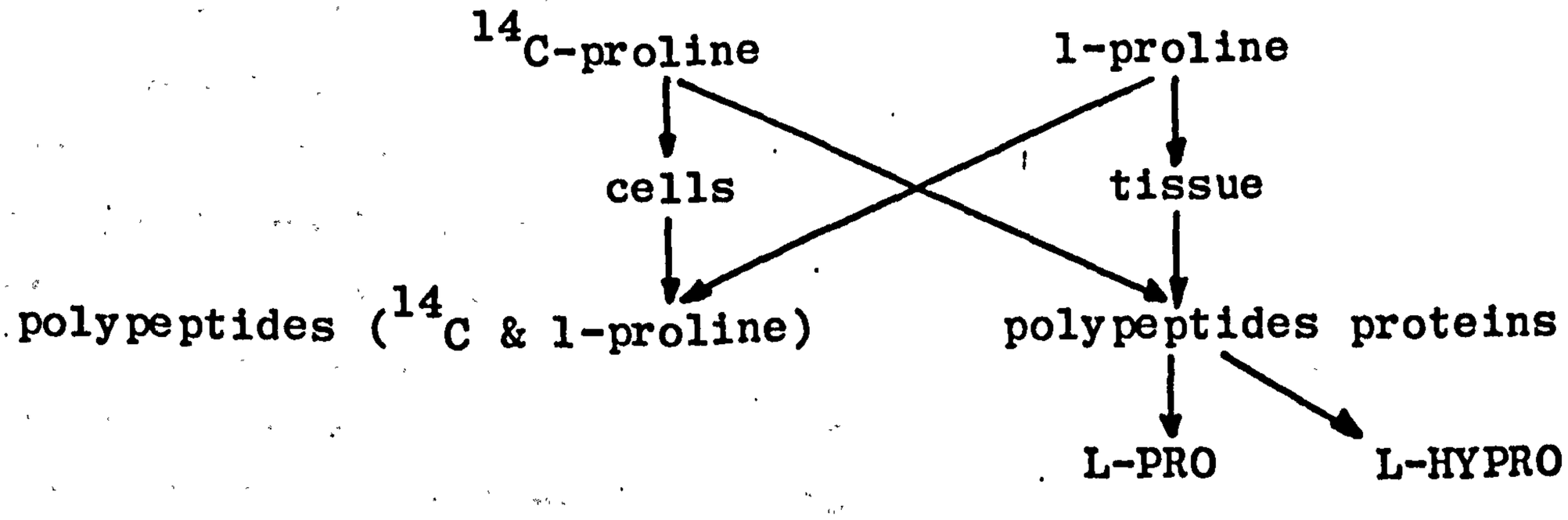

After the incubation incorporation of the free labelled and unlabelled proline into polypeptides, which are non-dialysable, occurs the tissues (proteins + polypeptides + AAcids) are then hydrolysed in 6N HCl for 6 hours at 135^{o}C and the polypeptides are then split into acid residues.

The amount of labelled proline-^{14}C at the beginning of the assay is 1 μC_i (2.2×10^6 dpm). From the specificativity 285mCi/mmol the number of labelled proline molecules in

1 μCi is 2.1×10^{15}.

However there are also free proline molecules in the AAcid pool in the tissue, but the number of molecules is at present indeterminate. Proline and hydroxyproline are also present in the tissue in polypeptides and proteins. The number of molecules of each present in 100 grams of fresh tissue can be calculated approximately as follows:-

in 100 grams of wet tissue, the weight of collagen in adult dermis is 4.57 g. (Loewi, G. Biochem. Biophys Acla. 52, 435, 1961).

The % of proline in collagen is 9.52 the % of hypro in collagen is 10.17 (Fitzak & Kuhn, Conn. Tiss. Res 1976).

i.e. the weight of proline in 100 grams of tissue is 0.434g

the weight of hydroxyproline in 100 grams of tissue is 0.447 g

i.e. number of proline molecules/100 grams tissue 22.69×10^{20} molecules

number of hydroxyproline molecules/100 grams tissue 20.52×10^{20} molecules.

At the end of the incubation 100 mg carrier proline is added i.e. 5.2×10^{20} molecules.

Assumption: If 5% maximum of radioactivity is incorporated, which is reasonable, then 95% of unlabelled proline from the AA pool is incorporated to the synthesised polypeptides. Therefore if each labelled and unlabelled proline molecule has an equal probability of being incorporated then we can assume that there is 20 times as much free l-Proline as ^{14}C-proline available prior to incubation.

i.e. the number of free L-proline molecules is then 42×10^{15}, and

if 5% of 42×10^{15} molecules are incorporated then 2.1×10^{15} L-proline molecules are incorporated.

Therefore 39.09×10^{15} L-proline molecules are <u>not</u> incorporated and 5% of the ^{14}C-proline molecules are incorporated then 0.1×10^{15} ^{14}C-proline molecules are incorporated therefore 2.0×10^{15} ^{14}C-proline molecules are not incorporated.

At the end of incubation there are

A) FREE molecules

(i) labelled: 2.0×10^{15} molecules

(ii) unlabelled: 39.9×10^{15} molecules + 5.2×10^{20} molecules

i.e. $5.2 \times 10^{20} + 39.9 \times 10^{15}$

i.e. 5.2×10^{20} ∴ free proline molecules

B) PEPTIDE-bound molecules

proline (i) labelled 0.1×10^{15} ^{14}C-proline molecules newly synthesised peptides

(ii) unlabelled 2.1×10^{15} L-proline molecules

From the specific activity of proline 285mCi/mmole)

number of moles of proline synthesised during incubation 0.36×10^{-8} mmoles

number of moles of ^{14}C-proline present approximately 3.4 mmoles

This is equivalent to 110,000 dpm.

At the end of dialysis the activity in disintigrations per minute was found to be about 80,000dpm

A comparison between theoretically derived and measured values for radioactivity incorporated during incubation shows a reasonable agreement.

DERIVATION OF THE EFFICIENCY VALUE FOR PACKARD 3255 SCINTILLATION COUNTER

A standardised ^{14}C-hexadecane source (Radiochemical Centre, Amersham) was used to check the efficiency of the counter. a 200 μl aliquot contained 88,000 dpm which is similar to the counts obtained after dialysis during the assay.

3 standards were made up, S_1, S_2, S_3 of 200 μl.

	cpm	actual	E (%)	
S_1	81,279	88,000	92.36	
S_2	77,951	"	88.58	1st count
S_3	78,929	"	89.69	
S_1	80,601	"	91.59	
S_2	78,479	"	89.18	
S_3	79,086	"	89.87	
		mean	90.21	
		S.D.	1.45	

i.e. overall uncertainty $< \pm$ 2%

i.e. counting efficiancy = 90.21%.

This is in concurrance with the value in the Packard Scintillator manual (91%).

A standardised (^{14}C)-hydroxyproline source was also used to check the efficiency of the counter. Three 60 µl samples each containing 66,000 dpm were used. The efficiency derived from counts measured was;

	cpm	actual	E(%)
S_1	59,410	66,000	90.06
S_2	58,941	66,000	89.30
S_3	58,754	66,000	89.02

The overall uncertainty $< \pm$ 2%

The counting efficiency is 89.46% and is similar to the value claimed in the Packard manual.

APPENDIX D

This Appendix contains a derivation of the relationship between the strain of a vessel and the blood flow within the vessel using a laminar flow model (refer Chapter 7).

DERIVATION OF RELATIONSHIP BETWEEN VESSEL STRAIN AND BLOOD FLOW

Consider a model in which the blood flow in a thin-walled tube is laminar. The tube is assumed to be incompressible and therefore under strain and isovolumetric. The blood flow rate for a particular length of vessel is expressed by Poiselles Law which states that

$$Q_t = \frac{\Pi r^4 \, dP}{8 \mu \, dx} \qquad D1$$

where r = inner radius of a thin-walled tube

x = tube length

dP = pressure differential along dx

μ = constant (C_1)

and if dx = x, dP = P = constant

then equation (D1) may be expressed as

$$Q_t = \frac{K \, r^4 \, P}{x} \qquad D2$$

where $K = \frac{\Pi}{8}$ = constant (C_2)

therefore for an unstrained tube

$$Q_1 = Q_t = \frac{K \, r^4 \, P}{x} \qquad D3$$

If a deformation is then applied to the tube such that

the new tube length = $x + \delta x$ and

the new tube radius = $r - \delta r$

then the flow within the tube may be expressed as

$$Q_2 = Q_t = \frac{K(r - \delta r)^4 p}{x + \delta x} \qquad D4$$

from equations D1 and D4, in which equation D4 is expanded, the ratio

$$\frac{Q_1}{Q_2} = \frac{(1 - 4r/\delta r)}{(1 + x/\delta x)} \qquad D5$$

Now the volume of an unstrained tube of length x,

$$V_1 = (\Pi r_1^2 - \Pi r_2^2)\, x_1, \qquad \begin{array}{l} r_1 = \text{outer radius} \\ r_2 = \text{inner radius} \end{array}$$

and volume of a tube strained to a new length x_2

$$V_2 = (\Pi r_3^2 - \Pi r_4^2)\, x_2, \qquad \begin{array}{l} r_3 = \text{strained tube outer radius} \\ r_4 = \text{strained tube inner radius} \end{array}$$

for incompressible material

$$V_1 = V_2;\ (\Pi r_1^2 - \Pi r_2^2)\, x_1 = (\Pi r_3^2 - \Pi r_4^2)\, x_2 \quad ...D6$$

and $(r_1^2 - r_2^2) = (r_1 - r_2)(r_1 + r_2)$

$(r_3^2 - r_4^2) = (r_3 - r_4)(r_3 + r_4)$

also $r_1 - r_2 = t$ where t = tube thickness

$r_3 - r_4 = t$

$t(r_1 + r_2)x_1 = t(r_3 + r_4)x_2$

for an axial or longitudinal strain of 20% which is quite common in capillaries

$x_2 = 1.2x_1$

$(r_1 + r_2) = (r_3 + r_4)\ 1.2$

and $(2r_2 + t) = (2r_4 + t)\ 1.2$ D7

for capillary dimensions $r_2 = 5\,\mu m$, $t = 2\,\mu m$

from (D7), $2r_4 + 2 = 10$

$$r_4 = 4\mu m$$

$$\% \text{ strain in radial direction} = \frac{r_2 - r_4}{r_2} \times 100 = 20\%$$

substituting axial and radial strains in equation D5 gives

$$\frac{Q_2}{Q_1} = \frac{(1 - 4.0.20)}{(1 + 0.20)}$$

$$= \underline{0.17}$$

The blood flow in a vessel strained in the axial or longitudinal direction by 20% is reduced to 17% of the flow in an unstrained vessel.

From Daly et al (1976) vide 3.2.1. (Figure 3.2) a reduction of flow to 17% of the original flow corresponds, approximately, to 50mmHg, which is around the threshold necessary to induce ischaemic necrosis.

From equation D5, for radial strain of 25% there is no flow (in fact there is always some flow, though it might not be easily detectable). However, if the expansion of equation D4 is not approximated then for a 25% decrease in the radius the flow is reduced by about 94% i.e. it is practically zero; the equivalent longitudinal strain being $\simeq 26.3\%$.